Characterization, toxicity, and biological activities of organometallic compounds and peptide nucleic acids for potential use as antimicrobials

Marigold Ellen Bethany Ernst

Dissertation submitted to the faculty of the Virginia Polytechnic Institute and State University in partial fulfillment of the requirements for the degree of

Doctor of Philosophy
In
Biomedical Sciences and Pathobiology

Nammalwar Sriranganathan
Joseph S. Merola
Katie M. Boes
Marion F. Ehrich

March 28, 2019
Blacksburg, VA

Keywords: antibiotic resistance, organometallic compounds, peptide nucleic acids, *Mycobacterium*, *Salmonella*

Characterization, toxicity, and biological activities of organometallic compounds and peptide nucleic acids for potential use as antimicrobials

Marigold Ellen Bethany Ernst

ABSTRACT

Bacterial antibiotic resistance is a globally recognized problem that has prompted extensive research into novel antimicrobial compounds. This dissertation describes research focusing on two types of potential antimicrobial molecules, organometallic compounds (OMC) and peptide nucleic acids (PNA). Organometallic compounds show promise as antimicrobial drugs because of their structural difference from conventional antibiotics and antimicrobials, and because of the ability to "tune" their chemical and biological properties by varying ligand attachments. Peptide nucleic acids, when linked to a cell-penetrating peptide (CPP), can suppress bacterial gene expression by an antisense mechanism and are attractive candidates for antimicrobial drugs because they bind strongly to target nucleic acids and are resistant to nucleases. Chapters 1 and 2 of the dissertation provide an introduction and broad literature review to frame the experimental questions addressed. Chapter 3 describes work to test the cytotoxicity and cellular penetration capabilities of novel OMCs by evaluating their effects on J774A.1 murine macrophage-like cells that were either uninfected or were infected with *Mycobacterium bovis* BCG. Results indicate that OMCs with an iridium (Ir) metal center and an amino acid ligand show minimal cytotoxicity against eukaryotic cells but likely do not penetrate the intracellular compartment in significant amounts. Chapter 4 presents research into *in vitro* effects of CPP-PNAs targeting the *tetA* and *tetR* antibiotic resistance genes (CPP-anti-tetA PNA and CPP-anti-tetR PNA, respectively) in tetracycline-resistant *Salmonella enterica* ssp. *enterica* serovar Typhimurium DT104 (DT104). Through the use of modified minimum inhibitory concentration (MIC) and minimum bactericidal concentration (MBC) assays it was shown that both the CPP-anti-tetA PNA and CPP-anti-tetR PNA increase tetracycline susceptibility in DT104. Chapter 5 explores the molecular mechanism of the CPP-anti-tetA PNA and CPP-anti-tetR PNA through the use of reverse transcriptase quantitative polymerase chain reaction (RT-qPCR). Results indicate good specificity of the CPP-anti-tetA PNA for its nucleic acid target as evidenced by suppression of *tetA* mRNA expression in DT104 cultures treated with a combination of tetracycline and the PNA. Chapter 6 describes the development of a mouse model of DT104 infection using BALB/c mice, followed by implementation of that model to test *in vivo* antimicrobial effects of the CPP-anti-tetA PNA and the CPP-Sal-tsf PNA, which targets expression of the essential *tsf* gene. An optimal dose of DT104 was identified that causes clinical illness within 2-4 days. At the doses tested, concurrent treatment of infected mice with tetracycline and the CPP-anti-tetA PNA or with the CPP-Sal-tsf PNA alone did not have a protective effect. Final conclusions are 1) that further research with the OMCs should focus on compounds with an Ir center and an amino acid ligand, and should explore ways to enhance intracellular penetration, 2) that the *in vitro* results of the PNA studies suggest that PNAs targeting expression of antibiotic resistance genes could allow for repurposing of antibiotics to which bacteria are resistant, and 3) additional study of the behavior of PNAs *in vivo* is advised.

General Audience Abstract

Antibiotic-resistant bacteria are increasingly recognized as a threat to global health, and new antibacterial drugs are urgently needed. Before a chemical compound can advance far in the journey to becoming a new drug it must be tested for toxicity against mammalian cells. A portion of this dissertation research involved testing the toxicity of several organometallic compounds (OMCs) previously shown to have antibacterial potential. Mouse-derived mammalian cells were treated with several of the OMCs, and initial results indicated that one of the OMCs is non-toxic and is likely a safe option for additional analysis. This OMC was further tested to see if it could inhibit mycobacterial growth inside of the mammalian cells. It did not effectively clear bacteria from inside of the mammalian cells, likely because of poor penetration of the cell membrane. Further research with this compound should focus on ways to effectively transport the OMC inside infected mammalian cells so that it can reach the bacteria it is meant to target. A second portion of this research involved using a peptide nucleic acid (PNA) to try and reverse tetracycline antibiotic resistance in the bacterial strain *Salmonella enterica* ssp. *enterica* serovar Typhimurium DT104 (DT104). Peptide nucleic acids are short linear molecules that can bind strongly to complementary DNA and RNA sequences and thus be used to interfere with expression of specific genes. A PNA was designed to inhibit expression of the bacterial *tetA* gene that codes for a protein called the TetA tetracycline efflux pump, which imparts resistances to tetracycline. Treating the bacteria with the PNA resulted in a lower dose of tetracycline needed to inhibit bacterial growth, indicating a successful increase in tetracycline susceptibility. By using a molecular analysis technique called reverse-transcriptase quantitative polymerase chain reaction (RT-qPCR), it was possible to measure the amount of *tetA* messenger RNA (mRNA) in cultures of DT104 treated only with tetracycline or with a combination of tetracycline and the PNA. As expected, bacteria treated with both the antibiotic and the PNA had less *tetA* mRNA than the cultures treated only with tetracycline, supporting the hypothesis that the PNA prevents the bacteria from effectively expressing the *tetA* gene. The PNA was next used in conjunction with tetracycline as an experimental treatment for mice infected with DT104. The PNA did not provide the expected protective effect under these circumstances. The overall conclusion for this part of the research is that PNAs offer an exciting potential avenue for counteracting antibiotic resistance, but additional experimentation is needed. Future research should focus on investigating more effective ways to get the PNAs inside the bacteria and on understanding more about how the PNAs behave in live animals. Several other PNAs targeting different genes involved in antibiotic resistance or essential bacterial functions were also tested against DT104 with variable success.

Dedication

This work is dedicated first to God. My desire is to honor him in whatever I do, whether it is related to relationships, work, or education.

This effort is secondly dedicated to my family

- To my incomparable husband Joey: thank you for the selfless support and unflagging encouragement you provided throughout this long academic journey. I promise that any benefits reaped from having this degree will go toward further nurturing the beautiful life and family we have built together.
- To our children Clara, Simon, and baby girl not yet born: thank you for your resilience and for the sacrifice of time you made when Mommy had to work on her "big project". I hope that by finishing this I can help teach you that persistence and discipline will pay off even if there are difficult periods. But enough of that for now – let's play!
- To my parents, Charles and Reine Bethany: thank you for always encouraging me to follow my chosen goals, and for providing such an excellent example of family love and support.

Thirdly, I dedicate this research to other family members, friends, colleagues, and mentors who offered support in any way over the past six years, be it through advice, babysitting, discussion of scientific ideas, cheerleading, or casseroles. There are too many of you to name, but each of your contributions helped me make it through the final push.

Finally, I dedicate this dissertation to myself, past, present, and future. Perhaps this is unconventional, but the combined pathology residency and PhD program was the most difficult challenge I have ever voluntarily undertaken, and I want this dissertation to remind me that past efforts prepared me for it, present perseverance brought it to completion, and future obstacles should not cause me to give up on something I deeply desire to finish.

Acknowledgements

I wish to first acknowledge my PhD committee. I was somehow blessed with a committee composed entirely of that special kind of mentor who calls you to academic excellence while still understanding what matters most in life. They made navigation of a demanding combined academic program possible.

- Dr. Nathan, you provided solid mentorship to help me plot out the bulk of this research, but still always challenged me to come up with my own scientific questions and answers. You also made sure that the "Philosophy" portion of the PhD was thoroughly addressed. Thanks for the lunchtime conversations ranging from molecular biology to metaphysics.
- Dr. Merola, you gave me the critical launch point I needed to get my PhD studies going, then graciously supported me as I figured out what research path made the most sense for me. Some would find this balance, "Inconceivable!" but you allowed me to make needed transitions without judgment or difficulty.
- Dr. Boes, you impressively had the double role of both training me in pathology and critically assessing my PhD research. You handled this with aplomb and helped me maintain the difficult balance between the two. Your support of my family needs is also gratefully recognized.
- Dr. Ehrich, to my knowledge, no one replies to emails as quickly as you do. I do not know how you do it, but your attention to my communications and your invaluable constructive criticism of my writing always made me feel that my efforts mattered.

I also acknowledge the intellectual contributions of my "second committee", the members of the PNAs research team who, along with Dr. Nathan, included Dr. Stephen Boyle, Dr. M. Renee Prater, and Dr. Shaadi El Swaifi.

My laboratory colleagues, including Dr. Neeta Jain-Gupta, lab manager Nancy Tenpenny, graduate students Grant Waldrop, Amanda Kravitz, and Chrissy Duchane, veterinary student Andrew Facchiano, and high school student Unmesha Vullikanti provided hands-on help and practical advice, without which, frankly, I would not have finished. My pathology colleagues, many of whom went through similar rigorous combined academic training, offered encouragement, gave much needed pathology fixes, and kept me laughing. I wish to solemnly acknowledge the sacrifice of the laboratory animals used in this research, and the help of the TRACSS staff who cared for them.

The administrators and staff of the Department of Biomedical Sciences and Pathobiology, the Biomedical and Veterinary Sciences program, and the Office of Research and Graduate Studies all enthusiastically guided me through the logistics of this program.

Funding for this work was generously provided by the VMCVM Office of Research and Graduate Studies, the Stamps Family Charitable Foundation Inc., a VCOM-VMCVM Center for One Health Research seed grant, and a Virginia Tech Center for Drug Discovery small grant.

Table of Contents

General Audience Abstract iii
Dedication iv
Acknowledgements v
Table of Contents vi
List of Figures viii
List of Tables xvii
List of Abbreviations xix
Attributions xx
1 Introduction 1
2 Literature review 3
2.1 Brief history of antibiotic discovery and early observations of antibiotic resistance 3
2.2 Brief review of mechanisms of antibiotic resistance 4
2.3 Call for new antimicrobial drugs that circumvent known mechanisms of antibiotic resistance 4
2.4 Organometallic compounds as possible antimicrobials 5
2.5 Antisense oligonucleotides (ASOs) as possible antimicrobials 6
2.6 Animal models for evaluation of PNA efficacy 11
2.7 References 12
3 Eukaryotic cell cytotoxicity and cellular penetration of novel organometallic compounds with inhibitory activity against nontuberculous mycobacteria 21
3.1 Introduction 21
3.2 Materials and Methods 22
3.3 Results 31
3.4 Discussion and Conclusions 43
3.5 References 47
4 Peptide nucleic acids targeting expression of tetracycline resistance genes increase tetracycline susceptibility in multidrug-resistant *Salmonella enterica* ssp. *enterica* serovar Typhimurium DT104 50
4.1 Introduction 50
4.2 Materials and Methods 53
4.3 Results 69
4.4 Discussion and Conclusions 91
4.5 References 95

5 Effect of cell penetrating peptide-peptide nucleic acid (CPP-PNA) conjugates on expression of *tetA* mRNA in *Salmonella enterica* ssp *enterica* serovar Typhimurium DT104 98
5.1 Introduction 98
5.2 Materials and Methods 99
5.3 Results 105
5.4 Discussion and conclusions 131
5.5 References 135
6 Development and implementation of a mouse model of oral *Salmonella* infection for *in vivo* testing of antimicrobial cell penetrating peptide-peptide nucleic acid conjugates 138
6.1 Introduction 138
6.2 Materials and Methods 139
6.3 Results 144
6.4 Discussion and conclusions 157
6.5 References 160
7 Conclusion 163
7.1 References 165

List of Figures

Figure 3.1 Structures of six novel OMCs chosen for eukaryotic cell cytotoxicity assays based on their inhibitory activity against several species of nontuberculous mycobacteria in pure culture. 23
Figure 3.2 Schematic of a 96-well cell culture plate seeded with 2 x 10^4 J774A.1 cells/well. Solutions containing OMCs in various concentrations were added and the cells were incubated for 24, 48, or 72 hours before measurement of cellular metabolism to assess cytotoxicity. Three compounds were tested on each 96-well plate. 25
Figure 3.3 24-well plate set up to evaluate the effect of experimental organometallic compounds on intracellular growth of *M. bovis* BCG Pasteur within J774A.1 murine macrophage-like cells. All wells contain J774A.1 cells infected overnight with *M. bovis* BCG Pasteur. Two 24-well plates with identical treatment arrangements were set up, one of which was incubated for 2 days before cell lysis and one of which was incubated for 5 days before cell lysis. Isoniazid was included as a conventional antimicrobial compound for mycobacterial infections. 28
Figure 3.4 24-well plate set-up to evaluate the ability of the compound IrCp*(L-pg)Cl to penetrate intracellularly within J774A.1 murine macrophage-like cells. All wells contain J774A.1 cells incubated with various concentrations of the compound for 24 or 48 hours before cell harvesting and measurement of the iridium concentration within cell lysates. 30
Figure 3.5 Charts showing relative cell viability of J774A.1 cells treated with six different OMCs at multiple concentrations for 24, 48, or 72 hours, compared to untreated control cells. After incubation, cell metabolism was assessed by performing an MTS assay and measuring absorbance of each well at 490 nm. Error bars indicate +/- 1 SD from the mean absorbance. 34
Figure 3.6 Graphs 6.A.1 and 6.B.1 show relative CFU/ml counts from the various treatment groups after the data was plotted on a log base 10 scale. Graphs 6.A.2 and 6.B.2 are close-up views of the tops of the data columns in Graphs 6.A.1 and 6.B.1, to allow for better visualization of error bars. The error bars show +/- one standard deviation from the mean CFU/ml count from each treatment group. No significant differences in bacterial CFU/ml were found among treatment groups using one factor ANOVA. 36
Figure 3.7 Appearance of J774A.1 cells after 5 days of incubation with the various treatments. Visual examination showed that the amount of cell death of the infected J774A.1 cells was similar among untreated cells (Figures 3.7B and 3.7C), cells treated with DMSO (Figure 3.7E, vehicle control for OMC 2), and cells treated with both of the OMCs (Figures 3.7F-3.7J). Cells treated with isoniazid (Figure 3.7D, antimicrobial-treated control) showed a large decrease in cell confluency, but had a greater number of live dividing cells at the end of five days of treatment than any of the other treatment groups. All of the infected cell cultures showed a large decrease in the amount of live cells compared to the uninfected, untreated control (Figure 3.7A). The amount of cell death was greater in the cultures treated for five days than in the cultures treated for two days (pictures for infected two day cultures not shown). 40
Figure 3.8 Dot plot showing the cell lysate iridium concentrations of each of the treatment wells that were analyzed by ICP-MS. Significant differences were found both between samples of the same concentration at different time points and between samples of different

concentrations at the same time points. * indicates $p < 0.05$, ** indicates $p < 0.01$, *** indicates $p < 0.001$. 42
Figure 4.1 Structure of a portion of a PNA (left) binding a complementary strand of DNA (right) by Watson-Crick base pairing. Unlike DNA, which has a sugar-phosphate backbone, PNAs have an N-(2-aminoethyl)-glycine (peptide) backbone that is not recognized by bacterial nucleases. This makes the PNAs resistant to cellular degradation. The peptide backbone is also uncharged, so there is no negative repulsion between the PNA and negatively charged DNA or RNA molecules. These characteristics make PNA-DNA or PNA-RNA bonds stronger and longer-lasting than DNA-DNA or RNA-DNA bonds..... 51
Figure 4.2 The proposed mechanism of action for PNA inhibition of gene expression is steric hindrance of ribosomal binding to the start codon region of mRNA (and likely DNA). The start codon is shown in green. After transcription of DNA to mRNA in the nucleus (first down arrow), the mRNA would ordinarily be bound by a ribosome and translated into a peptide sequence. If a complementary PNA molecule bound to a cell-penetrating peptide (CPP) encounters the mRNA (first curved arrow), a stable bond will form that interferes with ribosomal binding (crossed-out upward arrow) and prevents translation..... 52
Figure 4.3 Partial structure of an experimental CPP-PNA molecule showing the O-linker binding the CPP and the PNA together. Peptide nucleic acids alone do not penetrate bacterial membranes effectively. Cell-penetrating peptides facilitate crossing of bacterial membranes and allow the PNAs to reach the intended intracellular DNA or mRNA target. The O-linker binds the CPP and PNA together, and also has a chemical composition that improves solubility of the molecule..... 59
Figure 4.4 Set up of a 96-well microtiter plate to evaluate the effect of a PNA targeting the essential *tsf* gene on bacterial proliferation. Only a portion of the plate was used, so only the pertinent wells are shown. DT104 bacteria were seeded at a concentration of 2.7×10^4 CFU/ml in each well, then treated as shown for 8 hours. Samples from each well were then serially diluted and plated on TSA overnight for enumeration and comparison of CFU/ml among treatment groups. The wells surrounding the treated wells were filled with sterile water to decrease evaporation from the plate. Treatment key: CPP-Sal-tsf = PNA targeting the essential *tsf* gene and attached to a cell penetrating peptide (CPP); Sal-tsf = PNA targeting the essential tsf gene, but not attached to a CPP; Control-PNA = "scrambled" PNA-CPP conjugate designed for use as a negative control for PNA activity; "tx" = abbreviation for "treatment"..... 61
Figure 4.5 Set up of a 96-well culture plate to evaluate the direct effect of PNAs targeting the *tetA* and *tetR* genes on bacterial proliferation. Only a portion of the plate was used, so only the pertinent wells are shown. DT104 bacteria were seeded at a concentration of 2.7×10^4 CFU/ml in each well, then treated as shown for 8 hours. Samples from each well were then serially diluted and plated on TSA overnight for enumeration and comparison of CFU/ml among treatment groups. The wells surrounding the treated wells were filled with sterile water to decrease evaporation from the plate. The expectation was that treatment of DT104 with just these CPP-PNAs would not significantly inhibit bacterial growth, because *tetA* and *tetR* are not essential genes. Treatment key: CPP-Sal-tetR PNA = CPP-PNA designed to inhibit expression of the resistance regulatory TetR protein; CPP-Sal-tetA PNA = CPP-PNA designed to inhibit expression of the TetA tetracycline efflux pump..... 63
Figure 4.6 Set up of a 96-well culture plate to evaluate the effect of varying concentrations of the cell-penetrating peptide (CPP) on bacterial proliferation. Only a portion of the plate was

used, so only the pertinent wells are shown. DT104 bacteria were seeded at a concentration of 2.7 x 10^4 CFU/ml in each well, then treated as shown for 8 hours. Samples from each well were then serially diluted and plated on TSA overnight for enumeration and comparison of CFU/ml among treatment groups. The wells surrounding the treated wells were filled with sterile water to decrease evaporation from the plate. 65
Figure 4.7 Initial set up of the experiment to test the effect of various PNA treatments on the tetracycline MIC of DT104. This is an example of a modified MIC microtiter plate. Bacteria were seeded in each treatment well at a concentration of 5 x 10^5/µl and incubated with serial dilutions of tetracycline in conjunction with 15 µM CPP-PNA treatments or 7.5 µM CPP only treatment. Only two treatment groups could fit on each microtiter plate, so several plates were set up, and the designations of PNA Treatment 1 and PNA Treatment 2 refer to any of the following: 15 µM CPP-anti-tetR PNA, 15 µM CPP-anti-tetA PNA, 15 µM CPP-Control PNA, 7.5 µM CPP alone, and none (bacteria only control). After ~18 hours of incubation the MIC was interpreted and direct transfer of well contents onto TSA was done for determination of the MBC after overnight incubation. 67
Figure 4.8 Set up of the follow up experiment to allow for collection of replicate date showing the effect of various PNA treatments on the tetracycline MIC against DT104. Bacteria were seeded in each treatment well at a concentration of 5 x 10^5/µl and incubated with serial dilutions of tetracycline in conjunction with 15 µM CPP-PNA treatments or 7.5 µM CPP only treatment. The microtiter plate was incubated in a VersaMax plate reader and absorbance readings at 560 nm were taken every 15 minutes to generate growth curves for each treatment group. This provided a second way to interpret the MIC for each group. After ~18 hours of incubation the MIC was interpreted and direct transfer of well contents onto TSA was done for determination of the MBC after overnight incubation. This experimental set up was run three times. 68
Figure 4.9 Agarose gel stained with ethidium bromide showing successful amplification of ST104 from DT104 template DNA but not NalR template DNA. Lane 1 (far left): Gene Ruler 1 kb Plus DNA ladder; Lane 2: as expected, NalR template DNA combined with the ST104 primer did not result in DNA amplification; Lane 3: DT104 DNA template with ST104 primer resulted in the expected amplicon band (312 bp), confirming the DT104 phage type; Lanes 4 and 5: both NalR template DNA and DT104 template DNA with *InvA* primer resulted in the expected 521 bp amplicon band. The *InvA* gene is common to all *Salmonellae*; Lanes 6 and 7: template free controls did not amplify any product, as expected. 69
Figure 4.10 Results of treatment of DT104 with a CPP-PNA targeting the essential *tsf* gene, along with appropriate controls. When bound to the CPP, the PNA significantly inhibited bacterial growth at both 30 µM and 15 µM concentrations. No inhibition was observed when the PNA was not bound to CPP. Unexpectedly, the nonsense sequence CPP-Control PNA significantly inhibited bacterial growth at the higher concentration. The CPP alone significantly inhibited bacterial growth at both the high and low concentrations, although the effect was not nearly as pronounced at the lower concentration. The average CFU/ml in each treatment group was compared to that of the untreated control using a student's t-test. ** = $p < 0.01$. Error bars indicate +/- 1 standard deviation from the mean (log transformed values). 70
Figure 4.11 Results of treatment of DT104 with PNAs targeting the *tetA* and *tetR* resistance and resistance regulatory genes. The high concentration of the CPP-anti-tetA PNA and the high

and low concentrations of the CPP-anti-tetR PNA all cause significant inhibition of bacterial growth. For this reason, only the lower 15 μM concentration was used for further experiments. The average CFU/ml in each treatment group was compared to that of the untreated control using a student's t-test. ** = p <0.01. Error bars indicate +/- 1 standard deviation from the mean. 71
Figure 4.12 A nearly linear dose-dependent inhibition of bacterial growth was observed after treatment with increasing concentrations of the CPP. Controls treated with sterile water in volumes equal to those of the CPP treatments did not show growth inhibition. Statistical analysis was not performed because of the limited number of replicates, and because the statistical significance of the growth suppression was less important in this experiment than simply observing the trend of dose dependent growth inhibition. Error bars indicate +/- 1 standard deviation from the mean (log transformed values). 72
Figure 4.13 MIC microtiter plates, spectrophotometer absorbance readings, and MBC agar plates for each treatment group in the MIC/MBC pilot experiment. Bacteria were seeded in experimental wells at a concentration of 5 x 10^5/μl and incubated with serially diluted concentrations of tetracycline in conjunction with various CPP-PNA treatments. Results for the MICs were interpreted after 16-20 hours of incubation at 37 C˚, both visually and by taking a single absorbance reading of each well at 560 nm with a VersaMax spectrophotometer. Direct transfer of MIC plate well contents onto TSA was then performed and interpretation of the MBC was done after overnight incubation at 37 C˚. **A.** Control group treated with tetracycline only. **B.** Treatment with CPP-anti-tetA PNA and tetracycline. **C.** Treatment with CPP-anti-tetR PNA and tetracycline. **D.** Treatment with CPP-Control PNA and tetracycline and CPP only and tetracycline. Some wells on these plates were used for collection of data for a different experiment. Only the wells highlighted by colored boxes are pertinent to this dissertation. The recorded MICs and MBCs for each replicate are summarized in Table 4.5..... 80
Figure 4.14 MIC microtiter plates and MBC agar plates for each replicate of the MIC/MBC replicate experiments. **A.** Replicate 1. **B.** Replicate 2. **C.** Replicate 3. Bacteria were seeded in experimental wells at a concentration of 5 x 10^5/μl and incubated with serially diluted concentrations of tetracycline in conjunction with various CPP-PNA treatments. The MIC plates were incubated in a VersaMax spectrophotometer for 6-20 hours of incubation at 35 C˚ with absorbance readings taken every 15 minutes. The MIC was then interpreted both visually and by looking at growth curves plotted from the absorbance readings (see Figure 4.15). Direct transfer of MIC plate well content onto TSA was then performed and interpretation of the MBC was done after overnight incubation at 37 C˚. Yellow arrows indicate treatment with CPP-anti-TetR PNA and tetracycline, green arrows indicate treatment with CPP-anti-TetA PNA and tetracycline, blue arrows indicate treatment with CPP-Control PNA and tetracycline, red arrows indicate treatment with CPP alone and tetracycline, pink arrows indicate treatment with CPP-Sal-tsf PNA and tetracycline, and purple arrows indicate treatment with tetracycline only. The recorded MICs and MBCs for each replicate are summarized in Table 4.5..... 84
Figure 4.15 Serial spectrophotometer absorbance readings from the MIC microtiter plates for each treatment group in the MIC/MBC replicate experiments. The MIC plates were grown in the VersaMax microtiter plate reader at 35 ˚C for 17-18 hours. Absorbance readings at 560 nm were taken every 15 minutes after 30 seconds of shaking. Absorbance is indicated on the y-axis. The time in hours is indicated on the bottom x-axis of each set of graphs. The

color legend to the right indicates the tetracycline concentration (μg/ml) at which each growth curve was generated. The recorded MICs and MBCs for each replicate are summarized in Table 4.5. 91
Figure 4.16 The currently understood relationship between TetR protein function and *tetA* gene expression. **A.** Under normal conditions, the TetR protein dimer (green) binds a DNA dual operator region and prevents transcription of the *tetA* and *tetR* genes. **B.** When tetracycline (yellow) is present, it causes TetR to dissociate from the DNA, allowing for TetA and TetR production. 93
Figure 5.1 Simplified diagram of a 96-well plate set-up in which DT104 was grown with or without 8 μg/ml tetracycline for various lengths of time in order to detect upregulation of *tetA* expression in response to tetracycline. Bacteria were harvested for RNA stabilization and extraction, and RT-qPCR was performed to measure mRNA expression of the target *tetA* gene and a stably expressed reference gene, 16S. Expression of *tetA* mRNA relative to 16S mRNA was compared between treated and untreated cultures and among different time points. 104
Figure 5.2 Simplified diagram of a 96-well plate set-up in which DT104 was grown to examine the effect of various combinations of CPP-PNA, CPP only, and 8 μg/ml tetracycline on *tetA* expression. Bacteria were plated at a concentration of 5 x 10^5 CFU/ml in Mueller Hinton broth and cultured for 1 hour or 4 hours. Bacteria were harvested for RNA stabilization and extraction, and RT-qPCR was performed to measure mRNA expression of the target *tetA* gene and a stably expressed reference gene, 16S. Expression of *tetA* mRNA relative to 16S mRNA was compared among various treatment groups. 105
Figure 5.3 RT-qPCR tracings (top) and standard curve (bottom) generated to evaluate efficiency of the primer for the 16S gene. Total RNA was extracted from DT104 cultured in Mueller-Hinton broth and serial 10-fold dilutions of the RNA extract were done to make six standard samples with RNA concentrations of 100 ng, 10 ng, 1 ng, 100 pg, 10 pg, and 1 pg. RT-qPCR was done using SYBR green fluorescent dye as a detection method. In RT-qPCR, fluorescence increases over time with increasing amplification of the target DNA, generating a tracing for each PCR well. The top graph shows the PCR tracings generated for each standard solution. The samples were run in triplicate, so there are three tracings for each concentration of RNA template. The PCR cycle number at which a tracing crosses a fluorescence threshold is called the quantitation cycle or C_q. The greater the starting amount of RNA template, the further left the tracing, and the lower the C_q. The C_qs for the 100 ng and 1 pg samples are labeled. The C_q data is log transformed and plotted as a standard curve as shown in the lower graph, and the primer efficiency (E), coefficient of determination (R^2), and slope of the standard curve are calculated. An optimized qPCR assay ideally has E = 95-105%, R2 ≥ 0.980, and standard curve slope = -3.32.[11] 106
Figure 5.4 RT-qPCR tracings (top) and standard curve (bottom) generated to evaluate efficiency of the primer for the *tetA* gene. Total RNA was extracted from DT104 cultured in Mueller-Hinton broth and serial 10-fold dilutions of the RNA extract were done to make six standard samples with RNA concentrations of 100 ng, 10 ng, 1 ng, 100 pg, 10 pg, and 1 pg. RT-qPCR was done using SYBR green fluorescent dye as a detection method. In RT-qPCR, fluorescence increases over time with increasing amplification of the target DNA, generating a tracing for each PCR well. The top graph shows the PCR tracings generated for each standard solution. The samples were run in triplicate, so there are three tracings for each concentration of RNA template. The PCR cycle number at which a tracing crosses

a fluorescence threshold is called the quantitation cycle or C_q. The greater the starting amount of RNA template, the further left the tracing, and the lower the C_q. The C_qs for the 100 ng and 1 pg samples are labeled. The C_q data is log transformed and plotted as a standard curve as shown in the lower graph, and the primer efficiency (E), coefficient of determination (R^2), and slope of the standard curve are calculated. An optimized qPCR assay ideally has E = 95-105%, R2 ≥ 0.980, and standard curve slope = -3.32.[11] 107

Figure 5.5 Time-related PCR tracings showing *tetA* expression and 16S expression in cultures of DT104 incubated with or without tetracycline for **A.** ~18 hours, **B.** 4 hours, or **C.** 1 hour. Note the fairly stable expression of the 16S reference gene in both the untreated (dark orange) and tetracycline-treated (dark purple) cultures. Relative upregulation of *tetA* expression compared to 16S expression, indicated by a left shift of the light purple curve, was expected in cultures treated with tetracycline. This effect was only obvious at the 1 hour time point, suggesting a rapid and short-lived upregulation of gene transcription. 109

Figure 5.6 Summary of results presented in Figure 5.5. Purple bars show relative *tetA* expression in DT104 cultures treated with 8 μg/ml tetracycline for 1 hour, 4 hours, or 18 hours compared to untreated cultures (orange bar). Total RNA was extracted and gene expression was measured using RT-qPCR. Expression of *tetA* relative to the reference16S gene was calculated for each time point using the Pfaffl method to obtain an expression ratio. The ratios were $\log_2$ transformed to allow for better visualization of relative gene expression. The data indicate a rapid upregulation of *tetA* expression within the first hour after exposure to tetracycline that then dissipates over the next several hours. 110

Figure 5.7 PCR tracings of *tetA* and 16S expression in various treatment groups cultured with different combinations of CPP-PNA, CPP only, and/or tetracycline for 1 hour. In all treatment groups, DT104 at a concentration of 5 x 10^5 CFU/ml was cultured in Mueller-Hinton broth in 96-well microtiter plates. After incubation with treatments for 1 hour, total RNA was stabilized and extracted, and RT-qPCR was performed to amplify *tetA* mRNA and 16S mRNA (reference gene). Expression of *tetA* in each treatment group was calculated with the Pfaffl method. The two black tracings to the far right of each graph are tracings for the non-template control for each primer. 114

Figure 5.8 PCR tracings of *tetA* and 16S expression in various treatment groups cultured with different combinations of CPP-PNA, CPP only, and/or tetracycline for 4 hours. In all treatment groups, DT104 at a concentration of 5 x 10^5 CFU/ml was cultured in Mueller-Hinton broth in 96-well microtiter plates. After incubation with treatments for 4 hours, total RNA was stabilized and extracted, and RT-qPCR was performed to amplify *tetA* mRNA and 16S mRNA (reference gene). Expression of *tetA* in each treatment group was calculated with the Pfaffl method. The two black tracings to the far right of each graph are tracings for the non-template control for each primer. 117

Figure 5.9 PCR tracings from one replicate of 4 hour treatment of DT104 with different combinations of CPP-PNA, CPP only, and/or tetracycline for 4 hours. DT104 at a concentration of 5 x 10^5 CFU/ml was cultured in Mueller-Hinton broth in 96-well microtiter plates. After incubation with treatments for 4 hours, total RNA was stabilized and extracted, and RT-qPCR was performed to amplify *tetA* mRNA and 16S mRNA (stably expressed reference gene). Expression of *tetA* in each treatment group was calculated with the Pfaffl method. Three of these replicates were set up, but only one led to successful amplification of mRNA, and even this replicate showed some issues with expression stability. These RNA samples were kept in frozen storage at -20 ˚C for approximately three

months before RT-qPCR, which may have caused sample degradation. The two black tracings to the far right of each graph are tracings for the non-template control for each primer. 119
Figure 5.10 Summary of results presented in Figure 5.7, Figure 5.8, and Figure 5.9. Bars show *tetA* expression in cultures treated with tetracycline and CPP-anti-tetA PNA relative to that of cultures treated only with tetracycline, or with tetracycline and CPP alone at 1 hour and 4 hours. DT104 at a concentration of 5 x 10^5 CFU/ml was cultured in Mueller-Hinton broth in 96-well microtiter plates. After incubation with treatments for 1 hour or 4 hours, total RNA was stabilized and extracted, and RT-qPCR was performed to amplify *tetA* mRNA and 16S mRNA (reference gene). Relative *tetA* expression compared to the culture treated with tetracycline alone was calculated with the Pfaffl method. The calculated expression ratios were $\log_2$ transformed to allow for better visualization of relative gene expression. Patterned bars show results for 1 hour incubation (single replicate), and solid bars show results for 4 hour incubation (average of two replicates). Treatment with tetracycline and the CPP alone (red bars) did not cause a consistent difference in gene expression relative to treatment with tetracycline alone (purple bars). At the 1 hour time point, expression was slightly relatively downregulated, and at the 4 hour time point expression was slightly relatively upregulated. By contrast, treatment with tetracycline and the CPP-anti-tetA PNA (green) caused notable relative downregulation of *tetA* mRNA expression at both the 1 hour and 4 hour time points. 121
Figure 5.11 PCR tracings of *tetA* and 16S expression in DT104 among cultures treated for 1 hour with various combinations of CPP-anti-tetR PNA, CPP-anti-tetA PNA, and tetracycline. In all treatment groups, DT104 at a concentration of 5 x 10^5 CFU/ml was cultured in Mueller-Hinton broth in 96-well microtiter plates. After incubation with treatments for 1 hour, total RNA was stabilized and extracted, and RT-qPCR was performed to amplify *tetA* mRNA and 16S mRNA (reference gene). Expression of *tetA* in each treatment group was calculated with the Pfaffl method. 123
Figure 5.12 PCR tracings of *tetA* and 16S expression in DT104 among cultures treated for 1 hour with various combinations of CPP-anti-tetR PNA and tetracycline. In all treatment groups, DT104 at a concentration of 5 x 10^5 CFU/ml was cultured in Mueller-Hinton broth in 96-well microtiter plates. After incubation with treatments for 1 hour, total RNA was stabilized and extracted, and RT-qPCR was performed to amplify *tetA* mRNA and 16S mRNA (reference gene). Expression of *tetA* in each treatment group was calculated with the Pfaffl method. 125
Figure 5.13 PCR tracings of *tetA* and 16S expression in DT104 among cultures treated for 4 hours with various combinations of CPP-anti-tetR PNA, CPP-anti-tetA PNA, and tetracycline. In all treatment groups, DT104 at a concentration of 5 x 10^5 CFU/ml was cultured in Mueller-Hinton broth in 96-well microtiter plates. After incubation with treatments for 1 hour, total RNA was stabilized and extracted, and RT-qPCR was performed to amplify *tetA* mRNA and 16S mRNA (reference gene). Expression of *tetA* in each treatment group was calculated with the Pfaffl method. 127
Figure 5.14 PCR tracings of *tetA* and 16S expression in DT104 among cultures treated for 4 hours with various combinations of CPP-anti-tetR PNA and tetracycline. In all treatment groups, DT104 at a concentration of 5 x 10^5 CFU/ml was cultured in Mueller-Hinton broth in 96-well microtiter plates. After incubation with treatments for 4 hours, total RNA was stabilized and extracted, and RT-qPCR was performed to amplify *tetA* mRNA and 16S

mRNA (reference gene). Expression of *tetA* in each treatment group was calculated with the Pfaffl method..... 129
Figure 5.15. Summary of results shown in Figure 5.11, Figure 5.12, Figure 5.13, and Figure 5.14. Presented is *tetA* expression in cultures treated with CPP-anti-tetR PNA with or without tetracycline, relative to that of cultures treated with tetracycline and CPP-anti-tetA PNA, or only with tetracycline for **A.** 1 hour or **B.** 4 hours. DT104 at a concentration of 5 x 10^5 CFU/ml was cultured in Mueller-Hinton broth in 96-well microtiter plates. After incubation with treatments for 1 hour or 4 hours, total RNA was stabilized and extracted, and RT-qPCR was performed to amplify *tetA* mRNA and 16S mRNA (reference gene). Relative *tetA* expression compared to the culture treated with tetracycline alone was calculated with the Pfaffl method. The calculated expression ratios were $\log_2$ transformed to allow for better visualization of relative gene expression. Solid bars indicate treatment with CPP-anti-tetR PNA and tetracycline. Patterned bars indicate treatment with only CPP-anti-tetR PNA. The same major observation was evident at both time points, namely, that the expected upregulation of *tetA* expression in response to treatment with CPP-anti-tetR PNA occurred only when tetracycline was absent. Statistical analysis was not done due to insufficient data points. 130
Figure 6.1 Survival curves for each treatment group in the first replicate of a study to test the efficacy of an experimental treatment for systemic salmonellosis in a mouse model. Female BALB/c mice (n = 5/group) were orally infected with tetracycline-resistant *Salmonella enterica* ssp. *enterica* serovar Typhimurium DT104 and left untreated for three days to allow for development of clinical disease. Treatment was started on day 3 PI and continued for seven days. Treatments included a combination of tetracycline and CPP-anti-tetA PNA, a cell-penetrating peptide-peptide nucleic acid conjugate that suppresses expression of the TetA tetracycline efflux pump, as well as appropriate controls (see text for details). The x-axis of each plot indicates the number of days PI. The y-axis shows S(t), which is the probability of surviving to time (t) where (t) is the number of days PI. Brief captions under each plot indicate the treatment given. All groups had two or three mice clear the infection and survive to the end of the study except for the group treated with tetracycline and the CPP-Control PNA. The CPP-Control PNA has a nonsense nucleic acid sequence designed to be a negative control for PNA action. Except for this latter group, no obvious differences in survival were noted upon visual examination of the survival plots..... 148
Figure 6.2 Survival curves for each treatment group in the second replicate of a study to test the efficacy of an experimental treatment for systemic salmonellosis in a mouse model. Female BALB/c mice (n = 5/group) were orally infected with tetracycline-resistant *Salmonella enterica* ssp. *enterica* serovar Typhimurium DT104 and left untreated for three days to allow for development of clinical disease. Treatment was started on day 3 PI and continued for seven days. Treatments included a combination of tetracycline and CPP-anti-tetA PNA, a cell-penetrating peptide-peptide nucleic acid conjugate that suppresses expression of the TetA tetracycline efflux pump, CPP-Sal-tsf, a PNA targeting expression of an essential bacterial gene, as well as appropriate controls (see text for details). The x-axis of each plot indicates the number of days PI. The y-axis shows S(t), which is the probability of surviving to time (t) where (t) is the number of days PI. Brief captions under each plot indicate the treatment given. In this replicate, all mice progressed to severe clinical illness resulting in termination within 10 days PI, except for two mice in the group treated with tetracycline alone. These two mice went through a period of illness, but cleared the

infection and appeared clinically healthy by the end of the study. Except for this latter group, no obvious differences in survival were noted upon visual examination of the survival plots. 152
Figure 6.3 Survival curves for each treatment group generated with combined data from both replicates of a study to test the efficacy of an experimental treatment for systemic salmonellosis in a mouse model. Only the treatment groups common to both replicates of the experiment were included. Female BALB/c mice (n = 5/group in each replicate) were orally infected with tetracycline-resistant *Salmonella enterica* ssp. *enterica* serovar Typhimurium DT104 and left untreated for three days to allow for development of clinical disease. Treatment was started on day 3 PI and continued for seven days. Treatments included a combination of tetracycline and CPP-anti-tetA PNA, a cell-penetrating peptide-peptide nucleic acid conjugate that suppresses expression of the TetA tetracycline efflux pump, as well as appropriate controls (see text for details). The x-axis of each plot indicates the number of days PI. The y-axis shows S(t), which is the probability of surviving to time (t) where (t) is the number of days PI. Brief captions under each plot indicate the treatment given. The two observations that stand out upon visual examination of this combined data are 1) overall survival was worst in the group treated with a combination of tetracycline and the CPP-Control PNA and 2) overall survival was best (50%) in the group treated only with tetracycline. All of the other groups had an overall survival of 20%-30%. 155
Figure 6.4 Dot plots showing the number of *Salmonella* CFU/ml grown from internal organs of mice in a study to test the efficacy of an experimental treatment for systemic salmonellosis. Female BALB/c mice (n = 5/group x 2 replicates) were orally infected with tetracycline-resistant *Salmonella enterica* ssp. *enterica* serovar Typhimurium DT104 and left untreated for three days to allow for development of clinical disease. Treatment was started on day 3 PI and continued for seven days. Treatments included a combination of tetracycline and CPP-anti-tetA PNA, a cell-penetrating peptide-peptide nucleic acid conjugate that suppresses expression of the TetA tetracycline efflux pump, as well as appropriate controls (see text for details). Upon termination, portions of liver, spleen, small intestine, and large intestine were collected and frozen at -80 ˚C until they could be thawed, homogenized, serially diluted, and cultured on XLT-4 agar for CFU/ml quantification. Some groups do not have 10 data points because not all samples had a positive culture result. Treatment groups: 1) Tetracycline + CPP-anti-tetA PNA, 2) CPP-anti-tetA PNA, 3) Tetracycline + CPP-Control PNA, 4) CPP-Control PNA, 5) Tetracycline, 6) CPP, 7) Phosphate buffered saline. No statistical differences were found among treatment groups using one-factor ANOVA with significance set as $p < 0.05$. 157

List of Tables

Table 3.1 Dilutions of six OMCs were prepared in antibiotic-free DMEM based off the MICs for each compound against *M. bovis* BCG or *M. avium* A5. These dilutions were then added to cultures of J774A.1 cells at the concentrations shown in this table and plates were incubated for 24, 48, or 72 hours before measurement of cellular metabolism to assess cytotoxicity. 24

Table 3.2 Iridium concentrations measured in cell culture samples treated with 10 μg/ml or 100 μg/ml Compound 1 for 24 or 48 hours. S = supernatant from cell lysate. M = treated medium. 41

Table 4.1 Zones of resistance (mm) and susceptibility of eight strains of *Salmonella* after Kirby-Bauer susceptibility testing with 12 conventional antibiotics. The box where *S.* Typhimurium DT104 crosses with tetracycline is yellow to highlight the tetracycline-resistance of this organism. The mechanism of resistance is a tetracycline efflux pump, the gene for which was chosen as the target for experiments in reversing antibiotic resistance using PNAs. 54

Table 4.2 Primer sequences used to confirm the DT104 serotype of the *Salmonella* organism chosen for experimentation with PNAs. InvA is a gene common to all *Salmonella* species and was used as a positive control. ST104 is a prophage sequence unique to *S.* Typhimurium DT104 (DT104). The expectation was that ST104 DNA would be amplified from the laboratory stock bacterial strain presumed to be DT104, but not from the non-DT104 strain identified as NalR. 55

Table 4.3 Primer and DNA template combinations in PCR reaction mixes prepared for confirmation of the DT104 serotype of the *Salmonella* strain chosen for experiments with PNAs. 56

Table 4.4 Description of the PNA sequences chosen for experimental manipulation of the response of DT104 to tetracycline. The start codon for each gene is highlighted in green. In order to facilitate crossing of the cell membrane, the PNAs were bound to a cell-penetrating peptide, $(KFF)_3K$, by an O-linker. 58

Table 4.5 Summary of the tetracycline MICs and MBCs obtained for all treatment groups in each replicate of the MIC/MBC experiments. Some MICs were difficult to visually interpret due to turbidity imparted by the PNAs, so the absorbance data from spectrophotometer measurements in replicates 1-3 is considered the best way to interpret MICs. Treatment with the CPP-anti-tetA PNA and the CPP-Sal-tsf PNA consistently decreased both the MIC and MBC relative to tetracycline alone. Treatment with the CPP-anti-tetR PNA and the CPP without PNA substantially decreased the MIC, but not the MBC. Treatment with the CPP-Control PNA consistently caused a decrease in the MIC, but the MBC could not be interpreted due to skips in the growth pattern. See text for additional comments. 74

Table 5.1 The effect of these peptide nucleic acids and the cell penetrating peptide on *tetA* expression in DT104 was analyzed by RT-qPCR. Details of PNA design are in Chapter 4. 100

Table 5.2 Primer sequences used to evaluate *tetA* expression in DT104 treated with various combinations of CPP-PNAs, CPP only, and tetracycline. Expression of *tetA* mRNA was calculated relative to expression of 16S RNA, which was stably expressed under the various treatment conditions. 101

Table 6.1 Description of the peptide nucleic acid and cell penetrating peptide sequences used concurrently with tetracycline (CPP-anti-tetA PNA, CPP-Control PNA) or alone (CPP-Sal-tsf) to experimentally treat 6-to-8-week-old female BALB/c mice orally infected with *Salmonella enterica* ssp. *enterica* serovar Typhimurium DT104. 140
Table 6.2 List of treatment groups in the first replicate of a study to evaluate the efficacy of an experimental treatment for oral *Salmonella* infection in 6-8-week-old female BALB/c mice. The CPP-anti-tetA PNA is designed to inhibit expression of the TetA tetracycline efflux pump, which imparts resistance to tetracycline. The CPP-Control PNA has a mismatched nucleotide sequence and was designed for use as a negative control. Treatments were begun on day 3 PI and continued for seven days. Treatments were administered IP once every 24 hours. 142
Table 6.3 List of treatment groups in the second replicate of a study to evaluate the efficacy of an experimental treatment for oral *Salmonella* infection in 6-8-week-old female BALB/c mice. The CPP-anti-tetA PNA is designed to inhibit expression of the TetA tetracycline efflux pump, which imparts resistance to tetracycline. The CPP-Control PNA has a mismatched nucleotide sequence and was designed for use as a negative control. The CPP-Sal-tsf PNA targets expression of an essential bacterial gene involved in stabilization of new peptides during bacterial protein translation. Treatments were begun on day 3 PI and continued for seven days. Treatments were administered IP once every 24 hours. 143
Table 6.4 Progression of infection in groups of mice orally infected with three different concentrations of *Salmonella enterica* ssp. *enterica* serovar Typhimurium DT104. Mice were infected to determine an optimal infectious dose of DT104 for future use in experiments that required a model of systemic salmonellosis. The goal was to find a dose that was not acutely lethal, but that caused clinical disease in all mice within 2-3 days so that experimental treatments could be initiated after manifestation of clinical illness. This was to try and more closely mimic disease progression and intervention in clinical practice. 145

List of Abbreviations

AMP	antimicrobial peptide
ASO	antisense oligonucleotide
BSL	biosafety level
Cl	chlorine
Cp	cyclopentadiene
Cp*	pentamethylcyclopentadiene
CPP	cell-penetrating peptide
C_q	quantitation cycle
DNA	deoxyribonucleic acid
DMSO	dimethyl sulfoxide
DT104	*Salmonella enterica* ssp. *enterica* serovar Typhimurium DT104
F	phenylalanine
gDNA	genomic deoxyribonucleic acid
HIV-1	human immunodeficiency virus-1
IP	intraperitoneal
Ir	iridium
IV	intravenous
K	lysine
LNA	locked nucleic acid
L-pg	L-phenylglycine
MBC	minimum bactericidal concentration
MDR	multidrug resistant
MIC	minimum inhibitory concentration
MPO	methylphosphonate
mRNA	messenger ribonucleic acid
MTS	3-(4,5-dimethylthiazol-2-yl)-5-(3-carboxymethoxyphenyl)-2-(4-sulfophenyl)-2H-tetrazolium)
OMC	organometallic compound
PCR	polymerase chain reaction
PI	post-infection
PMO	phosphorodiamidate morpholino oligomer
PNA	peptide nucleic acid
PS-ODN	phosphorothioate oligonucleotides
Pt	platinum
RFU	relative fluorescence units
Rh	rhodium
RNA	ribonucleic acid
RT-qPCR	reverse transcriptase quantitative polymerase chain reaction
R-type ACSSuT	resistance type ampicillin, chloramphenicol, streptomycin, sulfonamides, tetracycline
SGI1	*Salmonella* genomic island 1
TetA	tetracycline resistance protein class A
TetR	tetracycline resistance regulator protein
tsf	translation elongation factor
XDR	extensively drug resistant

Attributions

Chapter 3.
The organometallic compounds used for the experiments were primarily synthesized by Dr. George Karpin, with some contribution from other Virginia Tech Department of Chemistry graduate students, under the mentorship of Dr. Joseph Merola. I designed and carried out all of the experiments with J774A.1 murine macrophage-like cells, wrote the manuscript, and generated the figures.

Chapter 4.
I was the major contributor to experimental design and carried out the bulk of the minimum inhibitory concentration experiments with guidance and occasional physical assistance from Dr. Nammalwar Sriranganathan. I wrote the manuscript and generated the figures.

Chapter 5.
I was the major contributor to experimental design with guidance from Dr. Nammalwar Sriranganathan. I performed the experiments, wrote the manuscript, and generated the figures.

Chapter 6.
I was the primary contributor to experimental design with guidance from Dr. Nammalwar Sriranganathan. Both of us were nearly equally involved in the physical execution of the experiments. I wrote the manuscript and generated the figures.

1 Introduction

The work described in this dissertation was ordered toward developing new approaches for treatment of antibiotic resistant bacterial infections. One set of experiments focused on the cytotoxicity and eukaryotic cellular penetration of novel organometallic compounds (OMCs) that show potential promise as antimycobacterial drugs. The remaining experiments involved use of antisense molecules called peptide nucleic acids (PNAs) to suppress expression of essential and antibiotic resistance genes in a drug-resistant strain of *Salmonella*.

Specific aims of this research:

1. Investigate the eukaryotic cytotoxicity of several novel OMCs that showed antimycobacterial activity *in vitro*, evaluate the antimycobacterial activity of one of these compounds in infected cell culture, and assess cellular penetration capabilities of that compound.
2. Evaluate the *in vitro* efficacy of PNAs targeting tetracycline resistance genes in *Salmonella enterica*, ssp. *enterica* serovar Typhimurium DT104 (DT104) by determining the effect of PNA treatment on the tetracycline minimum inhibitory concentration (MIC) and minimum bactericidal concentration (MBC).
3. Perform molecular analysis of the mechanism of action of the PNAs through use of reverse transcriptase-quantitative PCR (RT-qPCR).
4. Develop a mouse model of oral DT104 infection and use the model for testing *in vivo* efficacy of PNAs targeting bacterial essential and antibiotic resistance genes.

The dissertation is presented in manuscript format in anticipation of submission of various portions of the work for publication in scientific journals. Chapters 3, 4, 5, and 6 contain the descriptions of the experimental work performed to address the specific aims listed above, and each of these chapters is organized to include Introduction, Materials and Methods, Results, Discussion and Conclusions, and References sections. The aim was to minimize the amount of effort needed to prepare these chapters as standalone manuscripts for publication in the future. Chapter 2 is a literature review section that provides historical context and broad background information not covered in depth in the subsequent chapters. Effort was made to avoid unnecessary overlap between the literature review in Chapter 2 and the literature review information provided in the Introduction and Discussion sections of each of the experimental chapters, but there is some

unavoidable redundancy. Chapter 7 provides a brief overarching discussion about the dissertational research as a whole and states final conclusions and recommendations for future work incorporating information from all of the preceding chapters.

2 Literature review

2.1 Brief history of antibiotic discovery and early observations of antibiotic resistance

Since the fortuitous accidental discovery and subsequent isolation of penicillin in the first half of the 20th century[1-2] developed society has enjoyed a relative respite from the potentially devastating effects of bacterial infection. However, within just a few years of introducing penicillin for human use it was already evident that bacteria could make adjustments in response to exposure to antibiotic compounds, rendering the infectious organisms less susceptible to the drugs. The first clinical administration of penicillin in a human occurred in 1941, in Great Britain during World War II. During those first few months of experimental clinical treatments, several near miraculous recoveries were observed in patients diagnosed with what were previously considered to be incurable diseases.[3] However, by the end of the decade scientific articles discussing the therapeutic use of penicillin for bacterial endocarditis were already describing observations about how the efficacy of the dose was related to the resistance level of the cultured organisms, and recommending an increase in baseline doses.[4-5]

As new classes of antibiotics were discovered and introduced into common use over the mid- to late twentieth century the same types of patterns were observed. Bacterial resistance to each new drug usually emerged within 20 years, and sometimes in less than 2 years.[6] Antibiotic resistance is now considered one of the most serious health issues of this generation and could potentially lead to catastrophic disease outbreaks if alternative therapies are not discovered and applied soon. There is a global call for action to address this looming crisis.[7-9]

There are multiple management practices that can be undertaken to decrease the spread of antibiotic resistance, such as adherence to good basic hygiene, avoidance of over-prescribing or inappropriate prescribing of antibiotics in healthcare settings, and limiting the amount of antibiotics that are unnecessarily used in a preventative fashion in food production.[8] However, while compliance with good antibiotic stewardship may help slow the rate of antibiotic resistance development, such efforts alone will not eliminate the problem. There is also a pressing need for development of new antibacterial drugs.

2.2 Brief review of mechanisms of antibiotic resistance

As a refresher, bacteria can develop the capability to resist antibiotics through mutation or by acquiring non-native genetic material through horizontal gene transfer. General mechanisms of antibiotic resistance can mostly be grouped into four major categories: i) enzymatic modification of the antibiotic molecule to render it less functional or inactive, ii) impedance of the antibiotic's ability to achieve therapeutic intracellular concentrations, either by activating efflux mechanisms or by altering the cellular membrane to reduce drug infiltration, iii) modification of the antibiotic target molecule to decrease binding affinity, and iv) alteration of the metabolic processes of the cell to evade antibiotic action. Discussion of all the different types of antibiotic resistant bacterial species, and the details of the numerous specific antibiotic resistance mechanisms which they employ is beyond the purview of this work. For a clear and detailed recent review of antibiotic resistance mechanisms, the reader is directed to the 2016 article by Munita and Arias.[10]

2.3 Call for new antimicrobial drugs that circumvent known mechanisms of antibiotic resistance

Just as there are only a few main mechanisms of antibiotic resistance, the mechanisms of action of most of the clinically available antibiotic drugs also fall within just a few broad categories: i) interference with bacterial cell wall synthesis (e.g. beta-lactams), ii) disruption of folate synthesis (e.g. sulfonamides), iii) inhibition of enzymes involved in nucleic acid synthesis (e.g. quinolones), and iv) inhibition of ribosomes involved in protein translation (e.g. tetracyclines, macrolides, aminoglycosides).[11] While there is a benefit to developing new antibiotic drugs that are derivatives of existing medications, specifically, a relatively high chance of efficacy, this approach also runs the risk of bacteria becoming rapidly resistant to the new drugs because of their similarity to older platforms.[12] Therefore, an exciting new horizon to pursue is that of antibacterial molecules that are radically different from current clinically available antibiotics and that attack with new mechanisms of action. The work in this dissertation sought to take one or two steps further along the latter path of action, by examining the antimicrobial potential of organometallic compounds (OMCs) and antisense oligonucleotide (ASO) molecules that are structurally distinct from conventional antibiotics.

2.4 Organometallic compounds as possible antimicrobials

2.4.1 Characteristics of OMCs that allow them to interact with biological molecules

Organometallic compounds (OMCs) are molecules with at least one chemical bond between a carbon atom and a metal atom.[13] While historically used for catalysis in non-biological fields, these compounds are currently attractive candidates for biochemical and biopharmaceutical research because of their inherent structural modifiability. The metal centers of these complexes can have higher coordination numbers than most purely organic molecules, allowing for binding of multiple and diverse ligands. These ligands can be varied to alter chemical characteristics of the compound, such as hydrophobicity, acidity, and cytotoxicity. This ability to rapidly "tune" OMCs allows for deep exploration into structure-activity relationships between the compounds and possible biological targets.[14] In addition, the metal centers of the molecules are electrophiles and have the potential to react directly with biological molecules, thus causing metal-specific mechanisms of action that may either be the sole effect or work in conjunction with actions of the attached ligands.[15-16] Some basic biological applications of these compounds include enzyme inhibition,[17] organelle-specific staining,[18] and facilitation of cellular uptake of foreign molecules.[19] Of primary interest for this dissertation is the use of OMCs in medicinal therapy.

2.4.2 Initial medical use of OMCs as antineoplastics

A great deal of recent research into the medicinal properties of OMCs focuses on anti-neoplastic properties of these compounds.[20-23] The initial impetus for this branch of research was the discovery and characterization of the anti-proliferative platinum (Pt) compound now known as cisplatin.[24-25] A database search for cisplatin and related compounds yields tens of thousands of hits, indicating the importance of these drugs. However, many of the early inorganic metal-based antineoplastic drugs and their derivatives act by nonspecifically binding DNA, especially in fast-growing cells.[15] This frequently leads to side effects such as vomiting, ototoxicity, nephrotoxicity, and neurotoxicity which can vary from moderate to severely debilitating.[26] Organometallic compounds are promising alternatives for antineoplastic research because their structural flexibility may allow design of medications with fewer off-target toxic effects.[27]

2.4.3 Potential use of OMCs as antimicrobials

As the threats of antibiotic resistance became more evident it was natural that researchers also began exploring antimicrobial properties of OMCs. The same type of chemical tuning that makes OMCs attractive as antineoplastic drugs can be applied to identifying new antimicrobial drugs. One approach is to derivatize known antimicrobial drugs with a metal element, thus leading to enhanced or novel effects.[28] Some examples of this concept that have shown success in a laboratory setting include ferrocenyl derivatization of the antimalarial drug chloroquine;[29] complexation of the antimalarial drug sulfadoxine with ruthenium, rhodium, and iridium compounds;[30] and binding of isoniazid, a tuberculosis drug, to cyanoferrate(II).[31] Even more exciting is the testing of novel OMCs that are completely different from previous antibacterial drugs. Researchers have tested unique OMCs against various bacterial species such as *Staphylococcus aureus*, *Streptococcus pyogenes*, *Acinetobacter baumanii*, *Enterococcus faecium*, *Escherichia coli*, and *Pseudomonas aeruginosa*, and have found compounds with minimum inhibitory concentrations that are similar to or lower than conventional antibiotics.[32-35] Recently Karpin et al.[36] described the minimum inhibitory concentrations (MIC) of multiple OMCs against several nontuberculous *Mycobacterium* species, and this family of compounds is the focus of eukaryotic cytotoxicity experiments that make up part of this dissertation. Additional background about the structure of these compounds, the possible target organisms, and the type of experiments done is provided in Chapter 3.

A vast amount of the research into both antineoplastic and antibacterial properties of OMCs comes from the laboratory of Peter J. Sadler. The reader is encouraged to thoroughly explore his works for additional information about this field of research.

2.5 Antisense oligonucleotides (ASOs) as possible antimicrobials

2.5.1 Definition of antisense technology and brief history

Antisense technology is the use of synthetic nucleic acid molecules to bind a target ribonucleic acid (RNA) sequence, usually an mRNA sequence, to modulate or suppress gene expression.[37] For this review chapter, the term is used specifically to refer to a mechanism of inhibition involving direct complementary binding between an antisense oligomer (ASO) and its target RNA sequence, resulting either in steric hindrance of ribosomal binding to the mRNA, and thus inhibition of protein translation, or in activation of an endonuclease such as RNase H to degrade the ASO-RNA

complex.[38] Other types of gene silencing technologies such as RNA interference (RNAi), which operates by a more complex multi-step mechanism,[39] are not reviewed here.

The property of antisense inhibition in bacteria is actually a natural one, with examples in prokaryotes first described in the literature in 1981,[40-41] followed by the discovery of several more within a few years.[42] More and more examples of bacterial mRNA regulation by naturally-occurring antisense RNAs were discovered over the ensuing decades, and this is still an active area of investigation in biological research.[43] This chapter will now focus on synthetic ASOs.

Interestingly, what is likely the earliest use of synthetic antisense technology was described by Paterson et al. in 1977,[44] prior to the reports of naturally occurring antisense RNAs. Paterson's laboratory showed that binding a recombinant DNA molecule to a complementary mRNA sequence in a cell-free system inhibited expression of the known β-globin protein product of the mRNA. Not long after that, in 1978, Stephenson and Zamecnik showed that a synthetic oligodeoxynucleotide could inhibit translation of Rous sarcoma virus RNA in a cell-free environment.[45] Over the next several decades researchers enthusiastically pursued the concept that one type of nucleotide molecule binding to another could affect gene expression. It was demonstrated that in transgenic petunias the constitutive expression of anti-sense RNA complementary to the gene for chalcone synthase, an enzyme critical to floral pigmentation, resulted in decreased mRNA levels for the enzyme and a white (nonpigmented) phenotype.[46] Injection of *Drosophila melanogaster* (fruitfly) embryos with antisense RNA complementary to the Kruppel (Kr) gene, which is required for normal body segmentation, resulted in the embryos developing into Kr-inhibited mutants.[47] On paper, at least, it seemed that scientific researchers had hit on a method that would allow an easy tailored approach to genetic modulation that could address almost any type of disease. However, as with most new discoveries in the biological sciences, the situation is not as simple as it may have first appeared.

A major obstacle in the use of antisense RNA to inhibit gene expression is the susceptibility of the molecules to degradation by nucleases. Most prokaryotic mRNA transcripts in natural systems have half-lives of only a few seconds to an hour, with most in the range of a few minutes.[48-49] Artificial antisense RNAs introduced into living systems are subject to the same degradation

mechanisms as naturally-occurring mRNAs, so they do not exert their effects for long if there is no intervention to prolong their availability for binding to the target nucleic acid. Initial efforts to address this difficulty in bacterial model systems mostly involved creating copy DNA (cDNA) that coded for the antisense sequence of interest and inserting it a plasmid within the bacterium, so that the ASO was constitutively expressed.[50] While useful on a small scale for evaluating individual effects of one or several ASOs, such an approach is cumbersome and does not address the inherent challenge of molecular instability. The desire for more stable ASOs with improved binding capabilities prompted research into chemical modifications to antisense molecule backbones that would allow for exogenous synthesis of ASOs for introduction into various experimental systems.[51]

2.5.2 Major types of modified ASOs under investigation as possible antimicrobials

One way to modify the antisense molecule is to introduce chemical variations into the classic DNA/RNA sugar-phosphate backbone.[38,52-53] Examples of this technique include methylphosphonates (MPOs), in which one nonbridging oxygen molecule in the phosphate group is replaced with a methyl group, and phosphorothioates (PS-ODNs) in which one nonbridging oxygen is replaced with a sulfur.[52] Another option is to synthesize molecules that can bind DNA or RNA by Watson-Crick base-pairing but have a non-sugar-phosphate backbone. Examples include phosphorodiamidate morpholino oligomers (PMOs) in which a morpholine ring replaces the sugar molecule of the backbone,[54] locked nucleic acids (LNAs) in which an oxygen and a carbon in the ribose sugar ring are bridged with a methylene linkage to form a bicyclic structure,[55] and peptide nucleic acids (PNAs) in which the sugar-phosphate backbone is entirely replaced by a peptide backbone.[56]

2.5.3 Focus of this research on PNAs

The research presented in part of this dissertation investigated potential antimicrobial use of PNAs. These are linear, achiral, uncharged molecules consisting of nucleosides (e.g. cytosine, adenine) bound to an N-(2-aminoethyl)-glycine backbone. These molecules were developed by Nielsen et al. and first described in the early 1990s.[57-58] They have several qualities that make them attractive as potential antisense drug candidates. For one thing, they form unusually stable bonds with complementary RNA because the neutral backbone eliminates the negative repulsion that occurs

between natural nucleic acid molecules, which have anionic phosphate groups as part of the backbone.[59] Like the other ASOs listed above, they are resistant to degradation by normal cellular machinery because the atypical backbone is not recognized by nucleases.[60] The fact that they are achiral means that there is no risk of one diastereomer of a chiral center having different qualities than the other, as is the case for PS-ODNs.[61] Their specificity for the nucleic acid target raises the possibility of designer drugs that precisely eliminate only the intended pathogen without causing off-target effects.[62]

2.5.4 Examples of antibacterial effects of PNAs

There are multiple reports indicating that PNAs show promise as antibacterial agents. A PNA that binds a functional site of rRNA in *E. coli* in a cell-free transcription/translation system inhibited protein translation in a manner similar to that of the conventional antibiotic tetracycline.[63] A PNA designed to bind the 4.5S RNA portion of the *E. coli* Signal Recognition Particle (SRP), which transports proteins and cell membrane components to the plasma membrane, caused displacement of the FfH protein portion of the SRP and inhibited bacterial growth.[64] Peptide nucleic acids designed to inhibit the essential *groEL* gene were able to cause selective growth inhibition of the oral pathogenic bacteria *Porphyromonas gingivalis* and *Aggregatibacter actinomycetemcomitans* in mixed bacterial culture.[65] *Pseudomonas aeruginosa* growth was significantly inhibited by PNAs targeting the essential *acpP* (involved in fatty acid synthesis) and *ftsZ* (involved in cell division) genes.[66] There is also the possibility of repurposing conventional antibiotics by restoring bacterial susceptibility using PNAs. A PNA targeting expression of β-lactamase expression in antibiotic-resistant *E. coli* partially restored bacterial cefotaxime susceptibility.[67] Methicillin-resistant *Staphylococcus aureus* (MRSA) was re-sensitized to the conventional antibiotic oxacillin *in vitro* by treatment with a PNA targeting the resistance gene *mecA*.[68]

2.5.5 Disadvantages of PNAs

While PNAs offer an exciting option as possible candidates for antimicrobial therapy, they are not without disadvantages. Importantly, they do not effectively diffuse across phospholipid membranes on their own, and generally require a carrier molecule to reach the intended intracellular target.[69-71] Short amino acid sequences called cell-penetrating peptides (CPPs), are common choices, especially the cationic peptide KFFKFFKFFK, which is comprised of lysine (K)

and phenylalanine (F) residues. This choice of CPP is based on the report of its membrane permeabilizing effects published by Vaara and Porro.[72] However, this CPP has drawbacks of its own. The membrane permeabilization it causes is nonspecific and inconsistent among bacterial species, and also can potentially affect the phospholipid membranes of eukaryotic host cells.[73-74] This could negatively counteract the target specificity afforded by the PNAs.[66] Therefore, although $(KFF)_3K$ was the CPP of choice in this dissertation research, the aspiration of other researchers to identify improved methods of PNA delivery is acknowledged and supported. Some examples of alternative delivery molecules currently under investigation include natural antimicrobial peptides (AMPs) found in eukaryotes,[75] Vitamin B_{12},[76] and tetrahedral DNA nanoparticles.[77]

The other large issue with pursuing PNA research is not due to the structure or behavior of the molecule; quite simply, it is cost. Peptide nucleic acids are still expensive to manufacture and purify, and if a research group does not have the capability to synthesize the PNAs in-house, it can cost thousands of dollars to obtain just a few hundred nmol from a commercial manufacturer (known from personal experience).

The reader is directed to peruse the full published works of Peter Nielsen and Liam Good for additional information about the development, use, and future potential of PNAs. These researchers were part of the group who invented and first published information about these fascinating molecules, and both are still actively involved in PNA research. Many of the studies cited in this review were produced by researchers who trained with or currently work with Dr. Nielsen or Dr. Good.

2.5.6 Future of ASOs in medicine

Peptide nucleic acids and other ASOs offer a glimpse of hope in the effort to counter bacterial antibiotic resistance. The medicinal potential of this type of molecule is now recognized at the national level as evidenced by the fact that the United States Food and Drug Administration (FDA) has approved several ASO drugs, including fomivirsen for cytomegalovirus retinitis in immunosuppressed patients such as those suffering from AIDS,[78] and mipomersen for familial hypercholesterolemia.[79] More ASO drugs are currently in clinical trials.[51,80] Although, none of

those drugs are for antimicrobial use, the author is optimistic that such potential drugs will eventually come under serious consideration.

On a more sobering note, there are already a few reports documenting emergence of resistant mutants in experiments where bacteria were treated with CPP-PSO or CPP-PNA conjugates. Fortunately, the mechanism of resistance is most likely related to upregulation of efflux mechanisms in response to the CPP, rather than mutation of the ASO nucleic acid target, so the concept of antisense antibacterial drugs still seems valid.[81-82] However, these reports remind us that a panacea for antibiotic resistant bacteria is likely still out of reach.

2.6 Animal models for evaluation of PNA efficacy

Part of this research involved use of a mouse model of bacterial infection to test PNA action *in vivo*. The reasons for this are described in greater depth in Chapter 6, but briefly, results of *in vitro* PNA experiments provided positive results that were judged to merit *in vivo* testing. It is generally agreed in the drug development community that promising potential medications should be tested for toxicity and efficacy using non-human *in vivo* experimental systems.[83] The use of comparative physiology and animal experimentation to learn about human anatomic and medical properties can be traced to ancient times, with the first recorded studies originating from Greece in the 6th century B.C.[84] Regrettably, viable alternatives to animal modeling have not yet been found, although active searches for other options are underway.[85]

Previously published literature did not provide much guidance when deciding how to proceed with an *in vivo* PNA experiment to evaluate efficacy against an infectious organism. Only two studies describing PNA treatment for bacterial sepsis were found.[86-87] There are a few studies evaluating the effect of PNAs that target expression of specific receptors in the rat brain, but this information was not directly applicable to the current research.[88-89] Studies discussing PNA pharmacokinetics, pharmacodynamics, or toxicity in mice or rats are also sparse. Those that are available describe a variety of PNA molecules used in different doses.[90-93] Based on those few data sets it appears that PNAs administered intraperitoneally, intravenously, or orally have widespread but low tissue distribution, likely undergo renal excretion, and would probably not be toxic at therapeutic doses.

However, no solid conclusions are yet drawn about how PNAs might behave *in vivo*, especially in ill animals, and a great deal more research in this area is needed.

The author hopes that this background information drives home the need for new antibacterial drugs, and provides adequate historical and technical context for the reader to understand why the experiments described in the following chapters were considered worthwhile undertakings.

2.7 References

1. Fleming A. On the antibacterial action of cultures of a Penicillium, with special reference to their use in the isolation of B. influenzae. Br J Exp Pathol. May, 1929;10:226-236.
2. Chain E, Florey H, Adelaide MB, et al. Pencillin as a chemotherapeutic agent. Lancet. 1940;2:226-231.
3. Fletcher C. First clinical use of penicillin. Brit Med J. 1984;289(6460):1721-1723.
4. Guest C, Harrison F. Acute endocarditis due to *Staphylococcus aureus* treated with penicillin. Am J Med. 1948;5(6):908-911.
5. Christie R. Penicillin in subacute bacterial endocarditis. Brit Med J. 1949;2(4634):950-951.
6. Centers for Disease Control and Prevention (CDC). Antibiotic resistance threats in the United States, 2013. https://www.cdc.gov/drugresistance/threat-report-2013/pdf/ar-threats-2013-508.pdf. Accessed February 16, 2019.
7. Spellberg B, Guidos R, Gilbert D, et al. The Epidemic of Antibiotic-Resistant Infections: A Call to Action for the Medical Community from the Infectious Diseases Society of America. Clin Infect Dis. 2008;46(2):155-164.
8. World Health Organization. Antibiotic resistance (5 February 2018). http://www.who.int/news-room/fact-sheets/detail/antibiotic-resistance. Accessed March 2, 2019.
9. European Centre for Disease Prevention and Control/Europeans Medicines Agency joint technical report. The bacterial challenge: time to react (September 2009). https://ecdc.europa.eu/sites/portal/files/media/en/publications/Publications/0909_TER_The_Bacterial_Challenge_Time_to_React.pdf. Accessed March 11, 2019.

10. Munita JM, Arias CA. Mechanisms of antibiotic resistance. Microbiol Spectr. 2016;4(2). doi: 10.1128/microbiolspec.VMBF-0016-2015.
11. Kapoor G, Saigal S, Elongavan A. Action and resistance mechanisms of antibiotics: A guide for clinicians. J Anaesthesiol Clin Pharmacol. 2017;33(3):300-305.
12. Fair RJ, Tor Y. Antibiotics and Bacterial Resistance in the 21st Century. Perspect Medicin Chem. June 2014;6:25-64. doi: 10.4137/PMc.s14459.
13. Patra M, Gasser G. Organometallic Compounds: An Opportunity for Chemical Biology? Chembiochem. 2012;13(9):1232-1252.
14. Noffke AL, Habtemariam A, Pizarro AM, Sadler PJ. Designing organometallic compounds for catalysis and therapy. Chem Commun. 2012;48(43):5219-5246.
15. Dabrowiak JC. Metals in Medicine. Chichester, West Sussex, United Kingdom: John Wiley & Sons Ltd.; 2009.
16. Gasser G, Ott I, Metzler-Nolte N. Organometallic anticancer compounds. J Med Chem. 2001;54(1):3-25.
17. Feng L, Geisselbrecht Y, Blanck S, et al. Structurally sophisticated octahedral metal complexes as highly selective protein kinase inhibitors. J Am Chem Soc. 2011;133(15):5976-5986.
18. Li C, Yu M, Sun Y, Wu Y, Huang C, Li F. A nonemissive iridium(III) complex that specifically lights-up the nuclei of living cells. J Am Chem Soc. 2011;133(29)11231-11239.
19. Noor F, Kinscherf R, Bonaterra GA, Walczak S, Wolfl S, Metzler-Nolte N. Enhanced cellular uptake and cytotoxicity studies of organometallic bioconjugates of the NLS peptide in Hep G2 cells. Chembiochem. 2009;10(3):493-502.
20. Florindo PR, Pereira DM, Borralho PM, Rodrigues CMP, Piedade MFM, Fernandes AC. Cyclopentadienyl-ruthenium(II) and iron(II) organometallic compounds with carbohydrate derivative ligands as good colorectal anticancer agents. J Med Chem. 2015;58(10):4339-4347.
21. Mendes N, Tortosa F, Valente A, et al. *In vivo* performance of a ruthenium-cyclopentadienyl compound in an orthotopic triple negative breast cancer model. Anticancer Agents Med Chem. 2017;17(1):126-136.

22. Reidel T. Demaria O, Zava O, Joncic A, Gilliet M, Dyson PJ. Drug repurposing approach identifies a synergistic drug combination of an antifungal agent and an experimental organometallic drug for melanoma treatment. Mol Pharm. 2018;15(1):116-126.
23. Hearn J, Hughes GM, Romero-Canelon I, et al. Pharmaco-genomic investigations of organo-iridium anticancer complexes reveal novel mechanism of action. Metallomics. 2018;10(1):93-107.
24. Rosenberg B, Van Camp L, and Krigas T. Inhibition of cell division in *Escherichia coli* by electrolysis products from a platinum electrode. Nature. February 1965;205:698-699.
25. Rosenberg B, Van Camp L, Trosko JE, Mansour VH. Platinum compounds: a new class of potent antitumour agents. Nature. April 1969;222:385-386.
26. Ndagi U, Mhlongo N, Soliman ME. Metal complexes in cancer therapy-an update from drug design perspective. Drug Des Devel Ther. 2017;11:599-616.
27. Bruijnincx PCA, Sadler PJ. New trends for metal complexes with anticancer activity. 2008;12(2):197-206.
28. Patra M, Gasser G, Metzler-Nolte N. Small organometallic compounds as antibacterial agents. Dalton Trans. 2012;41(21):6350-6358.
29. Biot C, Glorian G, Maciejewski LA, Brocard JS. Synthesis and antimalarial activity *in vitro* and *in vivo* of a new ferrocene-chloroquine analogue. J Med Chem. 1997;40(23):3715-3718.
30. Chellan P, Avery VM, Duffy S, et al. Organometallic conjugates of the drug sulfadoxine for combatting antimicrobial resistance. Chem Eur J. 2018;24(40):10078-10090.
31. Oliveira JS, Sousa EHS, Basso L, et al. An inorganic iron complex that inhibits wild-type and an isoniazid-resistant mutant 2-trans-enoyl-ACP (CoA) reductase from Mycobacterium tuberculosis. Chem Commun. 2004:312-313.
32. Pandrala M, Li F, Feterl M, et al. Chlorido-containing ruthenium(II) and iridium(III) complexes as antimicrobial agents. Dalton Trans. 2013;42:4686.
33. Adb-El-Aziz AS, Agatemor C, Etkin N, et al. Antimicrobial organometallic dendrimers with tunable activity against multidrug-resistant bacteria. Biomacromolecules. 2015;16(11):3694-3703.

34. Karpin G, Morris DM, Ngo MT, Merola JS, Falkinham III JO. Transition metal diamine complexes with antimicrobial activity against *Staphylococcus aureus* and methicillin-resistant *S. aureus* (MRSA). Medchemcomm. 2015;6(8):1471-1478.
35. Chen F, Moat J, McFeely D, et al. Biguanide iridium(III) complexes with potent antimicrobial activity. J Med Chem. 2018;61:7330-7344.
36. Karpin GW, Merola JS, Falkinham III JO. Transition metal-α-amino acid complexes with antibiotic activity against Mycobacterium spp. Antimicro Agents Chemother. 2013;57(7):3434-3436.
37. Gupta S, Singh RP, Rabadia N, Patel G, Panchal H. Antisense technology. Int J Pharm Sci Rev Res. 2011;9(2);38-45 (article 007).
38. Rasmussen LCV, Sperling-Petersen HU, Mortensen KK. Hitting bacteria at the heart of the central dogma: sequence-specific inhibition. Microb Cell Fact. 2007;6(24). doi: 10.1186/1475-2859-6-24.
39. Agrawal N, Dasaradhi PVN, Mohmmed A, Malhotra P, Bhatnagar RK, Mukherjee SK. RNA interference: biology, mechanism, and applications. Microbiol Mol Biol Rev. 2003;67(4):657-685.
40. Tomizawa J, Itoh T, Selzer G, Som T. Inhibition of ColE1 RNA primer formation by a plasmid-specified small RNA. Proc Natl Acad Sci U S A. 1981;78(3):1421-1425.
41. Stougaard P, Molin S, Nordstrom K. RNAs involved in copy-number control and incompatibility of plasmid R1. Proc Natl Acad Sci U S A. 1981;78(10):6008-6012.
42. Inouye M. Antisense RNA: its functions and applications in gene regulation - a review. Gene. 1988;72:25-34.
43. Saberi F, Kamali M, Najafi A, Yazdanparast A, Moghaddam MM. Natural antisense RNAs as mRNA regulatory elements in bacteria: A review on function and applications. Cell Mol Biol Lett. 2016;21(6). doi: 10.1186/s11658-016-0007-z.
44. Paterson BM, Roberts BE, Kuff EL. Structural gene identification and mapping by DNA-mRNA hybrid-arrested cell-free translation. Proc Natl Acad Sci U S A. 1977;74(10):4370-4374.
45. Stephenson ML, Zamecnik PC. Inhibition of Rous sarcoma viral RNA translation by a specific oligodeoxyribonucleotide. Proc Natl Acad Sci U S A. 1978;75(1):285-288.

46. van der Krol AR, Lenting PE, Veenstra J, et al. An anti-sense chalcone synthase gene in transgenic plants inhibits flower pigmentation. Nature. 1988;333(6176:866-869.
47. Rosenberg U, Preiss A, Seifert E, Jackle H, Knipple DC. Production of phenocopies by Krüppel antisense RNA injection into Drosophila embryos. Nature. 1985;313(6004):703-706.
48. Rauhut R, Klug G. mRNA degradation in bacteria. FEMS Microbiol Rev. 1999;23(3):353-370.
49. Hui MP, Foley PL, Belasco JG. Messenger RNA degradation in bacterial cells. Annu Rev Genet. 2014:48:537-559.
50. Coleman J, Hirashima A, Inokuchi Y, Green PJ, Inouye M. A novel immune system against bacteriophage infection using complementary RNA (micRNA). Nature. 1985;315(6020):601-603.
51. Shen X, Corey DR. Chemistry, mechanism and clinical status of antisense oligonucleotides and duplex RNAs. Nucleic Acids Res. 2018;46(4):1584-1600. doi: 10.1093/nar/gkx1239.
52. Dias N, Stein CA. Antisense oligonucleotides: Basic concepts and Mechanisms. Mol Cancer Ther. 2002;1(5):347-55.
53. Oberemok V, Laikova KV, Repetskaya AI, et al. A Half-Century History of Applications of Antisense Oligonucleotides in Medicine, Agriculture and Forestry: We Should Continue the Journey. Molecules. 2018;23(6):1302. doi: 10.3390/molecules23061302.
54. Summerton J, Weller D. Morpholino antisense oligomers: design, preparation, and properties. Antisense Nucleic Acid Drug Dev. 1997;7:187-195.
55. Wahlestedt C, Salmi P, Good L, et al. Potent and nontoxic antisense oligonucleotides containing locked nucleic acids. Proc Natl Acad Sci U S A. 2009;97(10):5633-5638.
56. Nielsen PE, Egholm M, Berg RH, Buchardt O. Sequence specific inhibition of DNA restriction enzyme cleavage by PNA. Nucleic Acids Res. 1993;21(2):197-200.
57. Nielsen PE, Egholm M, Berg RH, Buchardt O. Sequence-selective recognition of DNA by strand displacement with a thymine-substituted polyamide. Science. 1991;254(5037):1497-1500.
58. Egholm M, Buchardt O, Nielsen P, Berg RH. Peptide nucleic acids (PNA). Oligonucleotide analogues with an achiral peptide backbone. J Am Chem Soc. 1992;114(5):1895-1897.

59. Egholm M, Nielsen PE, Buchardt O, Berg RH. Recognition of guanine and adenine in DNA by cytosine and thymine containing peptide nucleic acids (PNA). J Am Chem Soc. 1992;114(24):9677-9678.
60. Demidov VV, Potaman VN, Frank-Kamenetskil MD, et al. Stability of peptide nucleic acids in human serum and cellular extracts. Biochem Pharm. 1994;48(6):1310-1313.
61. Iwamoto N, Butler DCD, Svrzikapa N, et al. Control of phosphorothioate stereochemistry substantially increases the efficacy of antisense oligonucleotides. Nat Biotechnol. 2017;35(9):845-851.
62. Mondhe M, Chessher A, Goh S, Good L, Stach JEM. Species-selective killing of bacteria by antimicrobial peptide-PNAs. PLoS One. 2014;9(2):e89082. doi: 10.1371/journal.pone.0089082.
63. Good L, Nielsen PE. Antisense inhibition of gene expression in bacteria by PNA targeted to mRNA. Nat Biotechnol. April 1998;16:355-358.
64. Ghosh S, Saini S, Saraogi I. Peptide nucleic acid mediated inhibition of the bacterial signal recognition particle. Chem Commun. 2018;54(59):8257-8260.
65. Sugimoto S, Maeda H, Kitamatsu M, Nishikawa I, Shida M. Selective growth inhibition of Porphyromonas gingivalis and Aggregatibacter actinomycetemcomitans by antisense peptide nucleic acids. Mol Cell Probes. November 2019;43:45-49.
66. Ghosal A, Nielsen PE. Potent antibacterial antisense peptide–eptide nucleic acid conjugates against *Pseudomonas aeruginosa*. Nucleic Acid Ther. 2012;22(5):323-334.
67. Readman JB, Dickson G, Coldham NG. Translational inhibition of CTX-M extended spectrum beta-lactamase in clinical strains of *Escherichia coli* by synthetic antisense oligonucleotides partially restores sensitivity to cefotaxime. Front Microbiol. March 2016;7:373. doi: 10.3389/fmicb.2016.00373.
68. Goh S, Loeffler A, Lloyd DH, Nair SP, Good L. Oxacillin sensitization of methicillin-resistant *Staphylococcus aureus* and methicillin-resistant *Staphylococcus pseudintermedius* by antisense peptide nucleic acids *in vitro*. BMC Microbiol. 2015;15:262. doi 10.1186/s12866-015-0599-x.
69. Wittung P, Kajanus J, Haaima G, Nielsen PE, Norden B, Malmstrom BG. Phospholipid membrane permeability of peptide nucleic acid. 1995;375(3):27-29.

70. Eriksson M, Nielsen PE, Good L. Cell permeabilization and uptake of antisense peptide-peptide nucleic acid (PNA) into *Escherichia coli*. J Biol Chem. 2002;277(9):7144-7147.
71. Gasparello J, Manicardi A, Casnati A. Efficient cell penetration and delivery of peptide nucleic acids by an argininocalix[4]arene. Sci Rep. 2019;9:3036. doi: 10.1038/s41598-019-39211-4.
72. Vaara M, Porro M. Group of peptides that act synergistically with hydrophobic antibiotics against gram-negative enteric bacteria. Antimicrob Agents Chemother. 1996;40(8):1801-1805.
73. Pomares MF, Delgado MA, Corbalan NS, Farias RN, Vincent PA. Sensitization of Microcin J25-Resistant Strains by a Membrane- Permeabilizing Peptide. Appl Environ Microbiol. 2010;76(20):6837-6842.
74. Xue, X, Mao X, Zhou Y, et al. Advances in the delivery of antisense oligonucleotides for combating bacterial infectious diseases. Nanomedicine. 2018;19(3):745-758.
75. Hansen AM, Bonke G, Larsen CJ, Yavari N, Nielsen PE, Franzyk H. Antibacterial peptide nucleic acid-antimicrobial peptide (PNA-AMP) conjugates: antisense targeting of fatty acid biosynthesis. Bioconjug Chem. 2016;27(4):863-867.
76. Rownicki M, Wojciechowska M, Wierzba AJ, et al. Vitamin B_{12} as a carrier of peptide nucleic acid (PNA) into bacterial cells. Sci Rep. 2017;7:7644. doi: 10.1038/s41598-017-08032-8.
77. Readman JB, Dickson G, Coldham NG. Tetrahedral DNA nanoparticle vector for intracellular delivery of targeted peptide nucleic acid antisense agents to restore antibiotic sensitivity in cefotaxime-resistant *Escherichia coli*. Nucleic Acid Ther. 2017;27(3):176-181. doi: 10.1089/nat.2016.0644.
78. Stein CA, Castanotto D. FDA-Approved oligonucleotide therapies in 2017. Mol Ther. 2017;25(5):1069-1075.
79. Geary RS, Baker BF, Crooke ST. Clinical and preclinical pharmacokinetics and pharmacodynamics of Mipomersen (Kynamro®): A second-generation antisense oligonucleotide inhibitor of apolipoprotein B. Clin Pharmacokinet. 2015;54(2):133-146.
80. Morena PMD, Pego AP. Therapeutic antisense oligonucleotides against cancer: hurdling to the clinic. Front Chem. 2014;2:87. doi: 10.3389/fchem.2014.00087.

81. Puckett SE, Reese KA, Mitev GM, et al. Bacterial resistance to antisense peptide phosphorodiamidate morpholino oligomers. Antimicrob Agents Chemother. 2012;56(12):6147-6153.
82. Courtney CM, Chatterjee A. Sequence-specific peptide nucleic acid-based antisense inhibitors of TEM-1 β-lactamase and mechanism of adaptive resistance. ACS Infect Dis. 2015;1(6):253-263.
83. Denayer T, Stohr T, Van Roy M. Animal models in translational medicine: Validation and prediction. New Horiz Transl Med. 2014;2(1):5-11.
84. Ericsson AC, Crim MJ, Franklin CL. A brief history of animal modeling. Mo Med. 2013;110(3):201-205.
85. Powell K. Replacing the replacements: Animal model alternatives. Science. 2018;362(6411):243-245.
86. Tan X, Actor JK, Chen Y. Peptide nucleic acid antisense oligomer as a therapeutic strategy against bacterial infection: proof of principle using mouse intraperitoneal infection. Antimicrob Agents Chemother. 2005;49(8):3203-3207.
87. Bai H, You Y, Yan H, et al. Antisense inhibition of gene expression and growth in gram-negative bacteria by cell-penetrating peptide conjugates of peptide nucleic acids targeted to *rpoD* gene. Biomaterials. 2012;33(2):659-667.
88. Tyler BM, Jansen K, McCormick DJ, et al. Peptide nucleic acids targeted to the neurotensin receptor and administered i.p. cross the blood-brain barrier and specifically reduce gene expression. Proc Natl Acad Sci U S A. 1999;96(12):7053-7058.
89. McMahon BM, Stewart JA, Jackson J, Fauq A, McCormick DJ, Richelson E. Intraperitoneal injection of antisense peptide nucleic acids targeted to the mu receptor decreases response to morphine and receptor protein levels in rat brain. Brain Res. 2001;904(2):345-349.
90. McMahon BM, Mays D, Lipsky J, Stewart JA, Fauq A, Richelson E. Pharmacokinetics and tissue distribution of a peptide nucleic acid after intravenous administration. Antisense Nucleic Acid Drug Dev. 2002;12(2):65-70.
91. Hamzavi R, Dolle F, Tavitian B, Dahl O, Nielsen PE. Modulation of the pharmacokinetic properties of PNA: Preparation of galactosyl, mannosyl, fucosyl, N-acetylgalactosaminyl, and N-acetylglucosaminyl derivatives of aminoethylglycine peptide nucleic acid

monomers and their incorporation into PNA oligomers. Bioconjug Chem. 2003;14(5):941-954.

92. Chauby B, Tripathi S, Pandey V. Single acute-dose and repeat-doses toxicity of anti-HIV-1 PNA TAR–penetratin conjugate after intraperitoneal administration to mice. Oligonucleotides. 2008:18(1):9-20.
93. Ganguly S, Chaubey B, Tripathi S, et al. Polyamide nucleic-acid-cell penetrating peptide conjugates targeted against HIV-1 transactivation response element. Oligonucleotides. 2008;18(3):277-286.

3 Eukaryotic cell cytotoxicity and cellular penetration of novel organometallic compounds with inhibitory activity against nontuberculous mycobacteria

3.1 Introduction

Tuberculous and virulent nontuberculous mycobacteria are pathogens known for centuries to cause disease in humans and animals. Diseases include tuberculosis, caused by species in the *Mycobacterium tuberculosis* complex such as *M. tuberculosis* and *M. bovis*[1], pulmonary infections caused by nontuberculous species such as *M. avium*, and *M. abscessus*[2], and skin infections caused by *M. leprae.*[3] Despite ongoing efforts to maximize the effects of antibiotic therapy[4] and develop effective preventative and therapeutic vaccines[5], the organisms continue to evade humanity's attempts to treat and eradicate mycobacterial disease. Tuberculosis caused approximately 1.4 million human deaths worldwide in 2017, and it is estimated that there were at least 10 million new cases.[6] This is in part due to issues with hygiene and availability of adequate resources for treatment. Another major factor is the nature of how mycobacteria establish infection in a host. After entering the host by an appropriate route such as inhalation, the bacteria are recognized and taken up by macrophages, but instead of then being digested by phagolysosomes, they activate molecular mechanisms that prevent effective killing by the macrophages.[7-8] This allows the bacteria to persist and replicate intracellularly while essentially using the host's own immune cells as a shield, and also inhibits the ability of antibiotics to reach the bacteria. In addition, and central to the point of this dissertation research, drug-resistant strains of mycobacteria are emerging at alarming rates. Emergence of multi-drug resistant (MDR), extensively-drug resistant (XDR), or pan-resistant *M. tuberculosis* has been documented in multiple countries. [9-12] Thus, an important goal in the ongoing effort to eliminate mycobacterial infections is the development of novel antimicrobial compounds to which the organism is not resistant.

Karpin et al[13] recently described a novel group of "half-sandwich" organometallic compounds (OMCs) that inhibited the growth of several species of nontuberculous mycobacteria in pure culture. These (OMCs) have a heavy metal iridium (Ir) or rhodium (Rh) center bound to a cyclopentadiene (Cp) or paracymene ring and an organic ligand such as an amino acid. The chemical platform of these compounds is radically different from that of conventional antibiotics

in current use. The concept of using metal-based compounds in medicine is not new. Over the past century most of such compounds were used as antineoplastics, as an extension of the discovery and development of cisplatin in the 1960s.[14-15] However, there are recent reports of OMCs that show antibacterial activity against several bacterial and protozoal genera, including antibiotic-resistant strains.[16-19]

One of the advantages of working with compounds that contain second and third row transition metals is that these metals can occupy a range of oxidation states, allowing for relatively easy manipulation of organic ligand attachment. This in turn facilitates tailoring of the complexes to accommodate specific biological, chemical, and physiological conditions. In addition, functionalizing the Cp group of a half-sandwich organometallic compound can substantially affect properties such as compound acidity, hydrophobicity, and cytotoxicity.[20] Since part of what makes a compound suitable for study as a potential medication is the ability to chemically tune it in order to hone in on the ideal structure-activity relationship, research into the antimicrobial use of OMCs seems warranted. However, before a compound can progress far in the journey to becoming a clinical antimicrobial drug, the possibility of cytotoxicity against mammalian tissues must be explored and preferably ruled out.[21] This is especially important when the target organism sequesters itself intracellularly within host immune cells, as it is expected that an ideal drug would penetrate intracellularly and facilitate destruction of the pathogen without notable damage to the host cells. This chapter of the dissertation describes preliminary research done to assess the eukaryotic cytotoxicity of several of the compounds listed in the paper by Karpin et al, using J774A.1 murine macrophage-like cells. An attempt was also made to determine if one of those compounds, and a chemically similar derivative, could clear intracellular *M. bovis* from within infected J774A.1 cells. Finally, the ability of one compound of interest to cross J774A.1 cell membranes and penetrate the intracellular space was assessed.

3.2 Materials and Methods

3.2.1 Organometallic compounds

Six OMCs developed by the laboratory of Dr. Joseph Merola of the Virginia Tech Chemistry Department were chosen for cytotoxicity studies based on the finding of micromolar minimum inhibitory concentrations (MIC) against *M. bovis* BCG strain ATCC 35745 (Connaught) or *M.*

avium strain A5. The compounds were synthesized according to the scheme described by Karpin, et al.[13] The chemical structures are shown in Figure 3.1.

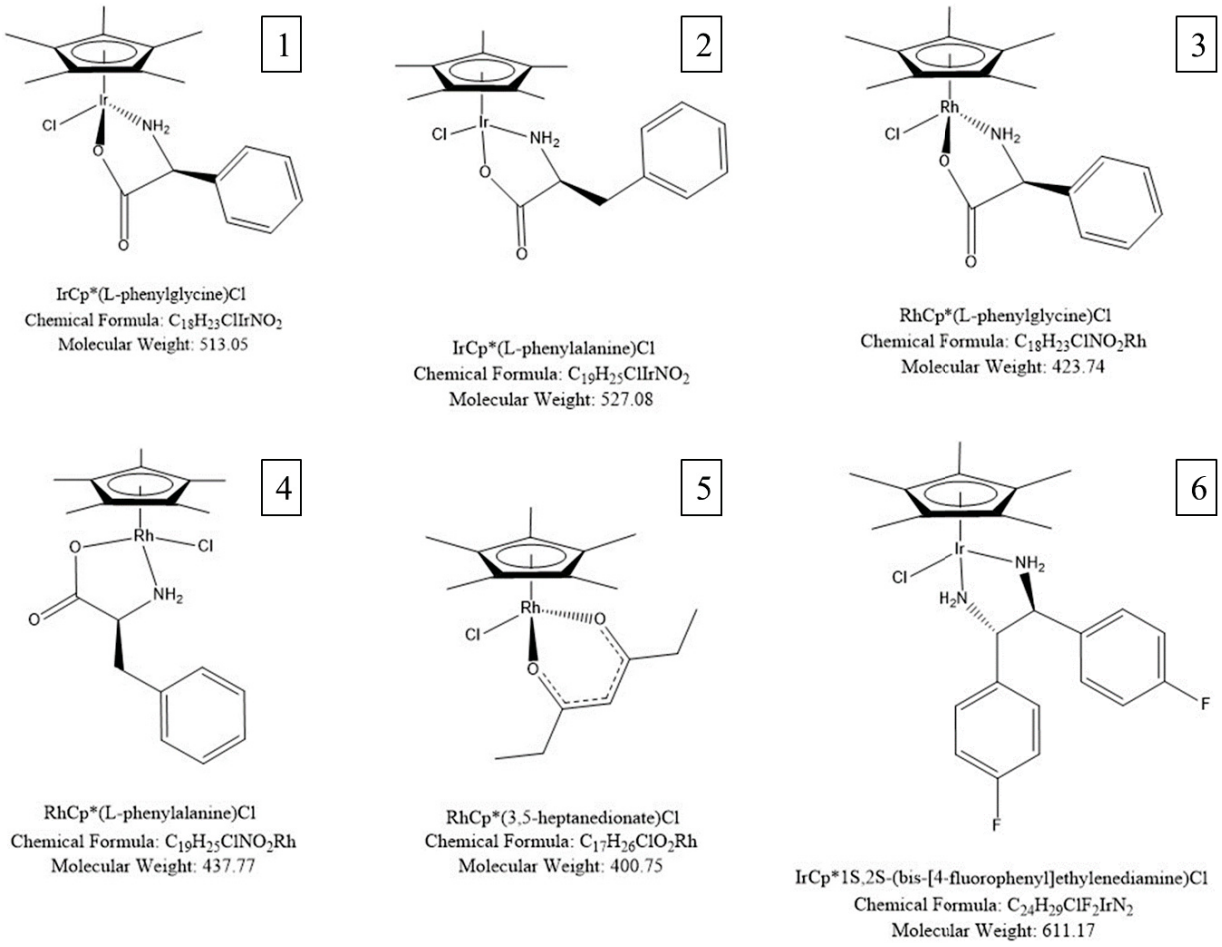

Figure 3.1 Structures of six novel OMCs chosen for eukaryotic cell cytotoxicity assays based on their inhibitory activity against several species of nontuberculous mycobacteria in pure culture.

3.2.2 MTS [3-(4,5-dimethylthiazol-2-yl)-5-(3-carboxymethoxyphenyl)-2-(4-sulfophenyl)-2H-tetrazolium)] cytotoxicity assay

For culturing cells, supplies were obtained from Sigma-Aldrich, St Louis MO, USA. Flasks of J774A.1 murine macrophage-like cells (ATCC® TIB-67™, Manassas, VA) at passage 8 or higher were grown to confluency in Dulbecco's Modified Eagle's Medium (DMEM) supplemented with 10% fetal bovine serum (FBS) and 1% penicillin/streptomycin (p/s) solution in 75 cm^2 culture flasks. Cells were then seeded in six flat bottom, 96-well culture plates at a density of 2 x 10^4/ml in antibiotic-free DMEM + 10% FBS and incubated at 37 C° with 5% CO_2 supplementation for

24 hours to allow cellular attachment to the plate surfaces. Stock solutions of the experimental compounds were prepared by dissolving appropriate amounts of purified powder in molecular grade sterile water and serial dilutions of the experimental compounds were prepared using antibiotic-free DMEM + 10% FBS. After cellular attachment, the culture medium was removed from the J774A.1 cells, the cells were washed once with antibiotic-free medium, and compound-treated medium was added to the cells in the concentrations shown in Table 3.1, and in the general arrangement shown in Figure 3.2. Three OMCs were tested on each culture plate, and cells were incubated with the treatments for 24, 48, or 72 hours. One hundred µl/well of OMC-treated medium was added to cells treated for 24 hours and 200 µl/well was added to cells treated for 48 or 72 hours to decrease the chance of detrimental medium evaporation. The cell culture plates were incubated at 37 C° with 5% CO_2 supplementation.

Table 3.1 Dilutions of six OMCs were prepared in antibiotic-free DMEM based off the MICs for each compound against *M. bovis* BCG or *M. avium* A5. These dilutions were then added to cultures of J774A.1 cells at the concentrations shown in this table and plates were incubated for 24, 48, or 72 hours before measurement of cellular metabolism to assess cytotoxicity.

Compound	*M. bovis* BCG MIC µg/ml	5x	10x	15x	20x	25x
1	10	50	100	150	200	250
2	15	75	150	225	300	375
3	7	35	70	105	140	175
4	12	60	120	180	240	300
	M. bovis BCG MIC µg/ml	2x	3x	4x	5x	
5	62.5	125	187.5	250	312.5	
	M. avium A5 MIC µg/ml	5x	10x	15x	20x	25x
6	8	40	80	120	160	200

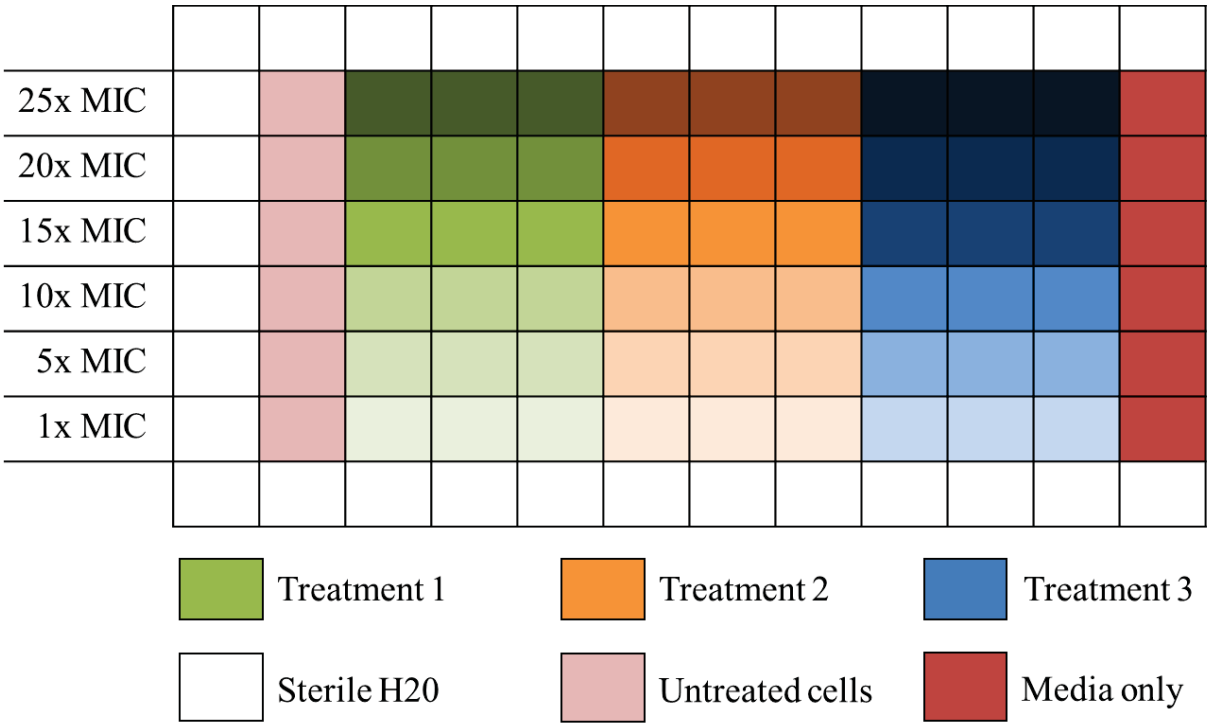

Figure 3.2 Schematic of a 96-well cell culture plate seeded with 2 x 10^4 J774A.1 cells/well. Solutions containing OMCs in various concentrations were added and the cells were incubated for 24, 48, or 72 hours before measurement of cellular metabolism to assess cytotoxicity. Three compounds were tested on each 96-well plate.

At each time point (24, 48, or 72 hours) of incubation, two of the 96-well plates with all 6 OMCs represented were removed from incubation and the CellTiter 96® Aqueous Non-Radioactive Cell Proliferation Assay was performed according to the manufacturer protocol. The absorbance of each well was immediately measured at 490 nm using a VersaMax™ Microplate Reader (Molecular Devices LLC, San Jose, CA, USA).

3.2.3 Treatment of *M. bovis* infected J774A.1 cells to evaluate bacterial clearance capabilities of two novel OMCs

Bacterial culture and preparation of inoculum

All work with *M. bovis* was carried out under Biosafety Level (BSL)-2 conditions. Bacterial manipulations were done in a Class II type A2 biosafety cabinet (Labconco, Kansas City, MO, USA). One 10 µl drop of previously frozen laboratory stock of *M. bovis* BCG Pasteur (ATCC 35734) was streaked onto Middlebrook 7H10 agar in a petri dish and incubated at 37 C˚ with 5% CO2 until colonies were visible. For bacterial passage 0, several colonies were plucked from the

agar culture and inoculated into 25 ml Middlebrook 7H9 broth in a loosely capped and parafilmed sidearm flask (nephelo flask) with 10% OADC supplementation (Sigma-Aldrich M0678) and 0.1% Tween-80 (Sigma-Aldrich CAS 9005-65-6) to decrease bacterial clumping. The culture was incubated at 37 C° with 5% CO_2 in a shaking incubator at 175-200 RPM, and turbidity was assessed by Klett readings and OD_{600} readings approximately once a week. For OD_{600} measurements a 1 ml sample of culture was removed from the shaken flask in the biosafety cabinet, sealed, and disinfected on the outside before placement in the spectrophotometer. After 22 days the culture was visibly turbid with an OD_{600} of 0.118. The culture was scaled up to a larger flask (passage 1) and a bacterial growth curve was performed over the next 12 days with daily Klett readings and OD_{600} and CFU/ml counts every 1-3 days. Klett and OD_{600} readings correlated well with each other but not with CFU/ml counts (data not shown). Also, there is a report that OD_{600} readings and comparison with McFarland standards provide reasonable real-time estimates of *M. tuberculosis* CFUs/ml and may be more reliable than CFU/ml counts on agar.[22] Therefore, the decision was made to use Klett readings, OD_{600} readings, and McFarland standard comparison to estimate CFU/ml concentrations needed for bacterial inocula. After this initial work to characterize bacterial growth under culture conditions specific to the laboratory where this research was performed, 1 ml of a third passage culture of *M. bovis* was inoculated into 49 ml Middlebrook 7H9 broth with 10% OADC and 0.1% Tween-80, and incubated with continuous shaking (175-200 RPM) at 37 C° and 5% CO_2 until the culture reached a turbidity corresponding to a Klett reading of 77, OD_{600} of 0.6, and #4 McFarland standard, which took approximately 4 days. The culture was estimated to be mid- to late log phase, with a bacterial concentration of ~3 x 10^7 CFU/ml and was then diluted to make an inoculum solution.

Culture and infection of eukaryotic cells

Appropriately passaged J774A.1 cells were seeded in 24-well plates at a density of 5 x 10^5 cells/well in 1 ml DMEM + 10% FBS + 1% p/s and allowed to attach for 24 hours at 37 C° with 5% CO_2 supplementation. The cell culture medium was removed and cells were washed 2x with sterile PBS before addition of 1 ml DMEM + 10% FBS/well. Based on the percentage of confluency, the number of cells were estimated to be approximately 1 x 10^6/well. The bacterial culture was diluted to a concentration of 1 x 10^8 CFU/ml and 100 µl of this suspension was added to each appropriate cell culture well for a multiplicity of infection (MOI) of 10:1. The 24-well

plates were incubated on a plate rotator at 37 C˚ for one hour to allow for bacterial uptake by the cells. After rotation, the medium containing bacteria was removed and 1 ml DMEM + 1% FBS + 50 μg/ml gentamicin was added to kill extracellular bacteria. The 24-well plates were incubated on a plate rotator at 37 C˚ for 30 minutes, then media was removed and 1 ml DMEM + 1% FBS + 25 μg/ml gentamicin was added to each appropriate well and plates were incubated at 37 C˚ with 5% CO_2 overnight to allow for establishment of intracellular infection.

Treatment of infected cell cultures with two OMCs

Two novel organometallic compounds were used for treatment of infected cells. The first compound, IrCp*(L-pg)Cl (Compound 1 in Figure 3.1) was determined by Karpin et al.[13] to have an MIC of 10 μg/ml against *M. Bovis* BCG. For this particular experiment, this compound is called OMC 1. The second compound is a slightly modified version of the first compound with a propyl group in place of one of the methyl groups on the Cp* ring. For this particular experiment, this compound is called OMC 2. The antimicrobial activity of this compound was not directly tested against *M. bovis* BGC, so the MIC was presumed to also be 10 μg/ml for the purpose of this experiment. The first compound is soluble in pure water, while the second compound is not and had to be dissolved in DMSO for preparation of a stock compound. The compounds were diluted in DMEM + 1% FBS to obtain treated medium solutions of 2x MIC (20 μg/ml), 1x MIC (10 μg/ml), and 0.5x MIC (5 μg/ml) for OMC 1, and 2x MIC (20 μg/ml) and 1x MIC (10 μg/ml) for OMC 2. Treatment solutions for OMC 2 contained 0.1% DMSO.

After overnight incubation, the gentamicin-treated medium was removed from the infected cell cultures and replaced with 2 ml of OMC-treated medium, 2 ml of 0.1% DMSO in DMEM + 1% FBS (vehicle control for second compound), 2 ml of 1 μg/ml isoniazid in DMEM + 1% FBS (conventional antimicrobial control), or 2 ml untreated DMEM + 1% FBS (untreated control). The experimental plate set up is shown in Figure 3.3. Two identical 24-well plate set-ups were treated, one for two days, and the other for five days. Four wells with uninfected, untreated J774A.1 cells were also maintained for the duration of the experiment to allow for serial visual comparison between infected and uninfected cells. After the appropriate number of days, the treated medium was removed, cells were washed 2x with DMEM and lysed by incubation with 0.1% Triton-X for 10 minutes, then cell lysates were serially diluted and plated on Middlebrook 7H10 agar. The agar

plates were covered with parafilm and incubated at 37 C˚ with 5% CO_2 for 6 weeks, then colonies were counted and the average CFU/ml from each treatment group was calculated. Although the initial experiments with bacterial growth under these culture conditions suggested that counting CFU/ml may underestimate bacterial concentration in a solution (see the first part of section 3.2.3), this was still determined to be the best way to compare relative bacterial proliferation among various treatment groups.

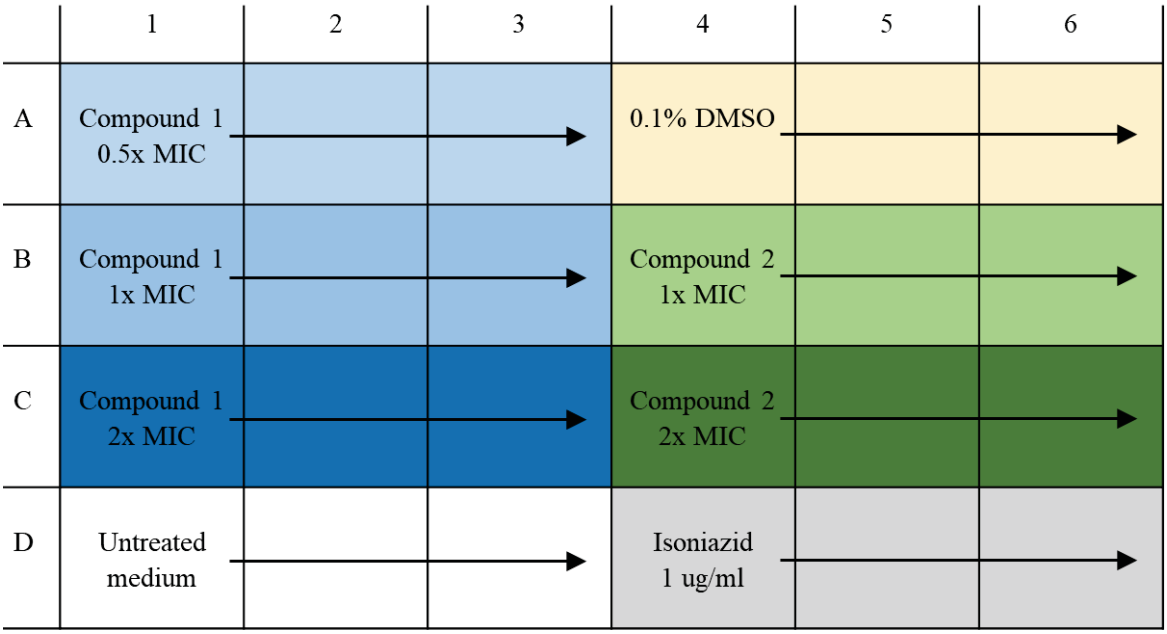

Figure 3.3 24-well plate set up to evaluate the effect of experimental organometallic compounds on intracellular growth of *M. bovis* BCG Pasteur within J774A.1 murine macrophage-like cells. All wells contain J774A.1 cells infected overnight with *M. bovis* BCG Pasteur. Two 24-well plates with identical treatment arrangements were set up, one of which was incubated for 2 days before cell lysis and one of which was incubated for 5 days before cell lysis. Isoniazid was included as a conventional antimicrobial compound for mycobacterial infections.

3.2.4 Assessment of cellular penetrance of Compound 1, IrCp*(L-pg)Cl

J774A.1 cells were cultured as described above and seeded in 24-well plates at a density of 1 x 10^5 cells/well in DMEM + 10% FBS without antibiotics. Cells were allowed to attach and proliferate to approximately 75% confluency (approximately 1-2 days). The medium was removed, cells were washed with PBS, then wells were filled with 2 ml of DMEM + 10% FBS containing the organometallic compound in concentrations 1x, 5x, and 10x the MIC against *M. bovis* BCG (10 µg/ml, 50 µg/ml, and 100 µg/ml, respectively). The set-up of the 24-well plate is shown in Figure

3.4. Cells were incubated with the compound for 24 or 48 hours, then the medium was removed, and one ml of medium from each well was stored for measurement of Ir concentration. Most wells were then washed 3x with sterile PBS before harvesting, but in one well from each treatment concentration the cells were left unwashed before harvesting, in order to allow for comparison between the effect of washing versus not washing the cells before measurement of Ir. The cells were lysed by incubation with 0.1% Triton-X for 10 minutes. The cell lysates were collected and centrifuged at 10,000 rpm for 5 minutes, then the supernatants were drawn off into separate tubes. Iridium concentration was measured in the treatment medium and the cell lysate supernatants by inductively coupled plasma mass spectrometry (ICP-MS) and compared between treatment concentrations and between washed and unwashed samples. The quantitation limit for the ICP-MS is approximately 5 ng/ml assuming a 50x dilution of the sample in 2% (w/w) HNO_3.

3.2.5 Statistical analysis

Data from the cytotoxicity experiment was recorded with the SoftMax® Pro Software (Molecular Devices LLC, San Jose, CA, USA) and transferred to Microsoft Excel (Microsoft Corporation, Redmond, WA, USA) for analysis. One-factor ANOVA using the Excel data analysis package (Microsoft Corporation, Redmond, WA, USA) was done on the data from each treatment plate in the bacterial clearance experiment in order to determine if there were any statistically detectable differences among the variances of the treatment groups. An unpaired student's t-test was performed using GraphPad Prism (San Diego, CA, USA) to compare iridium concentration between different treatment concentrations and time points in the cell penetration experiment.

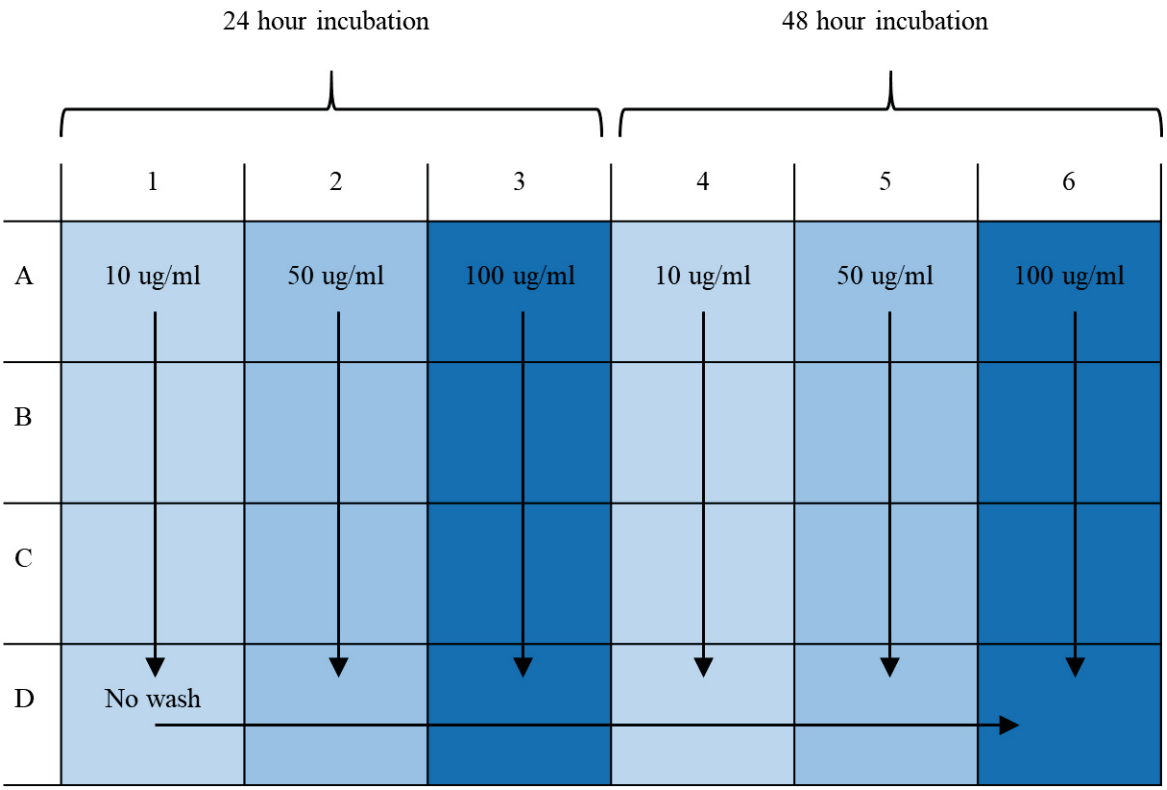

Figure 3.4 24-well plate set-up to evaluate the ability of the compound IrCp*(L-pg)Cl to penetrate intracellularly within J774A.1 murine macrophage-like cells. All wells contain J774A.1 cells incubated with various concentrations of the compound for 24 or 48 hours before cell harvesting and measurement of the iridium concentration within cell lysates.

3.3 Results

3.3.1 MTS cytotoxicity assay

Graphical representations for each of the six compounds are shown in Figure 3.5. For Compound 1 (Figure 3.5A), cell viability relative to untreated control wells was between 60% and 130% for all treatments at the 24 hour, 48 hour, and 72 hour time points without a clear trend except in the 48 hour series, in which cell viability generally showed a relative increase with increasing treatment concentration. At the highest two treatment concentrations (20x MIC and 25x MIC), the relative cell viability was greater than 100% at all time points. For Compound 2 (Figure 3.5B), cell viability relative to untreated controls was greater than 100% at the 24 hour mark for all treatment concentrations, and was between 80% and 110% at the 48 hour mark for all treatment concentrations, without a clear trend. For the 72 hour mark, relative viability for the lowest 5 treatment concentrations was approximately 80-90%, then there was a distinct drop to about 65% viability at the highest treatment concentration. For Compound 3 (Figure 3.5C), at the 24 hour time point the relative cell viability was 80-90% for the two lowest treatment concentrations and between 120-140% at the four higher treatment concentrations. At the 48 and 72 hour time points, relative cell viability was between 80% and 100% for the three lowest treatment concentrations, then dropped slightly to hover between 60% and 80% at the three highest treatment concentrations. For compound 4 (Figure 3.5D), both mild time dependent and mild treatment concentration dependent effects were observed. At the 24 hour time point relative cell viability was greater than 100% for all concentrations except the highest one, where there was a sharp drop to approximately 60% viability. At the 48 hour and 72 hour time points, relative cell viability was approximately 70-80% for the four lowest treatment concentrations but showed a sharp drop to 40% or lower at the two highest concentrations. Compound 5 (Figure 3.5E) showed clear time and dose dependent effects. At all three time points cell viability steadily dropped from 80% or higher at the lowest treatment concentration to below 20% at the highest concentration. Compound 6 (Figure 3.5F) also showed clear time and dose dependent effects. At all three time points cell viability steadily dropped from 60% or higher at the lowest treatment concentration to below 20% at the highest concentration. The only measurement that indicated cell viability similar to the untreated control was that for the lowest treatment concentration at 72 hours.

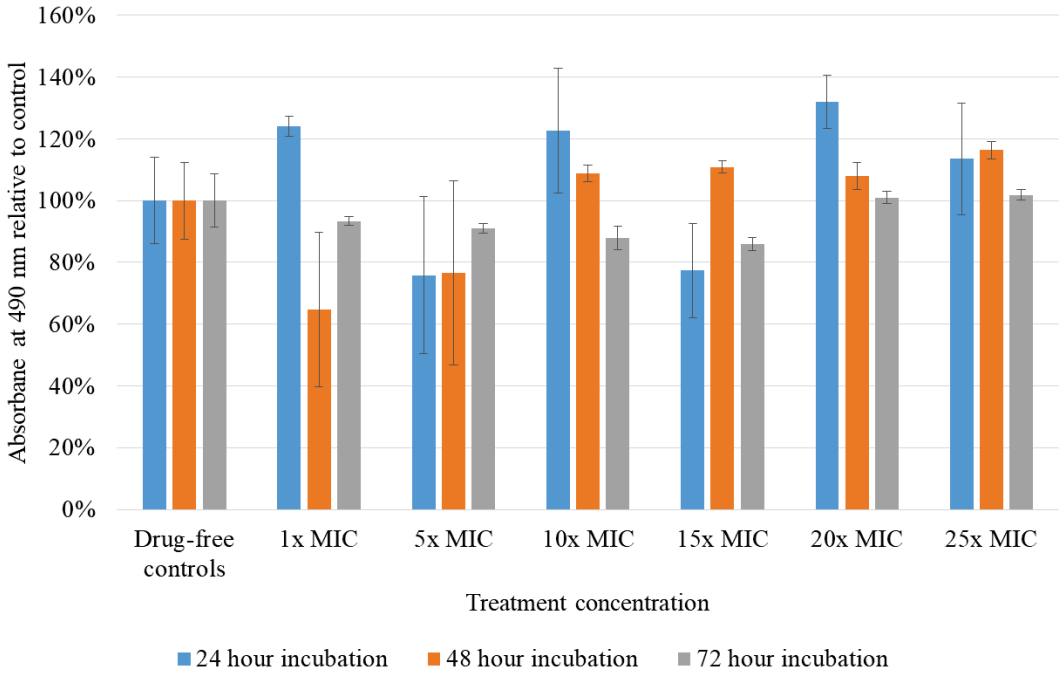

Figure 3.5A Compound 1

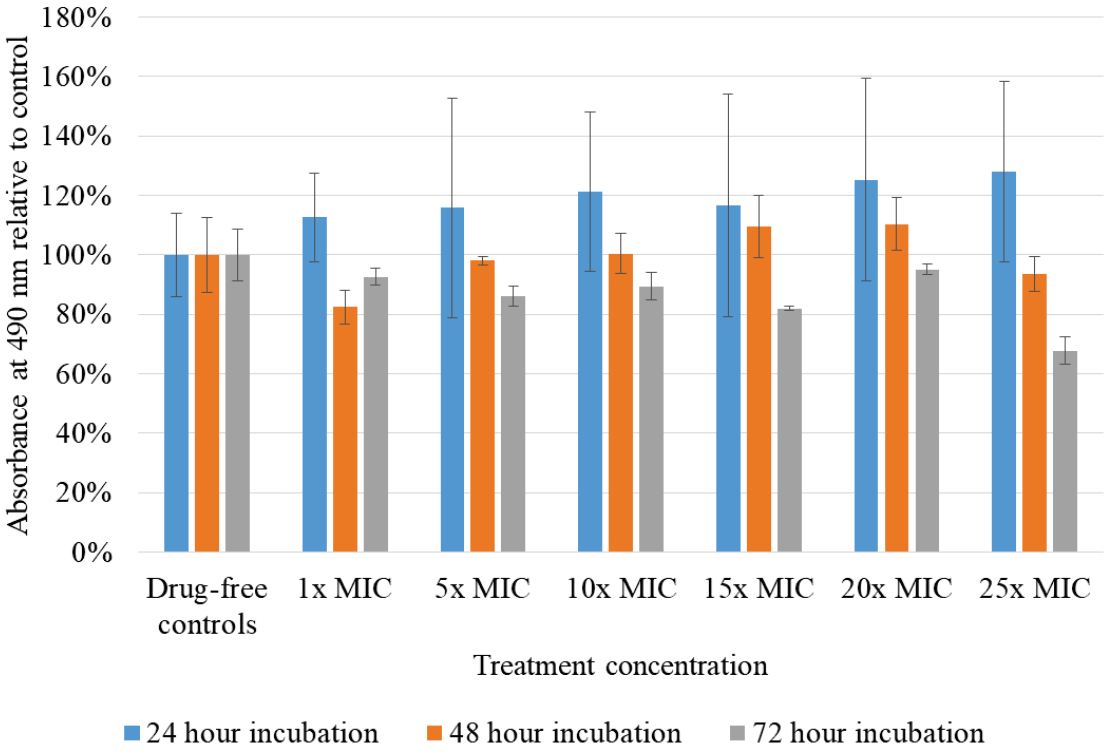

Figure 3.5B Compound 2

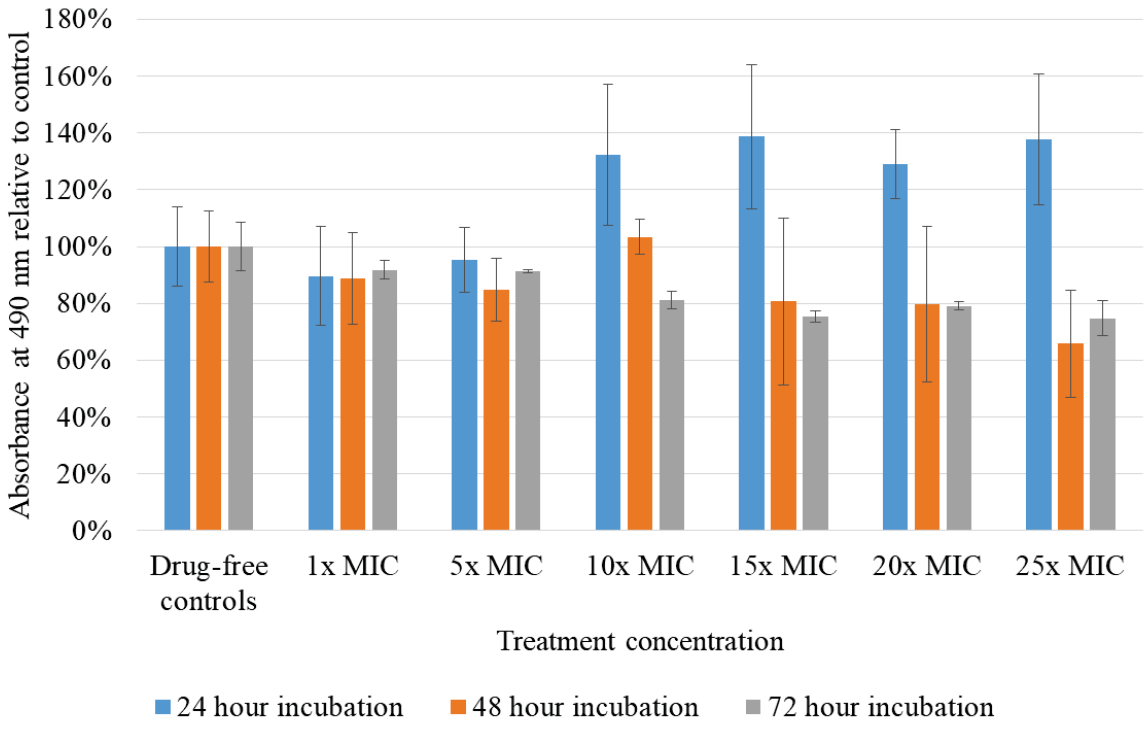

Figure 3.5C Compound 3

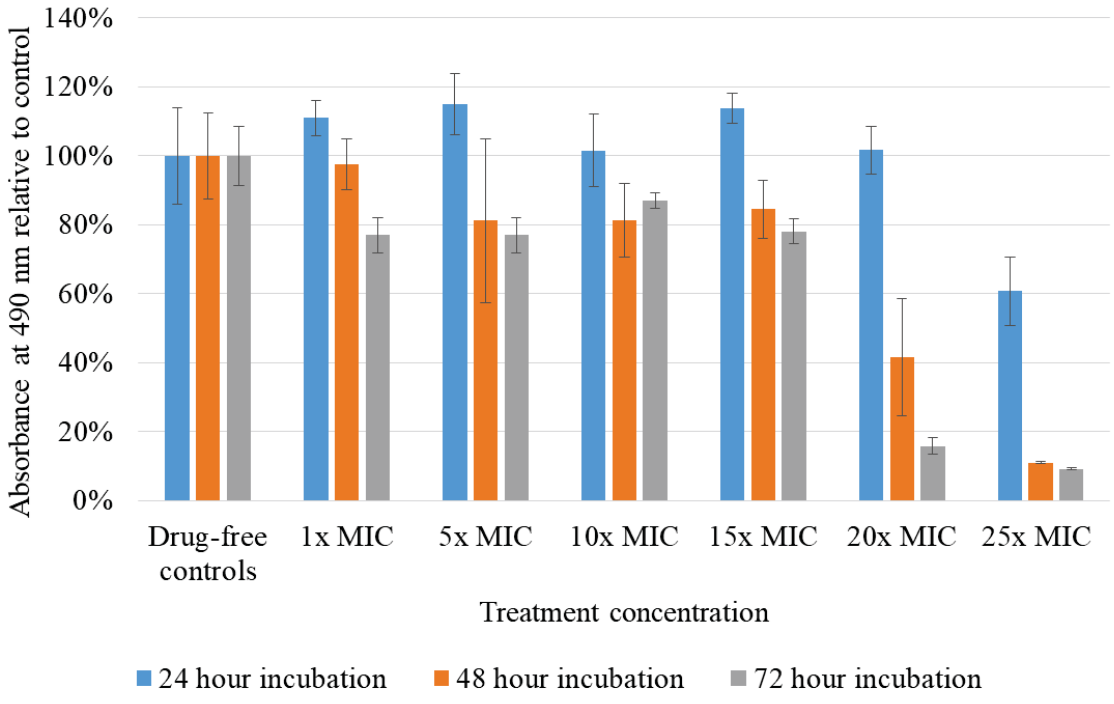

Figure 3.5D Compound 4

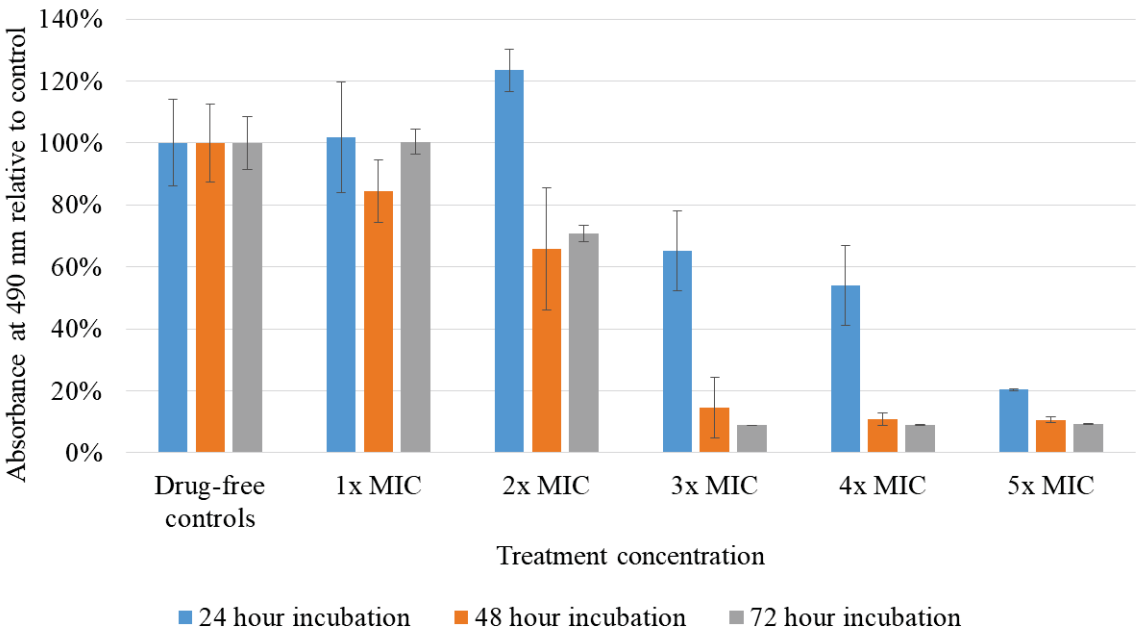

Figure 3.5E Compound 5

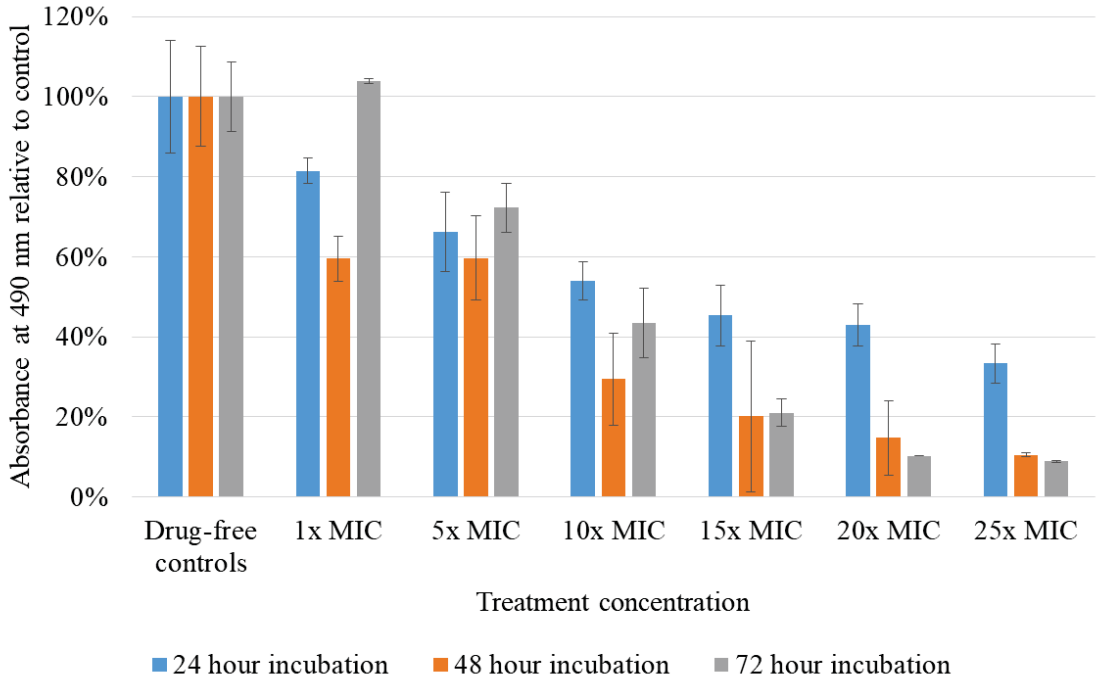

Figure 3.5F Compound 6

Figure 3.5 Charts showing relative cell viability of J774A.1 cells treated with six different OMCs at multiple concentrations for 24, 48, or 72 hours, compared to untreated control cells. After incubation, cell metabolism was assessed by performing an MTS assay and measuring absorbance of each well at 490 nm. Error bars indicate +/- 1 SD from the mean absorbance.

3.3.2 Treatment of *M. bovis* infected J774A.1 cells to evaluate bacterial clearance capabilities of two novel OMCs

One factor ANOVA analysis of the CFU/ml culture from each treatment group did not detect differences in variances among any of the treatment groups at either time point. Figure 3.6 shows bar charts comparing CFU/ml counts among various treatment groups at the two day (Figure Figure 3.6A.1 and Figure 3.6A.2) and five day (Figure 3.6B.1 and Figure 3.6B.2) time points.

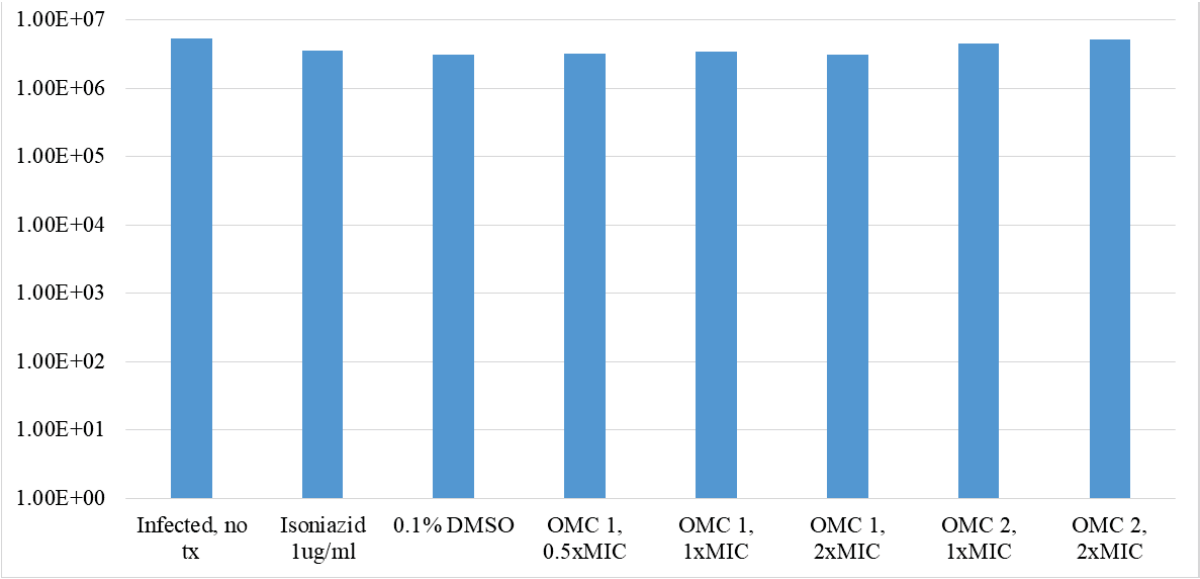

Figure 3.6A.1 Plate A, lysis after 2 days of treatment

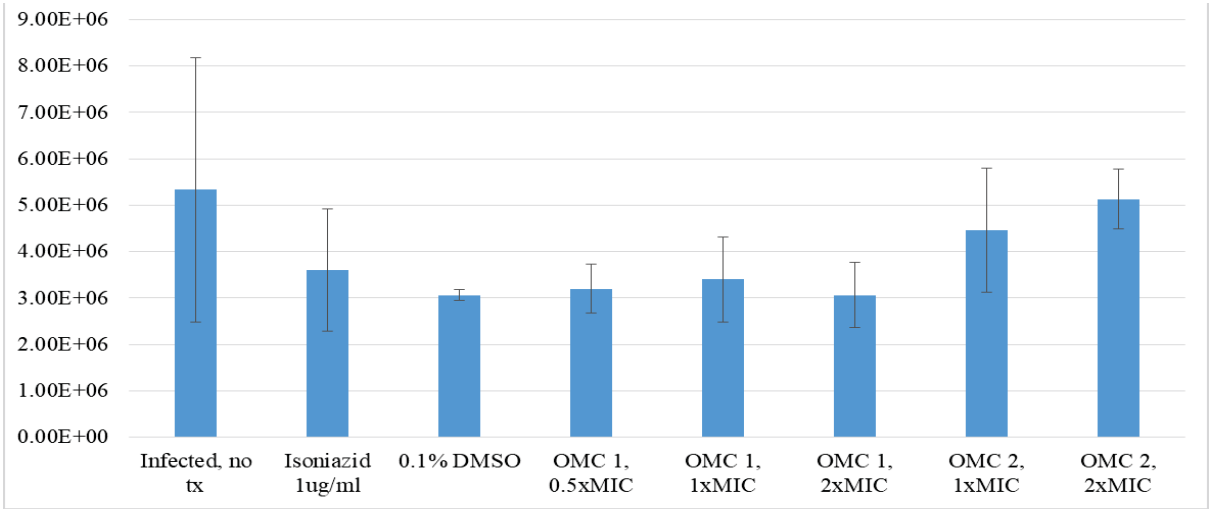

Figure 3.6A.2 Plate A, lysis after 2 days of treatment, close up to show error bars

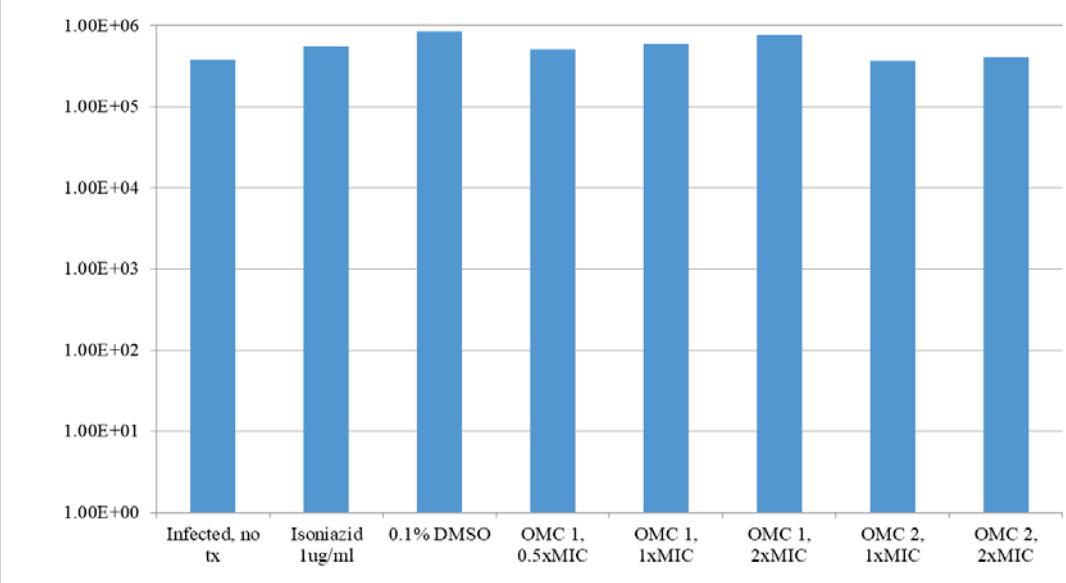

Figure 3.6B.1 Plate B, lysis after 5 days of treatment

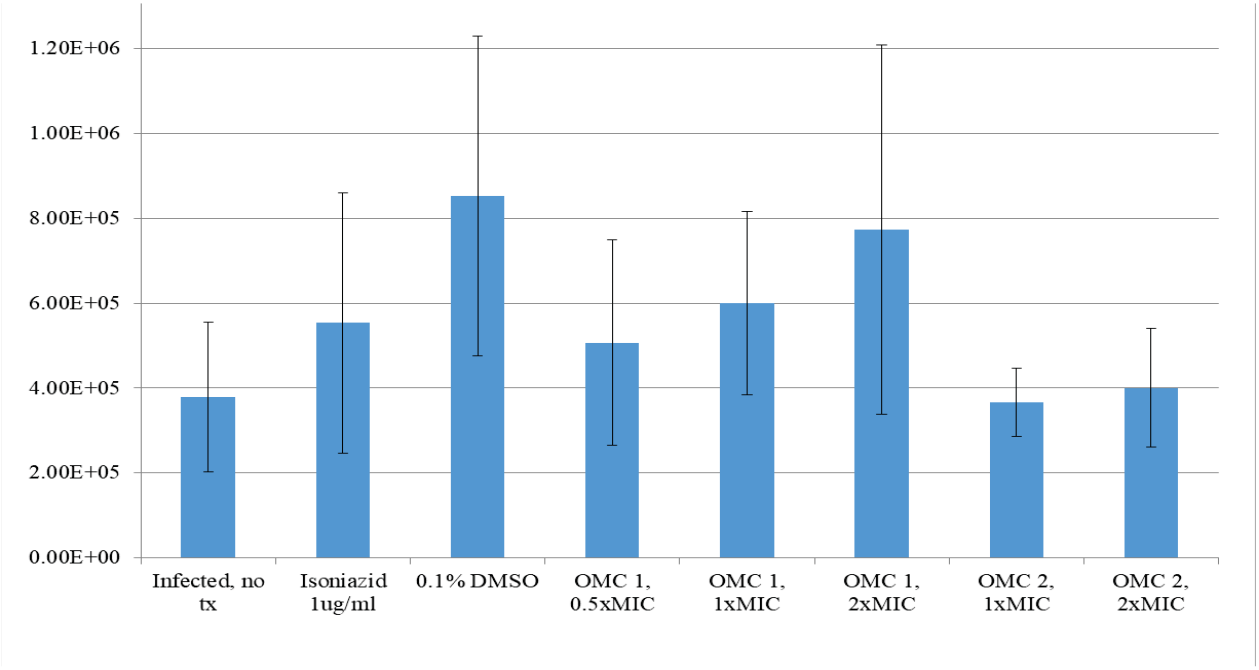

Figure 3.6B.2 Plate B, lysis after 5 days of treatment, close up to show error bars

Figure 3.6 Graphs 6.A.1 and 6.B.1 show relative CFU/ml counts from the various treatment groups after the data was plotted on a log base 10 scale. Graphs 6.A.2 and 6.B.2 are close-up views of the tops of the data columns in Graphs 6.A.1 and 6.B.1, to allow for better visualization of error bars. The error bars show +/- one standard deviation from the mean CFU/ml count from each treatment group. No significant differences in bacterial CFU/ml were found among treatment groups using one factor ANOVA.

The effects of various treatments were also assessed by visually comparing J774A.1 cell confluency and morphology among treated cultures. Photomicrographs of cells from each treatment group are shown in Figure 3.7. See the main figure legend for additional discussion.

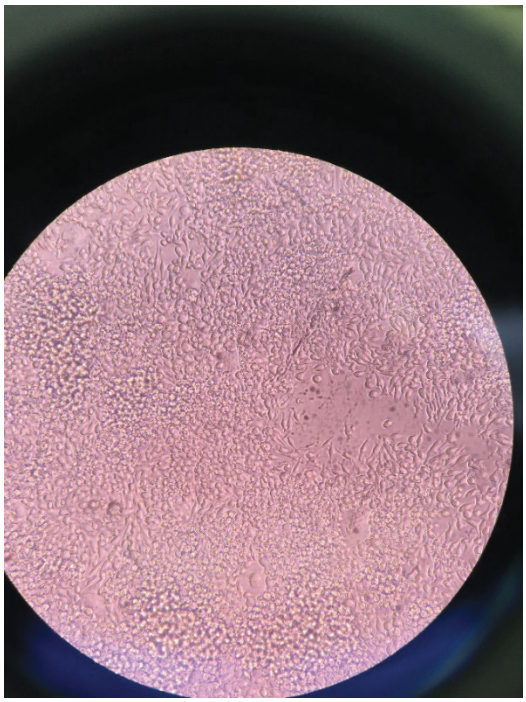

Figure 3.7A: Uninfected, untreated control J774A.1 cells after 5 days of incubation.

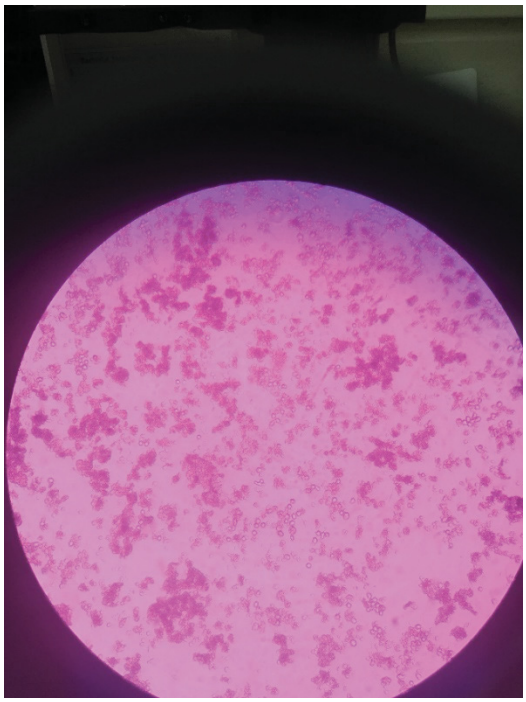

Figure 3.7B: Infected, untreated control J774A.1 cells after 2 days of incubation.

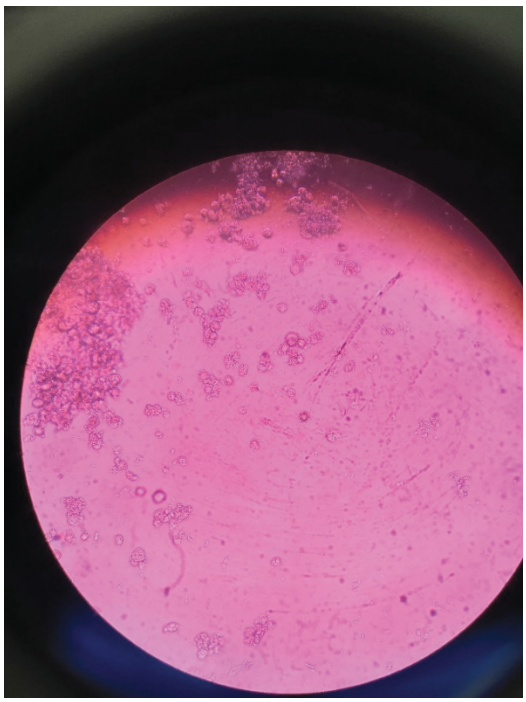

Figure 3.7C: Infected, untreated control J774A.1 cells after 5 days of incubation

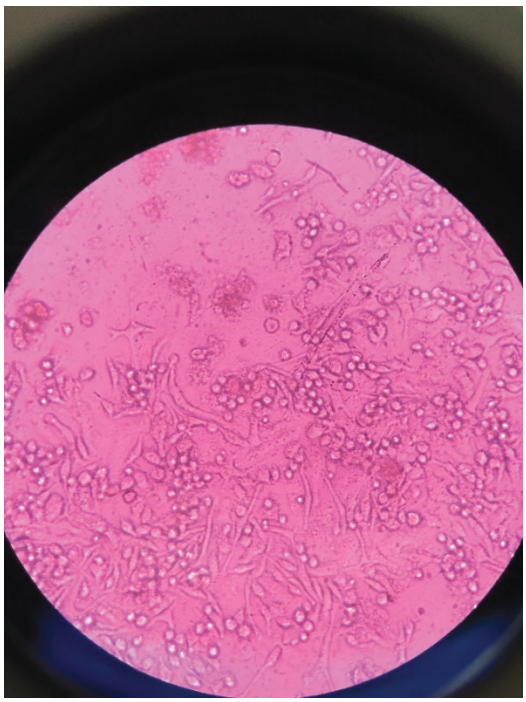

Figure 3.7D: Infected J774A.1 cells treated with 1 µg/ml isoniazid for 5 days.

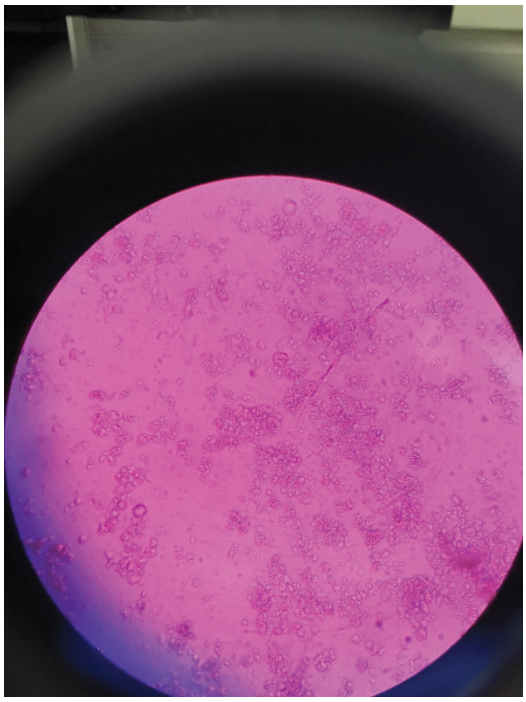

Figure 3.7E: Infected J774A.1 cells treated with 0.1% DMSO for 5 days.

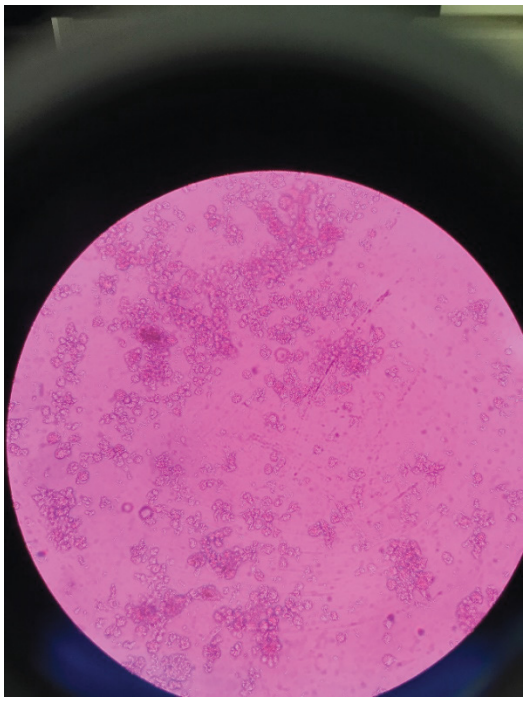

Figure 3.7F: Infected J774A.1 cells treated with OMC 1 at 0.5x MIC for 5 days.

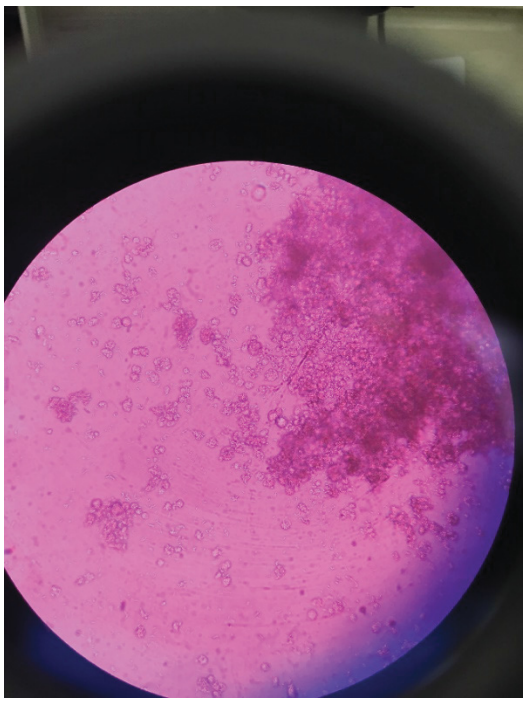

Figure 3.7G: Infected J774A.1 cells treated with OMC 1 at 1x MIC for 5 days.

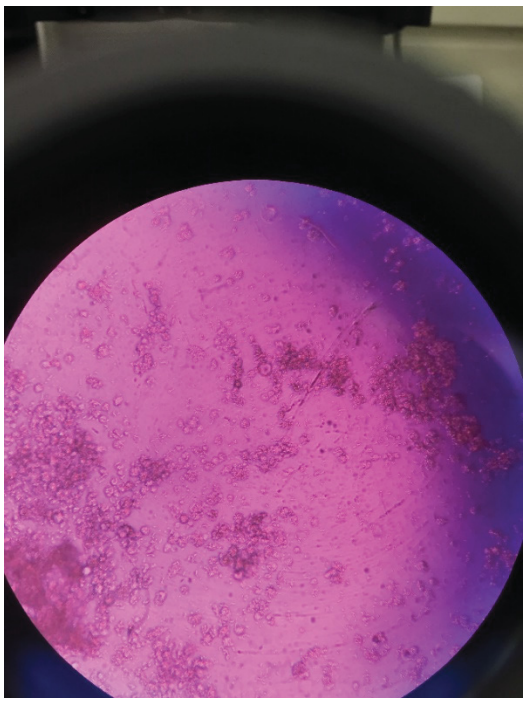

Figure 3.7H: Infected J774A.1 cells treated with OMC 1 at 2x MIC for 5 days.

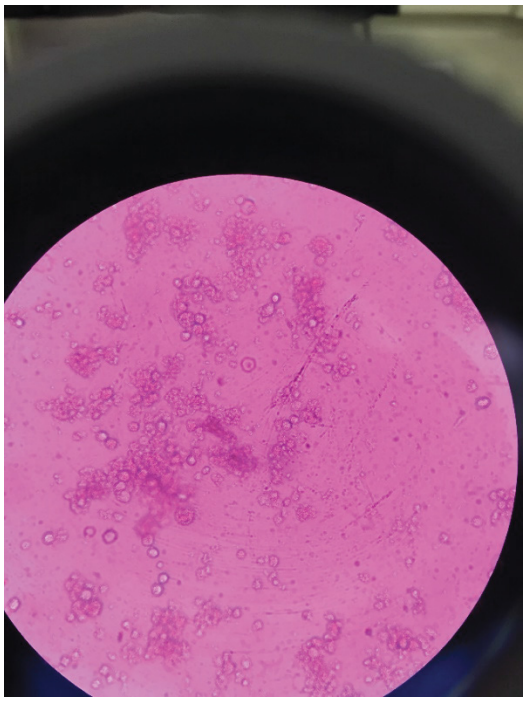

Figure 3.7I: Infected J774A.1 cells treated with OMC 2 at 1x MIC for 5 days.

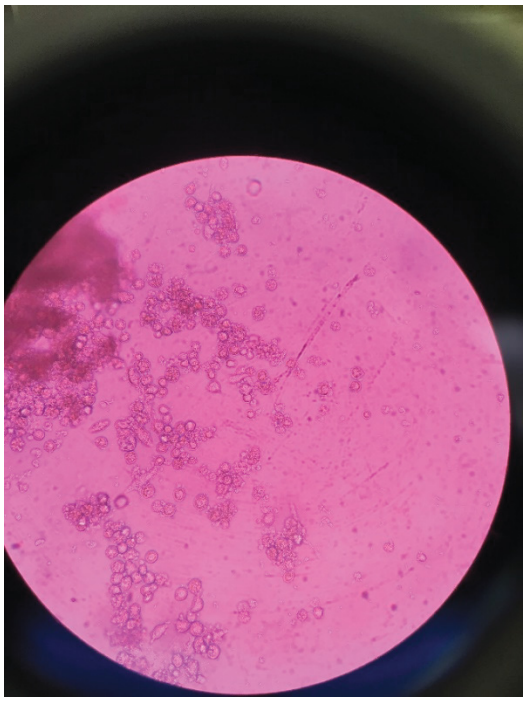

Figure 3.7J: Infected J774A.1 cells treated with OMC 2 at 2x MIC for 5 days.

Figure 3.7 Appearance of J774A.1 cells after 5 days of incubation with the various treatments. Visual examination showed that the amount of cell death of the infected J774A.1 cells was similar among untreated cells (Figures 3.7B and 3.7C), cells treated with DMSO (Figure 3.7E, vehicle control for OMC 2), and cells treated with both of the OMCs (Figures 3.7F-3.7J). Cells treated with isoniazid (Figure 3.7D, antimicrobial-treated control) showed a large decrease in cell confluency, but had a greater number of live dividing cells at the end of five days of treatment than any of the other treatment groups. All of the infected cell cultures showed a large decrease in the amount of live cells compared to the uninfected, untreated control (Figure 3.7A). The amount of cell death was greater in the cultures treated for five days than in the cultures treated for two days (pictures for infected two day cultures not shown).

3.3.3 Assessment of cellular penetrance of Compound 1, IrCp*(L-pg)Cl

Some cell culture wells were lost due to bacterial contamination. Samples were collected and analyzed for content of Ir in cells exposed to the 10 μg/ml 24 hour, 100 μg/ml 24 hour, 10 μg/ml 48 hour, and 100 μg/ml 48 hour treatments. The iridium concentrations measured from each sample are presented in Table 3.2. The table also includes a column with a calculated estimated concentration of Compound 1 in each sample, because the assay specifically measured the concentration of Ir in μg/ml, not the concentration of the whole compound. Iridium makes up only about 37% of the compound by molecular weight, so the Ir concentration was multiplied by a factor of 2.7 to obtain these estimates. Based on the estimated concentration of Compound 1 measured in the cell culture medium samples, recovery of iridium by the ICP-MS assay was approximately 60% in most measurements. Unfortunately, an estimation of the intracellular concentration for Compound 1 in each treatment group could not be calculated, because the total volume of the cell lysate plus the lysate solution (Triton-X), which is what was run through the analyzer, was not recorded. See the Discussion for further thoughts on this point.

The Ir concentrations among treatment groups are also presented graphically in Figure 3.8 to show significant differences among various treatment groups. Both time and dose dependent effects of treatment are observed.

Table 3.2 Iridium concentrations measured in cell culture samples treated with 10 μg/ml or 100 μg/ml Compound 1 for 24 or 48 hours. S = supernatant from cell lysate. M = treated medium.

Sample ID	[Compound 1] in culture medium (μg/ml)	Incubation time (hours)	PBS wash?	Sample type	[Ir] in sample (μg/ml)	Estimated [Compound 1] in sample (μg/ml)
P1A1	10	24	Yes	S	0.016	0.0432
				M	2.197	5.9319
P1A4	10	24	Yes	S	0.015	0.0405
				M	2.236	6.0372
P1C1	10	24	Yes	S	0.015	0.0405
				M	2.236	6.0372
P1D1	10	24	No	S	0.057	0.1539
				M	2.286	6.1722
P2A5	100	24`	Yes	S	0.158	0.4266
				M	15.730	42.471
P1B3	100	24	Yes	S	0.106	0.2862
				M	20.625	55.6875
P1C3	100	24	Yes	S	0.101	0.2727
				M	19.865	53.6355
P1D3	100	24	No	S	0.448	1.2096
				M	17.533	47.3391
P1B4	10	48	Yes	S	0.032	0.0864
				M	2.167	5.8509
P1C4	10	48	Yes	S	0.026	0.0702
				M	2.172	5.8644
P1D4	10	48	No	S	0.068	0.1836
					2.239	6.0453
P1A6	100	48	Yes	S	0.197	0.5319
				M	21.557	58.2039
P1B6	100	48	Yes	S	0.203	0.5481
				M	21.981	59.3487
P1C6	100	48	Yes	S	0.200	0.54
				M	22.335	60.3045
P1D6	100	48	No	S	0.562	1.5174
				M	22.439	60.5853

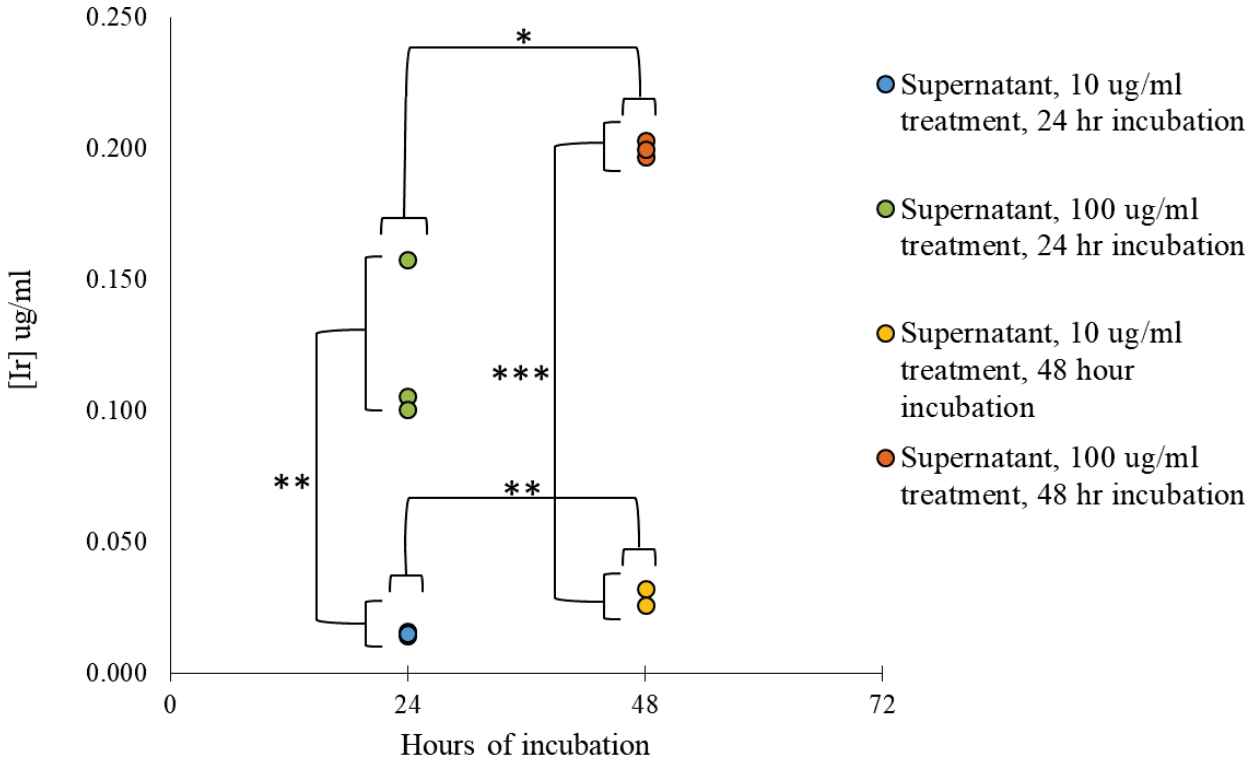

Figure 3.8 Dot plot showing the cell lysate iridium concentrations of each of the treatment wells that were analyzed by ICP-MS. Significant differences were found both between samples of the same concentration at different time points and between samples of different concentrations at the same time points. * indicates $p < 0.05$, ** indicates $p < 0.01$, *** indicates $p < 0.001$.

3.4 Discussion and Conclusions

This group of experiments sought to partially characterize the eukaryotic cell cytotoxicity and cellular penetration capabilities of novel organometallic compounds under study as possible future antimicrobial treatments. The six compounds tested using the MTS cytotoxicity assay were in part chosen based on their micromolar MICs against *M. bovis* BCG or *M. avium* A5. They were also chosen because they had a variety of organic ligands, and one aim was that the cytotoxicity assay could help determine which combinations of metal centers and organic ligands appeared safest in a biologic system and were thus good candidates for further experimentation. Interpretation of this assay is subjective. There are published recommendations on how to interpret cell viability assays, such as the ISO statement that a 30% reduction in cell viability indicates toxicity;[23] however, the decision of what constitutes cytotoxicity in a particular circumstance must be based at least partly on the intended future use of the molecule. In this instance, the long term goal is that some of these OMCs will be used as medicinal drugs, so it seemed prudent to err on the side of caution. A consistent decrease in cell viability below 90% relative to the untreated control was interpreted as a cytotoxic effect, and this interpretation affected the decision of which OMC to use in additional experiments. The results did indeed show notable differences among the various compounds based on ligand identity. The compounds with an iridium center and an amino acid ligand showed either mild or no cytotoxicity (relative cell viability ~ 80-120%), the compounds with a rhodium center and an amino acid ligand showed mild to moderate cytotoxicity (relative cell viability ~70-80%), especially at high concentrations, and the two compounds with either a heptanedionate or fluorophenyl-ethylenediamine ligand showed moderate to marked cytoxicity (relative cell viability 60% or below) in a dose dependent manner. Of the two compounds considered to be non-cytotoxic, Compound 1 was chosen as the focus for the next two experiments because it had the lower MIC. The decision to focus on just one compound was made out of an effort to simplify the experimental set up and pursue only the most promising molecules.

The bacterial clearance study used dilutions of Compound 1 and a second molecule that is identical except that one of the methyl groups on the Cp* ring was replaced with a propyl group. *In vitro* testing of bacterial clearance from infected eukaryotic cells cultures is one of the recommended steps in characterizing a potential antimicrobial substance because it gives some insight into how well the molecule crosses cell lipid membranes, and how the activity of the molecule against the

target organism may differ between pure bacterial cultures and a living system.[21] At the concentrations tested in this experiment, the two compounds did not significantly inhibit intracellular growth of *M. bovis* BCG relative to untreated controls or relative to isoniazid, a conventional antimicrobial used for treatment of tuberculosis. Two major possible reasons for this lack of statistical significance are considered. One is that the OMCs truly have no effect on bacterial proliferation at these concentrations. The other is that the small sample size – three replicate wells of each treatment – prevented detection of statistical significance. Either way, the minimal amount of difference in growth noted with visual evaluation of the bar charts is not considered clinically significant. In addition, during sample preparation for treatment of the cell cultures it became clear that the second compound, with an attached propyl group on the Cp* ring, was insoluble in water, and had to be dissolved in DMSO. This can be undesirable for a potential medicinal molecule because the goal in drug development is often to produce a hydrophilic compound that can be taken orally and absorbed into the bloodstream.[21] One other observation of interest is that isoniazid, used as a positive control for current treatment of mycobacterial infections also did not significantly decrease intracellular bacterial growth relative to the untreated control. The concentration of 1 μg/ml isoniazid was chosen based on published critical concentrations for isoniazid against *Mycobacterium tuberculosis* which are generally in the range of 0.2-1 μg/ml.[24-25] These reflect the concentrations effective in a pure culture of *M. tuberculosis* and it is possible that a concentration of 1 μg/ml was not high enough to cause effective intracellular bacterial inhibition.

To further evaluate the ability of Compound 1 to cross eukaryotic cell membranes, uninfected J774A.1 cells were incubated with various concentrations of the compound and the intracellular iridium concentration was measured. Comparison of the Ir concentrations in the cell lysate samples with those of the treated medium samples suggests that the compound does penetrate intracellularly, but only in minute amounts. It appears likely that intracellular penetration of the compound is low, and would not be enough to effectively clear bacteria. However, it actually cannot be said with certainty whether or not minimum inhibitory concentrations of the compound were achieved intracellularly because, unfortunately, the total volume of the cell lysate plus the lysate solution (Triton-X), which is what was run through the analyzer, was not recorded. Due to this omission the intracellular concentration of the compound could not be calculated with

certainty, because a dilution factor is missing. This experiment should be repeated and all applicable data collected so that a more accurate estimate of intracellular Compound 1 concentrations can be determined. One conclusion that can be made with certainty from the results of this experiment is that penetration of the compound is both time and dose dependent, as shown by the differences between the 24 hour and 48 hour treatments and the 10 μg/ml and 100 μg/ml treatments.

Several important limitations to these experiments are noted. Eukaryotic cell cytotoxicity was only evaluated using the MTS assay, which indirectly assesses cellular metabolic activity by measuring the ability of cells to reduce a tetrazolium salt to a colored product. However, there are multiple assays available for assessing cytotoxicity *in vitro*, such as the simple trypan blue evaluation, in which live and dead cells are visually counted on a hemocytometer, or bioluminescent ATP assays, which estimates the relative number of living cells by directly measuring the amount of ATP in a culture.[26] It is ideal to test the cytotoxicity of a compound using several different types of assays, as each has various advantages and disadvantages and provides slightly differing information about relative cell viability. In addition, only one non-human eukaryotic cell line was used for the experiments. Testing a compound against a variety of different cell lines, including human derivatives, is usually expected for a compound that may be used as a medicine. Also, the concentrations used for the bacterial clearance study were low, well below the recorded MIC for Compound 1 against *M. bovis* in pure culture, and also much lower than the concentrations determined to cause no or little cytotoxicity. It is possible that repeating this type of experiment with higher concentrations would yield different results.

The process of characterizing a novel chemical compound in anticipation of developing a new drug is long and arduous, and the vast majority of compounds do not progress beyond early stages of experimentation.[27-28] In order to seriously consider a compound as a candidate for additional study, one would want to see evidence of facile transit across cell membranes and a several-log decrease in bacterial CFU/ml counted in infected cell cultures treated with the molecule. Therefore, based on these initial results, Compound 1 does not at first appear as a highly desirable lead compound. However, the low cytotoxicity of the compound against a eukaryotic cell line is a positive finding, and there is actually still a great deal to learn about this molecule and its possible

derivatives before deciding whether or not they should be pursued as possible antimicrobials. Several future directions for this research are recommended. The cytotoxicity of the compound should be tested with at least two other types of cytotoxicity assays, and against other eukaryotic cells lines. After a more accurate idea of the cellular penetration abilities of the compound is obtained, experiments should be conducted to improve the ability of Compound 1 or a related compound to cross cell membranes while still maintaining hydrophilicity. Possible options include encapsulation of the compound in a lipophilic nanoparticle vehicle, or altering chemical groups on the Cp* ring or ligand.

In conclusion, these experiments show that several novel organometallic compounds under consideration as possible antimycobacterial drugs cause little to no cytotoxicity against J774A.1 murine macrophage-like cells, but likely do not easily penetrate eukaryotic cell membranes. They also do not inhibit intracellular bacterial growth at low concentrations. The lack of cytotoxicity is encouraging, but effort should go toward improving the ability of these compounds to cross cell membranes. Their ability to inhibit intracellular bacterial growth should also be further evaluated and improved before progressing to more advanced experimentation such as large scale toxicity studies in *in vivo* models.

3.5 References

1. Addo K, Owusu-Darko K, Yeboah-Manu D, et al. Mycobacterial species causing pulmonary tuberculosis at the Korle Bu Teaching Hospital, Accra, Ghana. Ghana Med J. 2007;41(2):52-57.
2. Adjemian J, Frankland TB, Daida YG, et al. Epidemiology of nontuberculous mycobacterial lung disease and tuberculosis, Hawaii, USA. Emerg Infect Dis.2017;23(3)439-447.
3. Rodrigues LC and Lockwood DNJ. Leprosy now: epidemiology, progress, challenges, and research gaps. Lancet Infect Dis. June 2011;11:464-470
4. World Health Organization. WHO treatment guidelines for drug-resistant tuberculosis 2016 update October 2016 revision. https://apps.who.int/iris/bitstream/handle/10665/250125/9789241549639-eng.pdf;jsessionid=6B4EE9CEADA3F5B7022359134F37F89D?sequence=1. Accessed January 31, 2019.
5. Tang J, Yam W, and Chen Z. Mycobacterium tuberculosis infection and vaccine development. Tuberculosis. February 2016;98:30-41.
6. World Health Organization. Global Tuberculosis Report 2018. https://www.who.int/tb/publications/global_report/en/. Accessed January 31, 2019.
7. Welin A, Winberg ME, Abdalla H, et al. Incorporation of Mycobacterium tuberculosis lipoarabinomannan into macrophage membrane rafts is a prerequisite for the phagosomal maturation block. Infect Immun. 2008;76(7):2882-2887.
8. Goldberg MF, Saini NK, Porcelli SA. Evasion of innate and adaptive immunity by Mycobacterium tuberculosis. Microbiol Spectr. 2014;2(5). doi: 10.1128/microbiolspec.MGM2-0005-2013.
9. Frieden TR, Sterling T, Pablos-Mendez A, Kilburn JO, Cauthen GM, and Dooley SW. The emergence of drug-resistant tuberculosis in New York City. N Engl J Med. 1993;328(8):521-526.
10. Rullan JV, Herrera D, Cano R, et al. Nosocomial transmission of multidrug-resistant Mycobacterium tuberculosis in Spain. Emerg Infect Dis. 1996;2(2):125-129.

11. Migliori GB, Ortmann J, Girardi E, et al. Extensively drug-resistant tuberculosis, Italy and Germany. Emerg Infect Dis. 2007;13(5):780-781.
12. Velayati AA, Masjedi MR, Farnia P, et al. Emergence of new forms of totally drug-resistant tuberculosis bacilli: super extensively drug-resistant tuberculosis or totally drug-resistant strains in Iran. Chest. 2009;136(2);420-425.
13. Karpin GW, Merola JS, and Falkinham JO. Transition metal-α-amino acid complexes with antibiotic activity against Mycobacterium spp. Antimicrob Agents Chemother. 2013;57(7):3434-3436. doi: 10.1128/AAC.00452-13.
14. Rosenberg B, Van Camp L, and Krigas T. Inhibition of cell division in *Escherichia coli* by electrolysis products from a platinum electrode. Nature. February 1965;205:698-699.
15. Rosenberg B, Van Camp L, Trosko JE, Mansour VH. Platinum compounds: a new class of potent antitumour agents. Nature. April 1969;222:385-386.
16. Patra M, Gasser G, and Metzler-Nolte N. Small organometallic compounds as antibacterial agents. Dalton Trans. 2012;41:6350-6358.
17. Pandrala M, Li F, Feterl M, et al. Chlorido-containing ruthenium(II) and iridium(III) complexes as antimicrobial agents. Dalton Trans. 2013;42:4686-4694.
18. Lu L, Liu L, Chao W, et al. Identification of an iridium(III) complex with anti-bacterial and anti-cancer activity. Sci Rep. January 2015. doi: 10.1038/srep14544.
19. Chellan P, Avery VM, Duffy S, et al. Organometallic conjugates of the drug sulfadoxine for combatting antimicrobial resistance. Chem Eur J. 2018;24:10078-10090.
20. Liu Z, Habtemariam A, Pizarro AM, et al. Organometallic half-sandwich iridium anticancer complexes. J Med Chem. January 2011;54:3011-3026.
21. Hughes D and Karlen A. Discovery and preclinical development of new antibiotics. Ups J Med Sci. 2014;119:162-169.
22. Penuelas-Urquides K, Villarreal-Trevino L, Silva-Ramirez B, Rivadeneyra-Espinoza L, Said-Fernandez S, and Bermudez de Leon M. Measuring of Mycobacterium tuberculosis growth. A correlation of the optical measurements with colony forming units. Braz J Microbiol. 2013;44(1):287-290.
23. International Standard. ISO 10993-5 Third Edition. Biological evaluation of medical devices – Part 5: Tests for *in vitro* cytotoxicity. 2009. Reference number ISO 10993-5;2009(E).

24. Gumbo T. New susceptibility breakpoints for first-line antituberculosis drugs based on antimicrobial pharmacokinetic/pharmacodynamic science and population pharmacokinetic variability. Antimicrob Agents Chemother. 2010;54(4):1484-1491.
25. Burke RM, Coronel J, Moore D. Minimum inhibitory concentration distributions for first- and second-line antimicrobials against *Mycobacterium tuberculosis*. J Med Microbiol. 2017;66(7):1023-1026.
26. Niles AL, Moravec RA, and Riss TL. Update on *in vitro* cytotoxicity assays for drug development. Expert Opin Drug Discov. 2008;3(6):655-669.
27. Corr P and Williams D. The pathway from idea to regulatory approval: examples for drug development. In: Lo B and Field MJ, eds. Conflict of Interest in Medical Research, Education, and Practice. Washington, DC: The National Academies Press; 2009:375-383.
28. Torjesen I. Drug development: the journey of a medicine from lab to shelf. The Pharm J. March 2015. https://www.pharmaceutical-journal.com/publications/tomorrows-pharmacist/drug-development-the-journey-of-a-medicine-from-lab-to-shelf/20068196.article?firstPass=false. Accessed January 31, 2019.

4 Peptide nucleic acids targeting expression of tetracycline resistance genes increase tetracycline susceptibility in multidrug-resistant *Salmonella enterica* ssp. *enterica* serovar Typhimurium DT104

4.1 Introduction

The CDC estimates that in the United States there are a minimum of 2,000,000 illnesses and 23,000 deaths due to antibiotic resistance annually.[1] Enteric pathogens such as nontyphoidal *Salmonella* are among those showing increased antibiotic resistance over the past century. Approximately 5% of nontyphoidal *Salmonella* isolates tested by the CDC are resistant to at least five classes of antibiotics,[1] and it is estimated that in the United States there are annually more than 1 million cases of salmonellosis, leading to thousands of hospitalizations and several hundred deaths.[2] *Salmonella enterica* ssp. *enterica* serovar Typhimurium DT104 (DT104) is of great concern due to its increasing prevalence among human and animal clinical isolates in multiple countries.[3-5] This phage type frequently shows resistance to ampicillin, chloramphenicol, streptomycin, sulfonamides, and tetracycline (R-type ACSSuT), due to a 43-kb chromosomal fragment called *Salmonella* genomic island 1 (SGI1) that contains multiple resistance genes, including that for the TetA tetracycline efflux pump.[6-8]

Research into potential new antimicrobials, or into ways to repurpose existing antibiotics is warranted. One possible approach is the use of antisense molecules to inhibit expression of bacterial essential or antibiotic resistance genes. Antisense antibacterials are linear molecules designed to bind mRNA or DNA in a complementary fashion such that bacterial protein translation or gene transcription is halted.[9] This can be accomplished with unmodified RNA or DNA sequences that directly complement the target gene, but such molecules may be easily displaced from the target gene and also are usually degraded quickly by bacterial nucleases. Modification of the chemical backbone of the antisense molecule can help address these limitations.[10] Peptide nucleic acids (PNAs), first described and characterized by Nielsen et al.[11] are uncharged antisense oligomers with a peptide backbone (Figure 4.1) that bind stably and strongly to target nucleic acids[12] and are resistant to degradation by intracellular nucleases and proteases.[13] The mechanism of action likely involves steric hindrance of DNA transcription or mRNA translation, by blocking access of ribosomes to binding sites on the nucleic acid (Figure 4.2).[10]

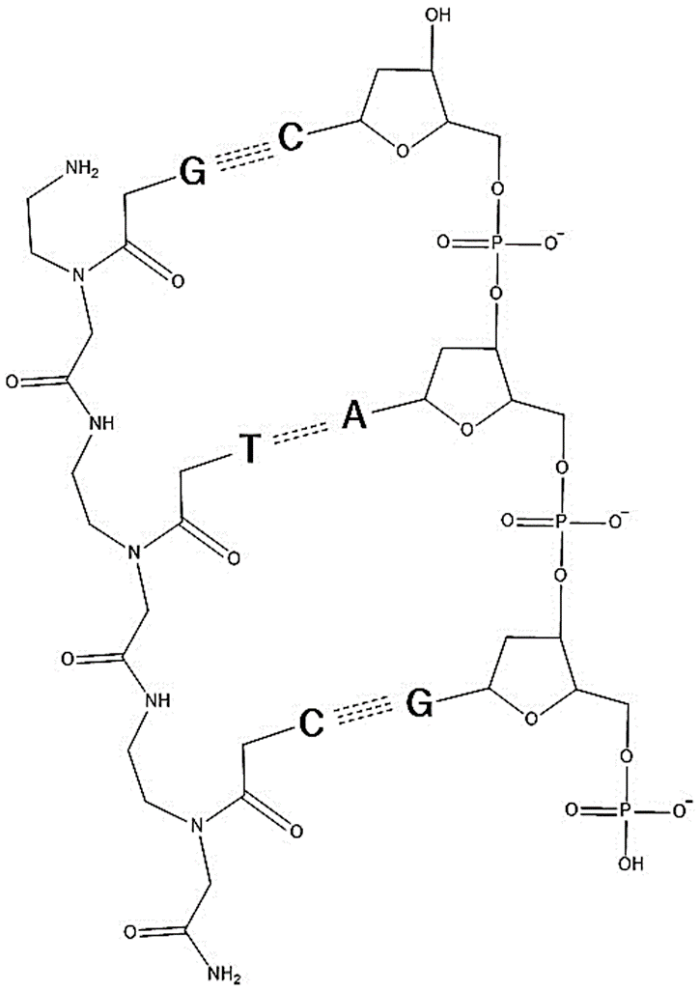

Figure 4.1 Structure of a portion of a PNA (left) binding a complementary strand of DNA (right) by Watson-Crick base pairing. Unlike DNA, which has a sugar-phosphate backbone, PNAs have an N-(2-aminoethyl)-glycine (peptide) backbone that is not recognized by bacterial nucleases. This makes the PNAs resistant to cellular degradation. The peptide backbone is also uncharged, so there is no negative repulsion between the PNA and negatively charged DNA or RNA molecules. These characteristics make PNA-DNA or PNA-RNA bonds stronger and longer-lasting than DNA-DNA or RNA-DNA bonds

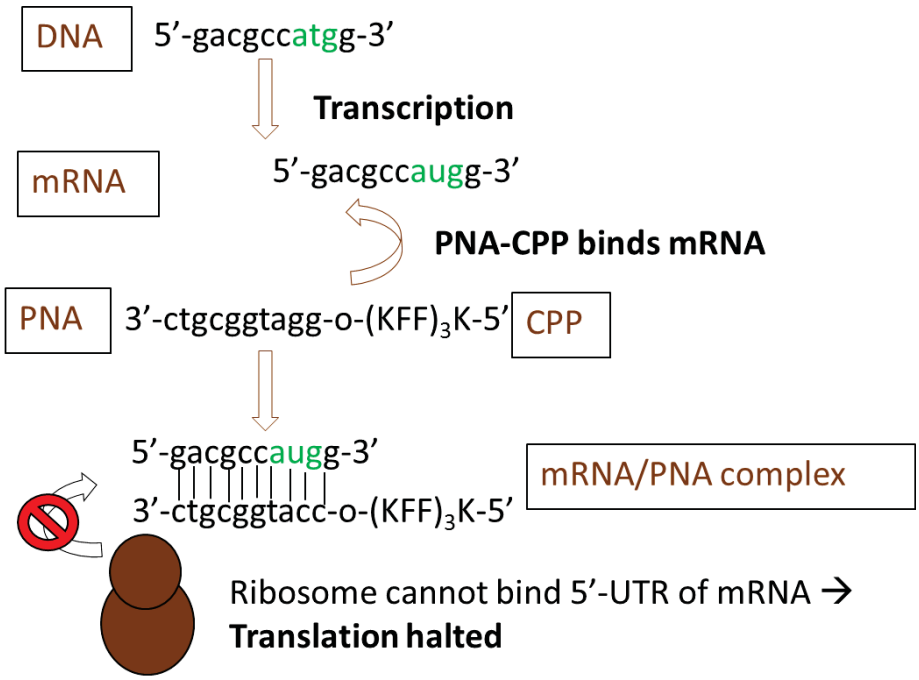

Figure 4.2 The proposed mechanism of action for PNA inhibition of gene expression is steric hindrance of ribosomal binding to the start codon region of mRNA (and likely DNA). The start codon is shown in green. After transcription of DNA to mRNA in the nucleus (first down arrow), the mRNA would ordinarily be bound by a ribosome and translated into a peptide sequence. If a complementary PNA molecule bound to a cell-penetrating peptide (CPP) encounters the mRNA (first curved arrow), a stable bond will form that interferes with ribosomal binding (crossed-out upward arrow) and prevents translation.

Peptide nucleic acids targeting essential bacterial genes have been shown to inhibit growth of pure cultures of various bacterial species including *Brucella suis*,[14] methicillin-resistant *Staphylococcus aureus* (MRSA),[15] and *Salmonella* Typhimurium,[16] and when appropriately designed they can even inhibit growth of selected species of bacteria within a mixed culture.[17] There are also a few reports of PNAs designed to target antibiotic resistance genes restoring antibiotic susceptibility in pure cultures of resistant bacteria. Examples include restoration of ampicillin susceptibility in resistant *Escherichia coli*[18] and restoration of oxacillin susceptibility in MRSA.[19]

Peptide nucleic acids do not readily cross cell membranes, so cellular penetration and bacterial inhibitory effects are often facilitated by linkage of PNAs to cationic cell penetrating peptides (CPPs)[20] These molecules increase permeability of anionic gram-negative bacterial membranes by

competing with stabilizing divalent cations in the lipopolysaccharide layer; one of the most commonly used CPPs is KFFKFFKFFK,[21] which consists of basic lysine (K) and hydrophobic phenylalanine (F) residues.[22] The primary aim of this study was to evaluate if a CPP-PNA targeting expression of the *tetA* gene, which codes for a tetracycline efflux pump, could restore tetracycline susceptibility in a resistant bacterial organism. A secondary goal was to evaluate the effect of a PNA targeting the resistance regulatory gene *tetR*, which has modulatory effects on *tetA* expression.[23]

4.2 Materials and Methods

4.2.1 Selection of model organism

Selection of a model organism was based on the desire to use a fast-growing, biosafety level-2 (BSL-2) or lower organism with a well-characterized genome and documented non-essential genes imparting resistance to at least one conventional antibiotic. Several strains of *Salmonella* from the Sriranganathan laboratory stock cultures were tested for susceptibility to multiple antibiotics (Table 4.1) using the Kirby-Bauer disc diffusion method. A culture of *Salmonella enterica* ssp. *enterica* serovar Typhimurium DT104 (DT104) was chosen for further experimentation based on its resistance to tetracycline and the availability of the DT104 genome in public databases including Pubmed Nucleotide and Pathosystems Resource Integration Center (PATRIC, patricbrc.org). This bacterial strain is a Biosafety Level 2 (BSL-2) organism, so all work was done under BSL-2 laboratory conditions, and any tasks requiring manipulation of open cultures was done in a Class II Type A2 biosafety cabinet (Labconco, Kansas City, MO).

A minimum inhibitory concentration (MIC) assay performed by the microbiology section of Virginia Tech Animal Laboratory Services at the Virginia-Maryland College of Veterinary Medicine confirmed tetracycline resistance in the chosen strain.

Table 4.1 Zones of resistance (mm) and susceptibility of eight strains of *Salmonella* after Kirby-Bauer susceptibility testing with 12 conventional antibiotics. The box where *S.* Typhimurium DT104 crosses with tetracycline is yellow to highlight the tetracycline-resistance of this organism. The mechanism of resistance is a tetracycline efflux pump, the gene for which was chosen as the target for experiments in reversing antibiotic resistance using PNAs.

***Salmonella* strain**	**AN**	**AM**	**TE**	**NA**	**GM**	**CRO**	**PB**	**XNL**	**RA**	**SXT**	**ENO**	**C**
S. enteritidis molR 20 ppm	28^S	23^S	25^S	0^R	28^S	33^S	17^S	25^S	0^R	28^S	23^S	22^S
S. Typhimurium molR 20 ppm	31^S	32^S	27^S	0^R	29^S	38^S	17^S	34^S	8^R	29^S	26^S	31^S
Wildtype *Salmonella*	28^S	26^S	25^S	31^S	28^S	34^S	18^S	29^S	20^S	30^S	38^S	0^R
S. Typhimurium NalR	33^S	34^S	29^S	0^R	32^S	40^S	18^S	34^S	9^R	30^S	27^S	30^S
S. Typhimurium 789	26^S	0^R	0^R	23^S	26^S	33^S	16^S	28^S	8^R	23^S	29^S	0^R
S. Typhimurium DT104	26^S	0^R	10^R	22^S	25^S	32^S	15^S	26^S	9^R	23^S	29^S	0^R
S. Typhimurium LT2 3552 flux 1	33^S	0^R	0^R	37^S	31^S	38^S	19^S	34^S	16^R	39^S	50^S	38^S
S. Typhimurium LT2 3394 flux 10	35^S	0^R	27^S	34^S	31^S	3^S	18^S	33^S	14^R	34^S	44^S	33^S

List of abbreviations: AN amikacin, AM ampicillin, TE tetracyline, NA nalidixic acid, GM gentamicin, CRO ceftriaxone, PB polymyxin B, XNL ceftiofur, RA rifampin, SXT sulfamethoxazole/trimethoprim, ENO enrofloxacin, C chloramphenicol. Superscripts: S indicates susceptible, R indicates resistant.

4.2.2 Confirmation of serotype

Verification of the serotype was performed because the original laboratory record indicating the source of the DT104 laboratory stock strain was not located. It was important to confirm that the serotype label was correct to ensure that PNA design would be accurate. To verify the serotype, PCR amplification of ST104, a prophage sequence unique to DT104, was performed as described by Yukawa et al (2015).[24] Cell pellets made from pure cultures of DT104 and NalR, another laboratory stock strain of *Salmonella* that is not tetracycline-resistant and is genetically distinct from DT104, were suspended in 2 ml tubes and floated in boiling water for 20 minutes to kill and lyse the cells and release genomic DNA (gDNA). The boiled tubes were spun at 13,000 x G for 3 minutes to pellet the cell debris, and the supernatants containing DNA were drawn off and stored at -20 C˚ in 50 ul aliquots until needed. Primers for *InvA*, a gene common to all *Salmonella* species/strains, and for ST104 were previously published by Yukawa et al.[24] These primer pairs were ordered from Sigma, resuspended, and stored at -20 ˚C as 10 μM forward/reverse primer mixes. The primer sequences are provided in Table 4.2. To validate these primers and verify the identity of the DT104 strain, six PCR tubes were set up as shown in Table 4.3.

Table 4.2 Primer sequences used to confirm the DT104 serotype of the *Salmonella* organism chosen for experimentation with PNAs. InvA is a gene common to all *Salmonella* species and was used as a positive control. ST104 is a prophage sequence unique to *S.* Typhimurium DT104 (DT104). The expectation was that ST104 DNA would be amplified from the laboratory stock bacterial strain presumed to be DT104, but not from the non-DT104 strain identified as NalR.

Gene	**Forward primer 5'-3'**	**Reverse primer 5'-3'**	**Product**
InvA	TTGTTACGGCTATTTTGACCA	CTGACTGCTACCTTGCTGATG	521 bp
ST104	TACCGCCATTCGCATAAACG	CAGAGGTTGGTATTGTAGCG	312 bp

Table 4.3 Primer and DNA template combinations in PCR reaction mixes prepared for confirmation of the DT104 serotype of the *Salmonella* strain chosen for experiments with PNAs.

Tube	**Primer mix**	**Template DNA**
1	ST104	NalR
2	ST104	DT104
3	*InvA*	NalR
4	*InvA*	DT104
5	ST104	None
6	*InvA*	None

The PCR reaction was run using a CFX96 Real-Time PCR Detection System (Bio-Rad, Hercules, CA). The reaction mixture in each PCR tube consisted of 20 µl GoTaq Green Master Mix, 16 µl sterile nuclease-free water (or 18 µl for DNA-free control tubes), 2 µl primer mix (1 µM final concentration), and 2 µl template DNA (or 0 µl for DNA-free control tubes), for a final volume of 40 µl. The PCR protocol was

1) 95 C˚ x 30 sec →
2) [95 C˚ x 30 sec → 55 C˚ x 30 sec → 72 C˚ x 1 min] x 30 cycles →
3) 72 C˚ x 5 min

Amplicon bands were visualized using conventional agarose gel electrophoresis with ethidium bromide staining. A DT104 sample was also sent out to the USDA National Veterinary Services Laboratories (NVSL, Ames, IA, USA) for independent verification of the serotype and phage type.

4.2.3 PNA design

Chosen genes

The GenBank genome for DT104 (reference number HF937208.1) was used as the standard when searching for target genes of interest. This genome was cross-referenced with the genome for DT104 on PATRIC, and good agreement was found between the recorded sequences. The genome was searched for genes that are known or theorized to impart resistance to tetracycline. Chosen genes included *tetA*, which codes for the TetA tetracycline efflux pump, and *tetR*, which codes for

the regulatory protein TetR. TetR is not an antibiotic resistance protein *per se*, but is understood to have modulatory effects on resistance proteins such as TetA. These two genes are part of the main chromosome, rather than on a plasmid, and are relatively close together. For these experiments, 10-mer (10 base-pairs long) PNAs were designed to complement the mRNA start codon and part of the 5'-untranslated region (UTR) of the target genes. These decisions were based on previously published literature indicating that the ideal length of bactericidal PNAs is 9- to 12-mer,[25] and that targeting the start codon region leads to the most effective gene inhibition.[26]

A previously designed PNA[16] targeting the essential *tsf* gene was chose as a positive control for PNA action. As a negative control for PNA action, a PNA with a nonspecific nucleic acid sequence was designed. Table 4.4 provides details about the target genes and PNA sequences. All PNAs were linked to a cell penetrating peptide (CPP) with the amino acid sequence $(KFF)_3K$, where K is lysine and F is phenylalanine. The PNAs and CPP were bound together with an O-linker, a 9-atom organic molecule that improves solubility (Figure 4.3). The PNAs were synthesized and tested for purity by PNA Bio (Newberry Park, CA), then shipped as a dry powder for reconstitution in the laboratory.

Table 4.4 Description of the PNA sequences chosen for experimental manipulation of the response of DT104 to tetracycline. The start codon for each gene is highlighted in green. In order to facilitate crossing of the cell membrane, the PNAs were bound to a cell-penetrating peptide, $(KFF)_3K$, by an O-linker.

GenBank gene reference number and/or name	**Function**	**Target DNA sequence (5'-3')**	**PNA sequence (5'-3') with attached CPP and o-linker**	**Name used in text**
DT104_38611 tetracycline resistance protein class A (*tetA*)	Codes for the TetA protein, a tetracycline efflux pump that is upregulated in the presence of intracellular tetracycline	gacgccatgg	(KFF)3K-o-ccatggcgtc	CPP-anti-tetA PNA
DT104_38601 tetracycline resistance regulator protein (*tetR*)	Codes for TetR, a protein that suppresses TetA expression under normal conditions, and is upregulated in the presence of intracellular tetracycline	cgtgaatgac	$(KFF)_3K$-o-gtcattcacg	CPP-anti-tetR PNA
tsf, translation elongation factor	Codes for an essential protein that forms part of a complex that stabilizes new peptides during the elongation stage of translation	ttagaatggc	(KFF)3K-o-gccattctaa	CPP-Sal-tsf
			This PNA was also ordered without an attached CPP	Sal-tsf
Control PNA	Nucleotide sequence with no known target in the DT104 genome	None	(KFF)3K-o-catactgcat	CPP-Control PNA
Cell penetrating peptide alone	Short amino acid sequence attached to PNAs to facilitate crossing cell membranes	N/A	KFFKFFKFFK	CPP

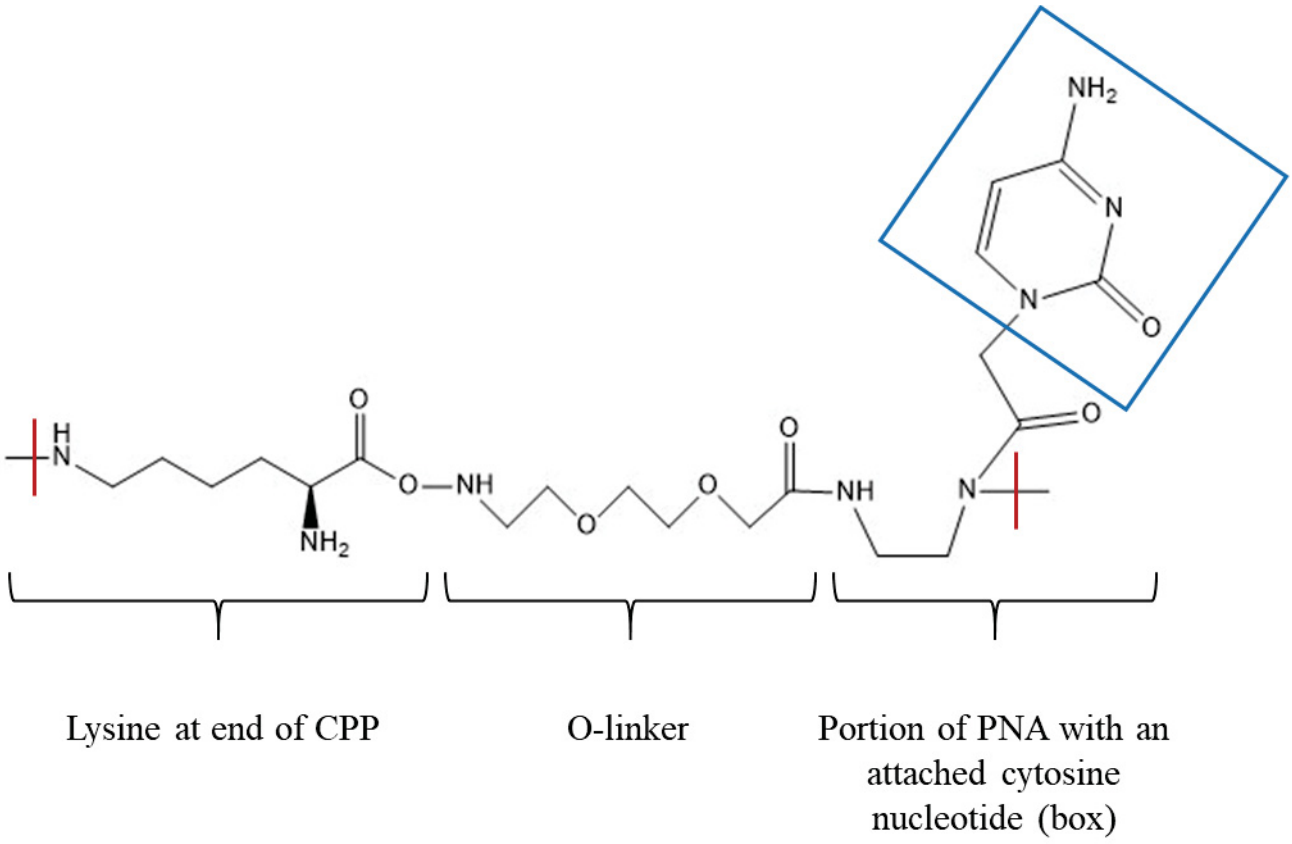

Figure 4.3 Partial structure of an experimental CPP-PNA molecule showing the O-linker binding the CPP and the PNA together. Peptide nucleic acids alone do not penetrate bacterial membranes effectively. Cell-penetrating peptides facilitate crossing of bacterial membranes and allow the PNAs to reach the intended intracellular DNA or mRNA target. The O-linker binds the CPP and PNA together, and also has a chemical composition that improves solubility of the molecule.

Preparation, storage, and thawing of stocks

Peptide nucleic acid stock solutions were made by resuspending the PNA-CPP or CPP powders in molecular grade nuclease-free sterile water to achieve a concentration of either 100 µg/ml (CPP only) or 200 µg/ml (CPP-PNA). Stocks were frozen in 250 µl aliquots at -20 C°. When used for experiments, PNA stocks were thawed and heated to 60 C° for 10 minutes, as per manufacturer recommendations.

4.2.4 Proof of concept: inhibition of bacterial growth with the CPP-Sal-tsf PNA

Before experimentation with PNAs targeting antibiotic resistance genes, the action of the CPP-Sal-tsf gene was confirmed by recapitulating the results reported by Soofi and Seleem.[16] This was

done to confirm that the positive control for PNA action behaved as expected. An overnight culture of DT104 grown in tryptic soy broth (TSB) was diluted with sterile PBS to match a 0.5 McFarland standard, which corresponds to approximately 1.5 x 10^8 CFU/ml, then further diluted in TSB to a concentration of 5.4 x 10^5 CFU/ml. Fifty microliters of this second dilution was added to the appropriate wells of a 96-well flat bottom microtiter plate, then a total of 50 µl of appropriate treatment solution was added to the wells for a final bacterial concentration of 2.7 x 10^4 CFU/ml. For wells with a 30 µM concentration of treatment, 30 µl of PNA or CPP stock was added to the wells, along with 20 µl of TSB. For wells with a 15 µM concentration of treatment, 15 µl of PNA or CPP stock was added to the wells along with 35 µl of TSB. The experimental plate set up is shown in Figure 4.4. Treatments were done in triplicate wells and included 15 µM and 30 µM CPP-Sal-tsf, Sal-tsf, CPP-Control-PNA, CPP only, and none. After 8 hours of incubation at 37 C˚ with 5% CO_2, cultures were serially diluted and plated on tryptic soy agar (TSA) for CFU/ml determination.

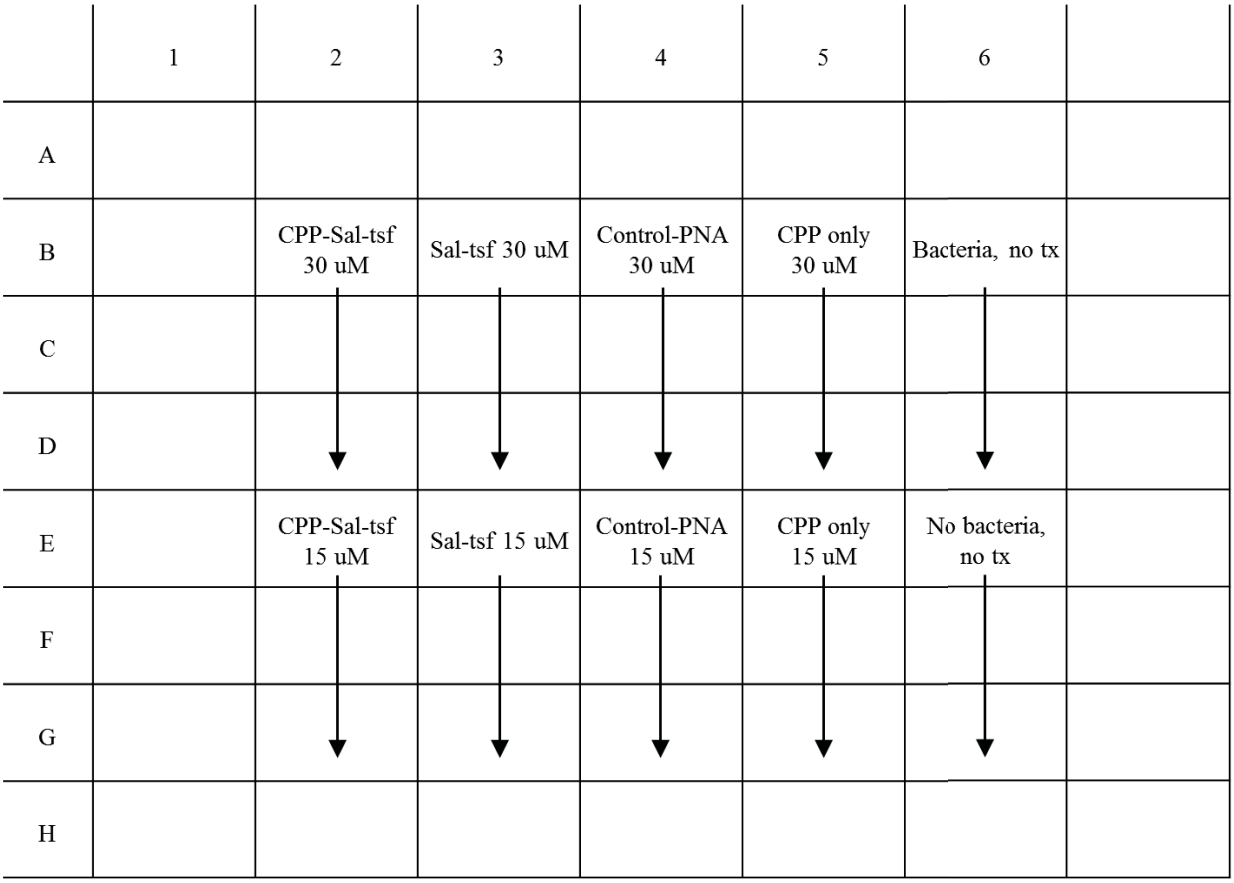

Figure 4.4 Set up of a 96-well microtiter plate to evaluate the effect of a PNA targeting the essential *tsf* gene on bacterial proliferation. Only a portion of the plate was used, so only the pertinent wells are shown. DT104 bacteria were seeded at a concentration of 2.7 x 10^4 CFU/ml in each well, then treated as shown for 8 hours. Samples from each well were then serially diluted and plated on TSA overnight for enumeration and comparison of CFU/ml among treatment groups. The wells surrounding the treated wells were filled with sterile water to decrease evaporation from the plate. Treatment key: CPP-Sal-tsf = PNA targeting the essential *tsf* gene and attached to a cell penetrating peptide (CPP); Sal-tsf = PNA targeting the essential tsf gene, but not attached to a CPP; Control-PNA = "scrambled" PNA-CPP conjugate designed for use as a negative control for PNA activity; "tx" = abbreviation for "treatment".

4.2.5 Evaluation of direct bactericidal activity of anti-resistance gene PNAs

Before treating the bacteria with both tetracycline and the CPP-anti-tetA and CPP-anti-tetR PNAs, it was necessary to determine if the resistance gene PNAs directly inhibited bacterial growth on their own. An overnight culture of DT104 grown in tryptic soy broth (TSB) was diluted with sterile PBS to match a 0.5 McFarland standard, corresponding to approximately 1.5 x 10^8 CFU/ml, then further diluted in TSB to a concentration of 5.4 x 10^5 CFU/ml. Fifty microliters of this second dilution was added to the appropriate wells of a 96-well flat bottom microtiter plate, then a total of 50 µl of treatment solution was added to the wells for a final bacterial concentration of 2.7 x 10^4 CFU/ml. For wells with a 30 µM concentration of treatment, 30 µl of PNA or CPP stock was added to the wells, along with 20 µl of TSB. For wells with a 15 µM concentration of treatment, 15 µl of PNA or CPP stock was added to the wells along with 35 µl of TSB. Treatments were done in triplicate wells and included 15 µM and 30 µM CPP-anti-tetA PNA, 15 µM and 30 µM CPP-anti-tetR PNA, and none. The experimental plate set up is shown in Figure 4.5. After 8 hours of incubation at 37 C˚ with 5% CO_2, cultures were serially diluted and plated on TSA for CFU/ml determination.

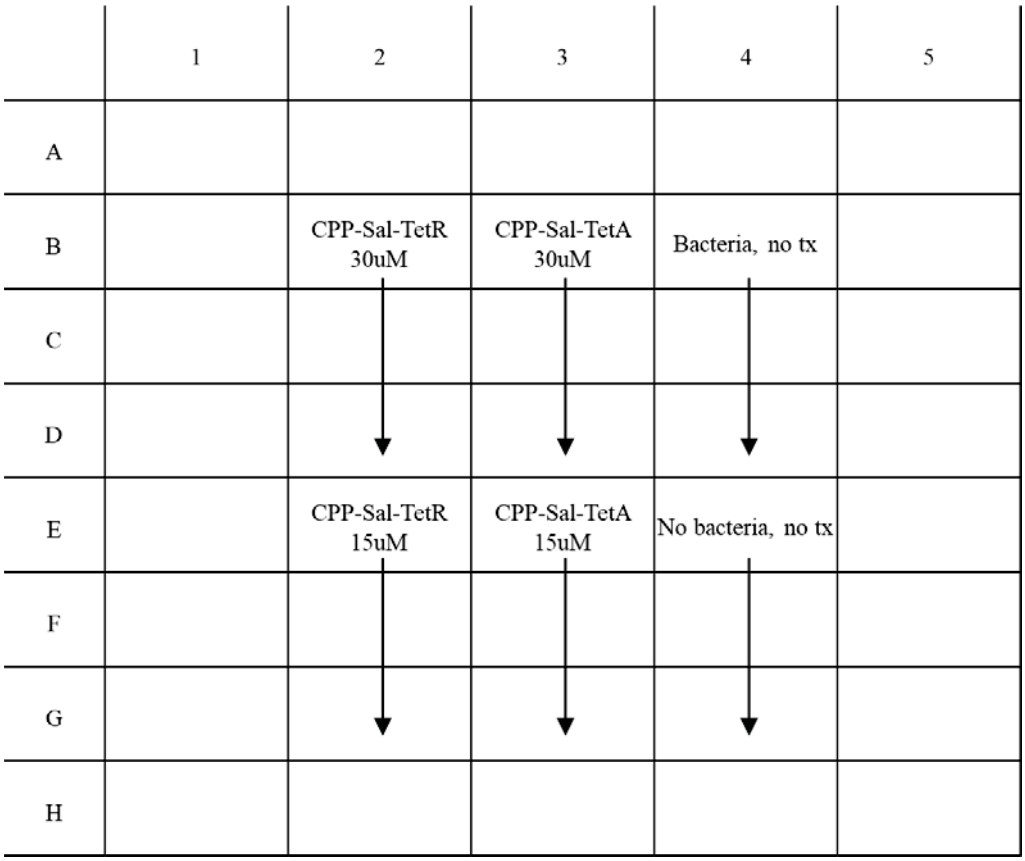

Figure 4.5 Set up of a 96-well culture plate to evaluate the direct effect of PNAs targeting the *tetA* and *tetR* genes on bacterial proliferation. Only a portion of the plate was used, so only the pertinent wells are shown. DT104 bacteria were seeded at a concentration of 2.7 x 10^4 CFU/ml in each well, then treated as shown for 8 hours. Samples from each well were then serially diluted and plated on TSA overnight for enumeration and comparison of CFU/ml among treatment groups. The wells surrounding the treated wells were filled with sterile water to decrease evaporation from the plate. The expectation was that treatment of DT104 with just these CPP-PNAs would not significantly inhibit bacterial growth, because *tetA* and *tetR* are not essential genes. Treatment key: CPP-Sal-tetR PNA = CPP-PNA designed to inhibit expression of the resistance regulatory TetR protein; CPP-Sal-tetA PNA = CPP-PNA designed to inhibit expression of the TetA tetracycline efflux pump.

4.2.6 Bacterial inhibitory effect of CPP alone

The CPP is reported to cause cell membrane permeability[20-21] and an inhibitory effect of the CPP alone was suggested by results of the experiment with CPP-Sal-tsf (see Results and Discussion sections). The decision was therefore made to test the bacterial inhibitory effect of the CPP alone in a dose dependent fashion to help determine how much the CPP may contribute to any observed inhibitory effects of CPP-PNA against DT104. An overnight culture of DT104 grown in tryptic soy broth (TSB) was diluted with sterile PBS to match a 0.5 McFarland standard, corresponding to approximately 1.5 x 10^8 CFU/ml, then further diluted in TSB to a concentration of 5.4 x 10^5 CFU/ml. One hundred µl of this second dilution was added to the appropriate wells of a 96-well flat bottom microtiter plate after addition of an identical volume of treated medium, then a total of 100 µl of treatment solution or additional TSB was added for a final bacterial concentration of 2.7 x 10^4 CFU/ml. Treatments were done in triplicate wells and included 7.5 µM, 10 µM, 15 µM, 30 µM, 40 µM, and 50 µM CPP, and none. The CPP stock solution is in sterile water, so there was some concern that the higher concentrations of CPP treatment would cause a relative decrease in available nutrients due to the large amount of water. To address this, an additional set of controls was set up in which sterile water was added to some wells in volumes equal to that of the CPP stock solution. The experimental plate set up is shown in Figure 4.6. After 8 hours of incubation at 37 C˚ with 5% CO_2, cultures were serially diluted and plated on TSA for CFU/ml determination.

	1	2	3	4	5	6	7	8
A	No CPP	CPP 7.5 uM (15 uL stock)	CPP 10 uM (20 uL stock)	CPP 15 uM (30 uL stock)	CPP 30 uM (60 uL stock)	CPP 40 uM (80 uL stock)	CPP 50 uM (100 uL stock)	Medium only
B	↓	↓	↓	↓	↓	↓	↓	↓
C	↓	↓	↓	↓	↓	↓	↓	↓
D		15 uL water	20 uL water	30 uL water	60 uL water	80 uL water	100 uL water	
E		↓	↓	↓	↓	↓	↓	
F		↓	↓	↓	↓	↓	↓	

Figure 4.6 Set up of a 96-well culture plate to evaluate the effect of varying concentrations of the cell-penetrating peptide (CPP) on bacterial proliferation. Only a portion of the plate was used, so only the pertinent wells are shown. DT104 bacteria were seeded at a concentration of 2.7×10^4 CFU/ml in each well, then treated as shown for 8 hours. Samples from each well were then serially diluted and plated on TSA overnight for enumeration and comparison of CFU/ml among treatment groups. The wells surrounding the treated wells were filled with sterile water to decrease evaporation from the plate.

4.2.7 Effect of PNAs on tetracycline minimum inhibitory concentration (MIC) and minimum bactericidal concentration (MBC) of DT104

The baseline MIC of tetracycline against DT104 was determined to be 32 μg/mL by performance of a microtiter plate MIC assay according to generally accepted laboratory standards.[27] The baseline MBC of tetracycline against DT104 was determined to be > 64 μg/mL by directly transferring the contents of each well of the MIC microtiter plate onto a designated square of TSA, incubating the agar plates overnight at 37 C˚ with 5% CO_2, and observing the concentration of tetracycline that prevented any visible bacterial growth. The conventional microtiter MIC assay was then modified to allow for assessment of the effect of PNAs on the tetracycline MIC and MBC against DT104. The initial experiment was set up as shown in Figure 4.7. Bacteria were seeded in each treatment well at a concentration of 5 x 10^5/μl. The bacteria were incubated with serial dilutions of tetracycline in conjunction with 15 μM PNA-CPP treatments or 7.5 μM CPP alone. Each treatment was done in triplicate. A 7.5 μM concentration of CPP alone was used because this molecule showed some direct bacterial inhibitory effects at concentrations greater than 10 μM when not linked to a PNA (see Results section). After approximately 18 hours of incubation the plate was visually inspected to determine the MIC. An initial estimate of the MIC for each treatment group was made, but it was noted that the PNAs imparted some turbidity to the medium, which complicated visual interpretation of the plate. To address this problem, the absorbance of each well was measured at 560 nm using a VersaMax microplate reader (Molecular Devices, LLC, San Jose, CA, USA), and the absorbance measurements were plotted to show differences in turbidity that could not be detected visually. Direct transfer of well contents onto TSA was then done for determination of the MBC of each treatment group.

To replicate the results obtained by this pilot experiment, a microtiter plate was set up as shown in Figure 4.8. Instead of incubation in a conventional incubator, this plate was incubated at 35 C˚ inside the VersaMax plate reader with serial measurement of well absorbance at 560 nm every 15 minutes for approximately 18 hours. The MIC was then determined both by visual inspection and by plotting the serial absorbance data to look for differences in growth curves of the various treatment groups. The MBC for each treatment group was then determined by direct transfer of well contents onto TSA. After determination of the MIC and MBC, this second set-up was repeated twice more to allow for triplicate data.

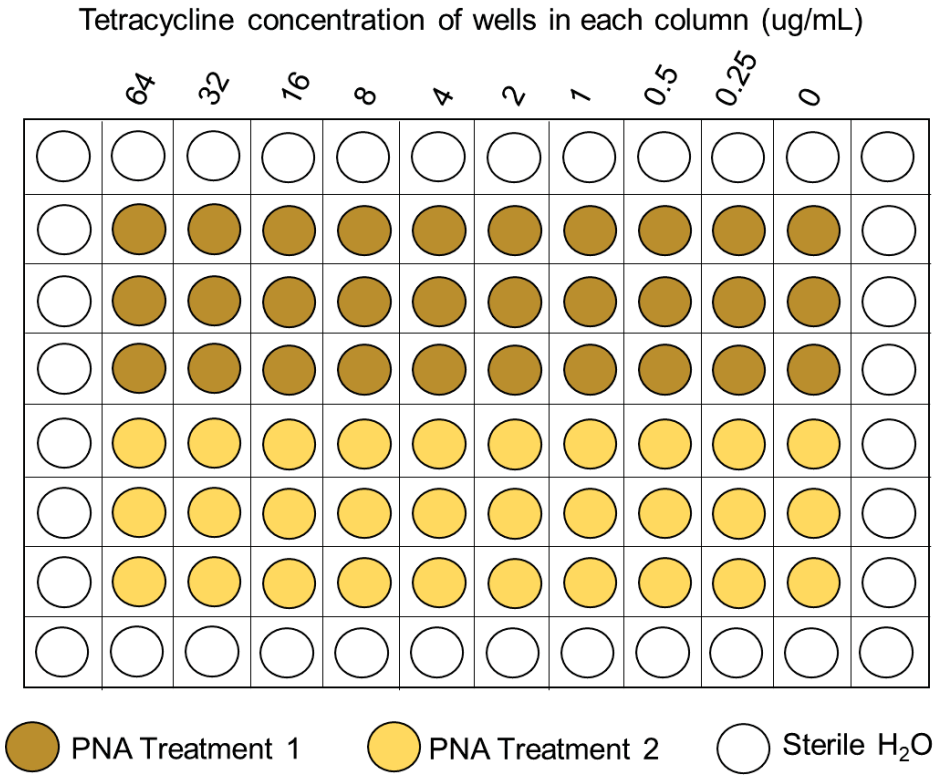

Figure 4.7 Initial set up of the experiment to test the effect of various PNA treatments on the tetracycline MIC of DT104. This is an example of a modified MIC microtiter plate. Bacteria were seeded in each treatment well at a concentration of 5 x 10^5/µl and incubated with serial dilutions of tetracycline in conjunction with 15 µM CPP-PNA treatments or 7.5 µM CPP only treatment. Only two treatment groups could fit on each microtiter plate, so several plates were set up, and the designations of PNA Treatment 1 and PNA Treatment 2 refer to any of the following: 15 µM CPP-anti-tetR PNA, 15 µM CPP-anti-tetA PNA, 15 µM CPP-Control PNA, 7.5 µM CPP alone, and none (bacteria only control). After ~18 hours of incubation the MIC was interpreted and direct transfer of well contents onto TSA was done for determination of the MBC after overnight incubation.

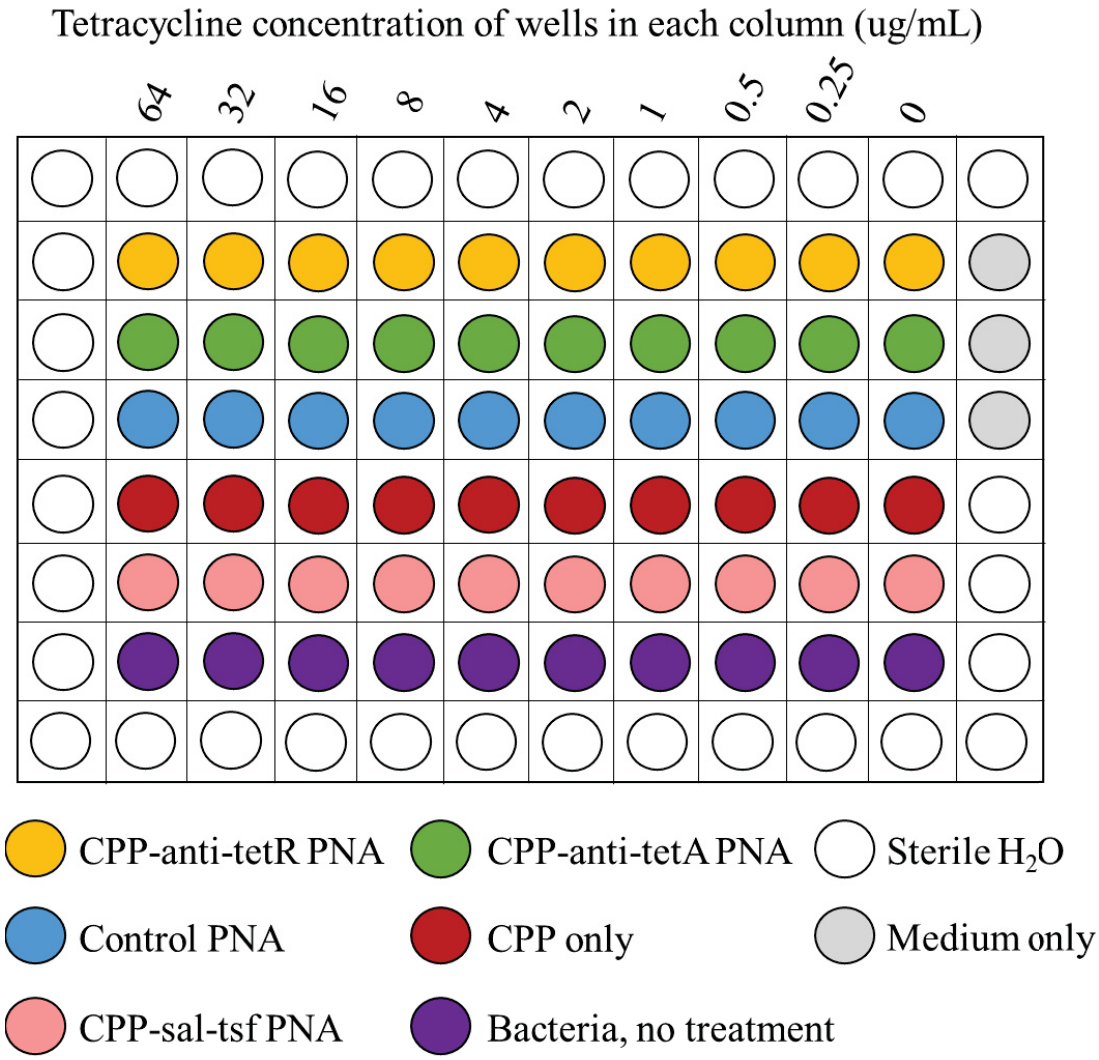

Figure 4.8 Set up of the follow up experiment to allow for collection of replicate date showing the effect of various PNA treatments on the tetracycline MIC against DT104. Bacteria were seeded in each treatment well at a concentration of 5 x 10^5/µl and incubated with serial dilutions of tetracycline in conjunction with 15 µM CPP-PNA treatments or 7.5 µM CPP only treatment. The microtiter plate was incubated in a VersaMax plate reader and absorbance readings at 560 nm were taken every 15 minutes to generate growth curves for each treatment group. This provided a second way to interpret the MIC for each group. After ~18 hours of incubation the MIC was interpreted and direct transfer of well contents onto TSA was done for determination of the MBC after overnight incubation. This experimental set up was run three times.

4.2.8 Statistical analysis

For experiments where bacterial CFU/ml counts were compared, a student's t-test was performed using Graphpad (San Diego, CA, USA) to compare means between untreated and treated cultures.

4.3 Results

4.3.1 Confirmation of serotype

The ST104 prophage sequence was successfully amplified from DT104 template DNA as shown in Figure 4.9. The independent testing by the NVSL also confirmed that the serotype was Typhimurium and the phage type was DT104.

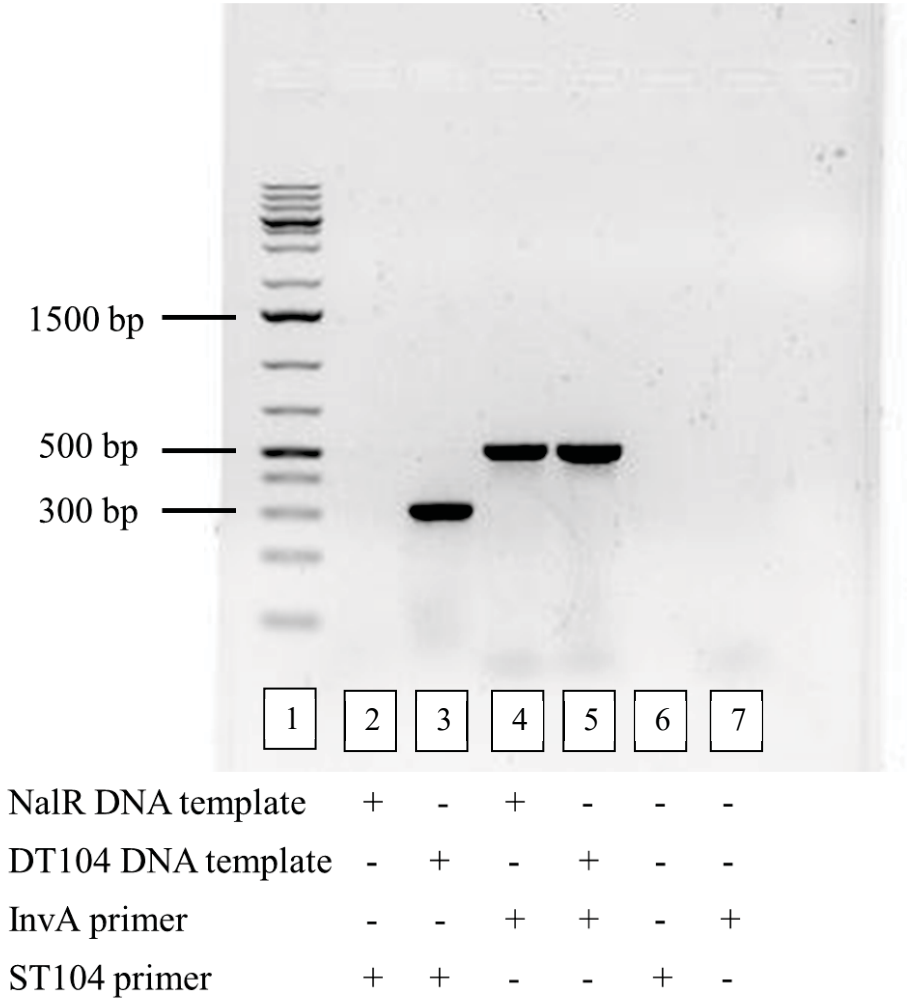

Figure 4.9 Agarose gel stained with ethidium bromide showing successful amplification of ST104 from DT104 template DNA but not NalR template DNA. Lane 1 (far left): Gene Ruler 1 kb Plus DNA ladder; Lane 2: as expected, NalR template DNA combined with the ST104 primer did not result in DNA amplification; Lane 3: DT104 DNA template with ST104 primer resulted in the expected amplicon band (312 bp), confirming the DT104 phage type; Lanes 4 and 5: both NalR template DNA and DT104 template DNA with *InvA* primer resulted in the expected 521 bp amplicon band. The *InvA* gene is common to all *Salmonellae*; Lanes 6 and 7: template free controls did not amplify any product, as expected.

4.3.2 Proof of concept: inhibition of bacterial growth with the CPP-Sal-tsf PNA

Relative growth of the various treatment groups is shown in Figure 4.10. The CPP-Sal-tsf PNA significantly inhibited bacterial growth relative to the untreated control culture at both the 15 µM and 30 µM concentrations. Cultures treated with Sal-tsf PNA without CPP did not have significantly reduced growth at either concentration, confirming the necessity of having the CPP attached to the PNA. The CPP-Control PNA significantly inhibited growth relative to the untreated control at the 30 µM concentration, but not the 15 µM concentration. The CPP alone significantly inhibited growth relative to the untreated control at both the 15 µM and 30 µM concentrations, although the effect was markedly more pronounced at the higher concentration.

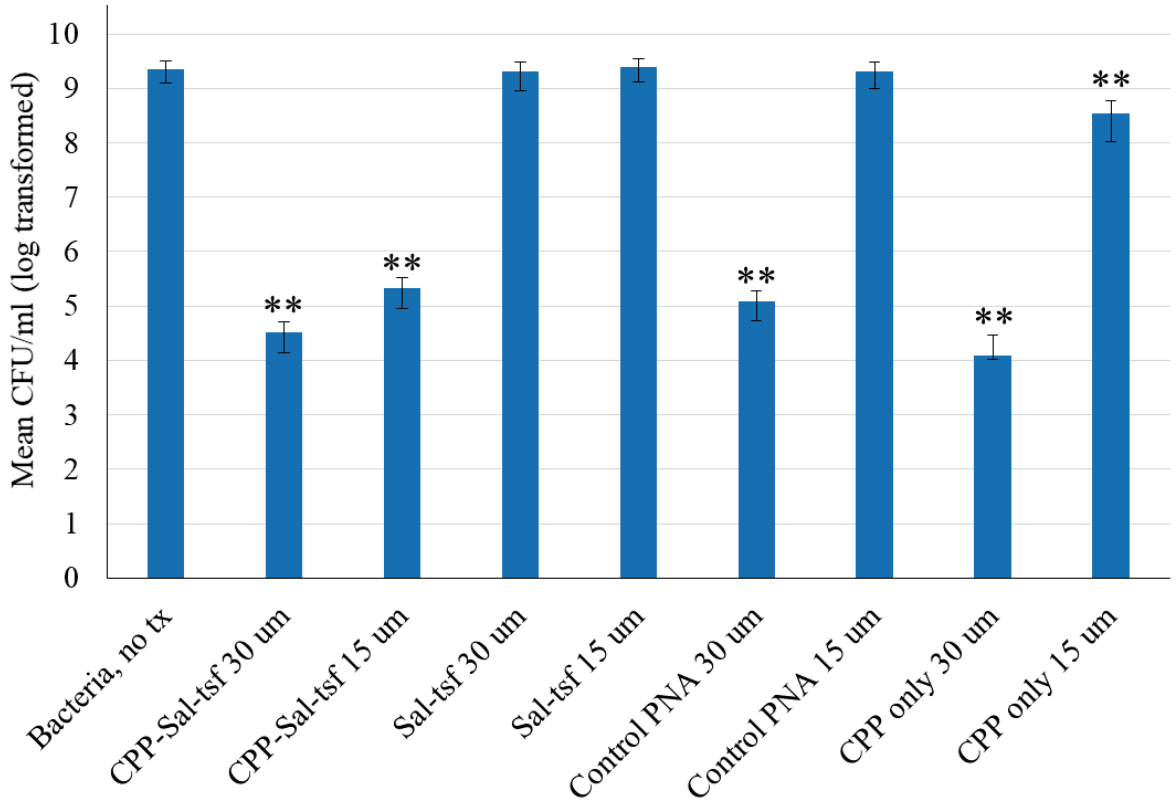

Figure 4.10 Results of treatment of DT104 with a CPP-PNA targeting the essential *tsf* gene, along with appropriate controls. When bound to the CPP, the PNA significantly inhibited bacterial growth at both 30 µM and 15 µM concentrations. No inhibition was observed when the PNA was not bound to CPP. Unexpectedly, the nonsense sequence CPP-Control PNA significantly inhibited bacterial growth at the higher concentration. The CPP alone significantly inhibited bacterial growth at both the high and low concentrations, although the effect was not nearly as pronounced at the lower concentration. The average CFU/ml in each treatment group was compared to that of the untreated control using a student's t-test. ** = $p < 0.01$. Error bars indicate +/- 1 standard deviation from the mean (log transformed values).

4.3.3 Evaluation of direct bactericidal activity of anti-resistance gene PNAs

Relative growth of the various treatment groups is shown in Figure 4.11. Statistically significant inhibition of bacterial growth relative to the untreated control was demonstrated by the 15 µM CPP-anti-tetR, 30 µM CPP-anti-tetR, and 30 µM CPP-anti-tetA PNAs, but not by the 15 µM CPP-anti-tetA PNA. None of the PNAs except the 30 µM CPP-anti-tetR PNA caused more than a one log decrease in bacterial growth, so from a practical standpoint they did not appear to directly inhibit bacterial growth to a degree that would prevent interpretation of their effects on DT104 growth when used concurrently with tetracycline.

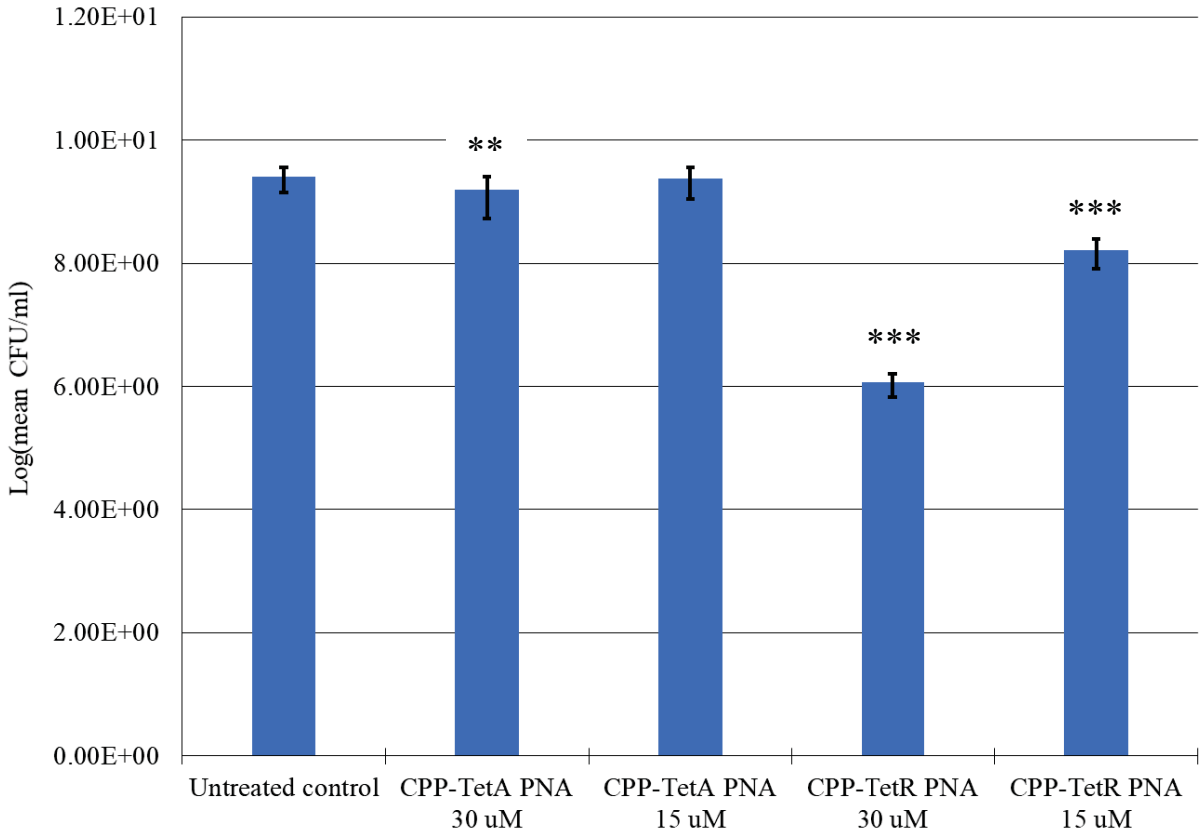

Figure 4.11 Results of treatment of DT104 with PNAs targeting the *tetA* and *tetR* resistance and resistance regulatory genes. The high concentration of the CPP-anti-tetA PNA and the high and low concentrations of the CPP-anti-tetR PNA all cause significant inhibition of bacterial growth. For this reason, only the lower 15 µM concentration was used for further experiments. The average CFU/ml in each treatment group was compared to that of the untreated control using a student's t-test. ** = $p < 0.01$. Error bars indicate +/- 1 standard deviation from the mean.

4.3.4 Bacterial inhibitory effect of CPP alone

A dose dependent inhibitory effect on bacterial growth was demonstrated, as shown in Figure 4.12.

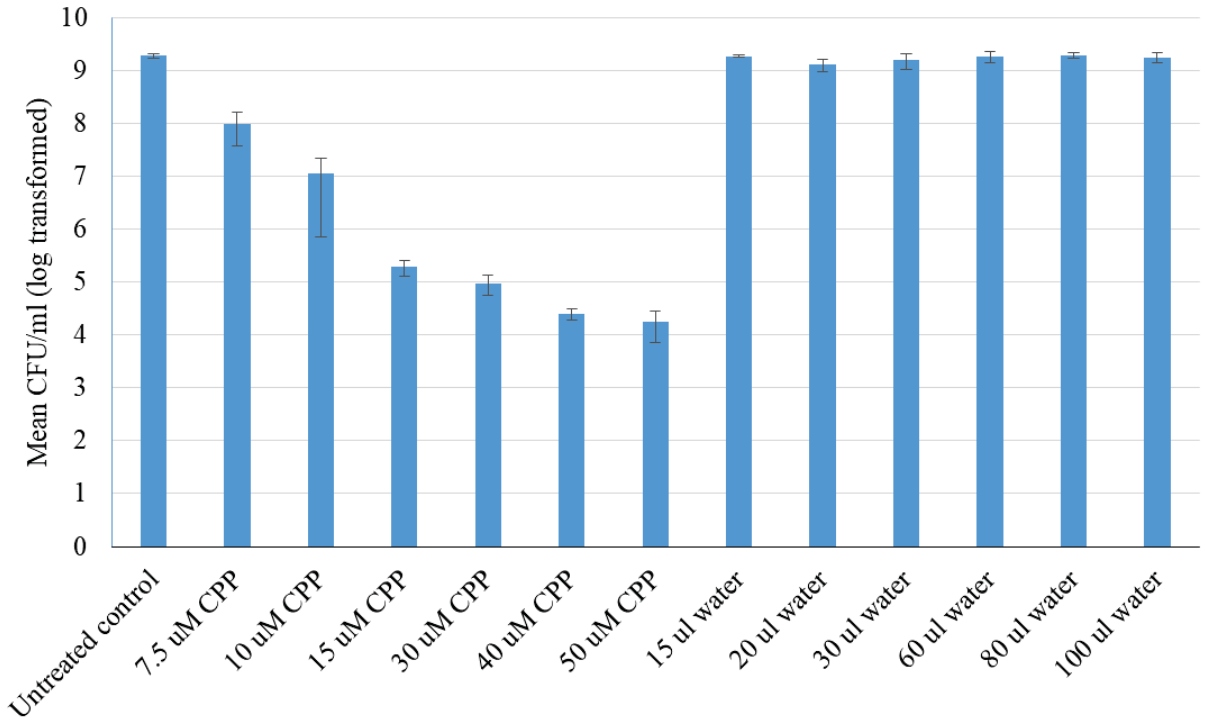

Figure 4.12 A nearly linear dose-dependent inhibition of bacterial growth was observed after treatment with increasing concentrations of the CPP. Controls treated with sterile water in volumes equal to those of the CPP treatments did not show growth inhibition. Statistical analysis was not performed because of the limited number of replicates, and because the statistical significance of the growth suppression was less important in this experiment than simply observing the trend of dose dependent growth inhibition. Error bars indicate +/- 1 standard deviation from the mean (log transformed values).

4.3.5 Effect of PNAs on tetracycline MIC and MBC of DT104

Table 4.5 and Figure 4.13-Figure 4.15 display the MIC and MBC readings obtained with various CPP-PNA treatments in conjunction with tetracycline. Bacteria treated with tetracycline alone most consistently had an MBC of 32 μg/ml and always had an MBC > 64 μg/ml. The CPP-anti-tetA PNA consistently decreased the tetracycline MIC and MBC of DT104 to 8 μg/ml and 16 μg/ml. The effects of the CPP-anti-tetR PNA varied between the pilot experiment and the subsequent replicates. In the pilot experiment this CPP-PNA appeared to cause a decrease in the MIC to 8 μg/ml and a decrease in the MBC to somewhere between 16 and 32 μg/ml. However, in replicates 1-3 the growth curves for the CPP-anti-tetR PNA consistently showed an MIC of <0.25 μg/ml, indicating a strong bacteriostatic effect, but did not cause a consistently notable decrease in the MBC. The reason for the discrepant results between the pilot experiment and the replicates for this PNA may be that turbidity caused by the PNA confounded interpretation of the pilot data; therefore, the data from the replicate experiments is considered more trustworthy for the CPP-anti-tetR PNA. The CPP-Control PNA also had variable MIC results between that pilot experiment and the replicates. In the pilot experiment it appeared to decrease the MIC to 8 μg/ml, but in the subsequent replicates it decreased the MIC to <0.25 μg/ml based on absorbance data. The MBC of the CPP-Control PNA was difficult or impossible to interpret in every replicate because "skips" were seen on the agar growth plate. This means that the bacteria did not consistently grow up to a certain concentration of tetracycline and then stop, but would instead do things like grow at low concentrations and high concentrations, but not at middle concentrations; no consistent pattern was found. The CPP alone consistently decreased the tetracycline MIC to either 16 or 8 μg/ml, but only decreased the MBC to 32 or 64 μg/ml. The CPP-Sal-tsf PNA showed strong bacteriostatic and bactericidal effects as evidenced by an MIC and MBC of 0.25 μg/ml or <0.25 μg/ml in every replicate.

Table 4.5 Summary of the tetracycline MICs and MBCs obtained for all treatment groups in each replicate of the MIC/MBC experiments. Some MICs were difficult to visually interpret due to turbidity imparted by the PNAs, so the absorbance data from spectrophotometer measurements in replicates 1-3 is considered the best way to interpret MICs. Treatment with the CPP-anti-tetA PNA and the CPP-Sal-tsf PNA consistently decreased both the MIC and MBC relative to tetracycline alone. Treatment with the CPP-anti-tetR PNA and the CPP without PNA substantially decreased the MIC, but not the MBC. Treatment with the CPP-Control PNA consistently caused a decrease in the MIC, but the MBC could not be interpreted due to skips in the growth pattern. See text for additional comments.

Treatment	**Replicate**	**Tetracycline MIC (µg/ml)**	**Tetracycline MBC (µg/ml)**
Tetracycline only	Pilot A	64	>64
	Pilot B	32	>64
	Pilot C	32	>64
	Rep 1	16	>64
	Rep 2	32	>64
	Rep 3	32	>64
CPP-anti-tetA PNA + tetracycline	Pilot A	8	16
	Pilot B	8	16
	Pilot C	8	16
	Rep 1	8	16
	Rep 2	8	16
	Rep 3	8	16
CPP-anti-tetR PNA + tetracycline	Pilot A	8	16
	Pilot B	8	16
	Pilot C	8	32
	Rep 1	<0.25	32
	Rep 2	<0.25	32
	Rep 3	0.25	64

CPP-Control PNA + tetracycline	Pilot A	8	16
	Pilot B	8	Skips
	Pilot C	8	32
	Rep 1	<0.25	Skips
	Rep 2	<0.25	Skips
	Rep 3	<0.25	Skips
CPP only + tetracycline	Pilot A	16	32
	Pilot B	16	32
	Pilot C	16	32
	Rep 1	8	64
	Rep 2	8	64
	Rep 3	8	64
CPP-Sal-tsf + tetracycline	Pilot A	Not done	Not done
	Pilot B	Not done	Not done
	Pilot C	Not done	Not done
	Rep 1	<0.25	<0.25
	Rep 2	<0.25	<0.25
	Rep 3	<0.25	0.25

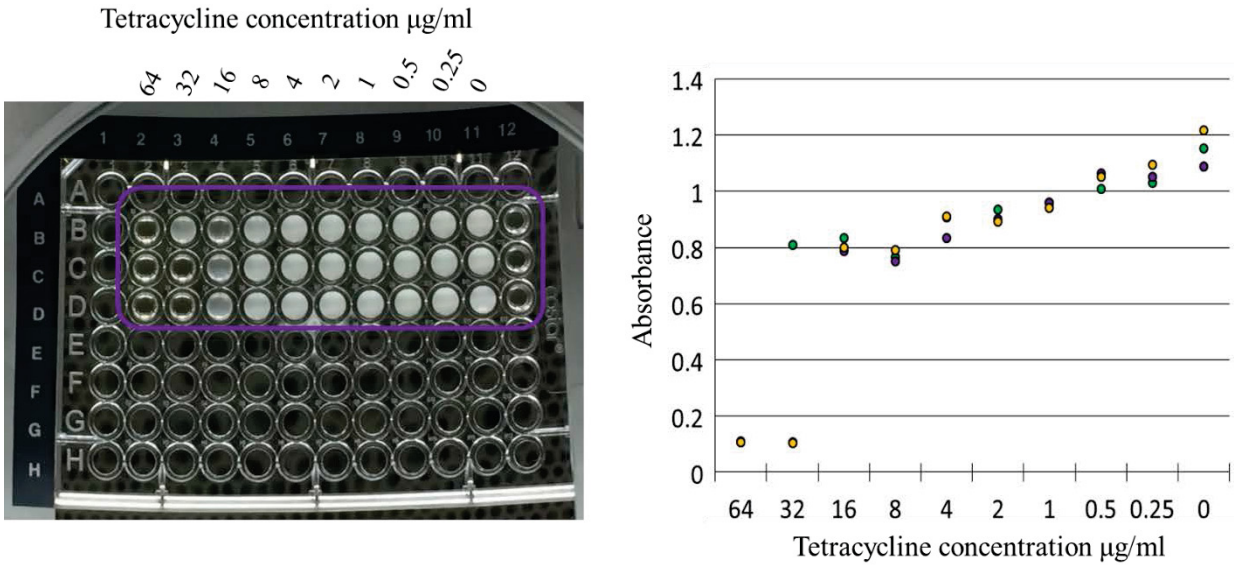

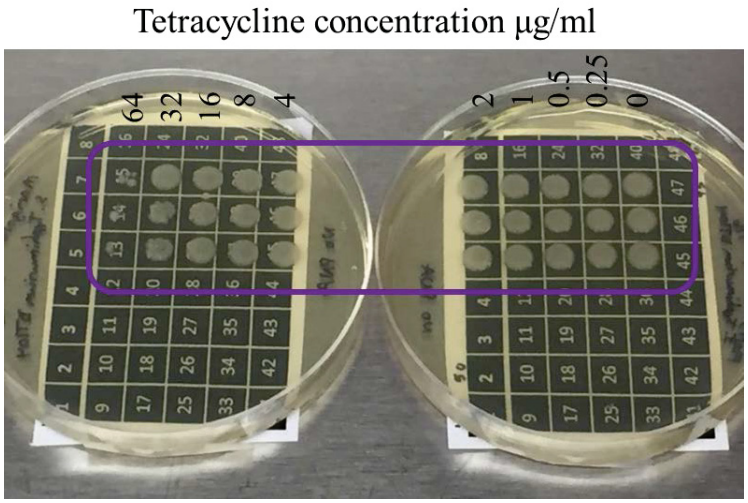

Figure 4.13A. MIC plate, spectrophotometry absorbance data, and MBC plate for bacteria treated with tetracycline only in the pilot MIC/MBC experiment. The purple boxes highlight the wells of interest on the MIC and MBC plates. Each set of three colored dots (green, yellow, purple) on the absorbance plot corresponds to triplicate wells treated with the same concentration of tetracycline. The MIC is interpreted as 32 µg/ml and the MBC is interpreted as >64 µg/ml.

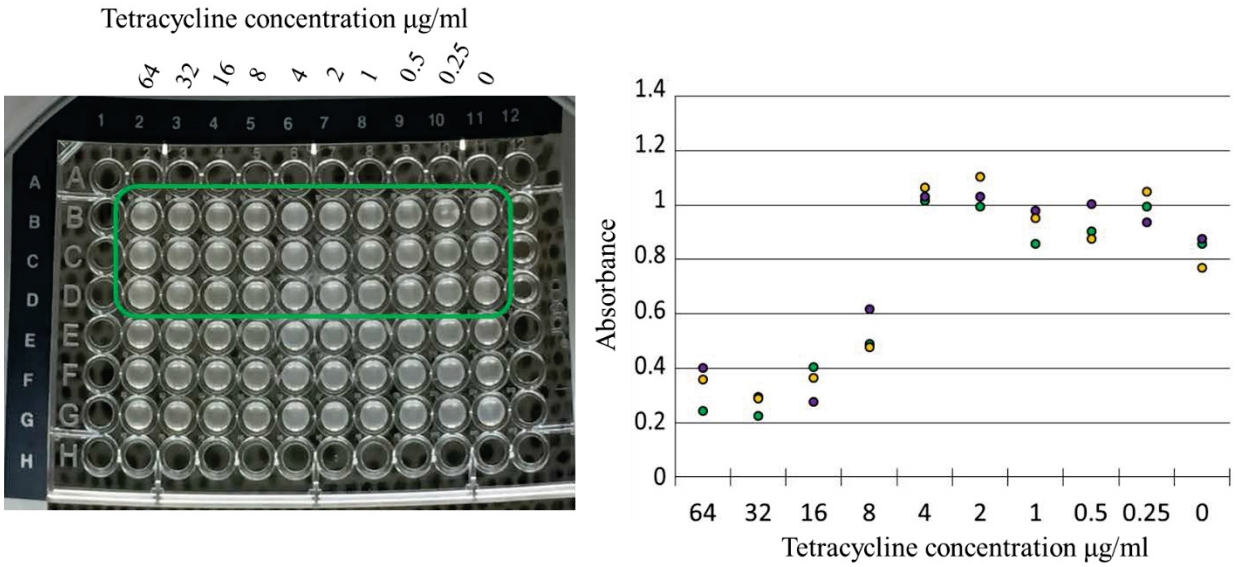

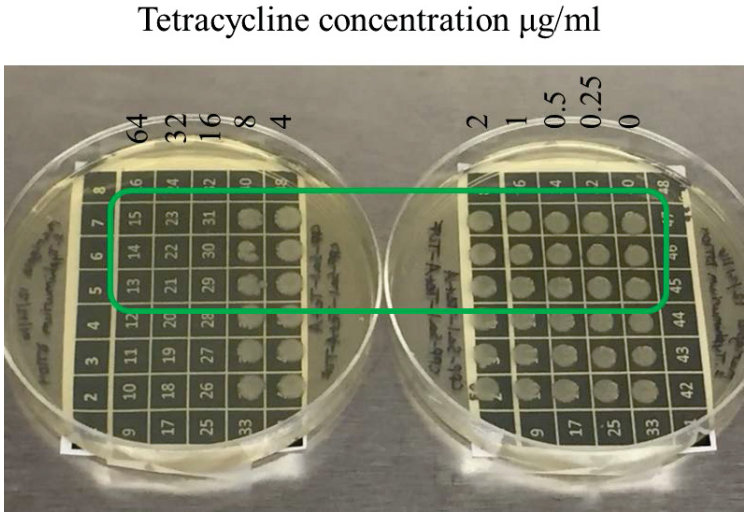

Figure 4.13B. MIC plate, spectrophotometry absorbance data, and MBC plate for bacteria treated with tetracycline and the CPP-anti-tetA PNA in the pilot MIC/MBC experiment. The green boxes highlight the wells of interest on the MIC and MBC plates. Each set of three colored dots (green, yellow, purple) on the absorbance plot corresponds to triplicate wells treated with the same concentration of tetracycline. The MIC is interpreted as 8 µg/ml and the MBC is interpreted as 16 µg/ml.

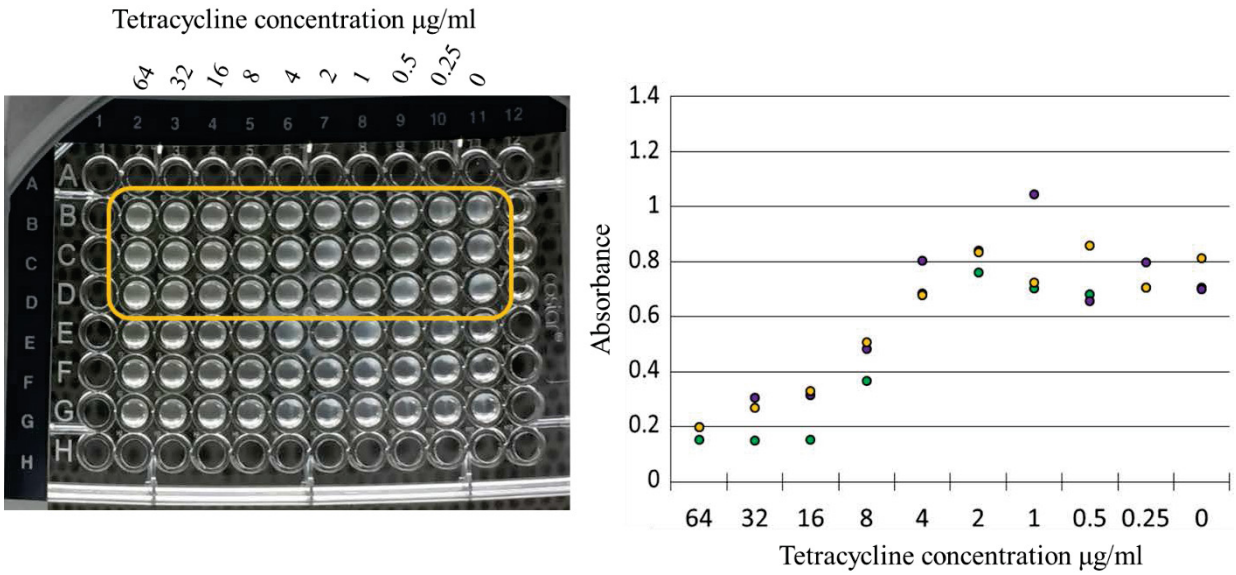

Tetracycline concentration µg/ml

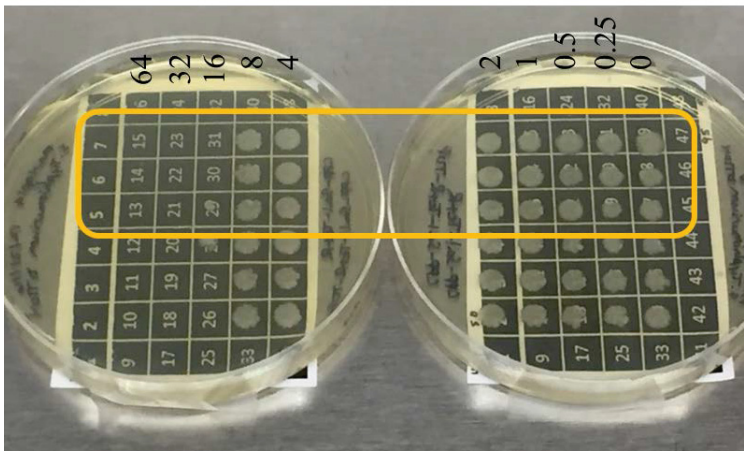

Figure 4.13C. MIC plate, spectrophotometry absorbance data, and MBC plate for bacteria treated with tetracycline and the CPP-anti-tetR PNA in the pilot MIC/MBC experiment. The yellow boxes highlight the wells of interest on the MIC and MBC plates. Each set of three colored dots (green, yellow, purple) on the absorbance plot corresponds to triplicate wells treated with the same concentration of tetracycline. The MIC is interpreted as 8 µg/ml and the MBC is interpreted as between 16 and 32 µg/ml.

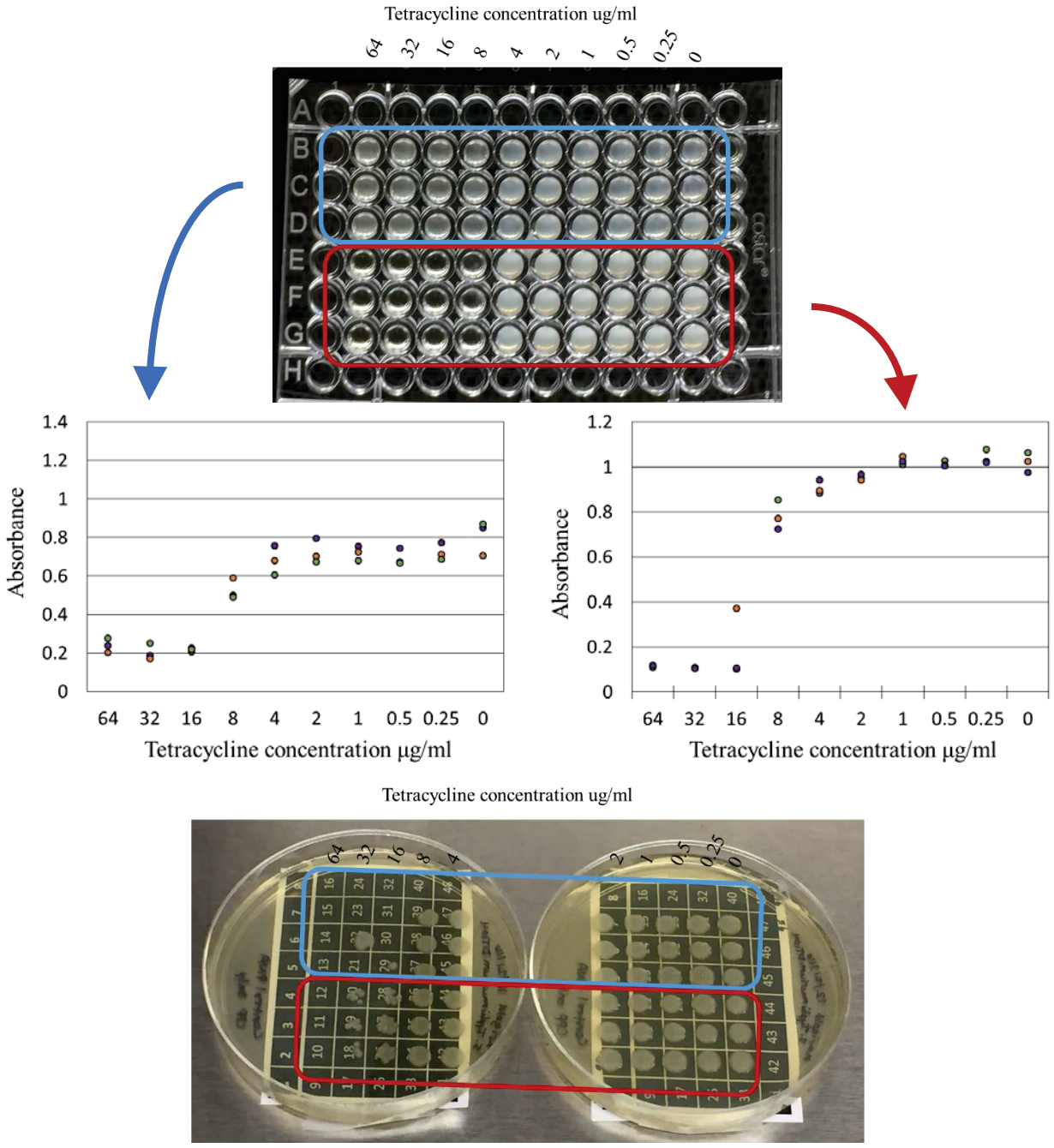

Figure 4.13D. MIC plate, spectrophotometry absorbance data, and MBC plate for bacteria treated with tetracycline and the CPP-Control PNA (blue boxes) and with tetracycline and the CPP alone in the pilot MIC/MBC experiment. The blue boxes highlight the wells of interest for the CPP-Control PNA and the red boxes highlight the wells on interested for the CPP alone on the MIC and MBC plates. Each set of three colored dots (green, yellow, purple) on the absorbance plots corresponds to triplicate wells treated with the same concentration of tetracycline. For the CPP-Control PNA the MIC is interpreted as 8 µg/ml and the MBC is interpreted as likely to be between 16 µg/ml and 32 µg/ml, but was equivocal because of a skip in the second row. For the CPP alone, the MIC is interpreted as 8 µg/ml and the MBC is interpreted as 64 µg/ml.

Figure 4.13 MIC microtiter plates, spectrophotometer absorbance readings, and MBC agar plates for each treatment group in the MIC/MBC pilot experiment. Bacteria were seeded in experimental wells at a concentration of 5 x 10^5/µl and incubated with serially diluted concentrations of tetracycline in conjunction with various CPP-PNA treatments. Results for the MICs were interpreted after 16-20 hours of incubation at 37 C˚, both visually and by taking a single absorbance reading of each well at 560 nm with a VersaMax spectrophotometer. Direct transfer of MIC plate well contents onto TSA was then performed and interpretation of the MBC was done after overnight incubation at 37 C˚. **A.** Control group treated with tetracycline only. **B.** Treatment with CPP-anti-tetA PNA and tetracycline. **C.** Treatment with CPP-anti-tetR PNA and tetracycline. **D.** Treatment with CPP-Control PNA and tetracycline and CPP only and tetracycline. Some wells on these plates were used for collection of data for a different experiment. Only the wells highlighted by colored boxes are pertinent to this dissertation. The recorded MICs and MBCs for each replicate are summarized in Table 4.5.

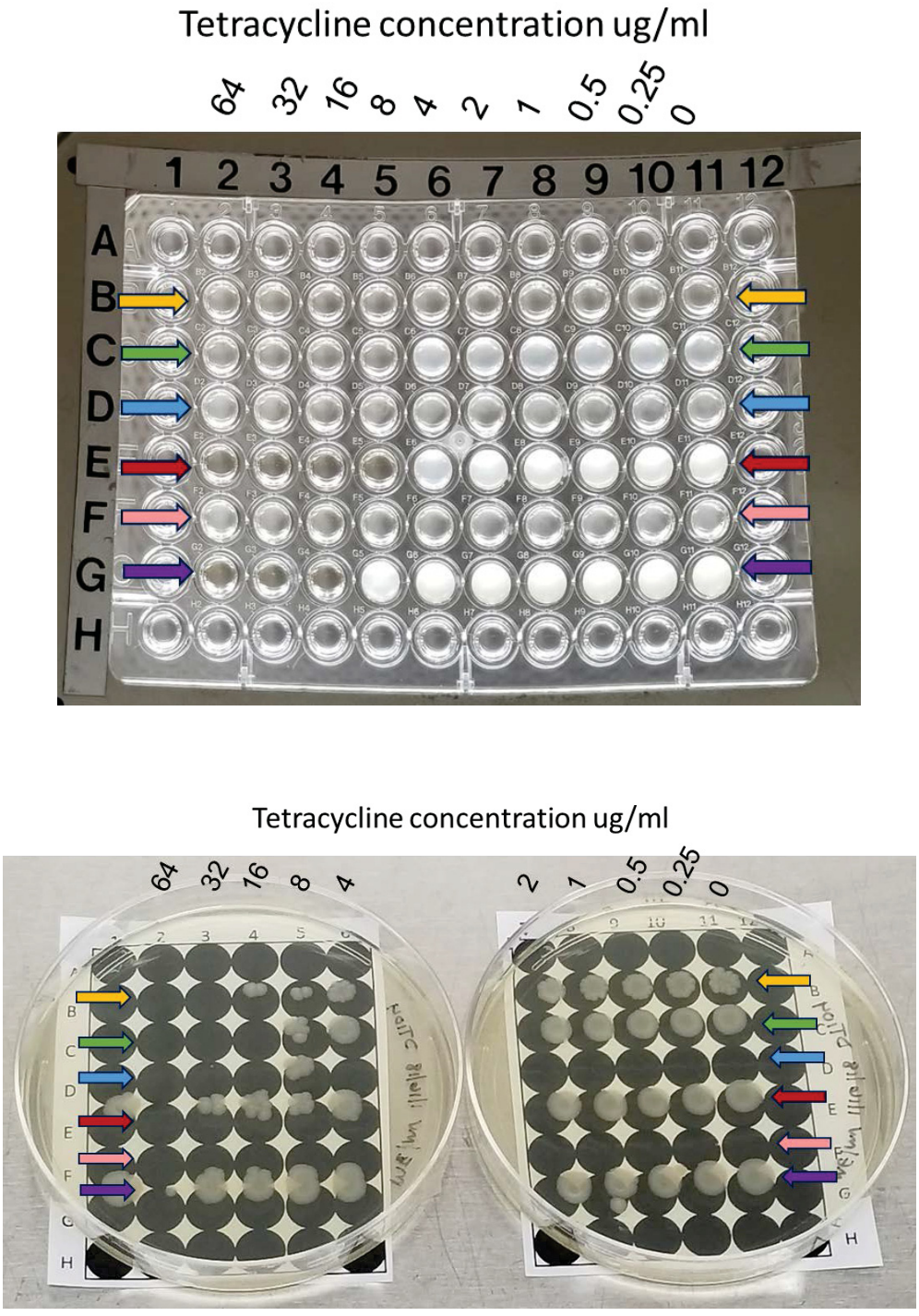

Figure 4.14A. MIC microtiter plate and MBC agar plates for replicate 1 of the MIC/MBC experiment. Yellow arrows indicate treatment with CPP-anti-TetR PNA and tetracycline, green arrows indicate treatment with CPP-anti-TetA PNA and tetracycline, blue arrows indicate treatment with CPP-Control PNA and tetracycline, red arrows indicate treatment with CPP alone and tetracycline, pink arrows indicate treatment with CPP-Sal-tsf PNA and tetracycline, and purple arrows indicate treatment with tetracycline only.

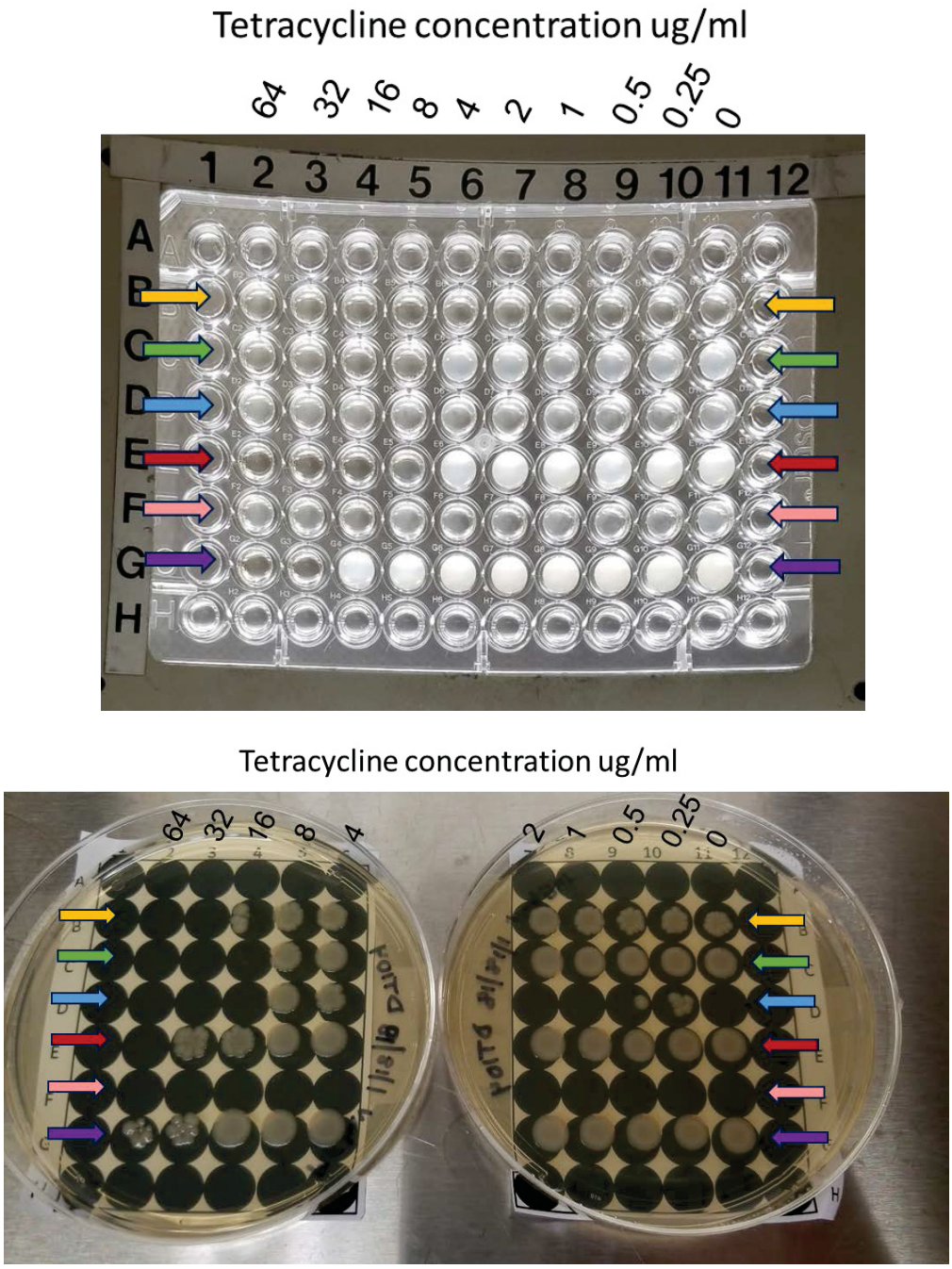

Figure 4.14B. MIC microtiter plate and MBC agar plates for replicate 2 of the MIC/MBC experiment. Yellow arrows indicate treatment with CPP-anti-TetR PNA and tetracycline, green arrows indicate treatment with CPP-anti-TetA PNA and tetracycline, blue arrows indicate treatment with CPP-Control PNA and tetracycline, red arrows indicate treatment with CPP alone and tetracycline, pink arrows indicate treatment with CPP-Sal-tsf PNA and tetracycline, and purple arrows indicate treatment with tetracycline only.

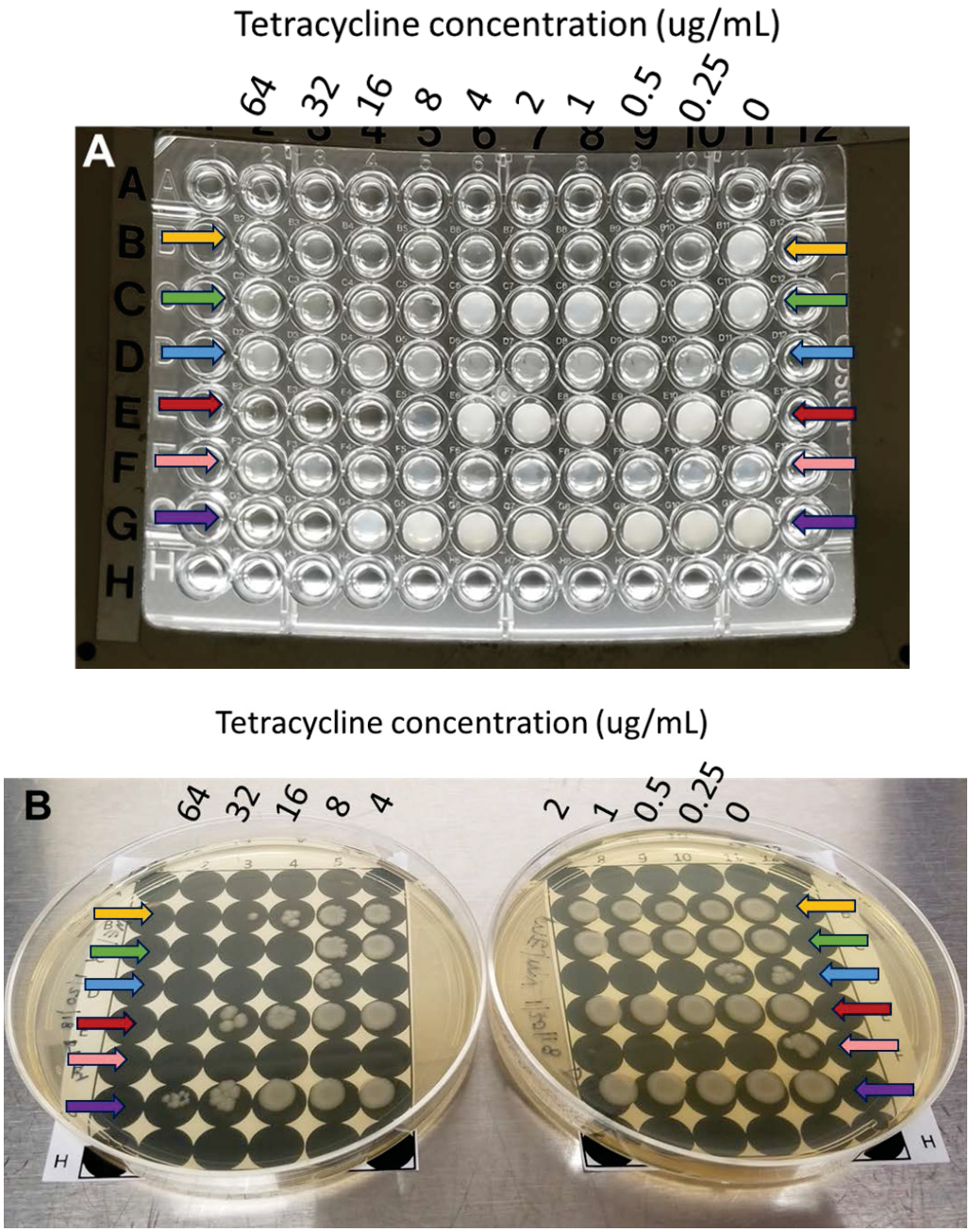

Figure 4.14C. MIC microtiter plate and MBC agar plates for replicate 3 of the MIC/MBC experiment. Yellow arrows indicate treatment with CPP-anti-TetR PNA and tetracycline, green arrows indicate treatment with CPP-anti-TetA PNA and tetracycline, blue arrows indicate treatment with CPP-Control PNA and tetracycline, red arrows indicate treatment with CPP alone and tetracycline, pink arrows indicate treatment with CPP-Sal-tsf PNA and tetracycline, and purple arrows indicate treatment with tetracycline only.

Figure 4.14 MIC microtiter plates and MBC agar plates for each replicate of the MIC/MBC replicate experiments. **A.** Replicate 1. **B.** Replicate 2. **C.** Replicate 3. Bacteria were seeded in experimental wells at a concentration of 5 x 10^5/µl and incubated with serially diluted concentrations of tetracycline in conjunction with various CPP-PNA treatments. The MIC plates were incubated in a VersaMax spectrophotometer for 6-20 hours of incubation at 35 C° with absorbance readings taken every 15 minutes. The MIC was then interpreted both visually and by looking at growth curves plotted from the absorbance readings (see Figure 4.15). Direct transfer of MIC plate well content onto TSA was then performed and interpretation of the MBC was done after overnight incubation at 37 C°. Yellow arrows indicate treatment with CPP-anti-TetR PNA and tetracycline, green arrows indicate treatment with CPP-anti-TetA PNA and tetracycline, blue arrows indicate treatment with CPP-Control PNA and tetracycline, red arrows indicate treatment with CPP alone and tetracycline, pink arrows indicate treatment with CPP-Sal-tsf PNA and tetracycline, and purple arrows indicate treatment with tetracycline only. The recorded MICs and MBCs for each replicate are summarized in Table 4.5.

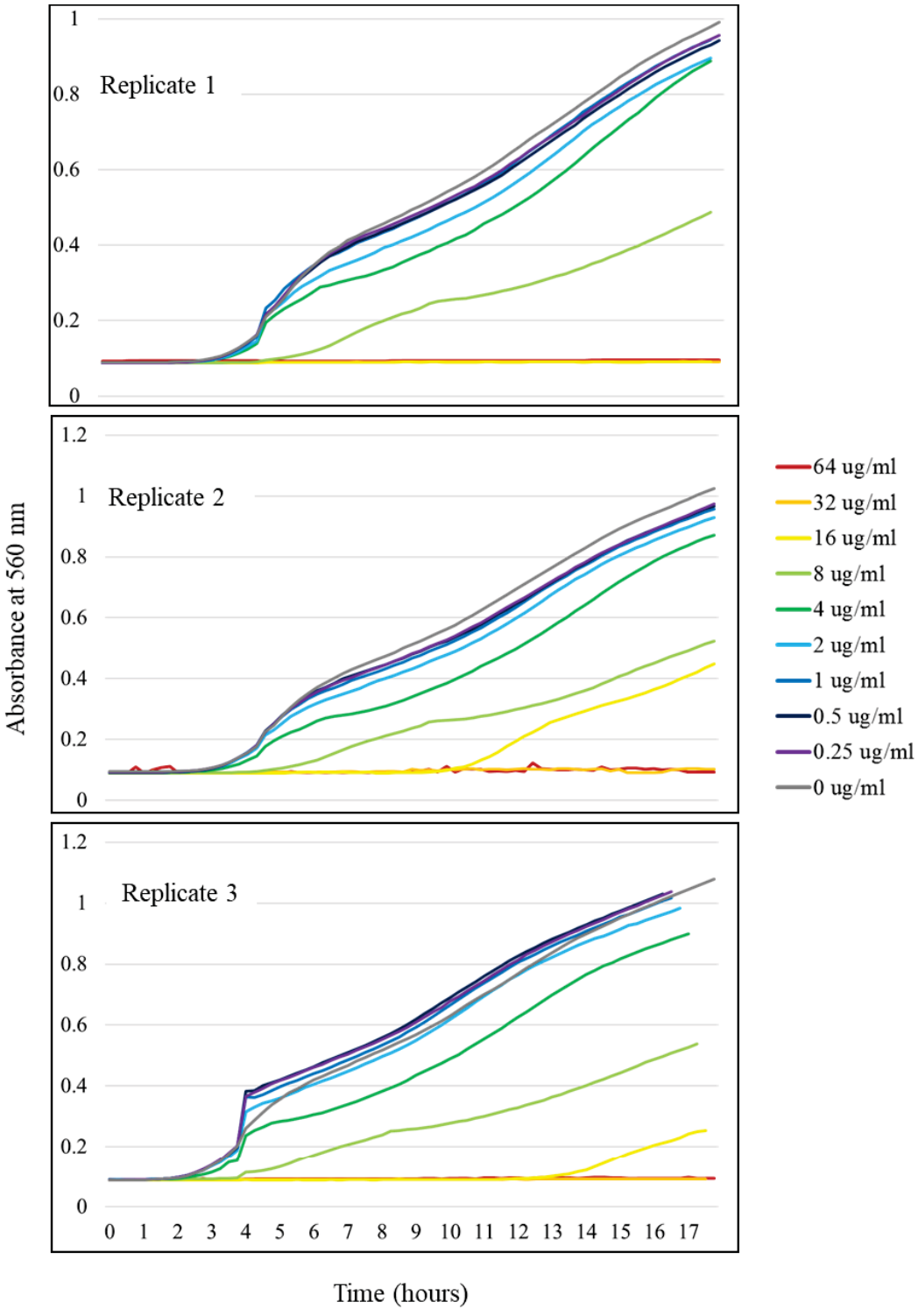

Figure 4.15A Growth curves generated from absorbance readings for bacteria treated with tetracycline only in the three replicates of the MIC/MBC study. The MIC is interpreted as 32 µg/ml.

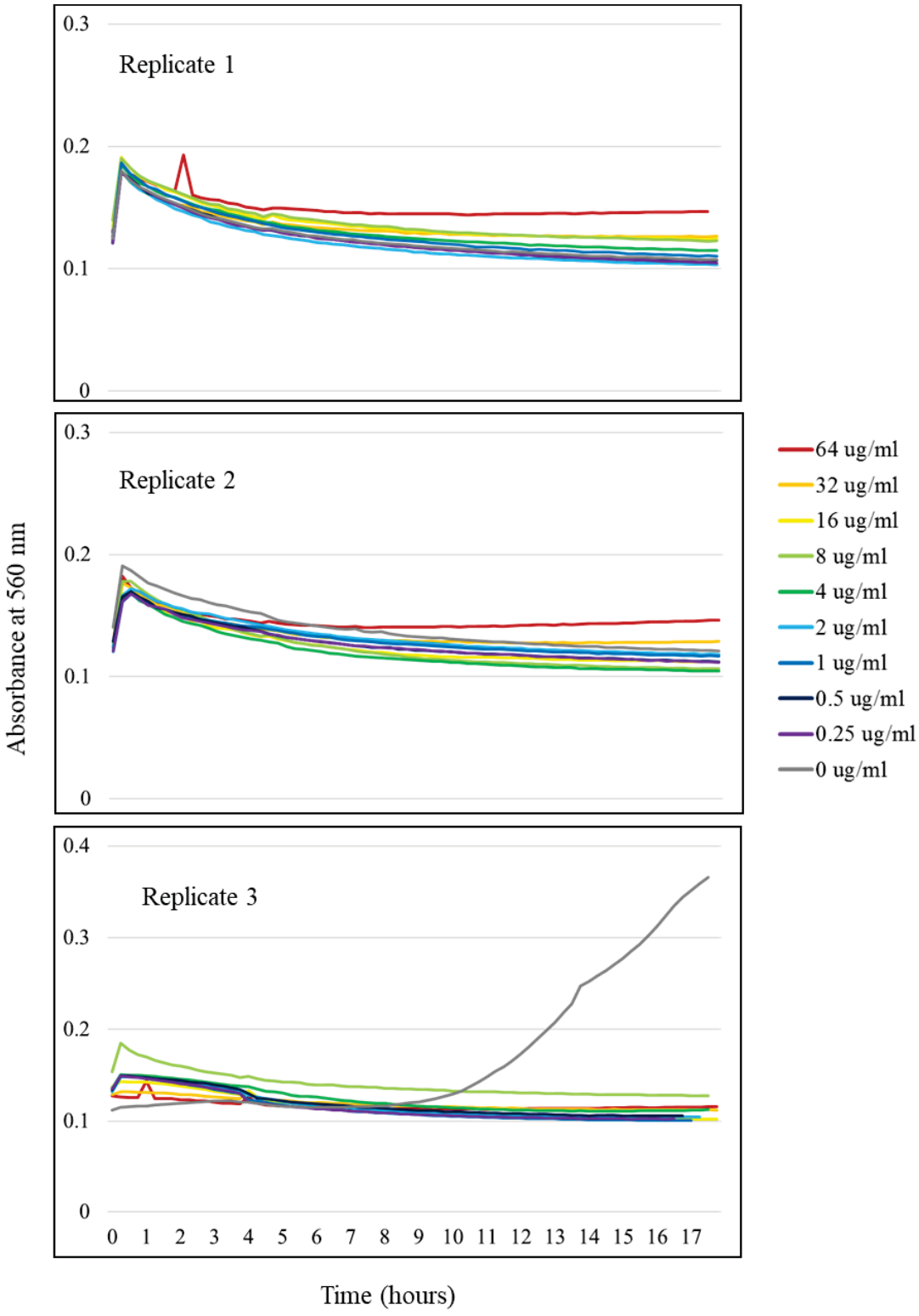

Figure 4.15B Growth curves generated from absorbance readings for bacteria treated with tetracycline and CPP-anti-tetR PNA in the three replicates of the MIC/MBC study. The MIC is interpreted as either 0.25 µg/ml or <0.25 µg/ml.

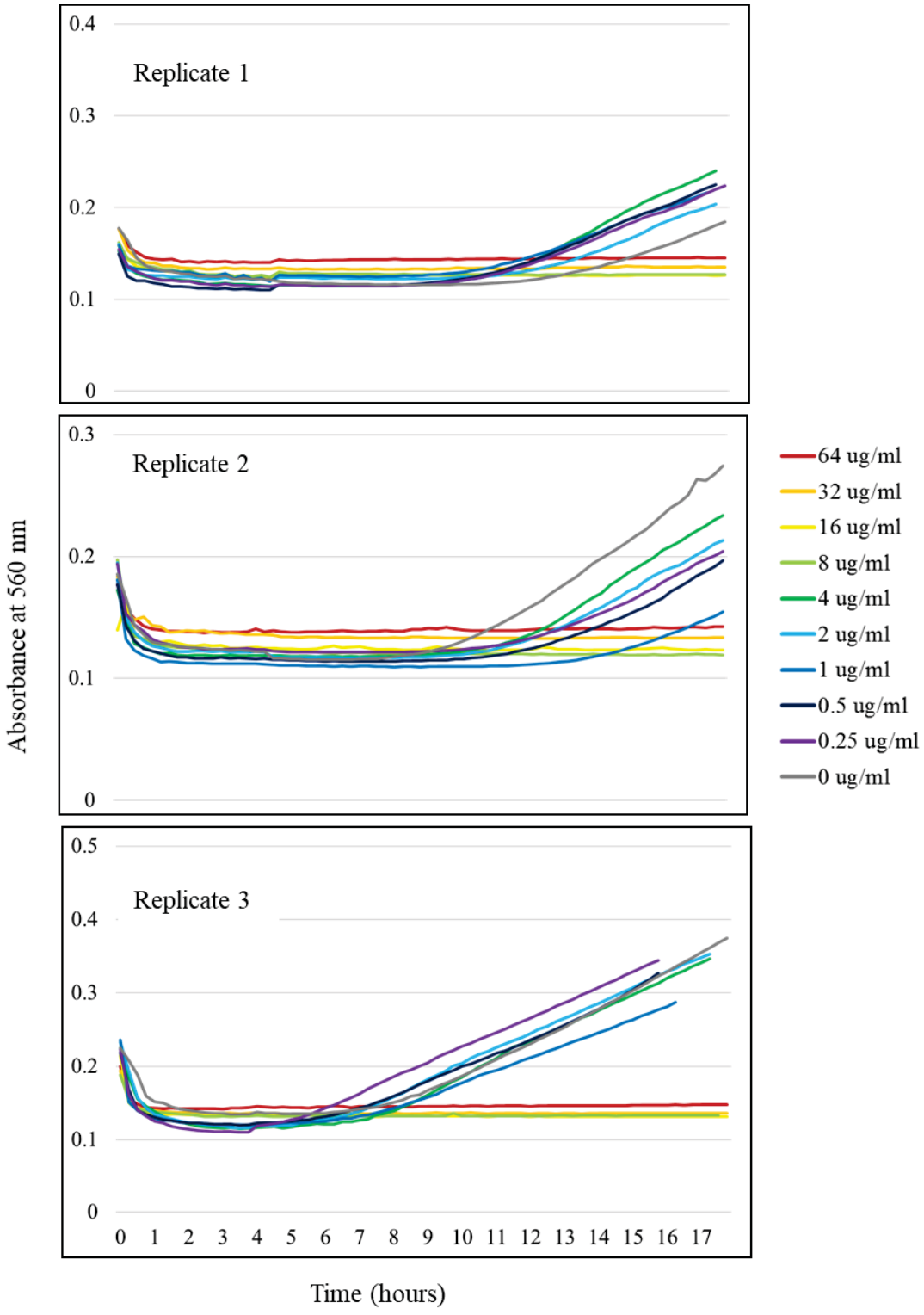

Figure 4.15C Growth curves generated from absorbance readings for bacteria treated with tetracycline and CPP-anti-tetA PNA in the three replicates of the MIC/MBC study. The MIC is interpreted as 8 µg/ml.

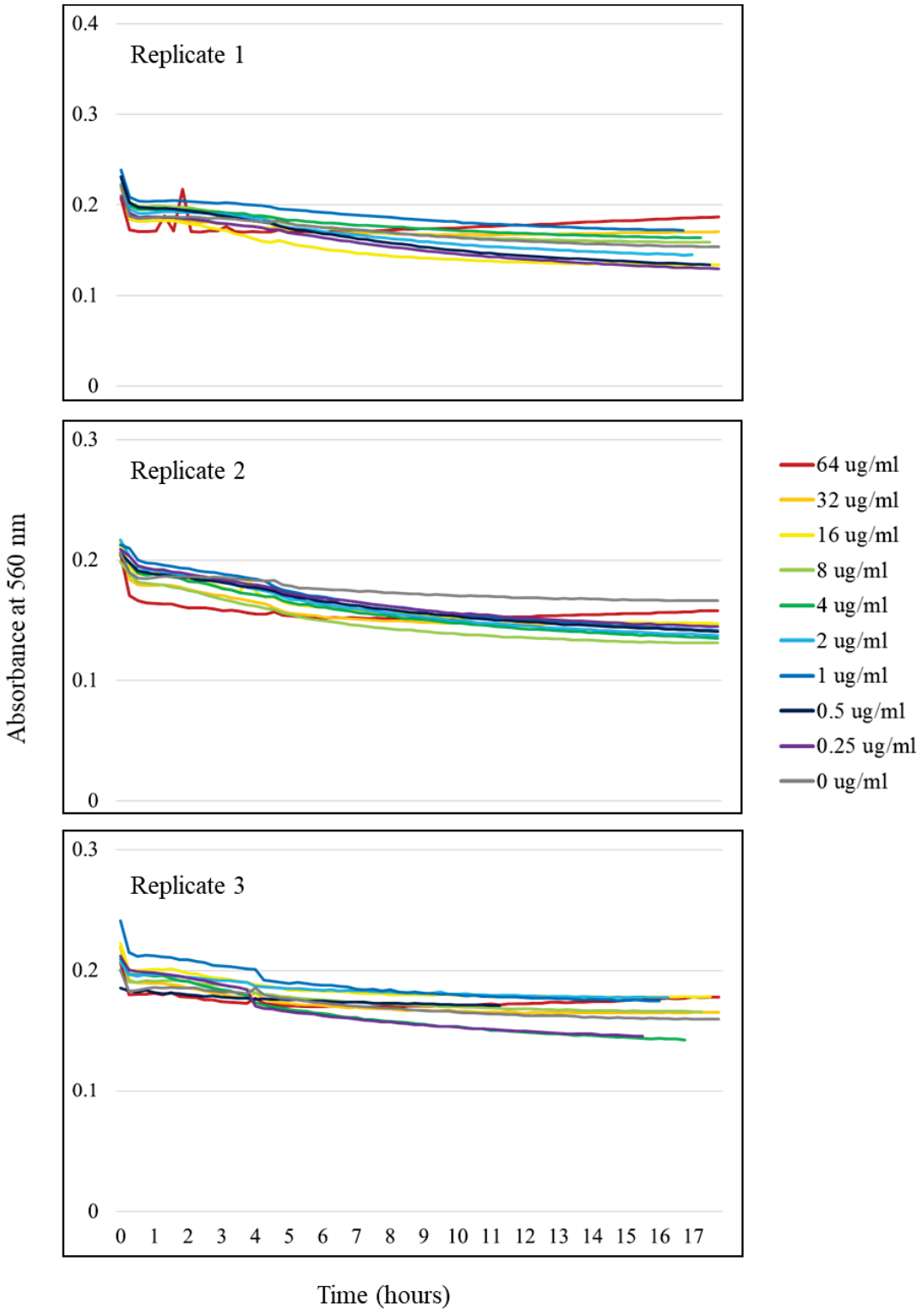

Figure 4.15D Growth curves generated from absorbance readings for bacteria treated with tetracycline and CPP-Control PNA in the three replicates of the MIC/MBC study. The MIC is interpreted as <0.25 µg/ml.

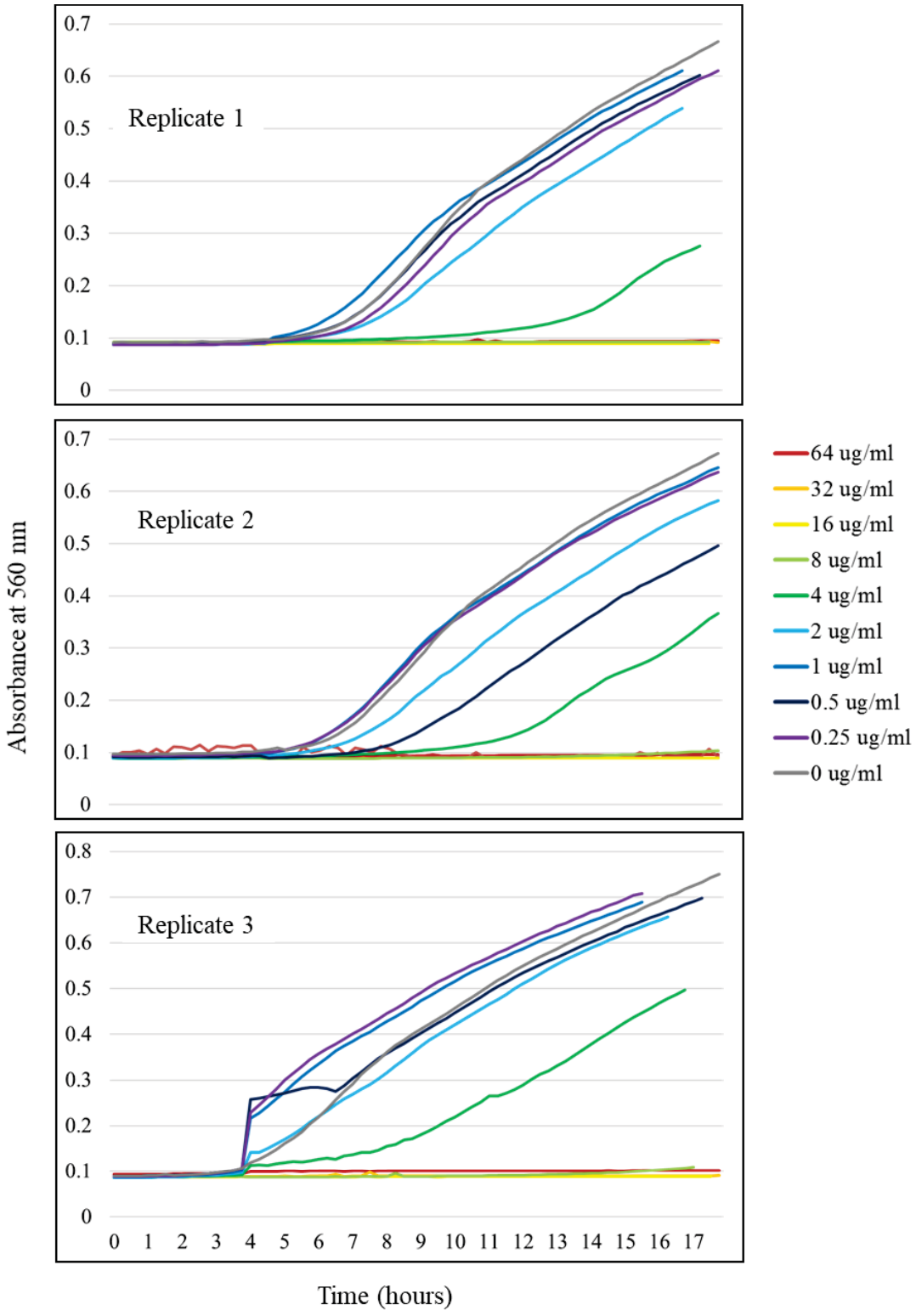

Figure 4.15E Growth curves generated from absorbance readings for bacteria treated with tetracycline and CPP alone the three replicates of the MIC/MBC study. The MIC is interpreted as 8 μg/ml.

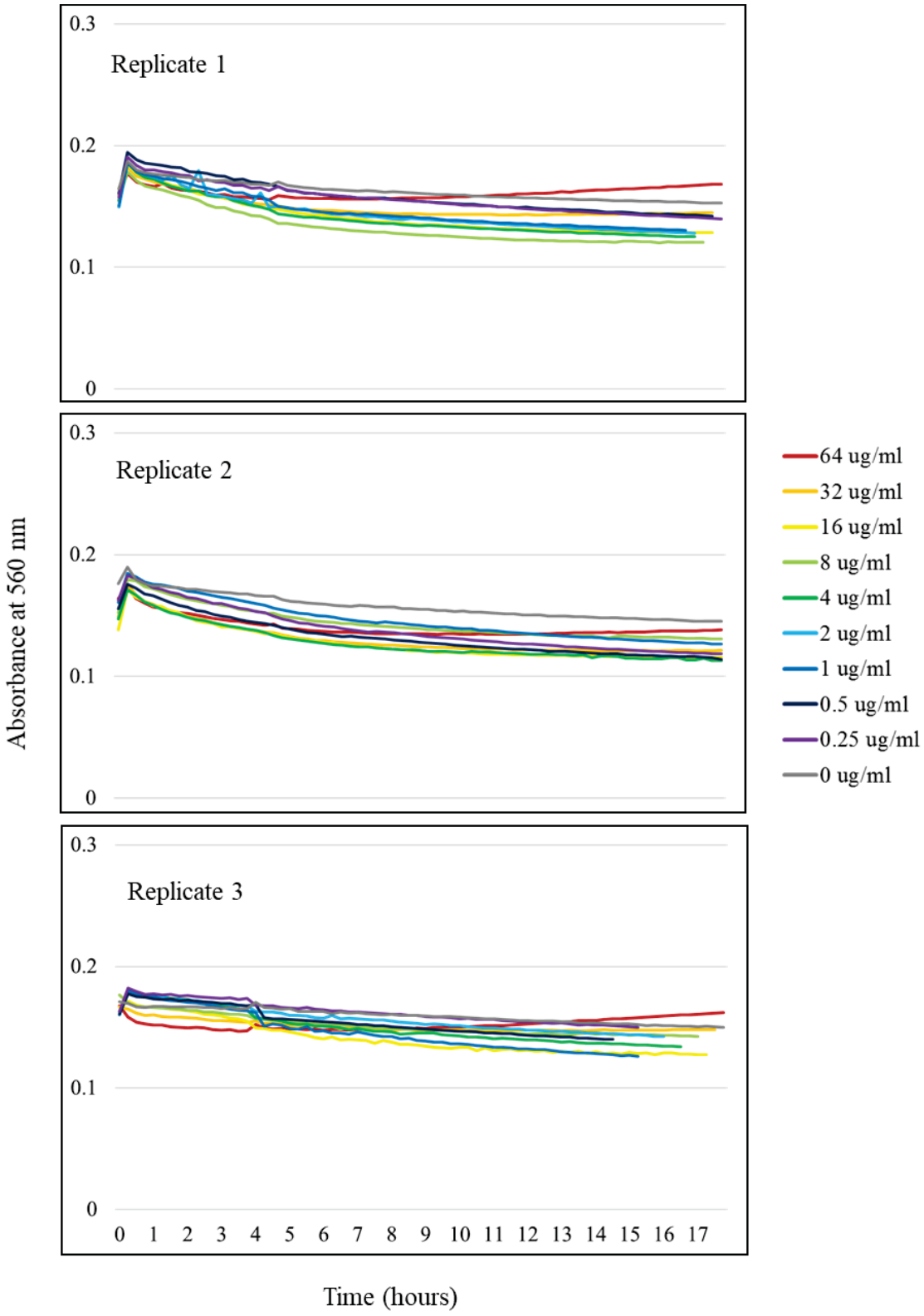

Figure 4.15F Growth curves generated from absorbance readings for bacteria treated with tetracycline and CPP-Sal-tsf in the three replicates of the MIC/MBC study. The MIC is interpreted as <0.25 µg/ml.

Figure 4.15 Serial spectrophotometer absorbance readings from the MIC microtiter plates for each treatment group in the MIC/MBC replicate experiments. The MIC plates were grown in the VersaMax microtiter plate reader at 35 ˚C for 17-18 hours. Absorbance readings at 560 nm were taken every 15 minutes after 30 seconds of shaking. Absorbance is indicated on the y-axis. The time in hours is indicated on the bottom x-axis of each set of graphs. The color legend to the right indicates the tetracycline concentration (μg/ml) at which each growth curve was generated. The recorded MICs and MBCs for each replicate are summarized in Table 4.5.

4.4 Discussion and Conclusions

This body of work demonstrates that CPP-PNA combinations targeting the *tetA* resistance gene and the *tetR* resistance regulatory gene cause notable decreases in the tetracycline MIC and MBC of tetracycline-resistant DT104. At a 15 μM concentration the CPP-anti-tetA PNA did not cause significant inhibition of bacterial growth on its own, which is expected as this gene is understood to be non-essential. When combined with tetracycline, the CPP-anti-tetA PNA behaved as expected and caused a decrease in both the MIC and MBC.

There was some concern that the presence of the CPP attached to the PNA would complicate interpretation of the results, because the CPP alone has inhibitory effects on bacterial growth. However, the results here show that even though the CPP MIC was consistently the same as that of the CPP-anti-tetA PNA, the CPP MBC was much higher, and close to that of bacteria treated only with tetracycline. This indicates a beneficial effect when the CPP and PNA are combined, leading to an increase in bactericidal capability not seen with the CPP alone. This is in line with previously reported results that a CPP-PNA combination caused greater cell membrane permeability in *E. coli* than a CPP alone.[20] An unexpected observation is that unbound CPP appears to have greater potency against DT104 than CPP bound to a PNA. When the CPP was unbound, it directly inhibited bacterial growth at concentrations as low as 7.5 μM, but conjugates of the CPP with PNAs such as the anti-tetA PNA or the Control PNA either did not cause significant direct bacterial inhibitory effects, or only did so at concentrations of 15 μM or higher. Because treatment doses were based on the molarity (μM) rather than weight (e.g. μg/ml) of the experimental molecules, the number of CPP particles present in a pure CPP treatment was the same as that in a solution of CPP-PNA, so it was surprising that differing effects were noted when CPP was bound versus unbound. A possible explanation is that CPP molecules bound to a PNA facilitate entrance of the conjugate molecule into the intracellular compartment, then at least some of the PNA

molecules stably bind to a complementary nucleic acid sequence. This may prevent the bound CPP from floating free and possibly leaving and re-entering the bacteria multiple times. The unbound CPP may have the capability to penetrate the bacterial membrane multiple times, thus causing more damage to the cell membrane than CPP that becomes trapped intracellularly when bound to PNA.

The CPP-anti-tetR PNA did cause inhibition of bacterial growth on its own. The effect at 15 μM was slight, but significant. The full role of *tetR* in overall bacterial fitness is still unknown, and the inhibitory effect on growth shown here suggests that suppression of the expression of this gene is detrimental to the bacterium. When the CPP-anti-tetR PNA was combined with tetracycline, it behaved in an unexpected manner. Based on the currently understood relationship between *tetR* and *tetA*[23] shown in Figure 4.16, TetR inhibits *tetA* expression under normal circumstances by binding an operon region. In the presence of tetracycline the TetR protein dissociates from the operon region, allowing upregulation of the *tetA* gene. Opening up this operon region also leads to upregulation of the *tetR* gene. This supposedly allows the bacterium to prevent an overly exuberant *tetA* response by making more *tetR*. It also ensures that ample TetR will be available to inhibit *tetA* expression upon removal of tetracycline. This is to the bacterium's advantage because there is evidence that constitutive expression of a nonessential protein such as a tetracycline efflux pump decreases bacterial fitness.[28] With this relationship in mind, it was expected that suppressing *tetR* in the presence of tetracycline would lead to increased expression of TetA, and thus preserve or even increase the degree of tetracycline resistance of the DT104. Instead, a notable inhibitory effect was seen at all concentrations of tetracycline, as evidenced by the decreased MIC values and flat growth curves. This suggests that the combined effect of tetracycline and the CPP-anti-tetR PNA was detrimental to the bacteria. Interestingly, the MBC was not consistently decreased with this combination, indicating that after removal of tetracycline the bacteria could recommence proliferation, and there is a not as significant a bactericidal effect as is seen with combined tetracycline and CPP-anti-tetA PNA treatment. One possible explanation is that suppression of *tetR* did indeed allow uncontrolled upregulation of *tetA* which put a burden on the bacteria preventing exponential growth in the presence of tetracycline, but allowed enough tetracycline to be removed that the bacteria were not killed and could grow again in the absence of tetracycline and the PNA.

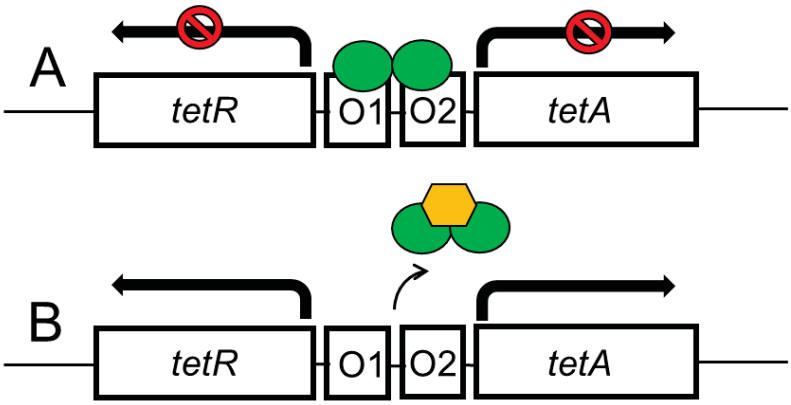

Figure 4.16 The currently understood relationship between TetR protein function and *tetA* gene expression. **A.** Under normal conditions, the TetR protein dimer (green) binds a DNA dual operator region and prevents transcription of the *tetA* and *tetR* genes. **B.** When tetracycline (yellow) is present, it causes TetR to dissociate from the DNA, allowing for TetA and TetR production.

Even more unexpected was the behavior of the CPP-Control PNA. This molecule was specifically designed to avoid complementarity with any known start codons in the DT104 genome, with the idea that it would be a negative control for PNA action. The sequence is complementary to regions in the middle of 10 confirmed or putative genes, but since the action of PNAs is greatest when the target sequence is slightly upstream to and including the mRNA start codon this was considered acceptable. In initial experiments to evaluate the direct effect of this PNA on bacterial growth, its effect was similar to that of CPP alone. No direct inhibition of bacterial growth was seen at 15 μM, the concentration used in subsequent experiments. However, when this molecule was used in conjunction with tetracycline a consistent marked inhibition of bacterial growth was seen, as evidenced by the growth curves in the replicates of the MIC/MBC experiments. The MBC for this molecule also repeatedly could not be interpreted because of skips in the growth pattern. Based on the pilot study it at first appeared that the tetracycline MBC for this molecule was likely between 16 and 32 μg/ml, but in all three of the subsequent replicates the growth was so inconsistent that a definitive MBC was not identified. No clear explanation for this phenomenon was found. These replicates were set up on three different days, two different people (the author and a student assistant) took turns setting up the microtiter plates, the skips were not always in the same place, and acceptable results were obtained for all the other treatment groups, so it is unlikely that the irregular growth pattern is due to operator error.

Several limitations to this study were identified. An unforeseen complication was that the PNAs imparted turbidity to the bacterial growth medium as soon as they were added, which made visual interpretation of the MIC difficult the next day. This was most pronounced for the CPP-anti-tetR PNA and the CPP-Control-PNA, and likely explains some discrepancies between the MIC interpretation for the pilot experiment and that for the subsequent replicates (see Table 4.5). A simple and straightforward relationship between *tetR* and *tetA* was assumed for the purpose of these experiments. The possibility of a more complex interplay between *tetR* and *tetA* or between *tetR* and other cellular mechanisms is not accounted for in the experimental design. Because of the unpredictable effects of the CPP-Control PNA, there was no solid negative control for PNA action to provide strong evidence for specificity of the CPP-anti-tetA PNA. Instead, the behavior of the Control PNA raised additional questions. The 15 μM concentration of the CPP-PNAs is high enough that some of the inhibitory effects could potentially be due to salt formation in the growth medium according to PNA Bio, the PNA manufacturer.

There are multiple possibilities for future work based on the results of this set of experiments. Peptide nucleic acids are expensive to manufacture (hundreds to thousands of dollars for a few hundred nanomoles), so it would be useful to try even lower concentrations of the PNAs and see if similar effects occur. Exploring alternatives to the CPP as a carrier molecule is also suggested. Since the CPP indiscriminately permeabilizes gram-negative bacterial membranes it could potentially have off-target effects such as damaging beneficial bacteria in the ill host organism. This would offset some of the benefits of the target specificity afforded by the PNAs. Comparison of bacterial cell membrane integrity among treatment groups may provide insight into why unbound CPP is apparently more potent than CPP bound to a PNA. Some options to explore this question include scanning electron microscopy of the treated bacteria, or measurement of molecules specific for leakage of intracellular contents such as potassium or adenosine triphosphate (ATP).[29] A more detailed analysis of the role of *tetR* in bacterial fitness and of the dynamic between *tetR* and *tetA* would be of interest to help determine if there are certain PNA combinations that may be even more effective in treating bacterial infection. Evaluating expression of the *tetA* and *tetR* mRNA transcripts, or measuring actual protein expression through use of Western blotting or other techniques are possible approaches. An inevitable next step in

determining the clinical use of these PNAs would be treatment of a DT104-infected live animal model with the PNA and tetracycline.

In conclusion, the decrease in tetracycline MIC and MBC that occurred after concurrent treatment with tetracycline and a PNA targeting expression of the TetA tetracycline efflux pump suggests that antisense therapy could allow for repurposing of antibiotics to which bacteria are resistant. Continuing to evaluate the efficacy of antisense antibacterial technology is a worthwhile pursuit in the ongoing effort to address the threat of antibiotic resistance.

4.5 References

1. Centers for Disease Control and Prevention (CDC). Antibiotic resistance threats in the United States, 2013. https://www.cdc.gov/drugresistance/threat-report-2013/pdf/ar-threats-2013-508.pdf. Accessed February 16, 2019.
2. Voetsch AC, Van Gilder TJ, Angulo FJ, et al. FoodNet estimate of the burden of illness caused by nontyphoidal *Salmonella* infections in the United. States. Clin Infect Dis. 2004;38(s3):S127-S134.
3. Glynn MK, Bopp C, Dewitt W, Dabney P, Mokhtar M, Angulo FJ. Emergence of multidrug-resistant *Salmonella enterica* serotype Typhimurium DT104 infections in the United States. N Engl J Med. 1998;338(19):1333-1338.
4. Threlfall EJ. Epidemic *Salmonella* Typhimurium DT104 – a truly international multiresistant clone. J Antimicrob Chemother. 2000;46:7-10.
5. Helms M, Ethelberg S, Kare M, and the DT104 Study Group. International *Salmonella* Typhimurium DT104 infections, 1992-2001. Emerg Inf Dis. 2005;11(6):859-867.
6. Briggs CE, Fratamico PM. Molecular characterization of an antibiotic resistance gene cluster of *Salmonella* Typhimurium DT104. Antimicrob Agents Chemother. 1999;43(4):846-849.
7. Boyd DA, Peters GA, Ng Lai-King, Mulvey MR. Partial characterization of a genomic island associated with the multidrug resistance region of *Salmonella enterica* Typhimurium DT104. FEMS Microbiol Lett. 200;189(2):285-291.
8. Boyd D, Peters GA, Cloeckaert A, et al. Complete nucleotide sequence of a 43-kilobase genomic island associated with the multidrug resistance region of *Salmonella enterica*

serovar Typhimurium DT104 and its identification in phage type DT120 and serovar Agona. J Bacteriol. 2001;183(19):5725-5732.

9. Bai H and Luo X. Antisense antibacterials: from proof-of-concept to therapeutic perspectives. In: Bobbarala V, ed. A Search for Antibacterial Agents. InTechOpen; 2012:319-344. doi: 10.5772/33347.
10. Rasmussen LCV, Sperling-Petersen HU, and Mortensen KK. Hitting bacteria at the heart of the central dogma: sequence-specific inhibition. Microb Cell Fact. 2007;6(24). doi: 10.1186/1475-2859-6-24.
11. Neilsen PE, Egholm M, Berg RH, Buchardt O. Sequence-selective recognition of DNA by strand displacement with a thymine-substituted polyamide. Science. 1991;254(5037):1497-1500.
12. Egholm M, Nielsen PE, Buchardt O, Berg RH. Recognition of guanine and adenine in DNA by cytosine and thymine containing peptide nucleic acids (PNA). J Am Chem Soc. 1992;114(24):9677-9678.
13. Demidov VV, Potaman VN, Frank-Kamenetskil MD, et al. Stability of peptide nucleic acids in human serum and cellular extracts. Biochem Pharm. 1994;48(6):1310-1313.
14. Rajasekaran P, Alexander JC, Seleem MN, et al. Peptide nucleic acids inhibit growth of *Brucella suis* in pure culture and in infected murine macrophages. Int J Antimicrob Agents. 2013;41(4):358-362.
15. Bai H, Sang G, You Y, et al. Targeting RNA polymerase primary σ^{70} as a therapeutic strategy against methicillin-resistant *Staphylococcus aureus* by antisense peptide nucleic acid. PLoS One. 2012;7(1):e29886. doi: 10.1371/journal.pone.0029886.
16. Soofi MA, Seleem MN. Targeting essential genes in *Salmonella enterica* serovar Typhimurium with antisense peptide nucleic acid. Antimicrob Agents Chemother. 2012;56(12):6407-6409.
17. Mondhe M, Chessher A, Goh S, Good L, Stach JEM. Species-selective killing of bacteria by antimicrobial peptide-PNAs. PLoS One. 2014;9(2):e89082. doi: 10.1371/journal.pone.0089082.
18. Good L, Nielsen PE. Antisense inhibition of gene expression in bacteria by PNA targeted to mRNA.Nat Biotechnol. April 1998;16:355-358.

19. Goh S, Loeffler A, Lloyd DH, Nair SP, Good L. Oxacillin sensitization of methicillin-resistant *Staphylococcus aureus* and methicillin-resistant *Staphylococcus pseudintermedius* by antisense peptide nucleic acids *in vitro*. BMC Microbiol. 2015;15:262. doi: 10.1186/s12866-015-0599-x.
20. Eriksson M, Nielsen PE, Good L. Cell permeabilization and uptake of antisense peptide-peptide nucleic acid (PNA) into *Escherichia coli*. J Biol Chem. 2002;277(9):7144-7147.
21. Vaara M, Porro M. Group of peptides that act synergistically with hydrophobic antibiotics against gram-negative enteric bacteria. Antimicrob Agents Chemother. 1996;40(8):1801-1805.
22. IUPAC-IUB Joint Commission on Biochemical Nomenclature (JCBN). Nomenclature and symbolism for amino acids and peptides. Eur J Biochem. 1984;138(1):9-37.
23. Moller TSB, Overgaard M, Nielsen SS, et al. Relation between tetR and tetA expression in tetracycline resistant *Escherichia coli*. BMC Microbiol. 2016;16:39. doi: 10.1186/s12866-016-0649-z.
24. Yukawa S, Tamura Y, Tanaka K, Uchida I. Rapid detection of *Salmonella enterica* serovar Typhimurium DT104 strains by the polymerase chain reaction. Acta Vet Scand. Spetember 2015;57:59. doi:10.1186/s13028-015-0143-x.
25. Good L, Awasthi SK, Dryselius R, Larsson O, Nielsen PE. Bactericidal antisense effects of peptide-PNA conjugates. Nat Biotech. April 2001;19:360-364.
26. Dryselius R, Aswasti SK, Rajaroa GK, Nielsen PE, and Good L. The translation start codon region is sensitive to antisense PNA inhibition in *Escherichia coli*. Oligonucleotides. 2004;13(6):427-433.
27. Andrews JM. Determination of minimum inhibitory concentrations. J Antimicrob Chemother. 2001;48(Suppl S1):5-16.
28. Nguyen TNM, Phan QG, Duong LP, Bertrand KP, Lenski RE. Effects of carriage and expression of the Tn10 tetracycline-resistance operon on the fitness of *Escherichia coli* K12. Mol Biol Evol. 1989;6(3):213-225.
29. Johnston MD, Hanlon GW, Denyer SP, Lambert RJW. Membrane damage to bacteria caused by single and combined biocides. J Appl Microbiol. 2003;94(6):1015-1023.

5 Effect of cell penetrating peptide-peptide nucleic acid (CPP-PNA) conjugates on expression of *tetA* mRNA in *Salmonella enterica* ssp *enterica* serovar Typhimurium DT104

5.1 Introduction

The worsening problem of antibiotic resistance presents a worldwide health threat.[1] In response to the need for novel antimicrobial drugs, there is a movement to evaluate the antibacterial effects of cell penetrating peptide (CPP)-bound antisense molecules such as phosphorothioate oligonucleotides (PS-ODN),[2] phosphorodiamidate morpholino oligomers (PMO),[3] and peptide nucleic acids (PNA).[4-5]

In Chapter 4 of this dissertation, it was shown that concurrent treatment with tetracycline and a CPP-PNA targeting expression of the TetA tetracycline efflux pump decreased the tetracycline MIC and MBC of tetracycline-resistant *Salmonella enterica* ssp. *enterica* serovar Typhimurium DT104 (DT104). These findings suggest that PNAs targeting antibiotic resistance genes can restore antibiotic susceptibility in resistant bacteria. However, the results of the Chapter 4 experiments also raised questions about the mechanism of action of the CPP-PNA molecules that could not be answered merely by reviewing the MIC and MBC data.

First of all, it was assumed that the *tetA* gene is functional in the laboratory stock strain of DT104 used for the experiments, based on literature review and on the documentation of the gene in the GenBank Nucleotide and PATRIC databases. However, it was not definitively known if tetracycline treatment actually causes upregulation of the tetA gene in DT104.

Second, there was uncertainty as to whether the CPP-anti-tetA PNA was truly suppressing expression of the *tetA* gene according to the currently accepted model of PNA action (see Chapter 4, Figure 4.2), which states that a PNA specifically binding the mRNA start codon and 5'-untranslated region of a target gene sterically hinders ribosome binding and prevents protein translation.[6] A common way to indirectly demonstrate sequence specificity of a PNA construct is to include a control group treated with a "scrambled" PNA that has a nonsense/mismatched nucleotide sequence.[7-8] If the expected phenotypic alteration (e.g. bacterial growth inhibition,

restoration of antibiotic susceptibility) is observed after treatment with the sequence specific PNA, but not the mismatched PNA, it strongly suggests suppression of the theoretical gene target. This approach was unsuccessful in experiments described in Chapter 4, because the scrambled control PNA had unpredictable inhibitory effects that as yet are not fully explained. Therefore, an alternative method to evaluate sequence specificity of the anti-tetA PNA was needed.

Third, some direct bacterial inhibitory activity of the CPP carrier molecule (peptide sequence KFFKFFKFFK) was observed in the experiments described in Chapter 4. A similar effect was previously reported in *Staphylococcus pseudintermedius*.[9] This prompted investigation into how much that CPP may be contributing to growth inhibition of DT104, and whether it affects expression of *tetA*.

Finally, it was noted that treatment of DT104 with a CPP-PNA targeting expression of the *tetR* gene had the opposite effect than expected. It is currently understood that TetR protein, the product of the *tetR* gene, suppresses expression of TetA (see Chapter 4, Figure 4.16),[10] so the presumption was that inhibiting *tetR* expression would allow for increased TetA expression and cause either unchanged or increased resistance to tetracycline relative to the untreated control. Instead, treatment with the CPP-anti-tetR PNA resulted in a moderate to marked decrease in the MIC and a slight decrease in the MBC. Therefore, there was a desire to gather evidence that the CPP-anti-tetR PNA actually targets *tetR* expression.

In the following set of experiments, reverse transcription quantitative polymerase chain reaction (RT-qPCR) was utilized to i) verify upregulation of *tetA* expression in DT104 in response to tetracycline, ii) characterize the effect of CPP-anti-tetA PNA and CPP alone on expression of *tetA* mRNA in the presence and absence of tetracycline, and iii) analyze the effect of CPP-anti-tetR PNA on expression of *tetA* mRNA in the presence and absence of tetracycline.

5.2 Materials and Methods

5.2.1 PNA design

See Chapter 4 of this dissertation for details on PNA design and synthesis. The relevant PNA and CPP sequences are repeated here in Table 5.1 for ease of reference.

Table 5.1 The effect of these peptide nucleic acids and the cell penetrating peptide on *tetA* expression in DT104 was analyzed by RT-qPCR. Details of PNA design are in Chapter 4.

GenBank gene reference number and/or name	**Function**	**Target DNA sequence (5'-3')**	**PNA sequence (5'-3') with attached CPP and o-linker**	**Name used in text**
DT104_38611 tetracycline resistance protein class A (*tetA*)	Codes for the TetA protein, a tetracycline efflux pump that is upregulated in the presence of intracellular tetracycline	gacgccatgg	(KFF)3K-o-ccatggcgtc	CPP-anti-tetA PNA
DT104_38601 tetracycline resistance regulator protein (*tetR*)	Codes for TetR, a protein that suppresses TetA expression under normal conditions, and is upregulated in the presence of intracellular tetracycline	cgtgaatgac	$(KFF)_3$K-o-gtcattcacg	CPP-anti-tetR PNA
Cell penetrating peptide alone	Short amino acid sequence attached to PNAs to facilitate crossing cell membranes	N/A	KFFKFFKFFK	CPP

5.2.2 Primer design

The NCBI Primer BLAST tool was used to generate 10 proposed primer pairs for sequences specific to the DT104 *tetA* gene. The input PCR template range was NCBI genome HF937208.1 from bp 4115970 to bp 4117097. The default entries were left in place for the remaining search parameters. An ideal RT-qPCR amplicon length is short, between 75-200 bp.[11-12] Using this guideline, three of the primer pairs designed by the BLAST tool were chosen and ordered from Sigma. These three primer pairs were validated by amplifying the target products from DT104 genomic DNA (gDNA) and visualizing the amplicon bands using agarose gel electrophoresis with ethidium bromide staining. The PCR reaction was run using a CFX96 Real-Time PCR Detection

System (Bio-Rad, Hercules, CA). The reaction mixture in each PCR tube consisted of 20 µl GoTaq Green Master Mix, 16 µl sterile nuclease-free water (or 18 µl for DNA-free control tubes), 2 µl primer mix (1 µM final concentration), and 2 µl template DNA (or 0 µl for DNA-free control tubes), for a final volume of 40 µl. The PCR protocol was

1) 95 C° x 30 sec →
2) [95 C° x 30 sec → 55 C° x 30 sec → 72 C° x 1 min] x 30 cycles →
3) 72 C° x 5 min

Amplicon bands were visualized using conventional agarose gel electrophoresis with ethidium bromide staining. The primer pair that resulted in the brightest band on the gel was then used routinely to detect the *tetA* gene for the remainder of the experiments.

The 16S ribosomal RNA gene was chosen as a stably expressed reference gene for comparison of the relative level of gene expression. The primer pair for this gene was previously published.[13] Primer sequences are shown in Table 5.2.

Table 5.2 Primer sequences used to evaluate *tetA* expression in DT104 treated with various combinations of CPP-PNAs, CPP only, and tetracycline. Expression of *tetA* mRNA was calculated relative to expression of 16S RNA, which was stably expressed under the various treatment conditions.

Gene	Forward primer 5'-3'	Reverse primer 5'-3'	Product
tetA	TTCCCGATTCTGTTGCTGCT	CAAGCGGTCCTGCGATAGAG	151 bp
16S	CGGGGAGGAAGGTGTTGTG	GAGCCCGGGGATTTCACATC	178 bp

5.2.3 RNA stabilization, extraction, and purification

Ribonucleic acid in bacterial cultures was stabilized with RNAprotect Bacteria Reagent (Qiagen, Germantown, MD) per manufacturer instructions. Briefly, one volume of bacterial broth culture was added to 2 volumes of RNAprotect Bacteria Reagent in a sterile capped tube, vortexed for 5 seconds and incubated at room temperature for 5 minutes. Tubes were then centrifuged for 10 min at 5000 x g to form an RNA-containing pellet, and the supernatant was decanted. At that point,

RNA extraction and purification were either performed immediately, or pellets were stored at -20 C° until RNA purification could be done (1 week to 3 months). For all experiments using RT-qPCR, RNA was purified using a Qiagen RNeasy Mini kit with on-column DNase digestion using a Qiagen RNase-free DNase set. All steps were carried out per manufacturer instructions. Purified RNA concentrations were measured with a NanoDrop™ 2000 spectrophotometer (Thermo Fisher Scientific, Waltham, MA).

5.2.4 PCR equipment, reagents, and process

RT-qPCR was done in 96 well PCR plates using a CFX Connect™ Real-Time PCR Detection System (Bio-Rad, Hercules, CA) and iTaq Universal One-Step RT-qPCR kits (Bio-Rad catalog number 1725151). SYBR green fluorescence was used to detect DNA amplification. Samples were always run in triplicate and each run include a non-template control for each primer, and a reverse-transcriptase-free control for each primer/target combination. Melt curve analysis was done at the end of each PCR run to evaluate primer specificity. Data was stored and visualized using CFX Manager™ Software (Bio-Rad, Hercules, CA).

5.2.5 Primer validation with standard curves

The primers for the *tetA* and 16S genes were validated for RT-qPCR by making six 10-fold serial dilutions of total RNA such that the starting RNA template in each well ranged from 100 nanogram (ng) to 1 picogram (pg). Triplicate wells of each RNA dilution were plated in a qPCR 96 well plate. The PCR reaction mixture was 15 µl 2x SYBR green master mix, 0.6 µl iScript reverse transcriptase (RT), 0.9 µl TetA primer (0.3 µM final concentration), 1 µl RNA template and 12.5 µl nuclease-free water, for a final volume of 30 µl/well. The PCR protocol was

1) 50 C˚ x 10 C˚ min →
2) 95 C˚ x 5 min →
3) [95 C˚ x 10 sec → 60 C˚ x 30 sec] x 40 cycles →
4) 95 C˚ x 1 min →
5) 55 C˚ x 1 min →
6) Melt curve 55 C˚ to 95 C˚ in 0.5 C˚ increments for 10 sec

An excellent standard curve was generated for each primer, and both showed good reaction efficiency (see Results section), indicating that these primers were acceptable choices for experimental comparison of relative *tetA* and 16S expression. Based on the C_q result of each starting RNA concentration in the standard curves, 1 ng of template RNA was chosen as the best amount of starting material for all future experiments, and RNA samples were subsequently adjusted accordingly to allow for 1 ng of RNA in each PCR reaction well.

5.2.6 Detection of tetA upregulation in response to tetracycline treatment

To determine if upregulation of the tetA gene in response to tetracycline could be detected with RT-qPCR, DT104 was plated into 96-well ultra-low attachment culture plates at a concentration of 5 x 10^5 CFU/ml in Mueller Hinton broth and cultured with 8 μg/ml tetracycline or no treatment for ~18 hours, 4 hours, or 1 hour. A simplified visual representation of the microtiter plate set-up is shown in Figure 5.1. Total RNA was extracted after stabilization with RNAprotect bacteria reagent and RT-qPCR was done with the *tetA* primer and 16S primer. Expression of *tetA* mRNA in tetracycline-treated and untreated cultures relative to expression of 16S mRNA was calculated using the Pfaffl method (Pfaffl 2001).[14] With this method an expression ratio is calculated with the following equation:

$$\text{Ratio} = \frac{(E_{\text{target}})^{\Delta C_q,\ \text{target (calibrator}-\text{test)}}}{(E_{\text{reference}})^{\Delta C_q,\ \text{reference (calibrator}-\text{test)}}}$$

where E_{target} = amplification efficiency of target gene (*tetA*), $E_{reference}$ = amplification efficiency of reference gene (16S), ΔC_q. target (calibrator – test) = C_q of the target gene (*tetA*) in the calibrator sample (no tetracycline) minus the C_q of the target gene in the test sample (8 μg/ml tetracycline), and ΔC_q, reference (calibrator – test) = C_q of the reference gene (16S) in the calibrator sample (no tetracycline) minus the C_q of the reference gene in the test sample (8 μg/ml tetracycline).

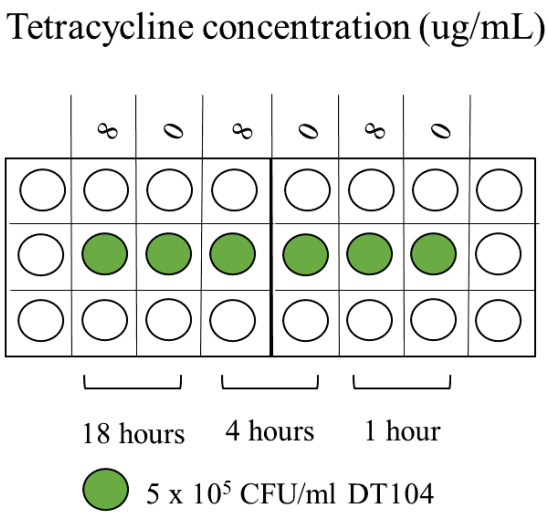

Figure 5.1 Simplified diagram of a 96-well plate set-up in which DT104 was grown with or without 8 µg/ml tetracycline for various lengths of time in order to detect upregulation of *tetA* expression in response to tetracycline. Bacteria were harvested for RNA stabilization and extraction, and RT-qPCR was performed to measure mRNA expression of the target *tetA* gene and a stably expressed reference gene, 16S. Expression of *tetA* mRNA relative to 16S mRNA was compared between treated and untreated cultures and among different time points.

5.2.7 Effect of CPP-anti-tetA PNA, CPP alone, and CPP-anti-tetR PNA on tetA expression in DT104 treated with tetracycline

To examine the effect of various combinations of CPP-PNA, CPP only, and tetracycline, DT104 was plated into 96-well ultra-low attachment culture plates at a concentration of 5 x 10^5 CFU/ml in Mueller Hinton broth and cultured for 1 hour or 4 hours. Treatments were added as shown in Figure 5.2. Total RNA was extracted and RT-qPCR was done with the *tetA* primer and 16S primer. Expression of *tetA* mRNA in various treatment groups relative to expression of 16S mRNA was calculated using the Pfaffl method. Comparisons included:

CPP-anti-tetA PNA + tetracycline vs. tetracycline only

CPP + tetracycline vs. tetracycline only

CPP-anti-tetA PNA + tetracycline vs. CPP + tetracycline

CPP-anti-tetR PNA + tetracycline vs. CPP-anti-tetA PNA + tetracycline

CPP-anti-tetR PNA without tetracycline vs. CPP-anti-tetA PNA + tetracycline

CPP-anti-tetR PNA + tetracycline vs. tetracycline only

CPP-anti-tetR PNA without tetracycline vs. tetracycline only

Three replicate cultures with 4 hour incubations were done for the following treatment groups: 8 µg/ml tetracycline only, CPP-anti-tetA PNA + 8 µg/ml tetracycline, and CPP only + 8 µg/ml tetracycline.

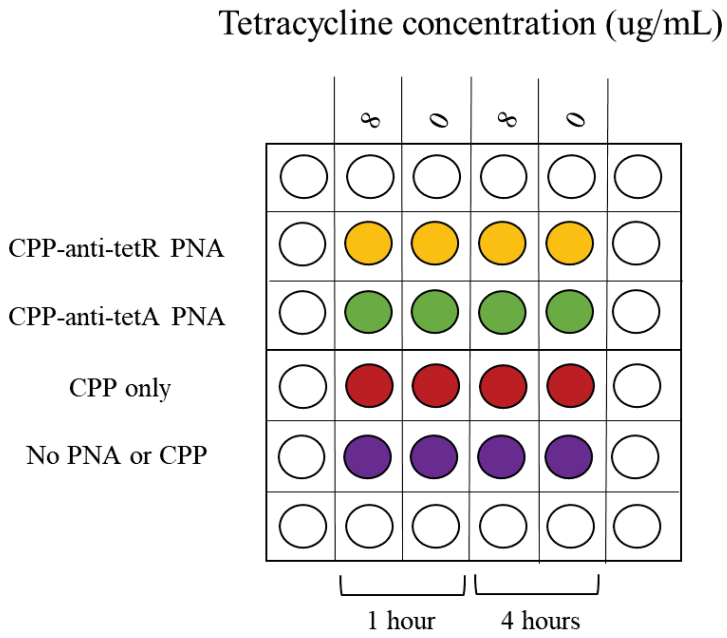

Figure 5.2 Simplified diagram of a 96-well plate set-up in which DT104 was grown to examine the effect of various combinations of CPP-PNA, CPP only, and 8 µg/ml tetracycline on *tetA* expression. Bacteria were plated at a concentration of 5 x 10^5 CFU/ml in Mueller Hinton broth and cultured for 1 hour or 4 hours. Bacteria were harvested for RNA stabilization and extraction, and RT-qPCR was performed to measure mRNA expression of the target *tetA* gene and a stably expressed reference gene, 16S. Expression of *tetA* mRNA relative to 16S mRNA was compared among various treatment groups.

5.3 Results

5.3.1 Primer validation with standard curves

Both the 16S and *tetA* primers generated standard curves with excellent linearity and acceptable efficiency (Figure 5.3 and Figure 5.4). Melt curve analysis for each primer demonstrated good primer specificity without evidence of primer-dimer formation (data not shown).

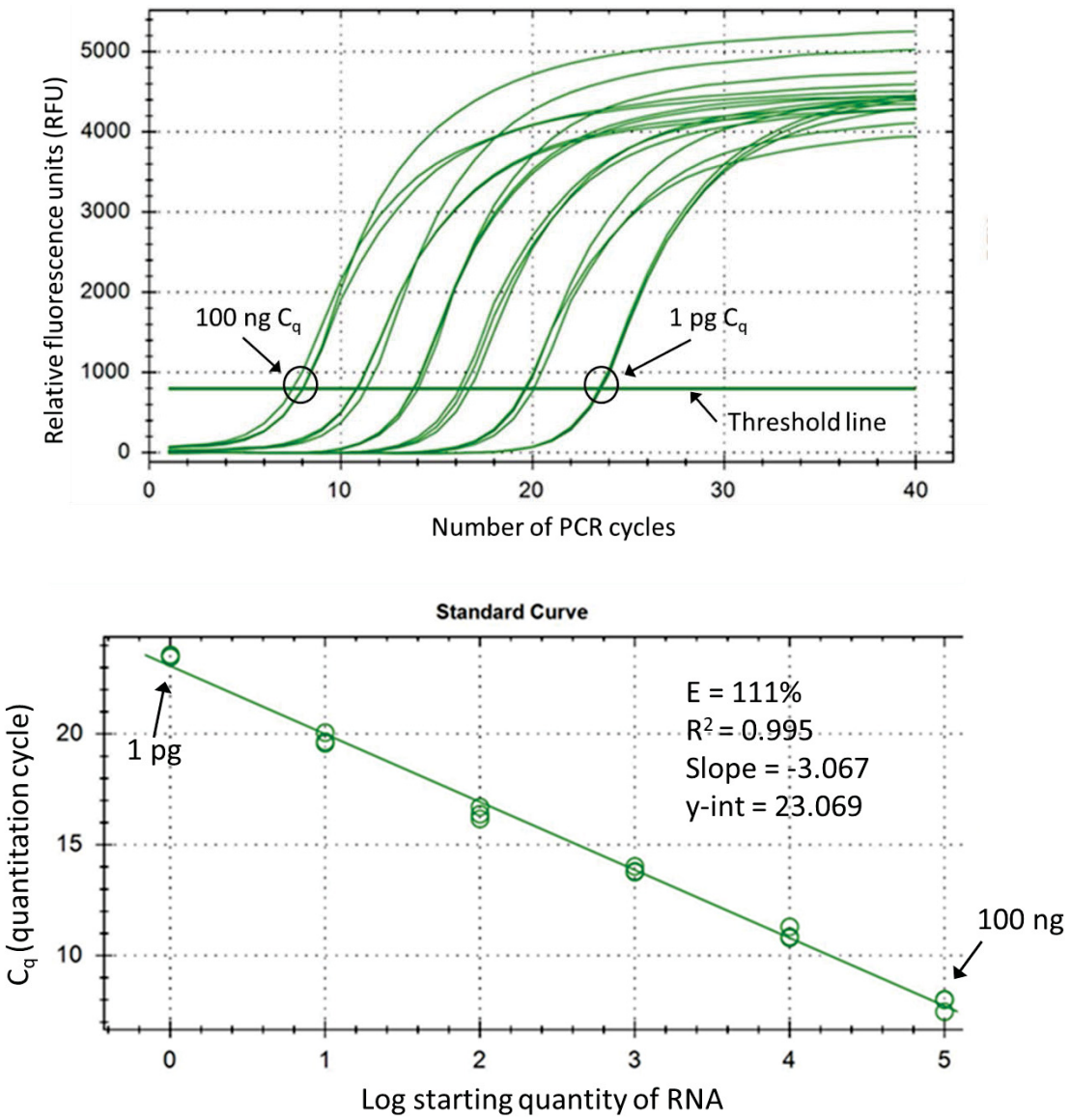

Figure 5.3 RT-qPCR tracings (top) and standard curve (bottom) generated to evaluate efficiency of the primer for the 16S gene. Total RNA was extracted from DT104 cultured in Mueller-Hinton broth and serial 10-fold dilutions of the RNA extract were done to make six standard samples with RNA concentrations of 100 ng, 10 ng, 1 ng, 100 pg, 10 pg, and 1 pg. RT-qPCR was done using SYBR green fluorescent dye as a detection method. In RT-qPCR, fluorescence increases over time with increasing amplification of the target DNA, generating a tracing for each PCR well. The top graph shows the PCR tracings generated for each standard solution. The samples were run in triplicate, so there are three tracings for each concentration of RNA template. The PCR cycle number at which a tracing crosses a fluorescence threshold is called the quantitation cycle or C_q. The greater the starting amount of RNA template, the further left the tracing, and the lower the C_q. The C_qs for the 100 ng and 1 pg samples are labeled. The C_q data is log transformed and plotted as a standard curve as shown in the lower graph, and the primer efficiency (E), coefficient of determination (R^2), and slope of the standard curve are calculated. An optimized qPCR assay ideally has E = 95-105%, R2 ≥ 0.980, and standard curve slope = -3.32.[11]

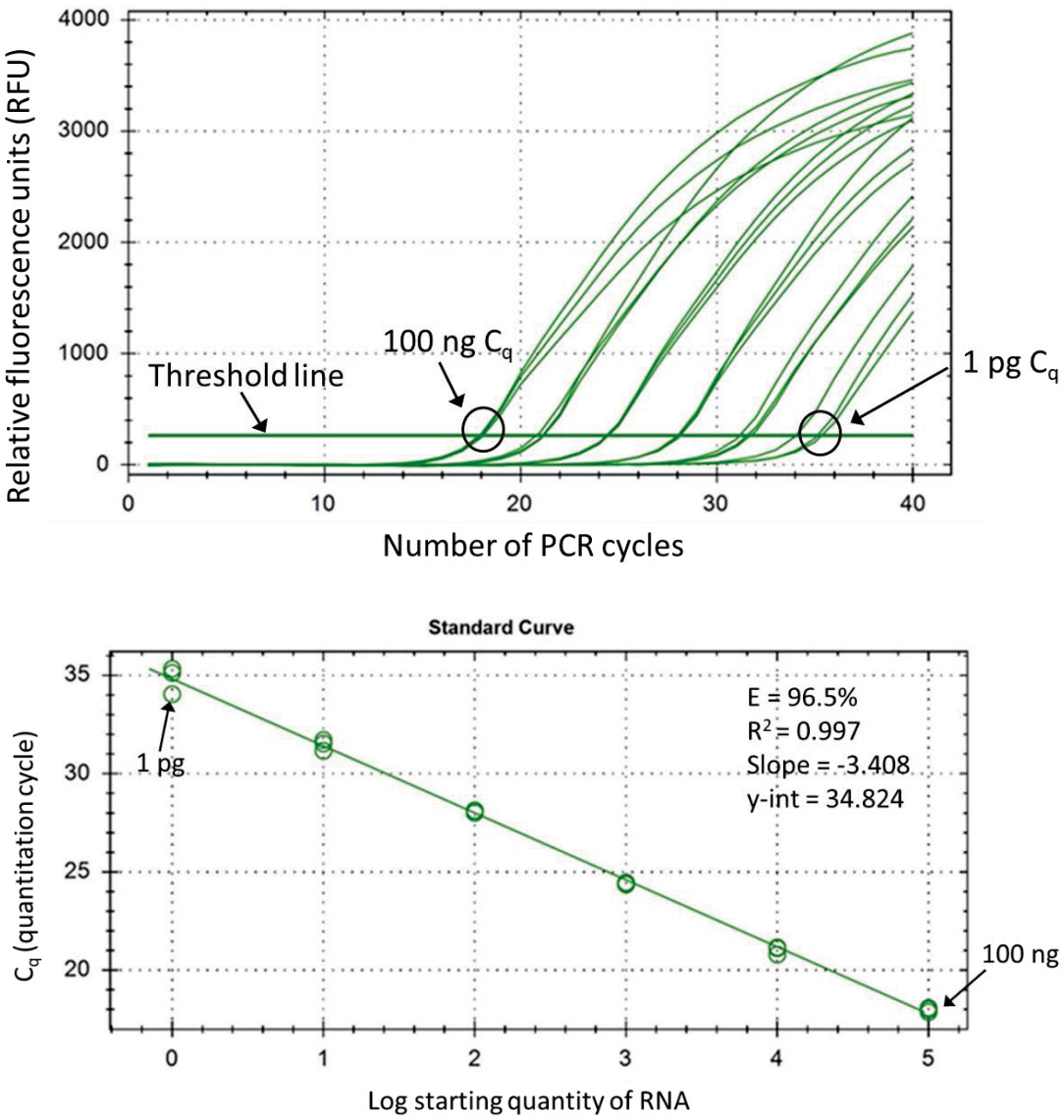

Figure 5.4 RT-qPCR tracings (top) and standard curve (bottom) generated to evaluate efficiency of the primer for the *tetA* gene. Total RNA was extracted from DT104 cultured in Mueller-Hinton broth and serial 10-fold dilutions of the RNA extract were done to make six standard samples with RNA concentrations of 100 ng, 10 ng, 1 ng, 100 pg, 10 pg, and 1 pg. RT-qPCR was done using SYBR green fluorescent dye as a detection method. In RT-qPCR, fluorescence increases over time with increasing amplification of the target DNA, generating a tracing for each PCR well. The top graph shows the PCR tracings generated for each standard solution. The samples were run in triplicate, so there are three tracings for each concentration of RNA template. The PCR cycle number at which a tracing crosses a fluorescence threshold is called the quantitation cycle or C_q. The greater the starting amount of RNA template, the further left the tracing, and the lower the C_q. The C_qs for the 100 ng and 1 pg samples are labeled. The C_q data is log transformed and plotted as a standard curve as shown in the lower graph, and the primer efficiency (E), coefficient of determination (R^2), and slope of the standard curve are calculated. An optimized qPCR assay ideally has E = 95-105%, R2 ≥ 0.980, and standard curve slope = -3.32.[11]

5.3.2 Detection of tetA upregulation in response to tetracycline treatment

Figure 5.5 shows the PCR tracings from DT104 cultures treated with tetracycline for 18 hours, 4 hours, or 1 hour, and Figure 5.6 summarizes the relative expression of *tetA* mRNA in tetracycline-treated cultures compared to untreated cultures at each time point. The first attempt at RNA amplification was done on the culture treated for approximately 18 hours. Little difference was observed in relative expression of *tetA* between the untreated culture and the culture treated with tetracycline (Figure 5.5.A). However, a slight difference was noted between the treated and untreated cultures incubated for 4 hours (Figure 5.5B), and a clear difference was seen between the cultures incubated for only 1 hour (Figure 5.C).

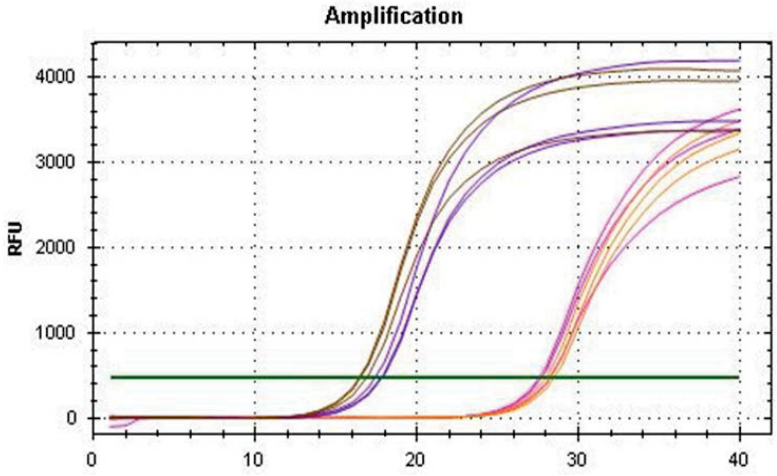

Figure 5.5A ~18 hours

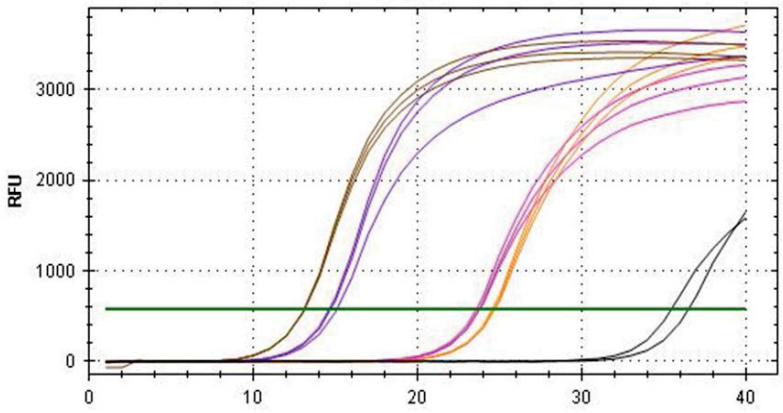

Figure 5.5B 4 hours

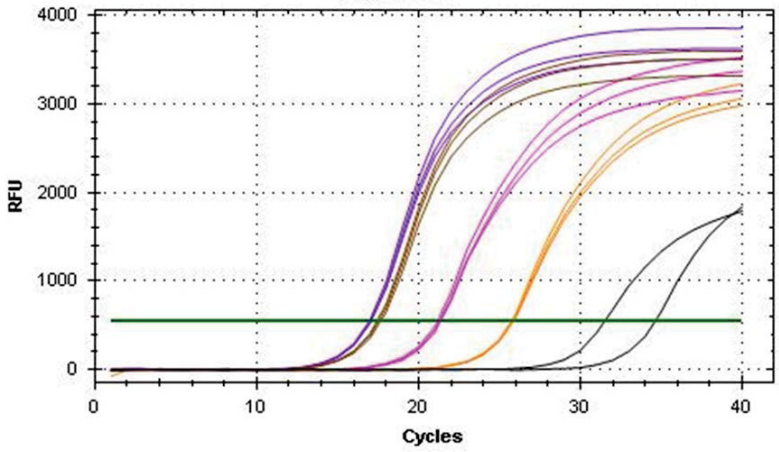

Figure 5.5C 1 hour

Figure 5.5 Time-related PCR tracings showing *tetA* expression and 16S expression in cultures of DT104 incubated with or without tetracycline for **A.** ~18 hours, **B.** 4 hours, or **C.** 1 hour. Note the fairly stable expression of the 16S reference gene in both the untreated (dark orange) and tetracycline-treated (dark purple) cultures. Relative upregulation of *tetA* expression compared to 16S expression, indicated by a left shift of the light purple curve, was expected in cultures treated with tetracycline. This effect was only obvious at the 1 hour time point, suggesting a rapid and short-lived upregulation of gene transcription.

PCR tracing color key indicating type of treatment and primer target:

No treatment, tetA

No treatment, 16S

8 µg/ml tetracycline, tetA

8µg/ml tetracycline, 16S

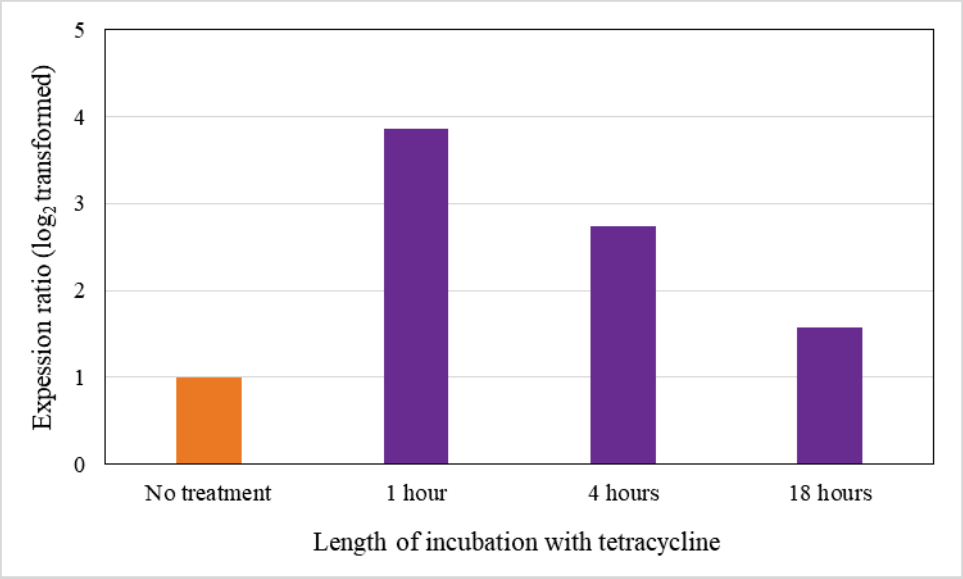

Figure 5.6 Summary of results presented in Figure 5.5. Purple bars show relative *tetA* expression in DT104 cultures treated with 8 µg/ml tetracycline for 1 hour, 4 hours, or 18 hours compared to untreated cultures (orange bar). Total RNA was extracted and gene expression was measured using RT-qPCR. Expression of *tetA* relative to the reference16S gene was calculated for each time point using the Pfaffl method to obtain an expression ratio. The ratios were $\log_2$ transformed to allow for better visualization of relative gene expression. The data indicate a rapid upregulation of *tetA* expression within the first hour after exposure to tetracycline that then dissipates over the next several hours.

5.3.3 Effect of CPP-anti-tetA PNA, CPP alone, and CPP-anti-tetR PNA on tetA expression in DT104 treated with tetracycline

The results of *tetA* expression in response to various combinations of CPP-PNA, CPP only, and tetracycline after 1 hour or 4 hours are detailed in Figure 5.7-Figure 5.15.

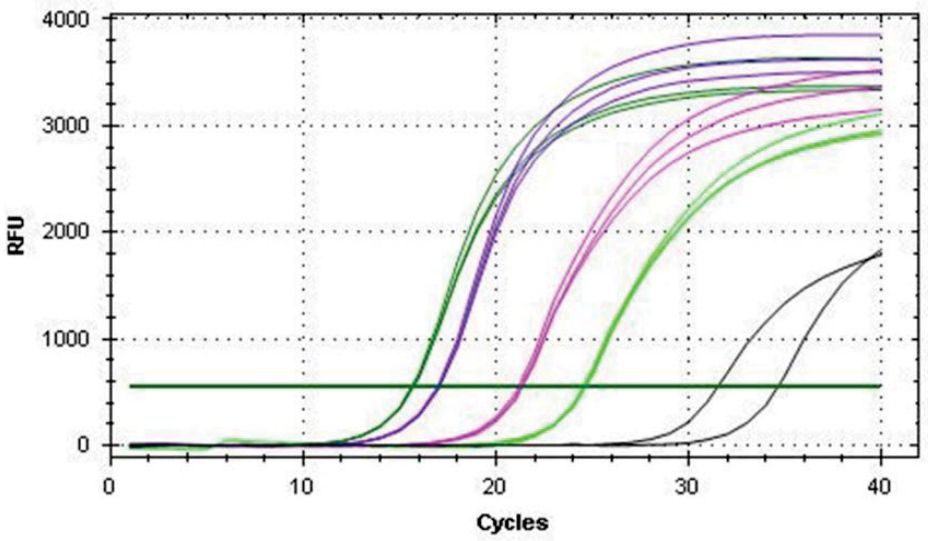

Figure 5.7A: Relative expression of *tetA* in a culture treated with tetracycline and CPP-anti-tetA PNA (light green) compared to a culture treated only with tetracycline (light purple). Incubation time was 1 hour. Note the relatively decreased expression of *tetA* in the PNA-treated culture as indicated by a right shift of the light green tracing. Expression of 16S was similar between treatment groups (dark green for CPP-PNA treated culture, dark purple for tetracycline only culture), as appropriate for a reference gene.

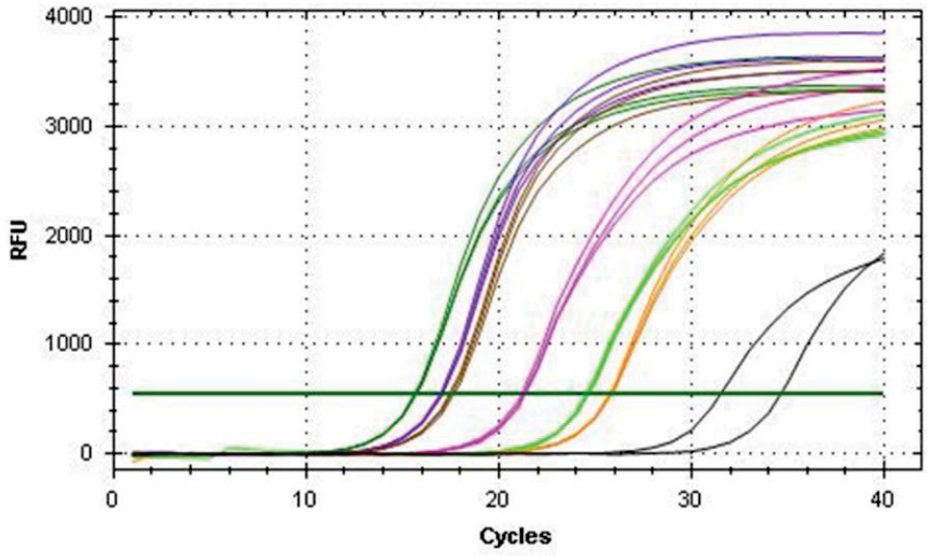

Figure 5.7B: This figure is the same as A. except that the tracings for the untreated culture are added in (light orange, *tetA* expression; dark orange, 16S expression). This shows that in the culture treated with both tetracycline and CPP-anti-tetA PNA, *tetA* expression (light green) is suppressed such that it is similar to that of the untreated culture. The culture treated with tetracycline alone shows *tetA* upregulation (light purple). Incubation time was 1 hour.

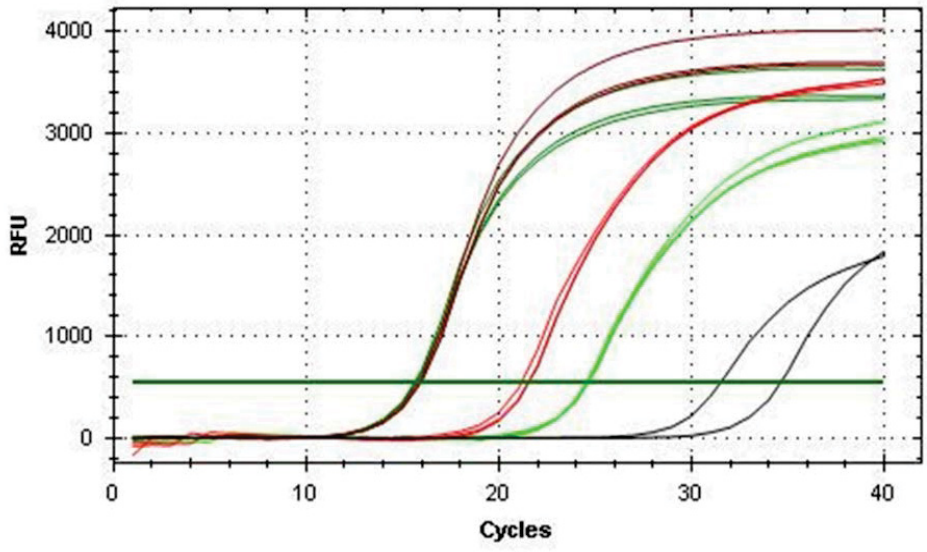

Figure 5.7C: Relative expression of tetA in a culture treated with tetracycline and CPP-anti-tetA PNA (light green) compared to a culture treated with tetracycline and CPP alone (light red). Incubation time was 1 hour. Note the relatively decreased expression of *tetA* in the PNA-treated culture as indicated by a right shift of the light green tracing. Expression of 16S was similar between treatment groups (dark green for CPP-PNA treated culture, dark red for CPP treated culture), as appropriate for a reference gene.

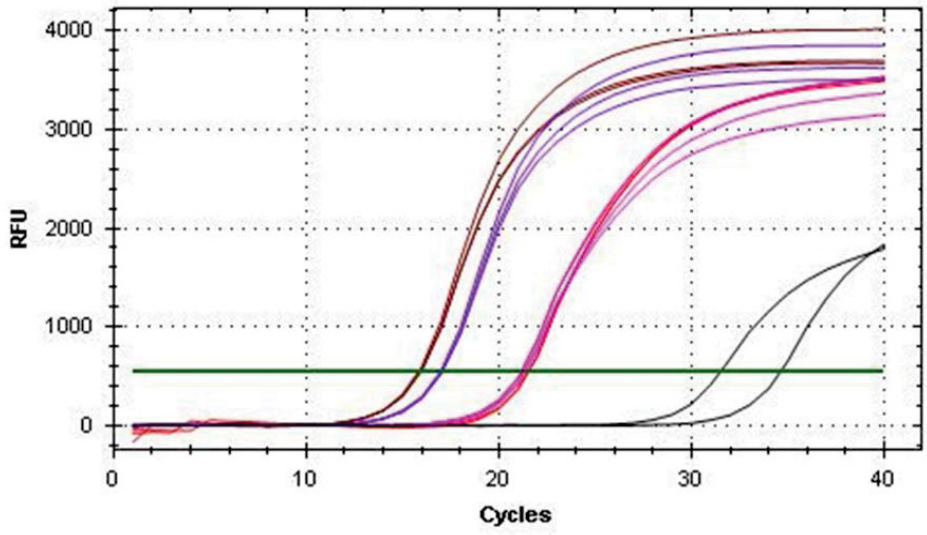

Figure 5.7D: Relative expression of *tetA* in a culture treated with tetracycline and CPP alone (light red), compared with the culture treated only with tetracycline (light purple). The tracings are nearly superimposed, indicating a similar degree of gene expression. Incubation time was 1 hour.

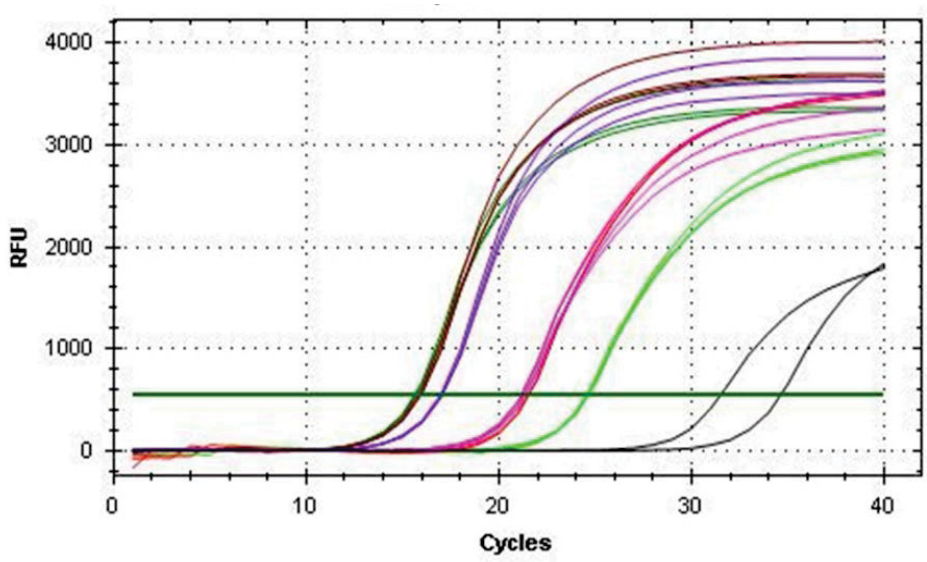

Figure 5.7E: Combination of tracings for the culture treated with tetracycline and CPP-anti-tetA PNA (light green), the culture treated with tetracycline and CPP alone (light red), and the culture treated only with tetracycline (light purple). This is to show that *tetA* expression is down-regulated in the CPP-PNA treated culture compared to both the culture treated with tetracycline alone and the culture treated only with tetracycline. Incubation time was 1 hour.

Figure 5.7 PCR tracings of *tetA* and 16S expression in various treatment groups cultured with different combinations of CPP-PNA, CPP only, and/or tetracycline for 1 hour. In all treatment groups, DT104 at a concentration of 5 x 10^5 CFU/ml was cultured in Mueller-Hinton broth in 96-well microtiter plates. After incubation with treatments for 1 hour, total RNA was stabilized and extracted, and RT-qPCR was performed to amplify *tetA* mRNA and 16S mRNA (reference gene). Expression of *tetA* in each treatment group was calculated with the Pfaffl method. The two black tracings to the far right of each graph are tracings for the non-template control for each primer.

PCR tracing color key indicating type of treatment and primer target:

8 µg/ml tetracycline + CPP-anti-tetA PNA, tetA

8 µg/ml tetracycline + CPP-anti-tetA PNA, 16S

8 µg/ml tetracycline + CPP, tetA

8 µg/ml tetracycline + CPP, 16s

Tetracycline only, tetA

Tetracyline only, 16S

No treatment, tetA

No treatment, 16S

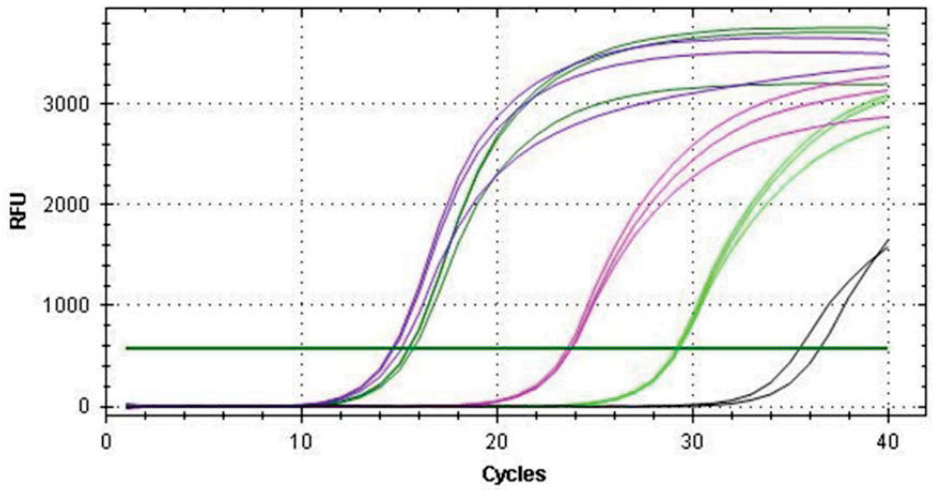

Figure 5.8A: Relative expression of tetA in a culture treated with tetracycline and CPP-anti-tetA PNA (light green) compared to a culture treated only with tetracycline (light purple). Incubation time was 4 hours. Note the relatively decreased expression of *tetA* in the PNA-treated culture as indicated by a right shift of the light green tracing. Expression of 16S was similar between treatment groups (dark green for CPP-PNA treated culture, dark purple for tetracycline only culture), as appropriate for a reference gene.

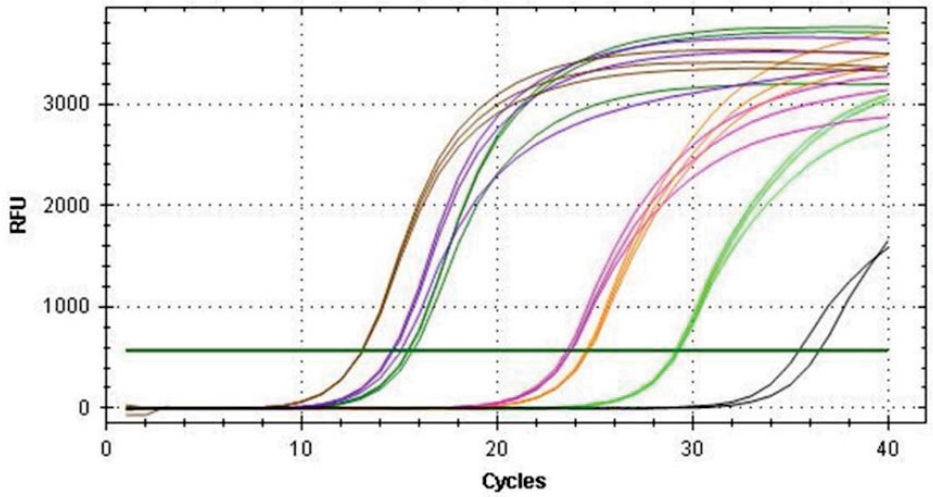

Figure 5.8B: This figure is the same as A. except that the tracings for the untreated culture are added in (light orange, *tetA* expression; dark orange, 16S expression). At this time point (4 hours), *tetA* expression in the culture treated only with tetracycline (light purple) has subsided somewhat, and is similar to that of the untreated culture (light orange). Expression of *tetA* in the culture treated with tetracycline and the CPP-anti-tetA PNA (light green) is suppressed relative to both of the other treatment groups.

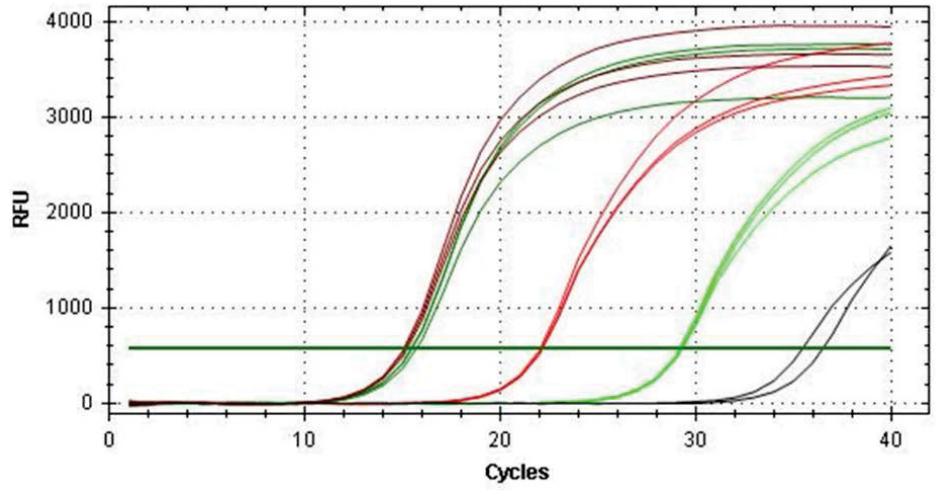

Figure 5.8C: Relative expression of *tetA* in a culture treated with tetracycline and CPP-anti-tetA PNA (light green) compared to a culture treated with tetracycline and CPP alone (light red). Incubation time was 4 hours. Note the relatively decreased expression of *tetA* in the PNA-treated culture as indicated by a right shift of the light green tracing. Expression of 16S was similar between treatment groups (dark green for CPP-PNA treated culture, dark red for CPP treated culture), as appropriate for a reference gene.

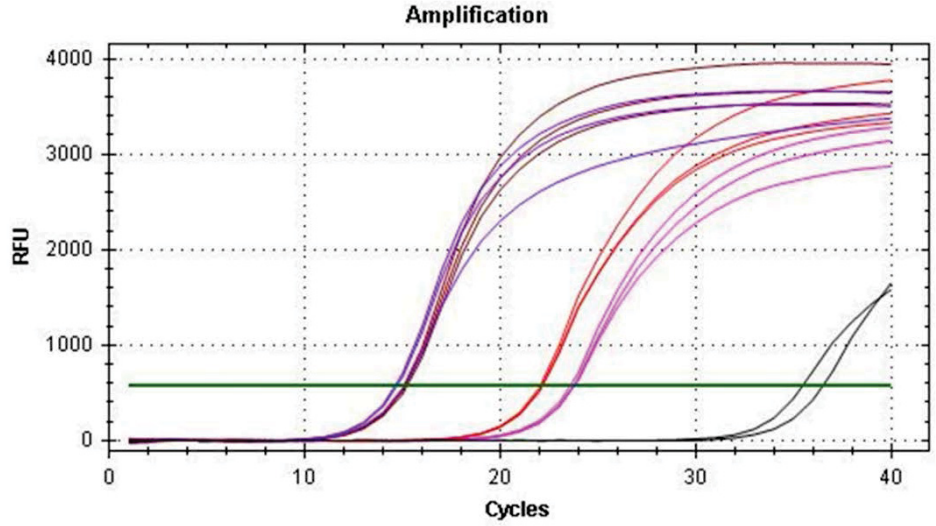

Figure 5.8D: Relative expression of *tetA* in a culture treated with tetracycline and CPP alone (light red), compared with the culture treated only with tetracycline (light purple). At this time point (4 hours), *tetA* expression in the culture treated with tetracycline and the CPP alone appears mildly increased relative to the culture treated only with tetracycline.

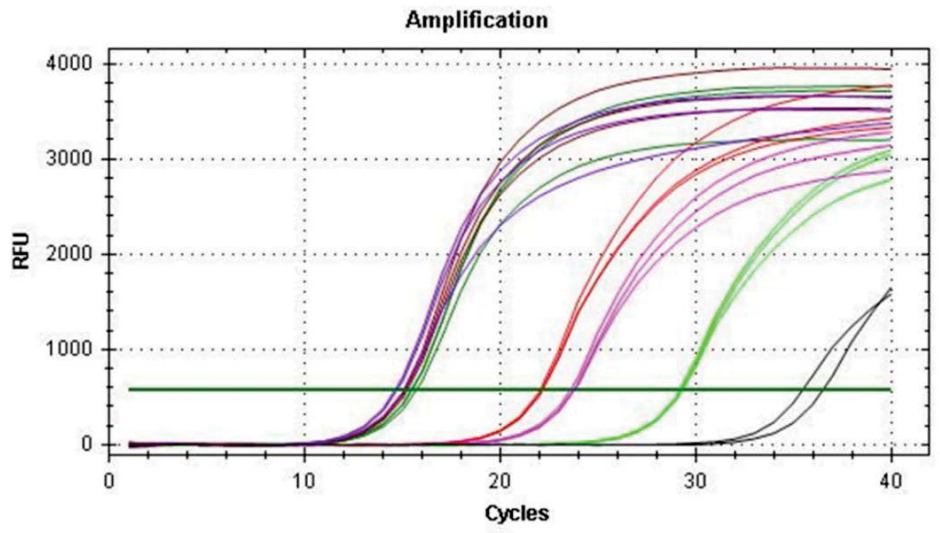

Figure 5.8E: Combination of tracings for the culture treated with tetracycline and CPP-anti-tetA PNA (light green), the culture treated with tetracycline and CPP alone (light red), and the culture treated only with tetracycline (light purple). Incubation time was 4 hours. This is to show that *tetA* expression is down-regulated in the CPP-PNA treated culture compared to both the culture treated with tetracycline alone and the culture treated only with tetracycline.

Figure 5.8 PCR tracings of *tetA* and 16S expression in various treatment groups cultured with different combinations of CPP-PNA, CPP only, and/or tetracycline for 4 hours. In all treatment groups, DT104 at a concentration of 5 x 10^5 CFU/ml was cultured in Mueller-Hinton broth in 96-well microtiter plates. After incubation with treatments for 4 hours, total RNA was stabilized and extracted, and RT-qPCR was performed to amplify *tetA* mRNA and 16S mRNA (reference gene). Expression of *tetA* in each treatment group was calculated with the Pfaffl method. The two black tracings to the far right of each graph are tracings for the non-template control for each primer.

PCR tracing color key indicating type of treatment and primer target:

8 µg/ml tetracycline + CPP-anti-tetA PNA, tetA

8 µg/ml tetracycline + CPP-anti-tetA PNA, 16S

8 µg/ml tetracycline + CPP, tetA

8 µg/ml tetracycline + CPP, 16s

Tetracycline only, tetA

Tetracyline only, 16S

No treatment, tetA

No treatment, 16S

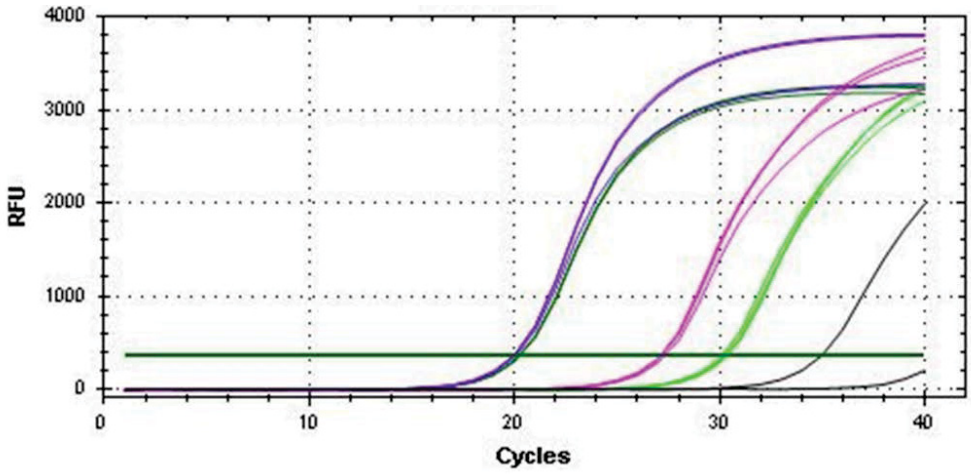

Figure 5.9A: Relative expression of *tetA* in a culture treated with tetracycline and CPP-anti-tetA PNA (light green) compared to a culture treated only with tetracycline (light purple). Incubation time was 4 hours. Note the relatively decreased expression of *tetA* in the PNA-treated culture as indicated by a right shift of the light green tracing. Expression of 16S was similar between treatment groups (dark green for CPP-PNA treated culture, dark purple for tetracycline only culture), as appropriate for a reference gene.

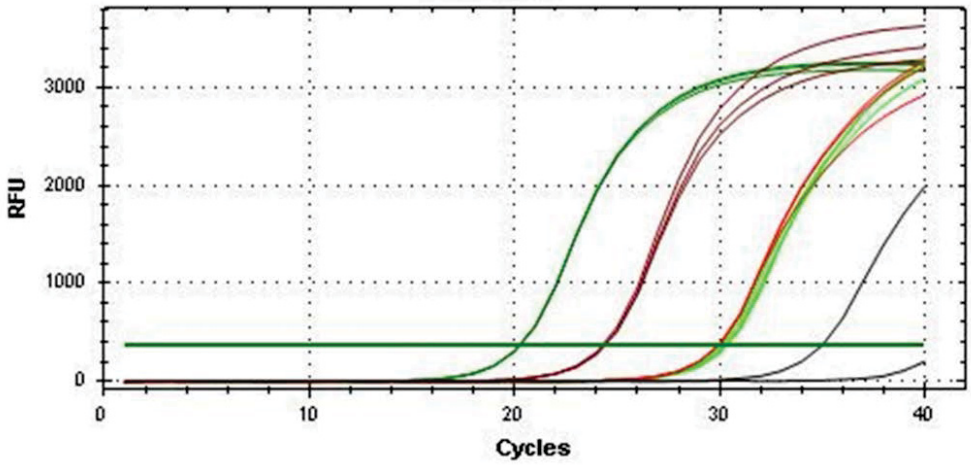

Figure 5.9B: Relative expression of *tetA* in a culture treated with tetracycline and CPP-anti-tetA PNA (light green) compared to a culture treated with tetracycline and CPP alone (light red). Incubation time was 4 hours. This set of tracings is difficult to interpret visually, because expression of the 16S reference was not stable between treatment groups as expected. Note how the 16S tracing for the culture treated with tetracycline and CPP (dark red) is substantially shifted to the right relative to the 16S tracing for the culture treated with tetracycline and the CPP-anti-tetA PNA (dark green). Mathematical calculation of the relative gene expression (see Figure 5.10) indicated a relative suppression of *tetA* in the culture treated with tetracycline and CPP-anti-tetA PNA, but the possible instability of 16S expression raises some concern about how well this result can be interpreted.

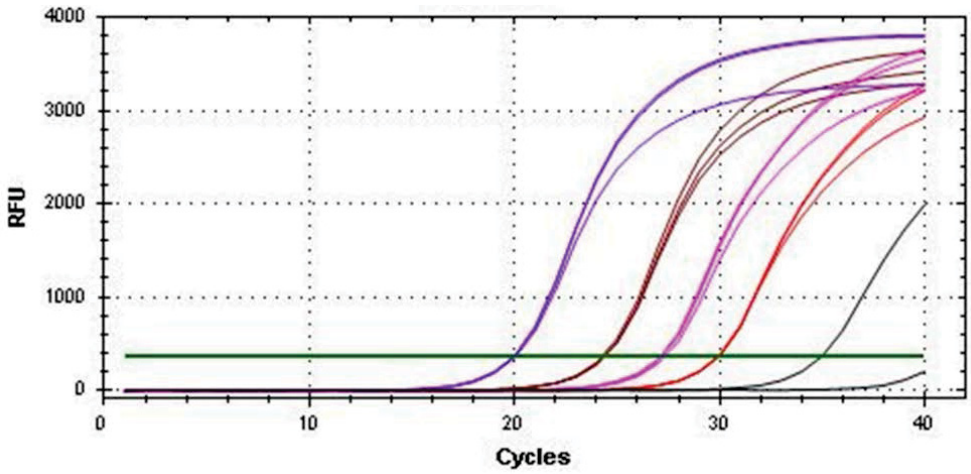

Figure 5.9C: Relative expression of *tetA* in a culture treated with tetracycline and CPP (light red) compared to a culture treated only with tetracycline (light purple). Incubation time was 4 hours. This set of tracings is difficult to interpret visually, because expression of the 16S reference was not stable between treatment groups as expected. Note how the 16S tracing for the culture treated with tetracycline and CPP (dark red) is substantially shifted to the right relative to the 16S tracing for the culture treated only with tetracycline (dark purple).

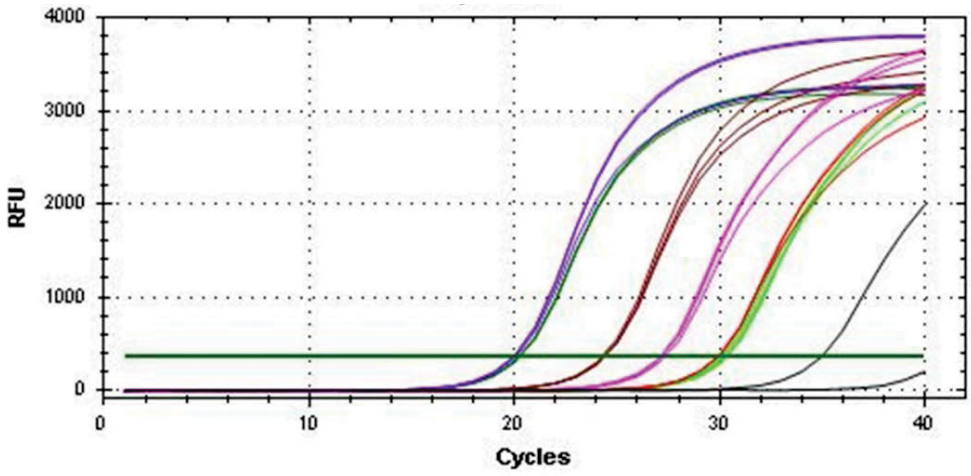

Figure 5.9D: Combination of tracings for the culture treated with tetracycline and CPP-anti-tetA PNA (light green), the culture treated with tetracycline and CPP alone (light red), and the culture treated only with tetracycline (light purple). Incubation time was 4 hours.

Figure 5.9 PCR tracings from one replicate of 4 hour treatment of DT104 with different combinations of CPP-PNA, CPP only, and/or tetracycline for 4 hours. DT104 at a concentration of 5 x 10^5 CFU/ml was cultured in Mueller-Hinton broth in 96-well microtiter plates. After incubation with treatments for 4 hours, total RNA was stabilized and extracted, and RT-qPCR was performed to amplify *tetA* mRNA and 16S mRNA (stably expressed reference gene). Expression of *tetA* in each treatment group was calculated with the Pfaffl method. Three of these replicates were set up, but only one led to successful amplification of mRNA, and even this replicate showed

some issues with expression stability. These RNA samples were kept in frozen storage at -20 ˚C for approximately three months before RT-qPCR, which may have caused sample degradation. The two black tracings to the far right of each graph are tracings for the non-template control for each primer.

PCR tracing color key indicating type of treatment and primer target:

8 µg/ml tetracycline + CPP-anti-tetA PNA, tetA

8 µg/ml tetracycline + CPP-anti-tetA PNA, 16S

8 µg/ml tetracycline + CPP, tetA

8 µg/ml tetracycline + CPP, 16s

Tetracycline only, tetA

Tetracyline only, 16S

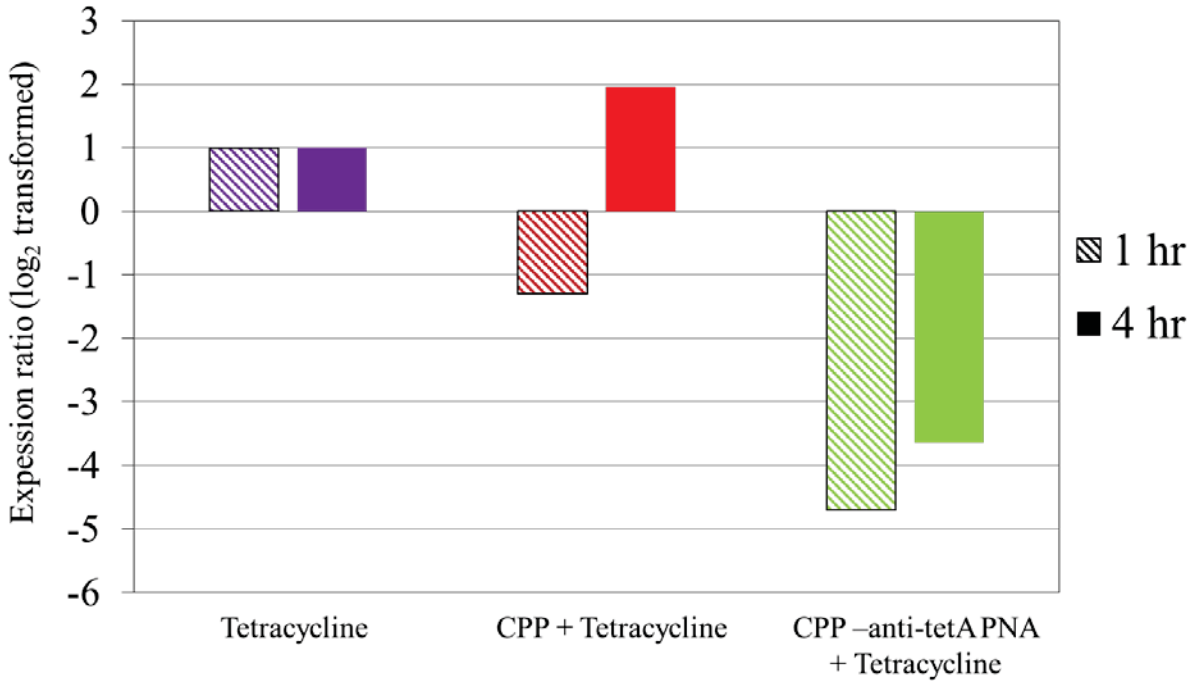

Figure 5.10 Summary of results presented in Figure 5.7, Figure 5.8, and Figure 5.9. Bars show *tetA* expression in cultures treated with tetracycline and CPP-anti-tetA PNA relative to that of cultures treated only with tetracycline, or with tetracycline and CPP alone at 1 hour and 4 hours. DT104 at a concentration of 5 x 10^5 CFU/ml was cultured in Mueller-Hinton broth in 96-well microtiter plates. After incubation with treatments for 1 hour or 4 hours, total RNA was stabilized and extracted, and RT-qPCR was performed to amplify *tetA* mRNA and 16S mRNA (reference gene). Relative *tetA* expression compared to the culture treated with tetracycline alone was calculated with the Pfaffl method. The calculated expression ratios were $\log_2$ transformed to allow for better visualization of relative gene expression. Patterned bars show results for 1 hour incubation (single replicate), and solid bars show results for 4 hour incubation (average of two replicates). Treatment with tetracycline and the CPP alone (red bars) did not cause a consistent difference in gene expression relative to treatment with tetracycline alone (purple bars). At the 1 hour time point, expression was slightly relatively downregulated, and at the 4 hour time point expression was slightly relatively upregulated. By contrast, treatment with tetracycline and the CPP-anti-tetA PNA (green) caused notable relative downregulation of *tetA* mRNA expression at both the 1 hour and 4 hour time points.

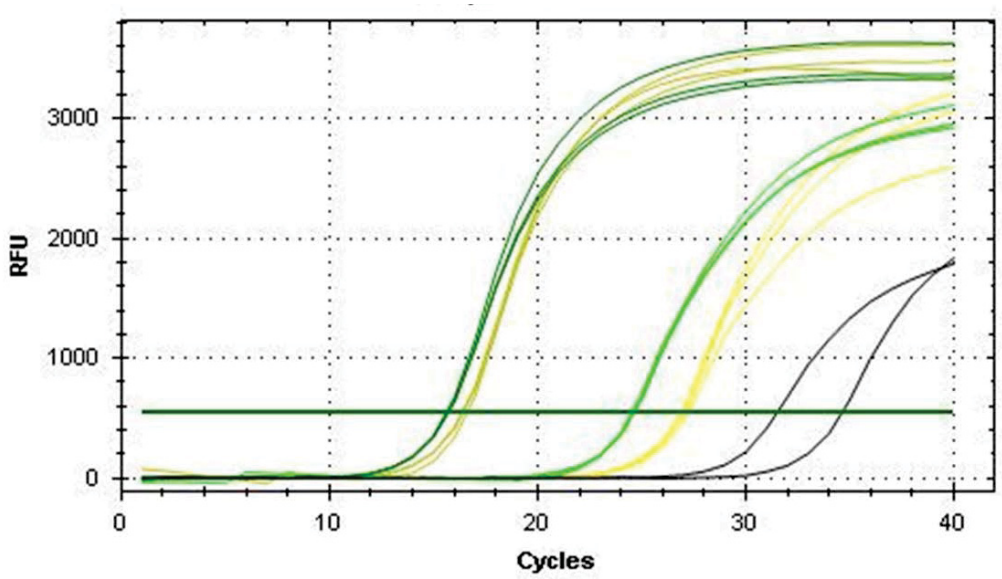

Figure 5.11A: Tracings of *tetA* expression in a culture treated with tetracycline and CPP-anti-tetR PNA (light yellow) compared to a culture treated with tetracycline and CPP-anti-tetA PNA (light green). Incubation time was 1 hour. Tracings of the 16S reference gene for each treatment are to the left (dark yellow and dark green, respectively). It was expected that *tetA* expression would be upregulated in the culture treated with tetracycline and CPP-anti-tetR PNA (light yellow) because this PNA is designed to inhibit expression of tetR, which codes for a protein that represses *tetA* expression. Instead, *tetA* expression in this culture is decreased relative to the culture treated with tetracycline and CPP-anti-tetA PNA.

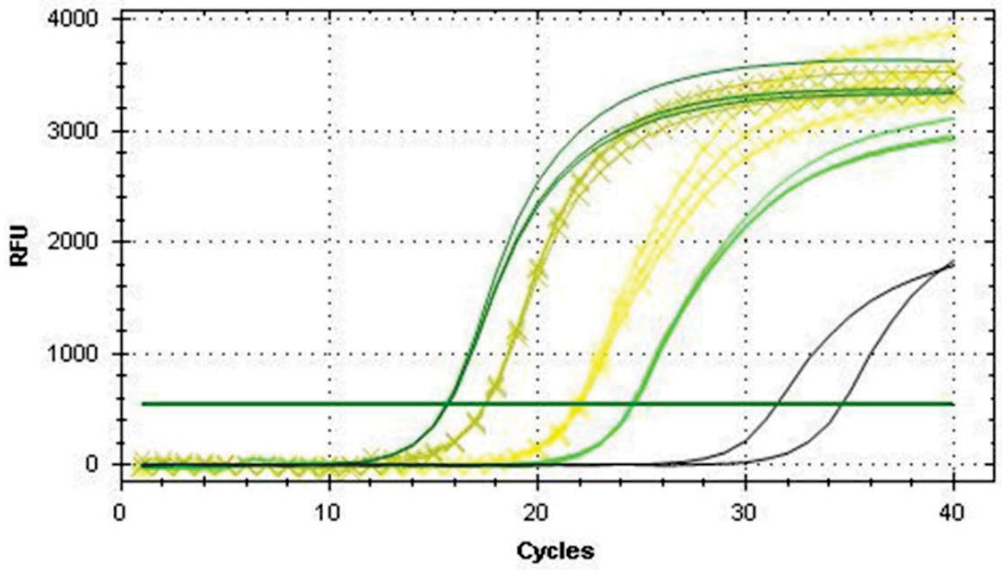

Figure 5.11B: Tracings of *tetA* expression in a culture treated only with CPP-anti-tetR PNA (light yellow crosses) and no tetracycline, compared to a culture treated with tetracycline and CPP-anti-tetA PNA (light green). Incubation time was 1 hour. Tracings of the 16S reference gene for each treatment are to the left (dark yellow crosses and dark green, respectively). Interestingly, the expected effect is now evident, with *tetA* expression apparently relatively upregulated in the culture treated with CPP-anti-tetR PNA alone.

Figure 5.11 PCR tracings of *tetA* and 16S expression in DT104 among cultures treated for 1 hour with various combinations of CPP-anti-tetR PNA, CPP-anti-tetA PNA, and tetracycline. In all treatment groups, DT104 at a concentration of 5 x 10^5 CFU/ml was cultured in Mueller-Hinton broth in 96-well microtiter plates. After incubation with treatments for 1 hour, total RNA was stabilized and extracted, and RT-qPCR was performed to amplify *tetA* mRNA and 16S mRNA (reference gene). Expression of *tetA* in each treatment group was calculated with the Pfaffl method.

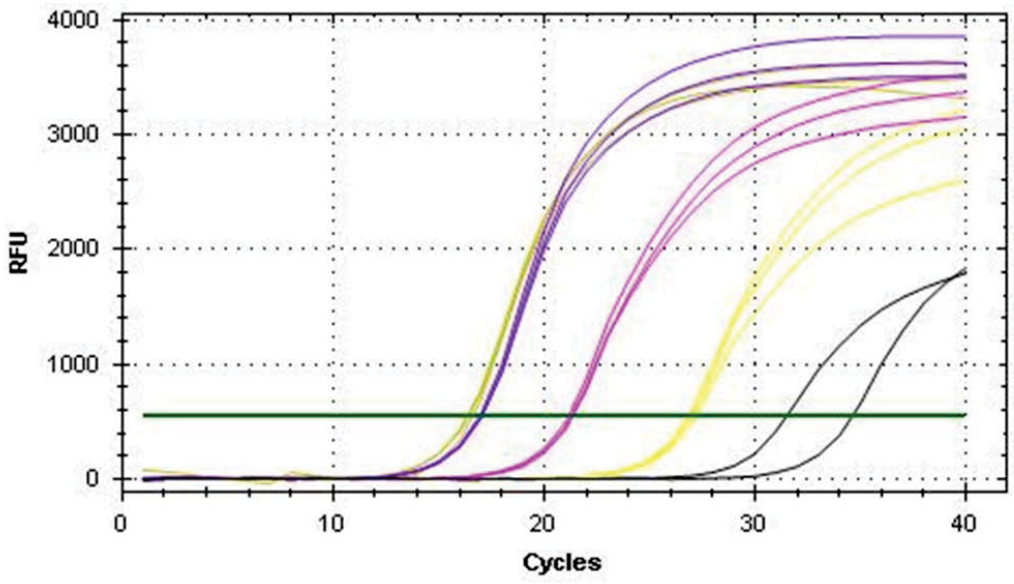

Figure 5.12A: Tracings of *tetA* expression in a culture treated with tetracycline and CPP-anti-tetR PNA (light yellow) compared to a culture treated only with tetracycline (light purple). Incubation time was 1 hour. Tracings of the 16S reference gene for each treatment are to the left (dark yellow and dark purple, respectively). It was expected that *tetA* expression would be similar between the two cultures, because both treatments should theoretically result in upregulation of tetA. Instead, *tetA* expression in the culture treated with tetracycline and CPP-anti-tetR PNA is decreased relative to the culture treated only with tetracycline.

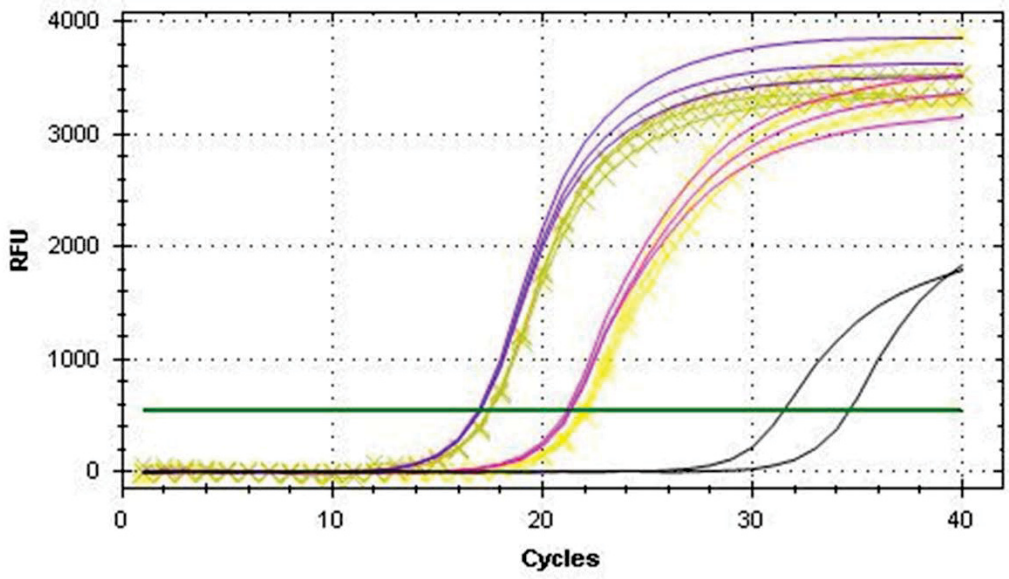

Figure 5.12B: Tracings of *tetA* expression in a culture treated only with CPP-anti-tetR PNA (light yellow crosses) and no tetracycline, compared to a culture treated only with tetracycline (light purple). Incubation time was 1 hour. Tracings of the 16S reference gene for each treatment are to the left (dark yellow crosses and dark purple, respectively). Interestingly, the expected effect is now evident, with *tetA* expression apparently similar between the two treatment groups.

Figure 5.12 PCR tracings of *tetA* and 16S expression in DT104 among cultures treated for 1 hour with various combinations of CPP-anti-tetR PNA and tetracycline. In all treatment groups, DT104 at a concentration of 5 x 10^5 CFU/ml was cultured in Mueller-Hinton broth in 96-well microtiter plates. After incubation with treatments for 1 hour, total RNA was stabilized and extracted, and RT-qPCR was performed to amplify *tetA* mRNA and 16S mRNA (reference gene). Expression of *tetA* in each treatment group was calculated with the Pfaffl method.

PCR tracing color key indicating type of treatment and primer target:

8 µg/ml tetracycline + CPP-anti-tetA PNA, tetA

8 µg/ml tetracycline + CPP-anti-tetA PNA, 16S

8 µg/ml tetracycline + CPP-anti-tetR PNA, tetA

8 µg/ml tetracycline + CPP-anti-tetR PNA, 16s

CPP-anti-tetR PNA, tetA

CPP-anti-tetR PNA, 16S

Tetracycline only, tetA

Tetracyline only, 16S

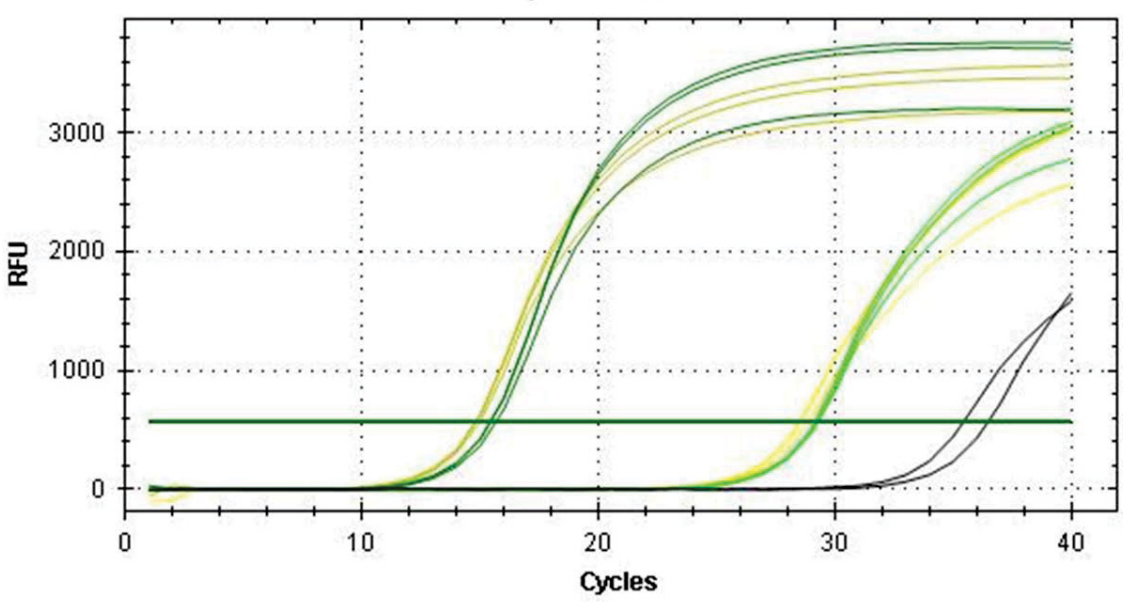

Figure 5.13A: Tracings of *tetA* expression in a culture treated with tetracycline and CPP-anti-tetR PNA (light yellow) compared to a culture treated with tetracycline and CPP-anti-tetA PNA (light green). Incubation time was 4 hours. Tracings of the 16S reference gene for each treatment are to the left (dark yellow and dark green, respectively). It was expected that *tetA* expression would be upregulated in the culture treated with tetracycline and CPP-anti-tetR PNA (light yellow) because this PNA is designed to inhibit expression of tetR, which codes for a protein that represses *tetA* expression. Instead, *tetA* expression in this culture is nearly identical that of the culture treated with tetracycline and CPP-anti-tetA PNA.

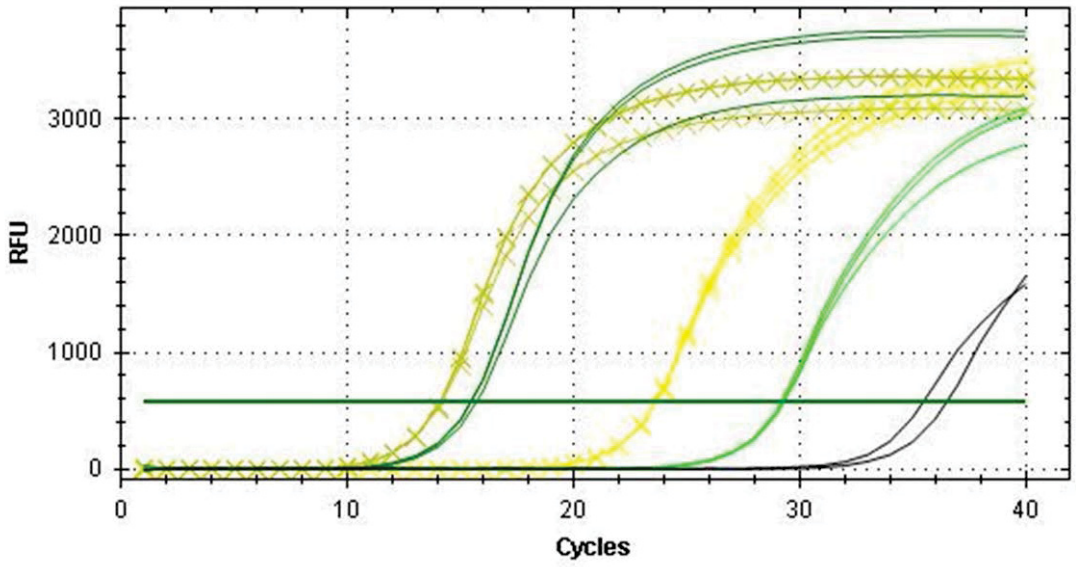

Figure 5.13B: Tracings of *tetA* expression in a culture treated only with CPP-anti-tetR PNA (light yellow crosses) and no tetracycline, compared to a culture treated with tetracycline and CPP-anti-tetA PNA (light green). Incubation time was 4 hours. Tracings of the 16S reference gene for each treatment are to the left (dark yellow crosses and dark green, respectively). As with the 1 hour culture (see Figure 5.11), the major observation is that the expected relative upregulation of *tetA* in response CPP-anti-tetR only occurred when tetracycline was absent.

Figure 5.13 PCR tracings of *tetA* and 16S expression in DT104 among cultures treated for 4 hours with various combinations of CPP-anti-tetR PNA, CPP-anti-tetA PNA, and tetracycline. In all treatment groups, DT104 at a concentration of 5 x 10^5 CFU/ml was cultured in Mueller-Hinton broth in 96-well microtiter plates. After incubation with treatments for 1 hour, total RNA was stabilized and extracted, and RT-qPCR was performed to amplify *tetA* mRNA and 16S mRNA (reference gene). Expression of *tetA* in each treatment group was calculated with the Pfaffl method.

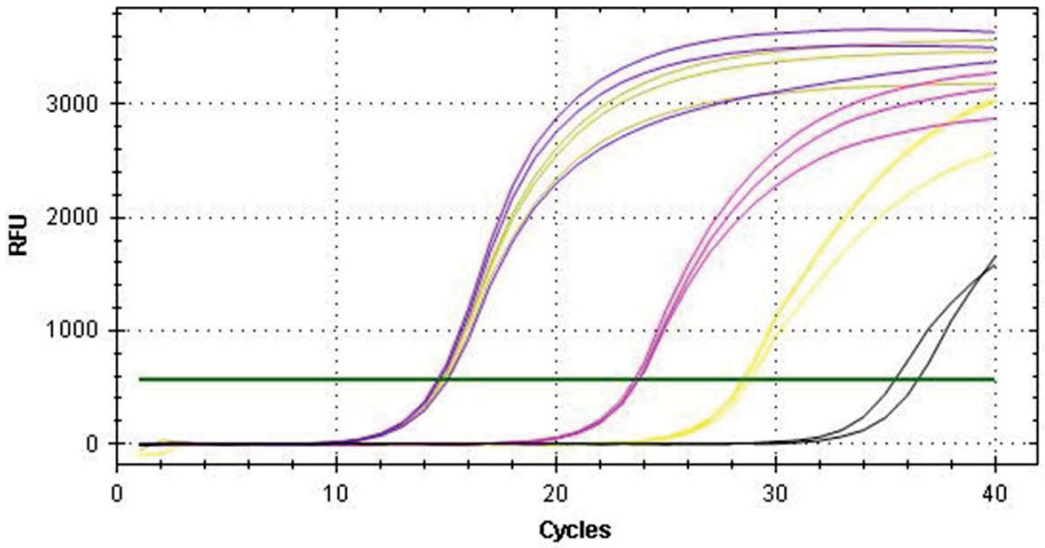

Figure 5.14A: Tracings of *tetA* expression in a culture treated with tetracycline and CPP-anti-tetR PNA (light yellow) compared to a culture treated only with tetracycline (light purple). Incubation time was 4 hours. Tracings of the 16S reference gene for each treatment are to the left (dark yellow and dark purple, respectively).

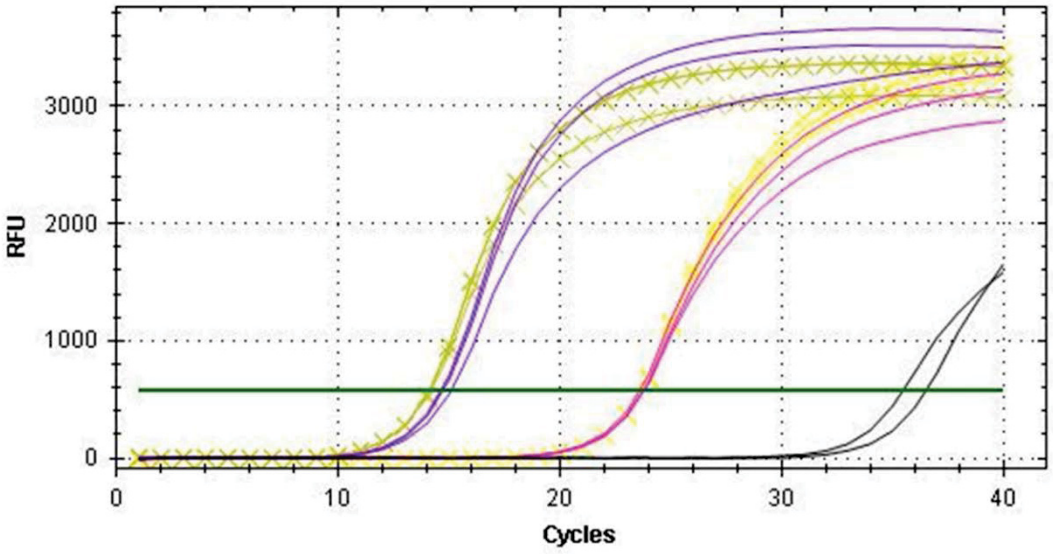

Figure 5.14B: Tracings of *tetA* expression in a culture treated only with CPP-anti-tetR PNA (light yellow crosses) and no tetracycline, compared to a culture treated only with tetracycline (light purple). Incubation time was 4 hours. Tracings of the 16S reference gene for each treatment are to the left (dark yellow crosses and dark purple, respectively). As with the 1 hour culture (see Figure 5.12) the expected similar *tetA* expression between the two groups only occurred when tetracycline was absent.

Figure 5.14 PCR tracings of *tetA* and 16S expression in DT104 among cultures treated for 4 hours with various combinations of CPP-anti-tetR PNA and tetracycline. In all treatment groups, DT104 at a concentration of 5 x 10^5 CFU/ml was cultured in Mueller-Hinton broth in 96-well microtiter plates. After incubation with treatments for 4 hours, total RNA was stabilized and extracted, and RT-qPCR was performed to amplify *tetA* mRNA and 16S mRNA (reference gene). Expression of *tetA* in each treatment group was calculated with the Pfaffl method.

<u>PCR tracing color key indicating type of treatment and primer target:</u>

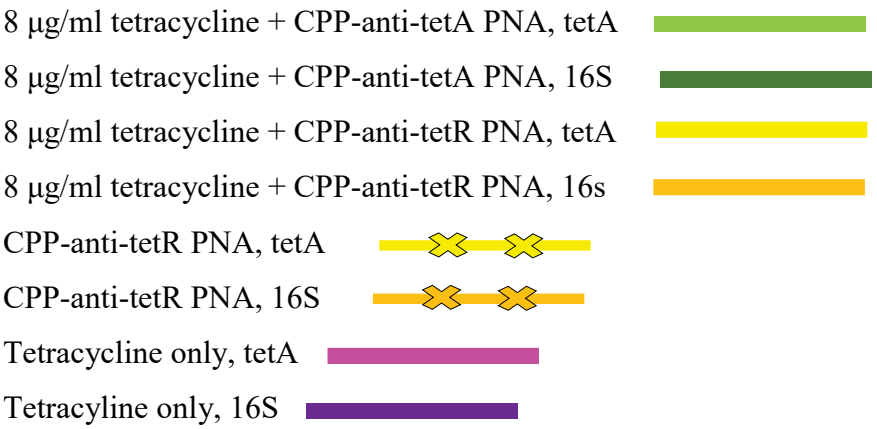

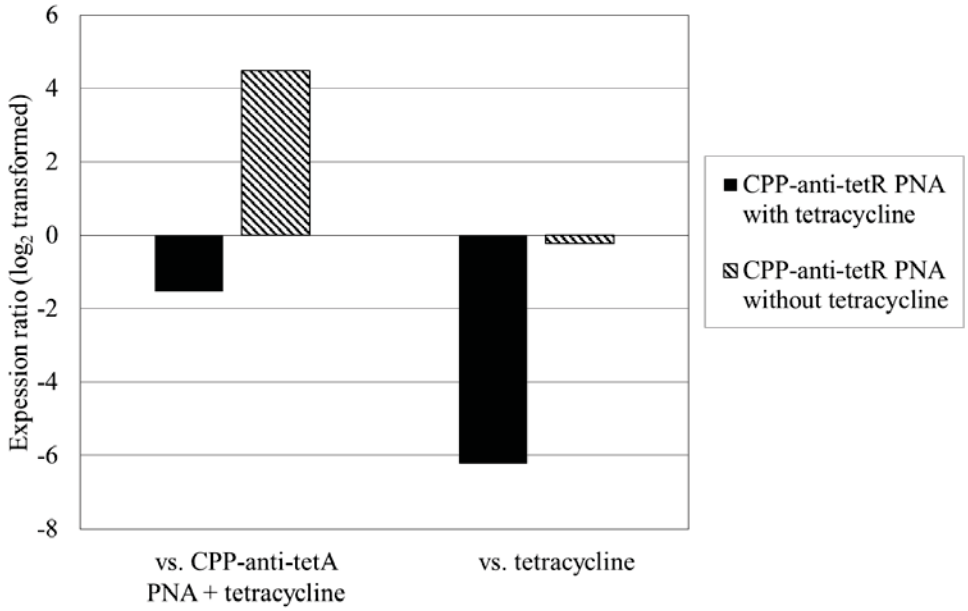

Figure 5.15A. 1 hour culture

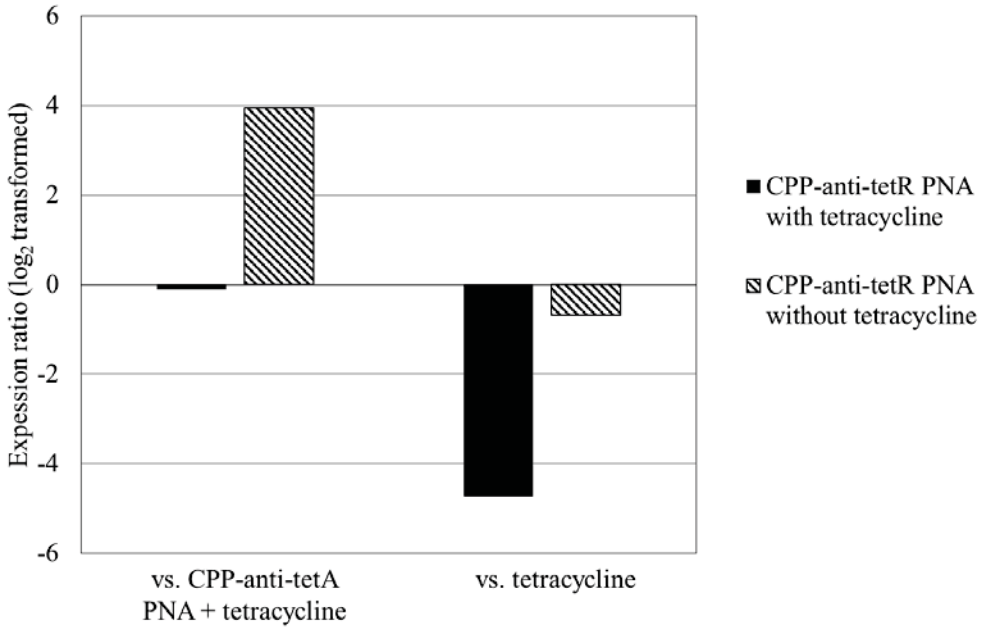

Figure 5.15B. 4 hour culture

Figure 5.15. Summary of results shown in Figure 5.11, Figure 5.12, Figure 5.13, and Figure 5.14. Presented is *tetA* expression in cultures treated with CPP-anti-tetR PNA with or without tetracycline, relative to that of cultures treated with tetracycline and CPP-anti-tetA PNA, or only with tetracycline for **A.** 1 hour or **B.** 4 hours. DT104 at a concentration of 5 x 10^5 CFU/ml was cultured in Mueller-Hinton broth in 96-well microtiter plates. After incubation with treatments for 1 hour or 4 hours, total RNA was stabilized and extracted, and RT-qPCR was performed to amplify *tetA* mRNA and 16S mRNA (reference gene). Relative *tetA* expression compared to the culture treated with tetracycline alone was calculated with the Pfaffl method. The calculated expression

ratios were $\log_2$ transformed to allow for better visualization of relative gene expression. Solid bars indicate treatment with CPP-anti-tetR PNA and tetracycline. Patterned bars indicate treatment with only CPP-anti-tetR PNA. The same major observation was evident at both time points, namely, that the expected upregulation of *tetA* expression in response to treatment with CPP-anti-tetR PNA occurred only when tetracycline was absent. Statistical analysis was not done due to insufficient data points.

5.4 Discussion and conclusions

This chapter described the use of RT-qPCR to explore *tetA* expression in DT104. The treatment conditions were chosen to address questions raised by the results of MIC and MBC experiments described in Chapter 4 of this dissertation. The choice of RT-qPCR as a method to evaluate gene expression was based on the existence of several other studies that successfully used RT-qPCR to evaluate relative gene expression in response to CPP-PNAs, both in eukaryotic[15] and prokaryotic cells.[2, 16] However, no previous studies were found that specifically reported RT-qPCR results related to concurrent treatment with tetracycline and with antisense oligonucleotides that manipulated expression of the *tetA* and *tetR* genes. Therefore, the results were interpreted as well as possible based on the author's understanding of cellular mechanisms and were not guided by similar results of previous researchers.

For the experiments presented in this chapter, any bacteria exposed to tetracycline were treated at a concentration of 8 μg/ml, which is known to be sub-inhibitory for this bacterial strain based on the results of minimum inhibitory concentration experiments described in Chapter 4 of this dissertation. The goal was to use an antibiotic concentration high enough to stimulate a robust genetic response in the bacterium without causing bacteriostatic or bactericidal effects that may skew evaluation of mRNA expression.

In the initial experiment to verify that the *tetA* gene is upregulated in DT104 in response to tetracycline, the bacteria were incubated with the antibiotic for approximately 18 hours. After this incubation period the difference in *tetA* expression between untreated and tetracycline-treated cultures was negligible. However, measurement of *tetA* expression in bacteria treated with tetracycline for only 1 or 4 hours did capture substantial relative upregulation of *tetA* compared to the untreated culture. This indicates a rapid and short-lived transcriptional response of the *tetA* gene in the presence of tetracycline. A probable explanation is that after the immediate demand

for and production of the TetA protein to facilitate tetracycline efflux, *tetA* mRNA transcription drops off due to suppression from concurrently increased levels of the *tetA* repressor protein TetR (see Chapter 4, Figure 4.16).[10] Self-regulation of the amount of TetA protein prevents unneeded overexpression of a non-essential gene product that may result in decreased bacterial fitness.[17]

Treatment with CPP-anti-tetA PNA decreased the measureable amount of *tetA* mRNA in tetracycline-treated cultures relative to cultures treated with tetracycline alone and cultures treated with tetracycline and just the CPP. The effect was seen at both 1 hour and 4 hours of treatment. These results support the hypothesis that the PNA effectively and specifically inhibits expression of its target gene. The results also show that the CPP alone does not appear to directly affect *tetA* mRNA expression, so the inhibitory effects of the CPP observed in the experiments described in Chapter 4 must be due to a different mechanism. This mechanism may be cell membrane disruption, given that this molecule is known to increase membrane permeabilization of gram negative bacteria.[18]

There is a question as to whether these results support the reported mechanism of action of PNAs, which states that PNA molecules primarily bind mRNA and prevent protein translation by hindering binding of the bacterial ribosome, but usually do not prevent mRNA transcription.[6] If this is the case, one could conceivably expect that *tetA* mRNA should be present and amplified in the RT-qPCR reaction, and measurement of the actual TetA protein would be necessary to evaluate the effect of the PNA. Since *tetA* mRNA expression was quantifiably decreased by the presence of CPP-anti-tetA PNA in these experiments, does it mean the mechanism is wrong and the PNA is inhibiting transcription? That is one possible explanation. However, it is also possible that the currently understood mechanism holds true and the reason *tetA* mRNA was not amplified in cultures treated with CPP-anti-tetA PNA is that the PNA bound irreversibly to target mRNA and interfered with reverse transcription, resulting in less cDNA for amplification. Another possibility is that PNA binding induced degradation of target mRNA. To date, the literature does not indicate that PNAs cause mRNA degradation, but that does not necessarily mean it does not occur; that possibility cannot be proven or disproven by this set of experiments.

The results of treatment with the CPP-anti-tetR PNA were interesting. Based on the current understanding of the relationship between *tetR* and *tetA*, it was thought that a PNA designed to suppress function of the *tetR* gene would allow for uncontrolled expression of the TetA protein in the presence of tetracycline and lead to unchanged or even increased tetracycline resistance of DT104. However, bacteria treated with both tetracycline and the CPP-anti-tetR protein showed relatively decreased *tetA* expression compared to bacteria treated with tetracycline and the CPP-anti-tetA PNA. The expected effect of *tetA* upregulation in the presence of CPP-anti-tetR PNA was only observed when tetracycline was absent. Under these circumstances, *tetA* expression was similar to that of cultures treated only with tetracycline. These findings suggest that if all else is unchanged, inhibiting *tetR* expression allows for abnormal upregulation of *tetA*, but the combined effect of CPP-anti-tetR PNA and tetracycline somehow overwhelms the bacterial metabolic balance. It is not clear why this is happening. The combination does not appear to kill the bacteria because 16S expression in the CPP-anti-tetR PNA treated cultures remained fairly stable whether tetracycline was present or not.

This work has limitations. One of the most obvious is that mRNA expression of a gene is not necessarily directly correlated with actual production of the protein product.[19] Thus, while these results strongly suggest that the CPP-anti-tetA PNA increases DT104 tetracycline susceptibility by targeting the *tetA* gene, it is unknown what effect the treatment has on the actual number of TetA protein molecules produced. Measurement of the TetA protein levels, such as through western blot analysis, would be necessary to more fully answer this question. To the author's knowledge, no antibodies specific for detection of DT104 TetA by western blotting have yet been characterized. Isolation of the TetA protein and validation of anti-TetA antibodies for development of a novel western blot protocol were beyond the scope of this dissertation, but may be of interest as future related work.

Another limitation is that only one reference gene, the gene coding for the 16S rRNA subunit, was used in the RT-qPCR assays. This gene is a common choice for use as a reference gene in studies using RT-qPCR for evaluation of bacterial gene expression; however, it is recommended that such experiments actually utilize several reference genes.[20-21] This is to account for potential unstable gene expression of at least one of the reference genes and to increase confidence in results by

showing that the experimental treatment effect is evident even after comparison with multiple reference genes. The DT104 *gyrB* gene was evaluated as a potential second reference gene for the experiments in this chapter, but expression was unpredictable among treatment groups, so it was not further pursed. It is also recommended that stability of potential reference genes be evaluated before use by analysis with software tools such as NormFinder (https://moma.dk/normfinder-software), based on the algorithm developed by Andersen, et al.[22] In this set of experiments software analysis was not done. Stable 16S expression was instead determined based on a good primer standard curve and observation of a similar 16S C_q among the various treatment groups. Before further in-depth evaluation of *tetA* expression in response to CPP-PNAs is pursued, it would be warranted to identify other reference genes and validate stability with at least one of the available software tools.

The study was possibly also adversely affected by some smaller technical issues. For example, the calculated efficiency of the 16S gene (111%) was considered acceptable but is slightly higher than desired. (Bio-Rad) It would be worthwhile to revalidate the 16S primers and see if a better reaction efficiency is achieved. Attempts to replicate the results of 4 hour treatment with the various CPP-PNA, CPP, and tetracycline combinations had limited success. Many of the samples did not show amplification better than the non-template controls or the melt curves indicated probably primer-dimer formation (data not shown), so they were excluded from analysis. These samples were in frozen storage longer than the others, which possibly caused sample degradation. Confidence in the conclusions drawn from these experiments would be increased by successfully recapitulating the study results with at least one more replicate.

The major finding from this set of experiments is that treatment with tetracycline and the CPP-anti-tetA PNA effectively suppressed expression of the *tetA* gene of tetracycline-resistant *Salmonella enterica* ssp. *enterica* serovar Typhimurium DT104. This reinforces the conclusion first stated in the discussion of Chapter 4 that treatment with CPP-PNAs may allow for repurposing of conventional antibiotics in resistant bacteria. The results also indicate that the overall effect of *tetR* on DT104 fitness is not fully understood. Future work should look more closely at how CPP-PNA treatment affects bacterial *tetA* gene expression and protein expression both *in vitro* and in

more complex systems such as eukaryotic cell culture. Additional analysis of *tetR* function, such as production of *tetR* knockdown bacterial culture systems would also be fascinating.

5.5 References

1. World Health Organization. Antibiotic resistance (5 February 2018). http://www.who.int/news-room/fact-sheets/detail/antibiotic-resistance. Accessed March 2, 2019.
2. Meng J, He G, Wang H, et al. Reversion of antibiotic resistance by inhibiting mecA in clinical methicillin-resistant Staphylococci by antisense phosphorothioate oligonucleotide. J Antibiot. 2015;68(3):158-164.
3. Mitev GM, Mellbye BL, Iversen PL, Geller BL. Inhibition of intracellular growth of *Salmonella enterica* serovar Typhimurium in tissue culture by antisense peptide-phosphorodiamidate morpholino oligomer. Antimicrob Agents Chemother. 2009;53(9):3700-3704.
4. Kiran D, Sriranganathan N. The antimicrobial effect of anti- dnaK peptide nucleic acids on multidrug resistant strains of *Escherichia coli* and *Salmonella enterica* serovar Typhimurium. BIOS. 2014;85(1):48-56.
5. Soofi MA, Seleem MN. Targeting essential genes in *Salmonella enterica* serovar Typhimurium with antisense peptide nucleic acid. Antimicrob Agents Chemother. 2012;56(12):6407-6409.
6. Rasmussen LCV, Sperling-Petersen HU, and Mortensen KK. Hitting bacteria at the heart of the central dogma: sequence-specific inhibition. Microb Cell Fact. 2007;6(24). doi: 10.1186/1475-2859-6-24.
7. Nielsen PE, Egholm M, Berg RH, Buchardt O. Sequence specific inhibition of DNA restriction enzyme cleavage by PNA. Nucleic Acids Res. 1993;21(2):197-200.
8. Bai H, You Y, Yan H, et al. Antisense inhibition of gene expression and growth in gram-negative bacteria by cell-penetrating peptide conjugates of peptide nucleic acids targeted to rpoD gene. Biomaterials. 2012;33(2):659-667.
9. Mohamed MF, Hammac GK, Guptill L, Seleem MN. Antibacterial activity of novel cationic peptides against clinical isolates of multi-drug resistant *Staphylococcus*

pseudintermedius from infected dogs. PLoS One. 2014;9(12): e116259. doi: 10.1371/journal.pone.0116259.

10. Moller TSB, Overgaard M, Nielsen SS, et al. Relation between tetR and tetA expression in tetracycline resistant *Escherichia coli*. BMC Microbiol. 2016;16:39. doi: 10.1186/s12866-016-0649-z.
11. Bio-Rad. Real-Time PCR Applications Guide 2006. http://www.bio-rad.com/webroot/web/pdf/lsr/literature/Bulletin_5279.pdf. Accessed April 8, 2019.
12. Debode F, Marien A, Janssen E, Bragard C, Berben G. The influence of amplicon length on real-time PCR results. Biotechnol Agron Soc Environ. 2017;21(1):3-11.
13. Fey A, Eichler S, Flavier S, Christen R, Hofle M G, Guzman CA. Establishment of a real-time PCR-based approach for accurate quantification of bacterial RNA targets in water, using *Salmonella* as a model organism. Appl Environ Microbiol. 2004;70(6):3618-3623.
14. Pfaffl MW. A new mathematical model for relative quantification in real-time RT-PCR. Nucleic Acids Res. 2001;29(9):e45.
15. Fabbri E, Tamanini A, Jakova T, et al. A peptide nucleic acid against microRNA miR-145-5p enhances the expression of the Cystic Fibrosis Transmembrane Conductance Regulator (CFTR) in Calu-3 Cells. Molecules. 2018;23(71). doi: 10.3390/molecules23010071.
16. Goh S, Loeffler A, Lloyd DH, Nair SP, Good L. Oxacillin sensitization of methicillin-resistant *Staphylococcus aureus* and methicillin-resistant *Staphylococcus pseudintermedius* by antisense peptide nucleic acids *in vitro*. BMC Microbiol. 2015;15:262. doi: 10.1186/s12866-015-0599-x.
17. Nguyen TNM, Phan QG, Duong LP, Bertrand KP, Lenski RE. Effects of carriage and expression of the Tn10 tetracycline-resistance operon on the fitness of *Escherichia coli* K12. Mol Biol Evol. 1989;6(3):213-225.
18. Vaara M, Porro M. Group of peptides that act synergistically with hydrophobic antibiotics against gram-negative enteric bacteria. Antimicrob Agents Chemother. 1996;40(8):1801-1805.
19. Liu Y, Beyer A, Aebersold R. On the dependency of cellular protein levels on mRNA abundance. Cell. 2016;165(3):535-550.

20. Rocha DJP, Santos CS, Pacheco LGC. Bacterial reference genes for gene expression studies by RT-qPCR: survey and analysis. Antonie Van Leeuwenhoek. 2015;109(3):685-693.
21. Bustin SA, Benes V, Garson JA, et al. The MIQE Guidelines: Minimum Information for publication of Quantitative real-time PCR Experiments. Clin Chem. 2009;55(4):611-622.
22. Andersen CL, Jensen JL, Orntoft TF. Normalization of real-time quantitative reverse transcription-PCR data: a model-based variance estimation approach to identify genes suited for normalization, applied to bladder and colon cancer data sets. Cancer Res. 2004;64:15:5245-5250.

6 Development and implementation of a mouse model of oral *Salmonella* infection for *in vivo* testing of antimicrobial cell penetrating peptide-peptide nucleic acid conjugates

6.1 Introduction

Antibiotic-resistant bacterial infections cause substantial human and animal morbidity and mortality, require prolonged treatment regimens, and contribute to increased healthcare expenses.[1] There is a global call for new antimicrobial drugs with novel mechanisms of action.[2] Antisense oligonucleotide molecules such as phosphorothioate oligonucleotides (PS-ODNs), phosphorodiamidate morpholino oligomers (PMOs), and peptide nucleic acids (PNAs) show great promise as alternatives to conventional antibiotics because of their ability to modulate or suppress bacterial gene expression by binding complementary DNA or RNA sequences.[3]

Peptide nucleic acids bound to a cell penetrating peptide (CPP) to facilitate cellular entry can inhibit bacterial growth by targeting essential genes,[4-5] and can also increase antibiotic susceptibility in resistant bacteria by targeting antibiotic resistance genes.[6] Chapters 4 and 5 of this dissertation describe work with a CPP-PNA conjugate (CPP-anti-tetA PNA) designed to target expression of the TetA tetracycline efflux pump in tetracycline resistant *Salmonella enterica* ssp. *enterica* serovar Typhimurium DT104 (DT104). Treatment of pure cultures of DT104 with CPP-anti-tetA PNA resulted in partial restoration of tetracycline susceptibility, as shown by a decreased minimum inhibitory concentration (MIC) and a minimum bactericidal concentration (MBC). The CPP-PNA also caused a substantial relative decrease in *tetA* mRNA expression as measured by RT-qPCR. Based on those results, the decision was made to test the CPP-PNA in a live mouse model infected with DT104. We also chose to test a CPP-PNA designed to target the essential *tsf* gene (CPP-Sal-tsf PNA).

An ideal model would use fully immunocompetent mice, would involve an oral infection route of DT104 to mimic how natural infection with this organism commonly occurs, and would result in clinically apparent systemic illness within a few days but not cause acute death, thus allowing for a window of time in which treatment could be initiated. A search for mouse models of S. Typhimurium infection in the literature indicated that the BALB/c strain is relatively susceptible

to *Salmonella* infection,[7-9] and that an oral infectious dose somewhere between 2 x 10^6 CFU and 1 x 10^9 was likely to result in clinical illness.[10-12] However, papers describing oral infection models often did not describe the clinical signs of illness that helped researchers track the course of infection or lacked detail about the timeline of development of clinical signs; the experiments also frequently involved pre-infection interventions such as antibiotic pretreatment.[10-11,13-14] Therefore, the decision was made to develop our own oral model of DT104 infection in BALB/c mice where the optimal infectious dose for our purposes was experimentally determined, and clinical signs of illness were documented to allow an informed clinical assessment of illness severity during future *in vivo* studies. This mouse model was then implemented to evaluate whether CPP-PNA treatment would attenuate or cure systemic salmonellosis caused by DT104 in mice.

6.2 Materials and Methods

6.2.1 Animal description, care, and handling

All protocols involving animal experimentation were reviewed and approved by the Virginia Tech (VT) Institutional Animal Care and Use Committee. These experiments all used six-to-eight-week-old female BALB/C mice. The animals were housed in an Animal Biosafety Level 2 (ABSL-2) facility in groups of five on cedar shaving bedding with a 12 hour light/dark cycle and an ambient temperature of ~25 C˚. The housing facility is accredited by the Association for Assessment and Accreditation of Laboratory Animal Care International (AAALAC) (accreditation #001123). Animals were provided free choice water and free choice standard rodent chow at all times, except for short periods of fasting when required for experimental procedures. Before being used for an experiment, mice were allowed to acclimate to the housing environment for a minimum of seven days. When euthanasia was performed as required by experimental protocols or at the end of a study, it was done by inhalation of compressed CO_2 gas according to American Veterinary Medical Association (AVMA) and VT University Veterinarian approved guidelines, followed by cervical dislocation to ensure death.

6.2.2 Bacterial model organism and cell penetrating peptide-peptide nucleic acid (CPP-PNA) sequences

The bacterial strain used for infection was *Salmonella enterica* ssp. *enterica* serovar Typhimurium DT104 (DT104). This bacterium is one of the stock strains in the Sriranganathan laboratory. The

CPP-PNAs used for these experiments are listed in Table 6.1. Details about design and storage of these molecules are found in Chapter 4.

Table 6.1 Description of the peptide nucleic acid and cell penetrating peptide sequences used concurrently with tetracycline (CPP-anti-tetA PNA, CPP-Control PNA) or alone (CPP-Sal-tsf) to experimentally treat 6-to-8-week-old female BALB/c mice orally infected with *Salmonella enterica* ssp. *enterica* serovar Typhimurium DT104.

GenBank gene reference number and/or name	**Function**	**Target DNA sequence (5'-3')**	**PNA sequence (5'-3') with attached CPP and o-linker**	**Name used in text**
DT104_38611 tetracycline resistance protein class A (TetA)	Codes for the TetA protein, a tetracycline efflux pump that is upregulated in the presence of intracellular tetracycline	gacgccatgg	(KFF)3K-o-ccatggcgtc	CPP-anti-tetA PNA
Control PNA	Nucleotide sequence with no known target in the DT104 genome	None	(KFF)3K-o-catactgcat	CPP-Control PNA
tsf, translation elongation factor	Codes for a protein that forms part of a complex that stabilizes new proteins during the elongation stage of translation	ttagaatggc	(KFF)3K-o-gccattctaa	CPP-Sal-tsf
Cell penetrating peptide alone	Short amino acid sequence attached to PNAs to facilitate crossing cell membranes	N/A	KFFKFFKFFK	CPP

6.2.3 Development of a mouse model of oral *Salmonella* infection

Dose experiment to establish the optimal infectious dose

A mid-log culture of DT104 grown in tryptic soy broth (TSB) was diluted in sterile PBS to make three inoculum cultures with approximate concentrations of 5 x 10^5 CFU/ml, 5 x 10^6 CFU/ml, and 5 x 10^7 CFU/ml. After a four hour fast (water was always freely available), five mice were orally infected with 0.2 ml of each inoculum by oral gavage with plastic gavage needles. This made three treatment groups of 5 mice each, infected with approximately 1 x 10^5, 1 x 10^6, and 1 x 10^7 CFU/mouse. Free choice food was returned immediately after gavage. Mice were observed twice a day for evidence of clinical illness, and more frequently if necessary based on the severity of clinical signs. Behavioral and physiologic changes such as activity level, respiratory effort, and evidence of dehydration were observed and recorded to map progression of systemic salmonellosis induced by the oral infection. After enough observational data were gathered at 7 days post-infection (PI), the animals were euthanized. The spleens were removed from mice that showed evidence of moderate to severe clinical illness, and cultured on MacConkey agar by first breaking open the splenic capsule, then gently smearing the spleen across the agar surface. MacConkey agar is a selective growth medium use for isolation of enteric bacterial bacilli. If a culture plate showed growth of colonies consistent with *Salmonella*, the genus was confirmed by agglutination of a pure sample of the bacteria after contact with *Salmonella* O antiserum. Organs harvested from mice in the PNA treatment experiment described below were also cultured, and bacterial CFUs/ml were determined. These organs included liver, spleen, small intestine, and large intestine. Comparing how many bacterial CFUs were cultured from each organ with the clinical status of the animal at time of death helped in further characterizing the infection model and mapping the timeline of infection and bacterial clearance in animals that recovered.

6.2.4 Implementation of the mouse model of oral *Salmonella* infection to test *in vivo* efficacy of concurrent treatment with tetracycline and the CPP-anti-tetA PNA

Replicate 1:

After a four hour fast, seven groups of five mice were orally infected with ~ 1 x 10^7 CFU/mouse of DT104. Free choice food was returned immediately after infection. The day of infection was designated Day 0. For the duration of the study, mice were monitored for clinical signs of illness by twice daily observation. If serious signs of illness were detected, observations were increased

to every four hours. Mice were euthanized if critical endpoints were reached, or at the completion of the study. Treatments were begun the afternoon of Day 3 post-infection (PI). Table 6.2 describes each treatment. All treatments were administered by intra-peritoneal injection (IP) once every 24 hours for seven days in a total volume of 100 µl.

Table 6.2 List of treatment groups in the first replicate of a study to evaluate the efficacy of an experimental treatment for oral *Salmonella* infection in 6-8-week-old female BALB/c mice. The CPP-anti-tetA PNA is designed to inhibit expression of the TetA tetracycline efflux pump, which imparts resistance to tetracycline. The CPP-Control PNA has a mismatched nucleotide sequence and was designed for use as a negative control. Treatments were begun on day 3 PI and continued for seven days. Treatments were administered IP once every 24 hours.

Treatment group	**Treatment**	**Fluid vehicle**
1	CPP-anti-tetA PNA 10 nmol/mouse + tetracycline 20 mg/kg	Sterile water
2	CPP-anti-tetA PNA 10 nmol/mouse	Sterile water
3	CPP-Control PNA 10 nmol/mouse + tetracycline 20 mg/kg	Sterile water
4	CPP-Control PNA 10 nmol/mouse	Sterile water
5	Tetracycline 20 mg/kg	Sterile water
6	CPP 5 nmol/mouse	Sterile water
7	Sterile PBS	Sterile PBS

After completion of the treatment regimen, mice were observed until Day 19 PI, and additional data related to behavior, physiologic changes, and number of deaths were collected. Any time a mouse was euthanized, either due to illness and progression to a critical endpoint, or because the study was ending, samples of liver, spleen, large intestine, and small intestine were collected for bacterial culture and frozen in sterile Petri dishes at -80 ˚C until culture on XLT-4 agar could be performed. This type of agar is selective for isolation of non-typhi *Salmonella* species. Samples were thawed in a refrigerator, then homogenized in sterile PBS using sterile glass tissue grinding rods and tubes, and serially diluted for culture and determination of CFU/ml.

Replicate 2:

After a four hour fast, eight groups of five mice were orally infected with ~ 1 x 10^7 CFU/mouse of DT104. Free choice food was returned immediately after infection. The day of infection was designated Day 0. For the duration of the study, mice were monitored for clinical signs of illness by twice daily observation. If serious signs of illness were detected, observations were increased

to every four hours. Mice were euthanized if critical endpoints were reached, or at the completion of the study. Treatments were begun the afternoon of Day 3 PI. Table 6.3 describes each treatment. All treatments were administered by intra-peritoneal injection once every 24 hours for seven days in a total volume of 100 µl.

Table 6.3 List of treatment groups in the second replicate of a study to evaluate the efficacy of an experimental treatment for oral *Salmonella* infection in 6-8-week-old female BALB/c mice. The CPP-anti-tetA PNA is designed to inhibit expression of the TetA tetracycline efflux pump, which imparts resistance to tetracycline. The CPP-Control PNA has a mismatched nucleotide sequence and was designed for use as a negative control. The CPP-Sal-tsf PNA targets expression of an essential bacterial gene involved in stabilization of new peptides during bacterial protein translation. Treatments were begun on day 3 PI and continued for seven days. Treatments were administered IP once every 24 hours.

Treatment group	**Treatment**	**Fluid vehicle**
1	Anti-tetA PNA-CPP 10 nmol/mouse + tetracycline 20 mg/kg	Sterile water
2	Anti-tetA PNA-CPP 10 nmol/mouse	Sterile water
3	Control PNA-CPP 10 nmol/mouse + tetracycline 20 mg/kg	Sterile water
4	Control PNA-CPP 10 nmol/mouse	Sterile water
5	Tetracycline 20 mg/kg	Sterile water
6	CPP 5 nmol/mouse	Sterile water
7	Sterile PBS	Sterile PBS
8	CPP-Sal-tsf 10 nmol/mouse	Sterile PBS

After completion of the treatment regimen, mice were observed until Day 10 PI, and additional data related to behavior, physiologic changes, and number of deaths were collected. Any time a mouse was euthanized, either due to illness and progression to a critical endpoint, or because the study was ending, samples of liver, spleen, large intestine, and small intestine were collected for bacterial culture and frozen in sterile Petri dishes at -80 ˚C until culture on XLT-4 agar could be performed. Samples for this replicate were prepared for culture slightly differently than those from Replicate 1. After thawing, the tissues were homogenized using the Precellys bead-mill tissue homogenizer system (Bertin Instruments, Rockville, MD) under vacuum. Samples were transferred under sterile conditions into 1 ml TSB in 2 ml Precellys vials and weighed after taring the scale with a blank vial. The vials were then agitated with the lysis beads in the homogenizer for 30 seconds, followed by 60 seconds of rest, then another 30 seconds of agitation. The tissue

homogenate was then plated on XLT-4 agar and incubated at 37 ˚C overnight. Final growth was tabulated after 48 hours.

Statistical analysis

Kaplan-Meier survival curves were plotted and visually compared among the treatment groups in each replicate. Survival curves were also plotted for treatment groups 1-7 using pooled data from both replicates of the experiments. The log-rank test was performed to detect statistical differences in mean probability of survival between the various experimental treatment groups and the control PBS-only group. One factor ANOVA was done to compare CFU/ml counts from each organ among treatment groups. Only sample sets with $n > 1$ were included in ANOVA analysis. For both the log-rank and ANOVA analyses, a p-value <0.05 was considered significant.

6.3 Results

6.3.1 Development of a mouse model of oral *Salmonella* infection

The following behavioral and physical exam changes were observed as clinical infection progressed, and are sorted according to time of appearance and severity:

- *Early mild clinical sign (apparent by 2-4 days PI)s:* huddling as a group, reluctance to move around the housing box without external stimulation
- *Moderate clinical signs (apparent by 3-7 days PI):* all mild signs along with hunched postured, ruffled fur, slightly decreased body condition, mild skin tenting indicating mild dehydration
- *Severe clinical signs (apparent by 7-8 days PI):* all mild and moderate signs along with reluctance or refusal to move around the housing box even with external stimulation, squinting/photophobia, loss of >20% of body weight, sunken eyes and moderate to marked skin tenting indicating severe dehydration.

Table 6.4 details the findings in each treatment group for the dose optimization study. Based on these results, an oral infectious dose of 1×10^7 CFU/ml was used for further implementation of the model, because this dose led to clinical illness in all mice, but did not cause immediate death.

During the two replicates of the study using CPP-PNA treatments, some additional observations were also made about progression of infection. The number of *Salmonella* CFU/ml was quantified

in organs from these mice where possible. It was noted that mice terminated earlier in progression of the disease often had higher CFU/ml counts in the small and large intestines than in the liver and spleen, whereas those terminated in a more advanced stage of clinical illness tended to have higher CFU/ml counts in the intestinal tract.

Table 6.4 Progression of infection in groups of mice orally infected with three different concentrations of *Salmonella enterica* ssp. *enterica* serovar Typhimurium DT104. Mice were infected to determine an optimal infectious dose of DT104 for future use in experiments that required a model of systemic salmonellosis. The goal was to find a dose that was not acutely lethal, but that caused clinical disease in all mice within 2-3 days so that experimental treatments could be initiated after manifestation of clinical illness. This was to try and more closely mimic disease progression and intervention in clinical practice.

Group	**Target infectious dose**	**Actual infectious dose (based on culture of inoculum)**	**Time to clinical signs**	**Bacteria cultured from spleen?**
1	1 x 10^5 CFU	~6 x 10^4 CFU	Did not develop clinical disease	Culture not done
2	1 x 10^6 CFU	~7 x 10^5 CFU	Mild clinical signs noted in all mice on Day 5, moderate signs progressing to severe in one mouse on Day 7	Yes, the spleen of the severely ill mouse was cultured and showed growth of numerous colonies of *Salmonella* spp.
3	1 x 10^7 CFU	~9 x 10^6 CFU	Possible mild clinical signs noted in all mice by Day 2, definite mild clinical signs noted in all mice by day 4, moderate signs noted in one mouse on Day 5, moderate signs in two mice on Day 6, signs ranging from mild (1 mouse) to moderate (2 mice) to severe (2 mice) in all 5 mice by day 7.	Yes, the spleens of all five mice were cultured. One yielded no growth, two yielded moderate growth, and two yielded marked growth of *Salmonella* spp.

6.3.2 Implementation of the mouse model of oral *Salmonella* infection to test *in vivo* efficacy of concurrent treatment with tetracycline and the CPP-anti-tetA PNA

Replicate 1

Culture of the inoculum solution indicated that mice received ~8 x 10^6 CFU/mouse for infection, which is slightly lower than the target dose of 1 x 10^7 CFU/mouse. By Day 3 PI when treatments were started, one or more mice were showing mild to moderate clinical signs of illness. Over 19 days PI, mice either progressed to severe clinical signs and were euthanized due to reaching critical endpoints, or progressed through mild or moderate clinical signs before undergoing recovery such that they were clinically health at the time of euthanasia at the end of the study. Kaplan-Meier survival curves were generated for each treatment group (Figure 6.1).

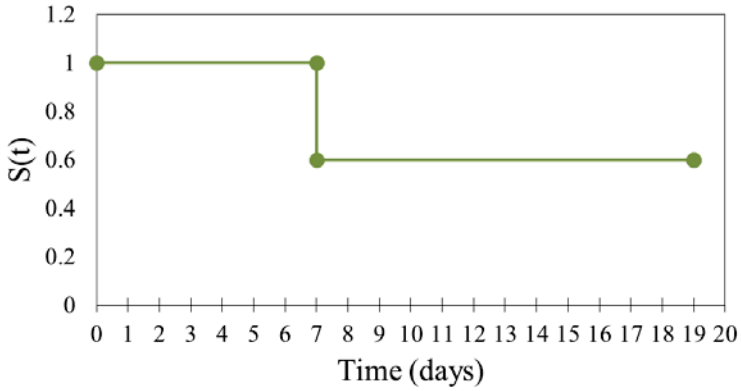

Figure 6.1A. CPP-anti-tetA PNA + Tetracycline

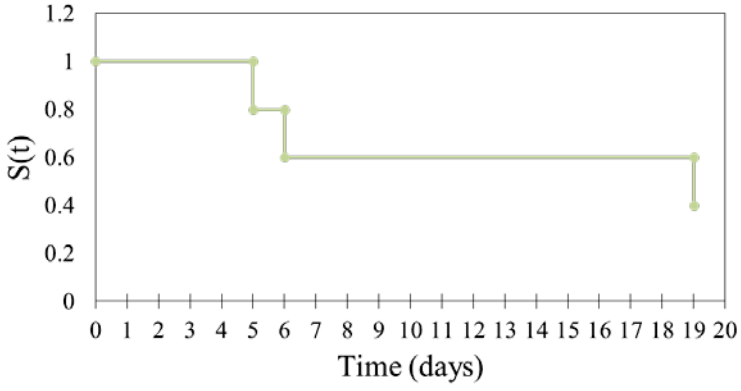

Figure 6.1B. CPP-anti-tetA PNA

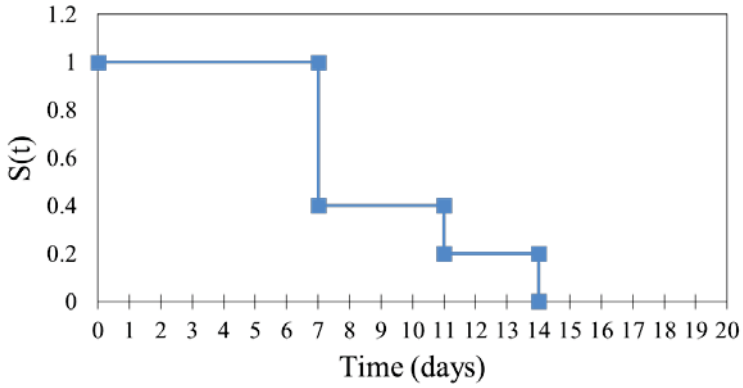

Figure 6.1C. CPP-Control PNA + Tetracycline

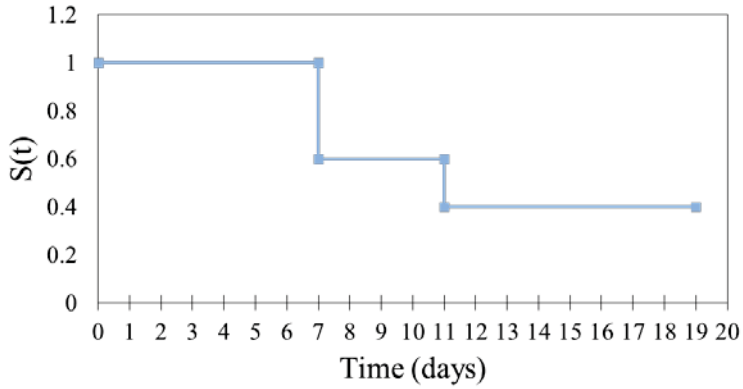

Figure 6.1D. CPP-Control PNA-CPP

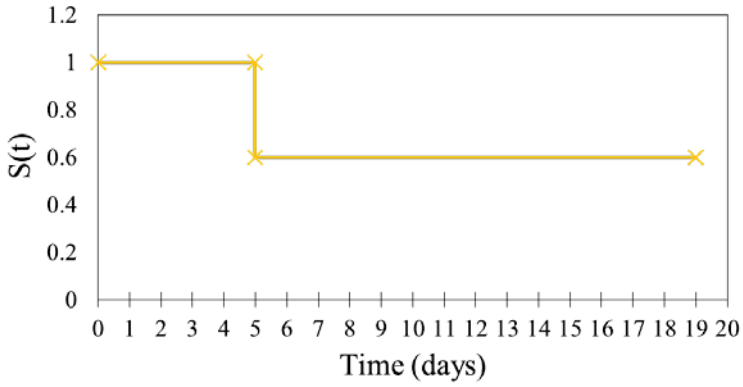

Figure 6.1E: Tetracycline

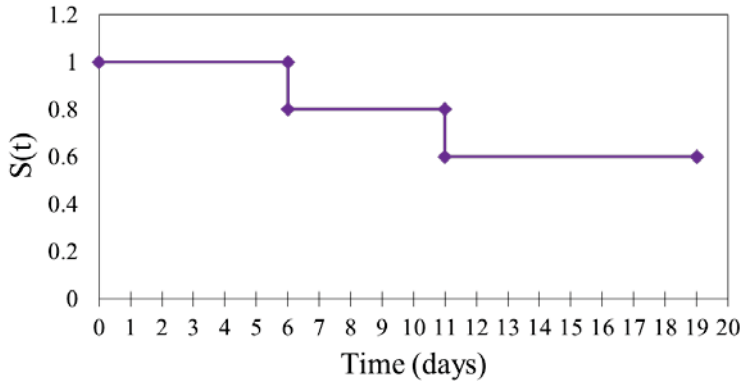

Figure 6.1F: PBS

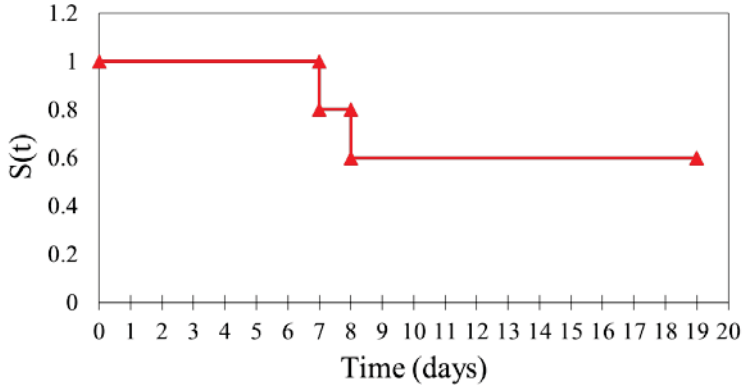

Figure 6.1G: CPP

Figure 6.1 Survival curves for each treatment group in the first replicate of a study to test the efficacy of an experimental treatment for systemic salmonellosis in a mouse model. Female BALB/c mice (n = 5/group) were orally infected with tetracycline-resistant *Salmonella enterica* ssp. *enterica* serovar Typhimurium DT104 and left untreated for three days to allow for development of clinical disease. Treatment was started on day 3 PI and continued for seven days. Treatments included a combination of tetracycline and CPP-anti-tetA PNA, a cell-penetrating peptide-peptide nucleic acid conjugate that suppresses expression of the TetA tetracycline efflux pump, as well as appropriate controls (see text for details). The x-axis of each plot indicates the number of days PI. The y-axis shows S(t), which is the probability of surviving to time (t) where (t) is the number of days PI. Brief captions under each plot indicate the treatment given. All groups had two or three mice clear the infection and survive to the end of the study except for the group treated with tetracycline and the CPP-Control PNA. The CPP-Control PNA has a nonsense nucleic acid sequence designed to be a negative control for PNA action. Except for this latter group, no obvious differences in survival were noted upon visual examination of the survival plots.

Replicate 2

Culture of the inoculum solution indicated that mice received ~1.2 x 10^7 CFU/mouse for infection, which is slightly higher than the target dose of 1 x 10^7 CFU/mouse. By Day 3 PI when treatments were started, one or more mice were showing mild to clinical signs of illness. Over 10 days PI, all mice except for two progressed to severe clinical signs and either died or were euthanized due to reaching critical endpoints. Two mice in treatment group 5 (tetracycline only) exhibited mild clinical signs for approximately seven days before undergoing recovery such that they were clinically health at the time of euthanasia at the end of the study. Kaplan-Meier survival curves were generated for each treatment group (Figure 6.2).

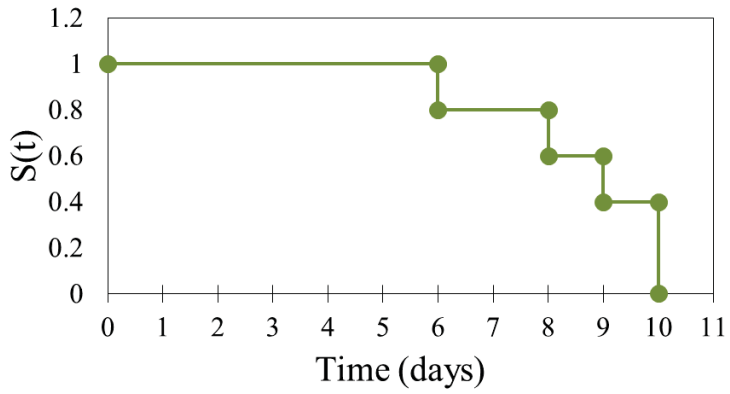

Figure 6.2A. CPP-anti-tetA PNA + Tetracycline

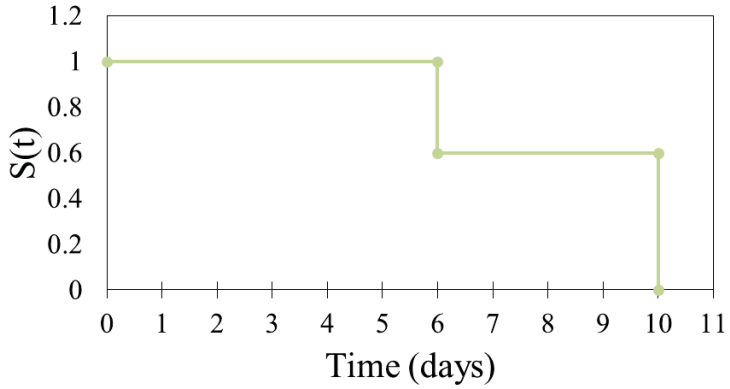

Figure 6.2B. CPP-anti-tetA PNA

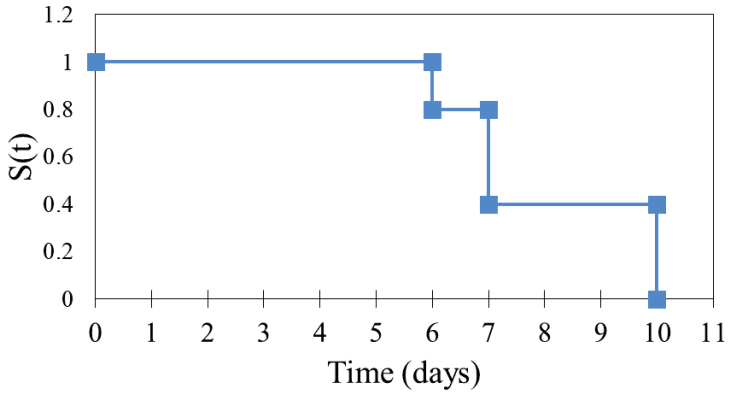

Figure 6.2C. CPP-Control PNA + Tetracycline

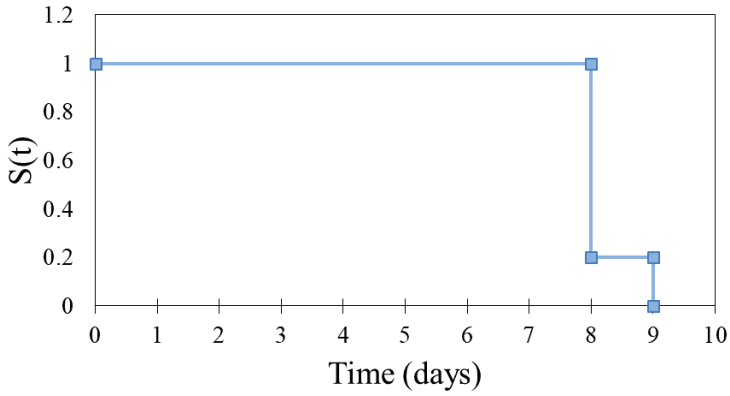

Figure 6.2D. CPP-Control PNA

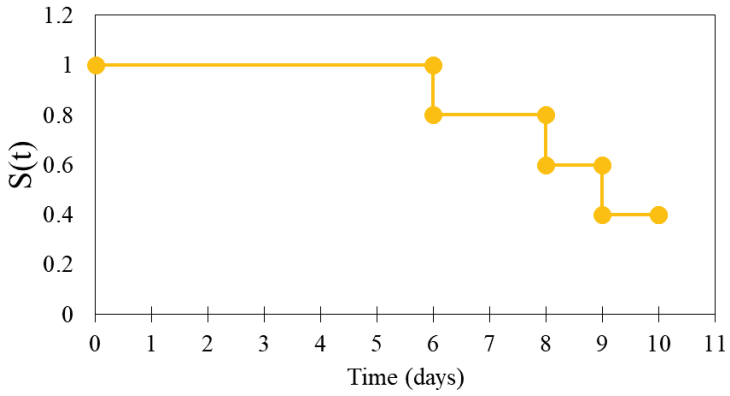

Figure 6.2E. Tetracycline

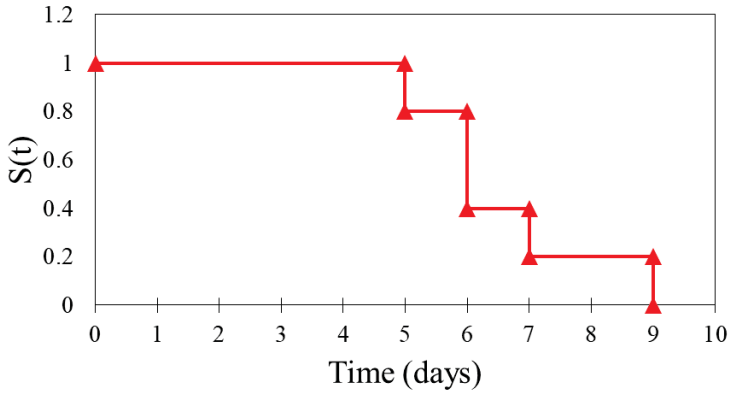

Figure 6.2F. CPP

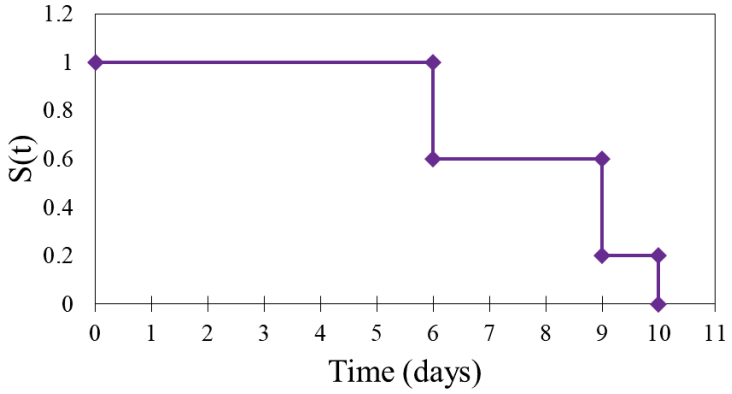

Figure 6.2G. PBS

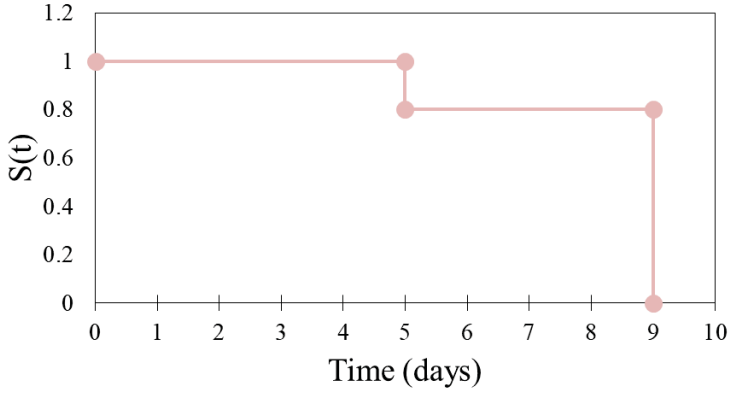

Figure 6.2H. CPP-Sal-tsf PNA

Figure 6.2 Survival curves for each treatment group in the second replicate of a study to test the efficacy of an experimental treatment for systemic salmonellosis in a mouse model. Female BALB/c mice (n = 5/group) were orally infected with tetracycline-resistant *Salmonella enterica* ssp. *enterica* serovar Typhimurium DT104 and left untreated for three days to allow for development of clinical disease. Treatment was started on day 3 PI and continued for seven days. Treatments included a combination of tetracycline and CPP-anti-tetA PNA, a cell-penetrating peptide-peptide nucleic acid conjugate that suppresses expression of the TetA tetracycline efflux pump, CPP-Sal-tsf, a PNA targeting expression of an essential bacterial gene, as well as appropriate controls (see text for details). The x-axis of each plot indicates the number of days PI. The y-axis shows S(t), which is the probability of surviving to time (t) where (t) is the number of days PI. Brief captions under each plot indicate the treatment given. In this replicate, all mice progressed to severe clinical illness resulting in termination within 10 days PI, except for two mice in the group treated with tetracycline alone. These two mice went through a period of illness, but cleared the infection and appeared clinically healthy by the end of the study. Except for this latter group, no obvious differences in survival were noted upon visual examination of the survival plots.

Kaplan-Meier survival curves were also generated using the combined data from both replicates of the mouse experiment (Figure 6.3). The log-rank test did not detect a significant difference in the probability of survival between any of the interventional treatment groups and the PBS-only control group.

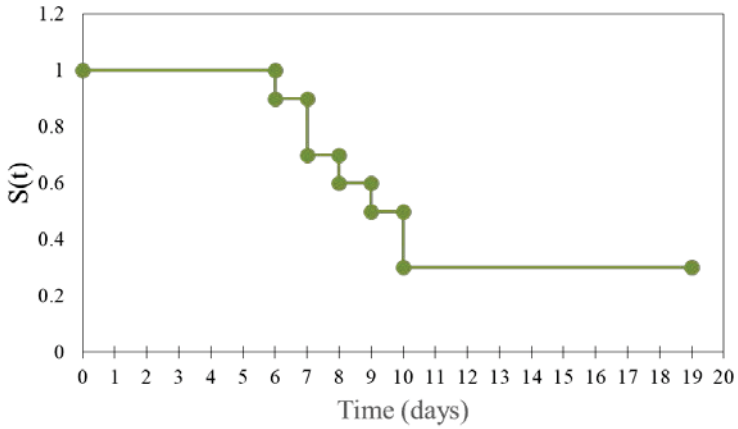

Figure 6.3A. CPP-anti-tetA PNA + Tetracycline

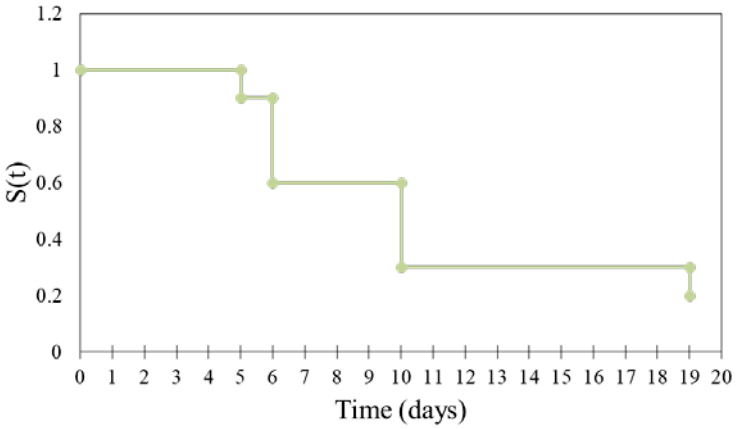

Figure 6.3B. CPP-anti-tetA PNA

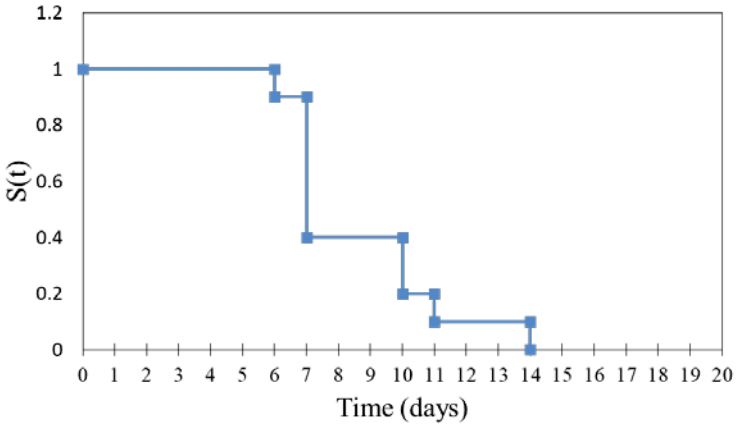

Figure 6.3C. CPP-Control PNA + Tetracycline

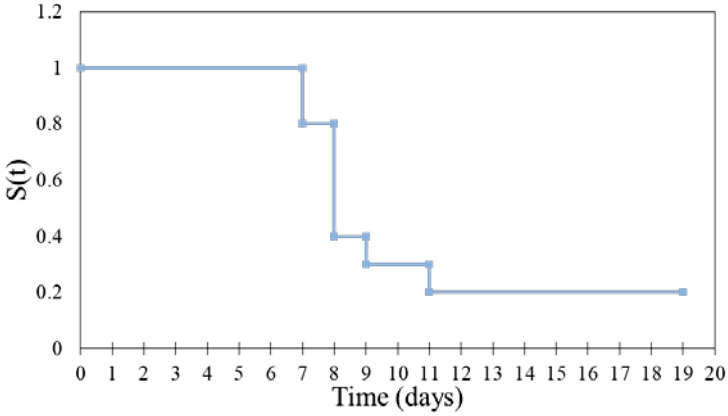

Figure 6.3D. CPP-Control PNA

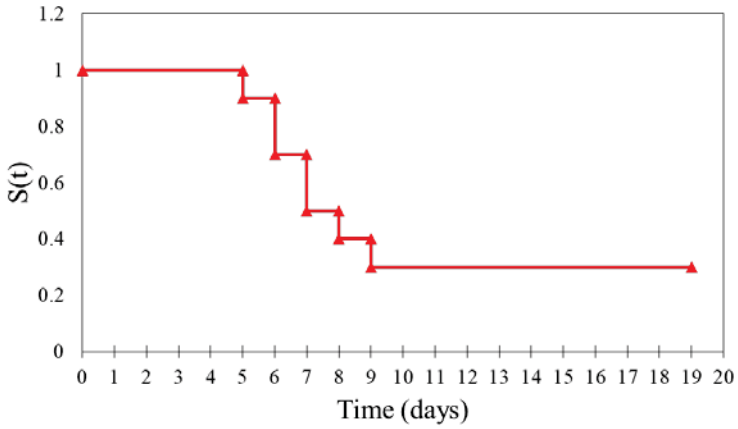

Figure 6.3E. CPP only

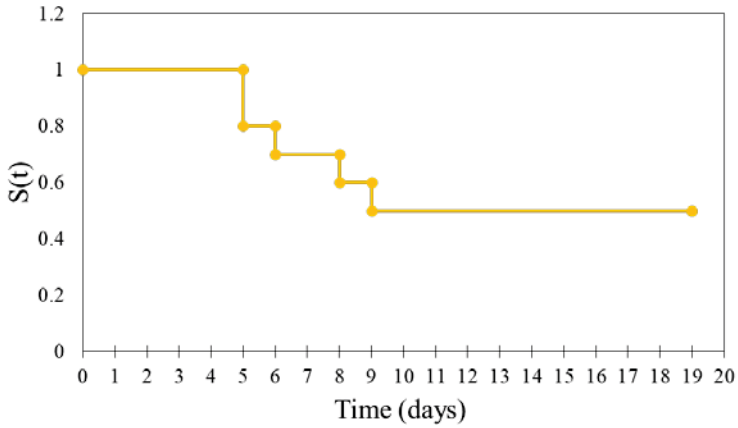

Figure 6.3F. Tetracycline only

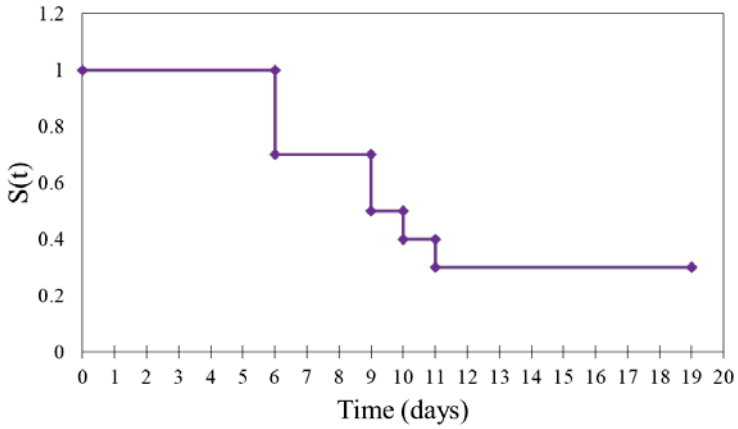

Figure 6.3G. PBS only

Figure 6.3 Survival curves for each treatment group generated with combined data from both replicates of a study to test the efficacy of an experimental treatment for systemic salmonellosis in a mouse model. Only the treatment groups common to both replicates of the experiment were included. Female BALB/c mice (n = 5/group in each replicate) were orally infected with tetracycline-resistant *Salmonella enterica* ssp. *enterica* serovar Typhimurium DT104 and left untreated for three days to allow for development of clinical disease. Treatment was started on day 3 PI and continued for seven days. Treatments included a combination of tetracycline and CPP-anti-tetA PNA, a cell-penetrating peptide-peptide nucleic acid conjugate that suppresses expression of the TetA tetracycline efflux pump, as well as appropriate controls (see text for details). The x-axis of each plot indicates the number of days PI. The y-axis shows S(t), which is the probability of surviving to time (t) where (t) is the number of days PI. Brief captions under each plot indicate the treatment given. The two observations that stand out upon visual examination of this combined data are 1) overall survival was worst in the group treated with a combination of tetracycline and the CPP-Control PNA and 2) overall survival was best (50%) in the group treated only with tetracycline. All of the other groups had an overall survival of 20%-30%.

The results from organs that grew *Salmonella* colonies are shown graphically in Figure 6.4. Not all samples had a positive culture. No statistically significant differences were found among the group variances with one-factor ANOVA.

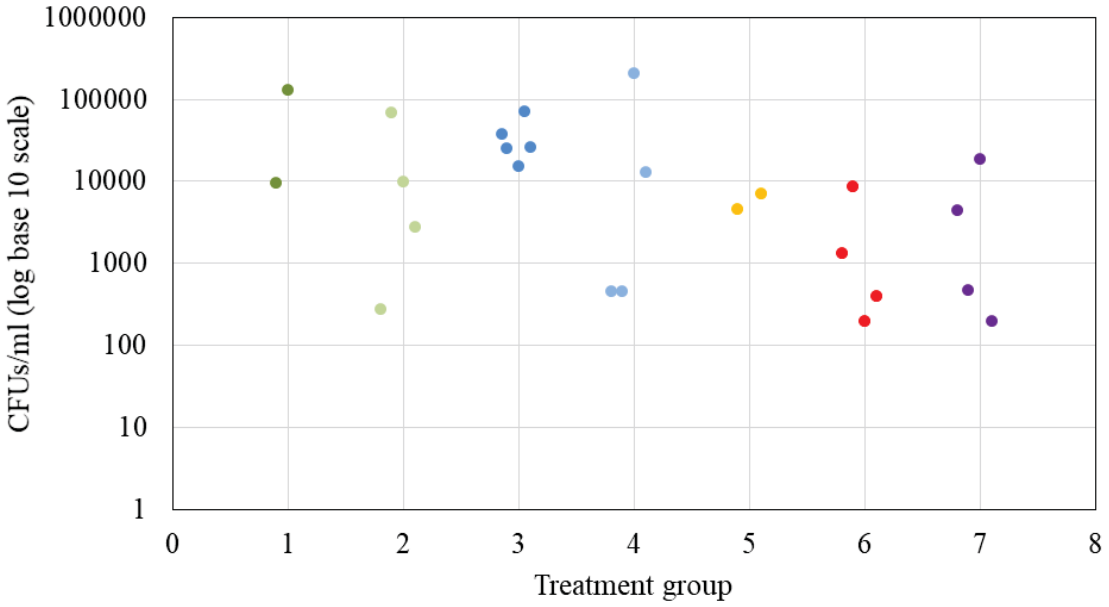

Figure 6.4A. CFUs/ml cultured from spleen

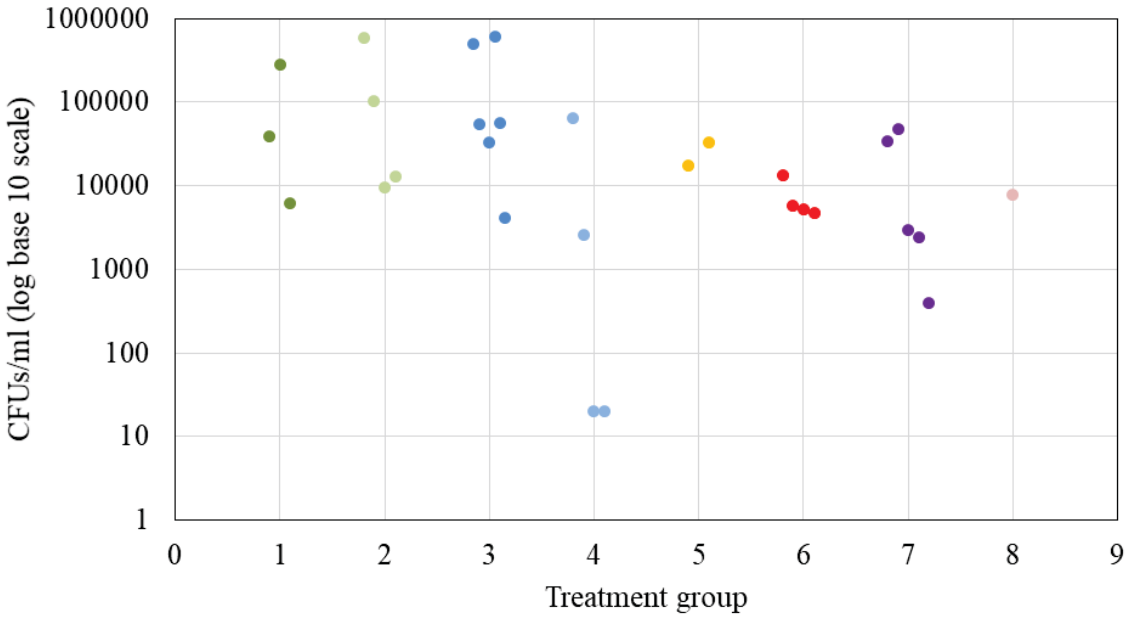

Figure 6.4B. CFUs/ml cultured from liver

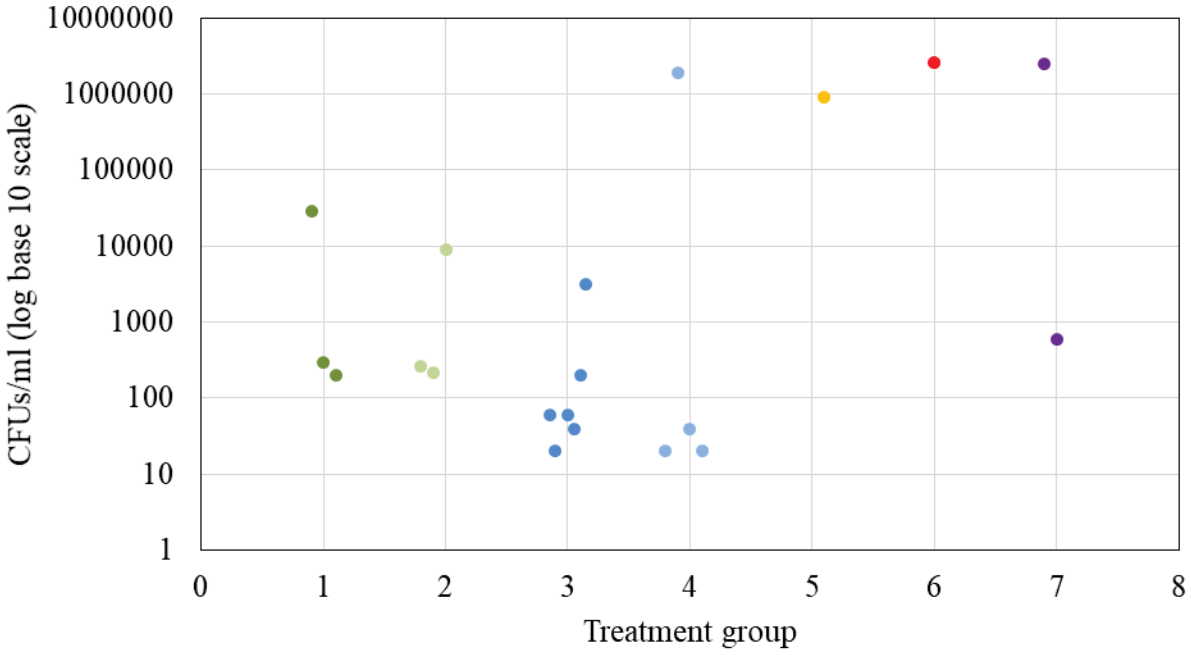

Figure 6.4C. CFUs/ml cultured from small intestine

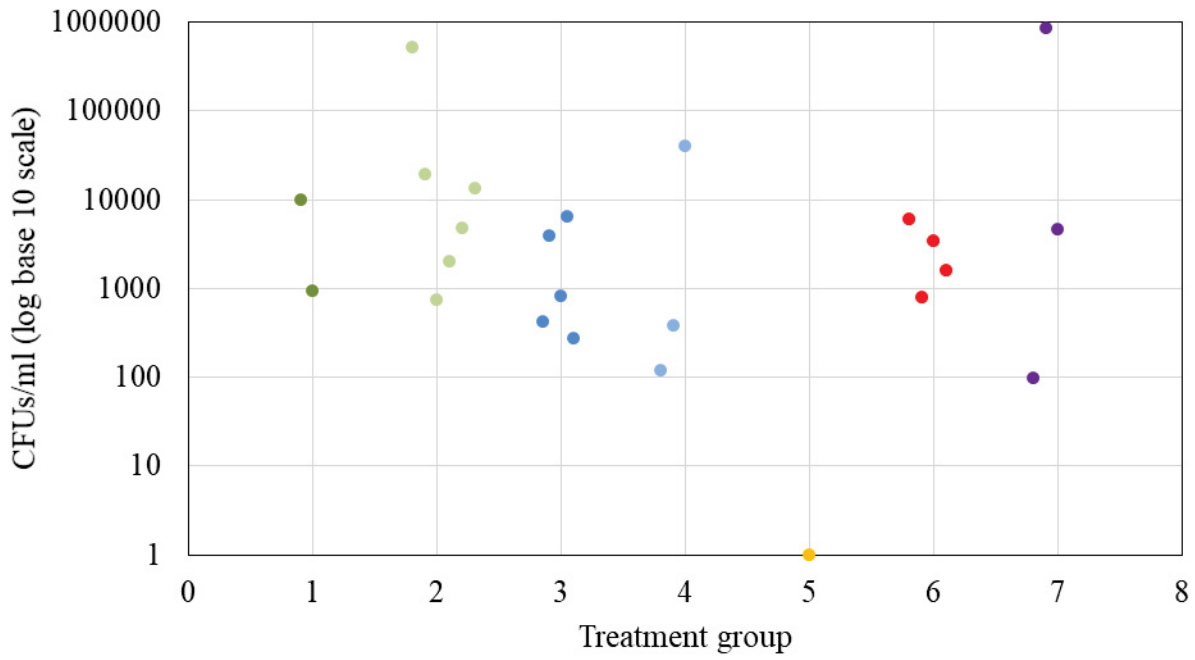

Figure 6.4D. CFUs/ml cultured from large intestine

Figure 6.4 Dot plots showing the number of *Salmonella* CFU/ml grown from internal organs of mice in a study to test the efficacy of an experimental treatment for systemic salmonellosis. Female BALB/c mice (n = 5/group x 2 replicates) were orally infected with tetracycline-resistant *Salmonella enterica* ssp. *enterica* serovar Typhimurium DT104 and left untreated for three days to allow for development of clinical disease. Treatment was started on day 3 PI and continued for seven days. Treatments included a combination of tetracycline and CPP-anti-tetA PNA, a cell-penetrating peptide-peptide nucleic acid conjugate that suppresses expression of the TetA tetracycline efflux pump, as well as appropriate controls (see text for details). Upon termination, portions of liver, spleen, small intestine, and large intestine were collected and frozen at -80 ˚C until they could be thawed, homogenized, serially diluted, and cultured on XLT-4 agar for CFU/ml quantification. Some groups do not have 10 data points because not all samples had a positive culture result. Treatment groups: 1) Tetracycline + CPP-anti-tetA PNA, 2) CPP-anti-tetA PNA, 3) Tetracycline + CPP-Control PNA, 4) CPP-Control PNA, 5) Tetracycline, 6) CPP, 7) Phosphate buffered saline. No statistical differences were found among treatment groups using one-factor ANOVA with significance set as $p < 0.05$.

6.4 Discussion and conclusions

This chapter describes the development of a mouse model of salmonellosis by oral infection with *Salmonella enterica* ssp. *enterica* serovar Typhimurium DT104, followed by use of that model to evaluate antimicrobial efficacy of CPP-PNA conjugates *in vivo*. The decision to develop and

optimize our own model was made because the literature did not present an oral DT104 infection model that mimicked natural infection to our satisfaction.

There are only a few reports describing the use of anti-sense oligomers such as PNAs or PMOs to inhibit bacterial growth or treat sepsis in mice. One study showed that when a PMO targeting the essential *acpP* gene in *E. coli* AS19 was injected intraperitoneally at the same time as a non-lethal dose of the bacterium, CFU/ml counts from peritoneal lavages were significantly lower than those from control mice that were injected with bacteria and phosphate buffered saline.[15] In a more recent paper Geller et al.[16] intranasally infected mice with *Klebsiella pneumoniae* and initiated treatment with an intranasal PMO targeting the essential acpP gene at 0, 8, 24, or 48 hours PI. Mouse survival showed both dose and time-dependent improvement relative to controls. Another set of experiments using both defective and wild type strains of *E. coli*, showed that injecting mice intraperitoneally 30 minutes before or intravenously 30 minutes after intraperitoneal injection of bacteria resulted in reduced peritoneal CFU/ml counts and reduced mortality compared to control mice treated with PBS.[17]

In each of these experiments using live animal models, the antisense molecules were administered either at the time of infection or within 48 hours PI. In addition, none of the mouse model studies utilizing antisense molecules involved oral infection with the bacterial organism of interest. These studies also all used PNAs or PMOs designed to suppress expression of essential bacterial genes. To the authors' knowledge, this dissertation chapter describes the first use of a mouse model of oral bacterial infection with *S.* Typhimurium DT104, a mouse pathogen, in which one of the experimental treatments involved concurrent use of a conventional antibiotic and a PNA targeting a corresponding bacterial antibiotic resistance gene, and treatment was not instituted until the mice had time to develop clinical signs of illness. Thus, this model mimics the type of timeline that is more likely to occur in cases of real illness, in which the patient becomes clinically ill before seeking treatment

Under the circumstances of these experiments, no clear protective effect was observed with the experimental treatments. Several possible reasons for this outcome are considered. For one, the dose of CPP-PNA may not have been high enough for effective action, especially since the mice

were allowed to develop clinical illness before intervention. Due to the cost of PNAs (often several thousand dollars for a few hundred nmole) there is a paucity of studies that examine pharmacokinetics, pharmacodynamics, or dose optimization for these molecules, so clear guidelines on choice of dose are not available. The dose was chosen to fall within ranges previously reported for PNA or PMO treatment in mice or rats,[15,17-18] and is admittedly at the lower end of what has been tried before. It is also possible that the PNAs were not effectively delivered to the bacteria due to inability to cross multiple cell membranes or low bioavailability. Another factor that could be in play is that there are differences in the metabolic processes activated by bacteria *in vitro* versus *in vivo*, potentially leading to different responses to the same molecule depending on the conditions.

Although no statistically significant differences in survival were seen among various treatment groups in the CPP-PNA experiments, there were several observations that stood out. The mice treated with tetracycline had the highest overall survival rate when data from both replicates were pooled. This suggests a slight protective effect of tetracycline, which was unexpected since DT104 is tetracycline-resistant. The combination of tetracycline and the CPP-Control PNA subjectively appeared to increase the risk of mortality. The reason for this is unknown. The CPP-Control PNA also had unexpected and unpredictable bacterial inhibitory effects against DT104 *in vitro* (see Chapter 4), so there is interest in better characterizing this molecule to try and explain its unexpected behavior. A favorable observation was that no signs of acute toxicity or hypersensitivity were seen in response to administration of the PNAs.

Several limitations of this study are noted. The small sample sizes were small, which in turn prevented thorough and robust statistical analysis of all of the various results. There was some inevitable variation in infectious dose due to the method of inoculum preparation, which likely affected the timeline and severity of disease. In the second replicate of the CPP-PNA experiment the retrospectively calculated infectious dose of DT104 was higher than that of the first replicate, which may explain why the clinical course of disease was more rapid and mortality was higher. Due to cost, no previous work was done to evaluate the acute or chronic toxicity or PK/PD of the PNAs specifically designed for these experiments. It is possible that such an analysis would have flagged the CPP-Control PNA as unsuitable for use in a live animal model. Recommendations for

future work include testing PNA PK/PD and toxicity at several different doses and for different lengths of time, trying similar experiments with a larger animal sample size, and investigating other drug delivery systems for the CPP-PNAs such as nanoparticles.

In conclusion, under the circumstances of this particular study, no significant protective effect against DT104 infection was seen in BALB/c mice treated with tetracycline and the CPP-anti-tetA PNA targeting expression of the TetA tetracycline efflux pump, or with CPP-Sal-tsf PNA targeting an essential gene. However, the oral DT104 infection model could be of use for future experiments both for this laboratory and for others.

6.5 References

1. Centers for Disease Control and Prevention (CDC). Antibiotic resistance threats in the United States, 2013. https://www.cdc.gov/drugresistance/threat-report-2013/pdf/ar-threats-2013-508.pdf. Accessed February 16, 2019.
2. World Health Organization. Antibiotic resistance (5 February 2018). http://www.who.int/news-room/fact-sheets/detail/antibiotic-resistance. Accessed March 2, 2019.
3. Rasmussen LCV, Sperling-Petersen HU, and Mortensen KK. Hitting bacteria at the heart of the central dogma: sequence-specific inhibition. Microb Cell Fact. 2007;6(24). doi: 10.1186/1475-2859-6-24.
4. Bai H, Sang G, You Y, et al. Targeting RNA polymerase primary σ70 as a therapeutic strategy against methicillin-resistant *Staphylococcus aureus* by antisense peptide nucleic acid. PLoS One. 2012;7(1):e29886. doi: 10.1371/journal.pone.0029886.
5. Abushahba MFN, Mohammad H, Seleem MN. Targeting multidrug-resistant Staphylococci with an anti-rpoA peptide nucleic acid conjugated to the HIV-1 TAT cell penetrating peptide. Mol Ther Nucleic Acids. July 2019;5:e339. doi:10.1038/mtna.2016.5.
6. Readman JB, Dickson G, Coldham NG. Translational inhibition of CTX-M extended spectrum β-lactamase in clinical strains of *Escherichia coli* by synthetic antisense oligonucleotides partially restores sensitivity to cefotaxime. Front Microbiol. March 2016;7:373. doi: 10.3389/fmicb.2016.00373.

7. Plant J, Glynn AA. Natural resistance to *Salmonella* infection, delayed hypersensitivity and Ir genes in different strains of mice. Nature. March 1974;248:345-347.
8. Mastroeni P, Villarreal-Ramos B, Hormaeche CE. Adoptive transfer of immunity to oral challenge with virulent *Salmonellae* in innately susceptible BALB/c mice requires both immune serum and T cells. Infect Immun. 1993;61(9):3981-3984.
9. Roy MF, Malo D. Genetic regulation of host responses to *Salmonella* infection in mice. Genes Immun. 2002;3(7):381-393.
10. Allen CA, Fedorka-Cray PJ, Vazquez-Torres A, et al. *In vitro* and *in vivo* assessment of *Salmonella enterica* serovar Typhimurium DT104 virulence. Infect Immun. 2001;69(7):4673-4677.
11. Asahara T, Shimizu K, Takada T, et al. Protective effect of Lactobacillus casei strain Shirota against lethal infection with multi-drug resistant *Salmonella enterica* serovar Typhimurium DT104 in mice. J Apple Microbiol. 2011;110(1):163-173.
12. Erova TE, Kirtley ML, Fitts EC, et al. Protective immunity elicited by oral immunization of mice with *Salmonella enterica* serovar Typhimurium Braun lipoprotein (Lpp) and acetyltransferase (MsbB) mutants. Front Cell Infect Microbiol. November 2016;6:148. doi: 10.3389/fcimb.2016.00148.
13. Wickham ME, Brown NF, Provias J, Finlay BB, Coombes BK. Oral infection of mice with *Salmonella enterica* serovar Typhimurium causes meningitis and infection of the brain. BMC Inf Dis. 2007;7:65. doi:10.1186/1471-2334-7-6.
14. Wagner RD, Johnson SJ. Probiotic bacteria prevent *Salmonella*-induced suppression of lymphoproliferation in mice by an immunomodulatory mechanism. BMC Microbiol. 2017;17:77. doi 10.1186/s12866-017-0990-x.
15. Geller BL, Deere J, Tilley L, Iversen PL. Antisense phosphorodiamidate morpholino oligomer inhibits viability of *Escherichia coli* in pure culture and in mouse peritonitis. J Antimicrob Chemother. 2005;55(6):983-988.
16. Geller BL, Li L, Martinez F, et al. Morpholino oligomers tested *in vitro*, in biofilm and *in vivo* against multidrug-resistant *Klebsiella pneumoniae*. J Antimicrob Chemother. 2018;73(6):1611-1619.

17. Tan X, Actor JK, Chen Y. Peptide nucleic acid antisense oligomer as a therapeutic strategy against bacterial infection: proof of principle using mouse intraperitoneal infection. Antimicrob Agents Chemother. 2005;49(8):3203-3207.
18. McMahan BM, Stewart JA, Jackson J, Fauq A, McCormick DJ, Richelson E. Intraperitoneal injection of antisense peptide nucleic acids targeted to the mu receptor decreases response to morphine and receptor protein levels in rat brain. Brain Res. 2001;904(2):345-349.

7 Conclusion

This dissertation is a culmination of work that, interspersed with time devoted to also completing requirements for a veterinary clinical pathology residency, spanned nearly six years and two disciplines, chemistry and bacteriology. The unifying goal for this research was the desire to play at least a small part in addressing the worldwide problem of bacterial antibiotic resistance. During the time spent in this PhD program it seems that the call for action has only gotten more frantic, and there is still so much to be done.

This field of research is exciting, but there are multiple difficulties to overcome, not the least of which is the unfortunate disparity between the pressing need for antimicrobial drug research and the lack of commercial interest in the process due to concerns about poor return on investment. It can take years and upwards of $1 billion for a new antibiotic to become commercially available, at which point it is usually prescribed only for short lengths of time (days to weeks). If it is not a first-line drug, it is often not used at all unless other treatments fail. This combination of factors is financially discouraging, to say the least, and limits the amount of funding made available for antibiotic research.[1]

From a researcher's perspective, drug discovery is often not an easy field in which to be, in part because of the diminished funding opportunities touched on above, but also because of the low chance of any particular new lead compound making it all the way from an initial hit to a sleekly packaged medication on the shelves of the local pharmacy.[2] Due to the myriad variables that can cause a molecule's action to differ among *in vitro*, *ex vivo*, and *in vivo* environments, it is difficult to predict the success of a compound of interest, so the investigator must be persistent despite likely discarding the majority of what initially appeared to be promising leads. In addition, the stringent governmental requirements for drug performance and safety, while necessary, impose another layer of stress and prolong the drug development process.[3]

It is now necessary to set aside those reflections on the potential obstacles in the field of drug discovery research and optimistically examine the chief take-away points from this body of work. With regard to the organometallic compounds (OMCs) from the laboratory of Dr. Joseph Merola

(focus of Chapter 3), the major conclusions are that OMCs with an iridium metal center and an amino acid ligand are the best candidates for further research into antimicrobial effects because of low cytotoxicity against a mammalian cell line and good solubility in an aqueous medium. However, more work is needed to investigate cellular penetration capabilities of the compounds.

As for the peptide nucleic acids (PNAs) targeting bacterial genes (focus of Chapters 4, 5, and 6), the conclusion was reached that these compounds indeed hold promise as antibacterial agents. As shown in Chapter 4, both a PNA targeting the essential *tsf* gene and a PNA targeting the *tetA* antibiotic resistance gene coding for a tetracycline efflux pump in *Salmonella enterica* ssp. *enterica* serovar Typhimurium showed notable antibacterial activity *in vitro*. However, similar results were not achieved *in vivo* with a mouse model of infection (Chapter 6), so additional emphasis on PNA toxicity, pharmacodynamics, pharmacokinetics, and dose optimization is necessary. Chapter 5 lends strong support for the specificity of the anti-tetA PNA for its nucleic acid target, as shown by a relative decrease in *tetA* mRNA in bacterial cultures treated concurrently with tetracycline and the PNA compared to cultures treated only with tetracycline. This is encouraging for the possibility of "designer drugs" that can be chosen to specifically treat a patient's infection without causing off target effects such as depleting beneficial bacteria or adversely affecting the patient's own cells.

There were some unexpected observations from this work. One was that a PNA targeting expression of the TetR resistance regulatory protein has a bacterial inhibitory effect. In addition, this PNA did not have the expected effect on *tetA* expression when tetracycline was present, but did have the expected effect if tetracycline was absent. The role of TetR in bacterial fitness is not yet fully elucidated; for this research it was assumed to be a non-essential gene, but the results suggest it is more important for bacterial function than originally understood. The second unforeseen observation was that a control PNA molecule with a scrambled nucleotide sequence did not behave at all as expected. The nucleotide sequence was designed to avoid targeting expression of any known genes, with the intention of using it as a relatively inert negative control. Instead, it had nonspecific and unpredictable bacterial inhibitory effects and when combined with tetracycline it subjectively appeared to contribute to increased mortality in mice infected with

Salmonella. This raises the question of whether that particular nucleotide sequence is somehow toxic or perhaps alters bacterial gene expression after all.

A concern common to both the OMC and PNA experiments is effective delivery of the proposed drug to its target. The OMC of most interest appears to have poor intracellular penetration on its own. The PNAs had repeatable bacterial inhibitory effects *in vitro*, but no clear antibacterial efficacy was observed *in vivo*. This could be because the dose was too low, but could also indicate that the PNAs did not reach the intended target.

Recommendations for future research are as follows:

- Pursue ways to increase the intracellular penetration capabilities of the OMC and experiment further with different ligand and Cp variations to continue searching for structures with even greater antimycobacterial activity
- Explore drug-delivery systems for both the OMCs and PNAs such as nanoparticle encapsulation and different cell-penetrating peptides or other carrier molecules
- Evaluate PNA action in infected eukaryotic cell culture
- Consider additional *in vivo* animal studies with PNAs, but first learn more about PK/PD and PNA stability

It is the author's hope that what was learned during this PhD research, and what will be learned in future related work, will help avoid a crisis of uncontrolled bacterial antibiotic resistance.

7.1 References

1. Fair RJ, Tor Y. Antibiotics and bacterial resistance in the 21st century. Perspect Medicin Chem. 2014;6:25-64. doi: 10.4137/PMc.s14459.
2. Mohs RC, Greig NH. Drug discovery and development: role of basic biological research. Alzheimers Dement. 2017;3(4):651-657.
3. U.S. Food and Drug Administration. The Drug Development Process. https://www.fda.gov/ForPatients/Approvals/Drugs/default.htm. Accessed March 4, 2019.